

**EXPLORING THE BIOLOGICAL
DOMAIN OF THE CARDIAC
EMBRYONIC STEM CELL TEST**

**In search for biomarkers of developmental
toxicity for optimizing an animal-free
alternative test system**

Gina Mennen

EXPLORING THE BIOLOGICAL DOMAIN OF THE CARDIAC EMBRYONIC STEM CELL TEST

In search for biomarkers of developmental
toxicity for optimizing an animal-free alternative
test system

Gina Mennen

Exploring the biological domain of the cardiac embryonic stem cell test - In search for biomarkers of developmental toxicity for optimizing an animal-free alternative test system

ISBN: 978-94-6458-406-6
DOI: doi.org/10.33540/1244
Cover: Shutterstock
Lay-out: Publiss | www.publiss.nl
Print: Ridderprint | www.ridderprint.nl

© Copyright 2022: Gina Mennen, The Netherlands

All rights reserved. No part of this publication may be reproduced, stored in a retrieval system, or transmitted in any form or by any means, electronic, mechanical, by photocopying, recording, or otherwise, without the prior written permission of the author.

EXPLORING THE BIOLOGICAL DOMAIN OF THE CARDIAC EMBRYONIC STEM CELL TEST

In search for biomarkers of developmental toxicity for optimizing an animal-free alternative test system

VERKENNING VAN HET BIOLOGISCH DOMEIN VAN DE EMBRYONALE STAMCEL TEST

Op zoek naar biomarkers van ontwikkelingstoxiciteit ter optimalisatie van een proefdiervrij alternatief testsysteem

(met een samenvatting in het Nederlands)

Proefschrift

Ter verkrijging van de graad van doctor aan de Universiteit Utrecht op gezag van de rector magnificus, prof. dr. H.R.B.M. Kummeling, ingevolge het besluit van het college voor promoties in het openbaar te verdedigen op dinsdag 30 augustus des middags te 12.15 uur

door

Regina Helena Mennen

geboren op 15 augustus 1992 te Helmond

Promotoren

Prof. dr. A. H. Piersma

Prof. dr. M. Pallardy

Copromotor

Dr. R. Bars

The degree is awarded as part of a Joint Doctorate with Université Paris-Saclay.

Dit proefschrift werd mede mogelijk gemaakt door financiële steun van CIFRE vanuit l'Association Nationale de la Recherche et de la Technologie (ANRT) grant no. 2018-0682.

"All models are wrong, but some are useful."

- George E.P. Box -

Contents

Chapter 1	General introduction	11
Section 1	A hypothesis-driven literature based approach for biomarker selection	33
Chapter 2	Neural crest related gene transcript regulation by valproic acid analogues in the cardiac embryonic stem cell test	35
Chapter 3	Molecular neural crest cell markers enable discrimination of organophosphates in the murine cardiac embryonic stem cell test	63
Chapter 4	Gene regulation by morpholines and piperidines in the cardiac embryonic stem cell test	89
Section 2	A hypothesis-generating data-driven approach for biomarker selection	119
Chapter 5	Genome-wide expression screening in the cardiac embryonic stem cell test shows additional differentiation routes that are regulated by morpholines and piperidines	121
Section 3	Enhancing the sensitivity to biomarkers	175
Chapter 6	Oxygen tension influences embryonic stem cell maintenance and has lineage specific effects on neural and cardiac differentiation	177
Chapter 7	Cell differentiation in the cardiac embryonic stem cell test (ESTc) is influenced by the oxygen tension in its underlying embryonic stem cell culture	207
Chapter 8	Endoderm and mesoderm derivatives in embryonic stem cell differentiation and their use in developmental toxicity testing	229
Chapter 9	Summary and general discussion	275

Appendix	
Nederlandse samenvatting	299
List of publications	305
Curriculum Vitae	309
Dankwoord	313

Abbreviations

3R	Replacement, Reduction, Refinement
AOP	Adverse outcome pathway
ATRA	All-trans retinoic acid
BMD	Benchmark dose
BMR	Benchmark response
cDNA	Complementary DNA
CPF	Chlorpyrifos
DAPI	4',6-diamidino-2-phenylindole
DEGs	Differentially Expressed Genes
DMSO	Dimethyl sulfoxide
DNA	Deoxyribonucleic acid
EB	Embryoid body
EHA	2-ethylhexanoic acid
EHOL	2-ethylhexanol
FA	Folic acid
FC	Fold change
FPD	Fenpropidin
FPM	Fenpropimorph
hESC	Human embryonic stem cells
hiPSC	Human induced pluripotent stem cells
HTS	high-throughput screening
ICxx	Inhibitory concentration of viability xx%

IDxx Inhibitory concentration of differentiation xx%

GO Gene ontology

mESC Murine/mouse embryonic stem cells

mESTc Murine/mouse cardiac embryonic stem cell test

mESTn Murine/mouse neural embryonic stem cell test

MLT Malathion

mRNA Messenger ribonucleic acid

NGS Next generation sequencing

qPCR Quantitative polymerase chain reaction

RNA Ribonucleic acid

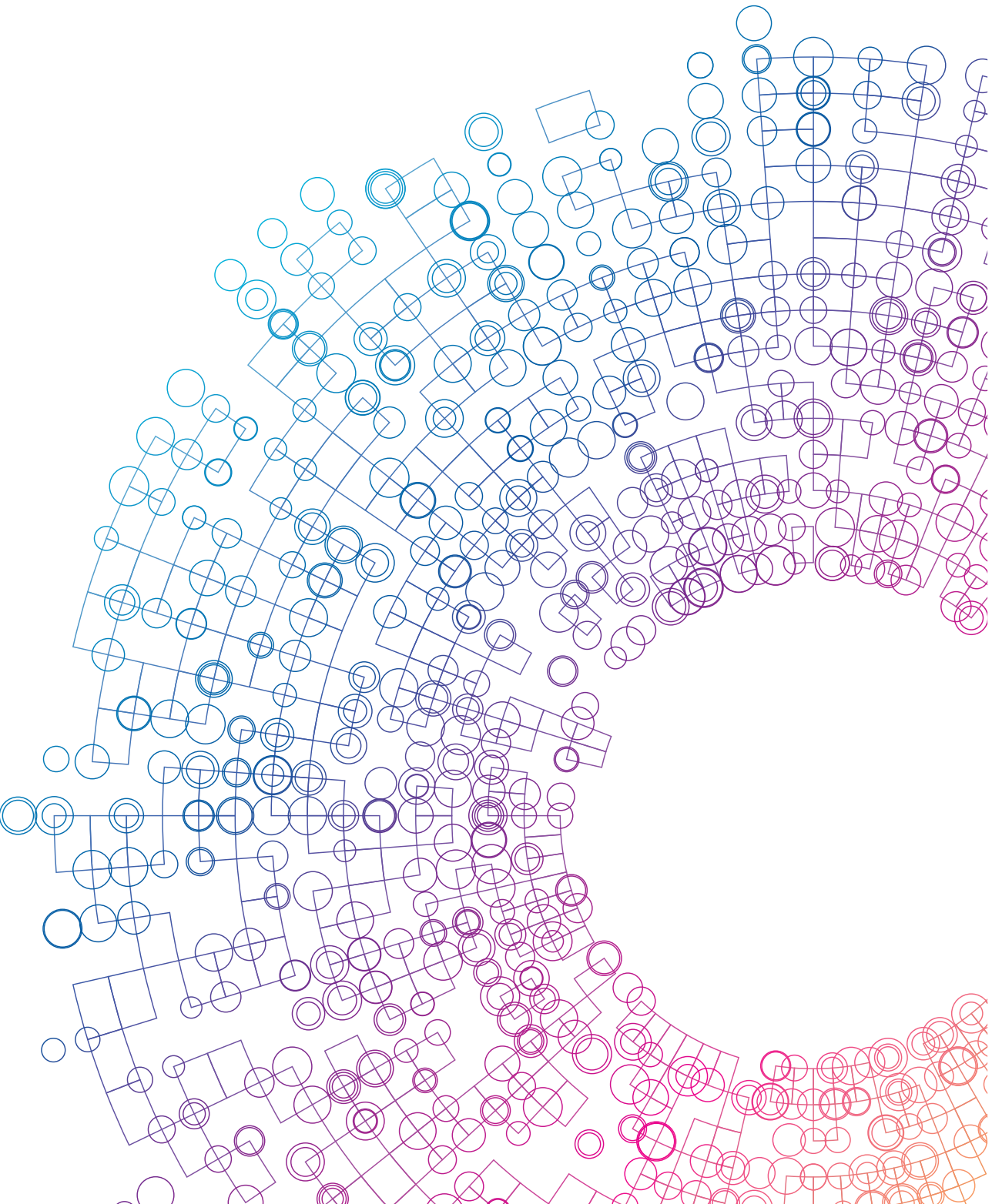
RNA-seq RNA-sequencing

SPX Spiroxamine

TDM Tridemorph

TPP Triphenylphosphate

VPA Valproic acid



CHAPTER

General introduction

1

Chemical safety assessment and prediction for human health

We use animal models to assess the safety of chemicals and drugs for humans, in order to protect humans at all life stages from adverse effects resulting from exposure to toxicants. In history, we have not always been able to preserve ourselves and our progeny from harmful chemicals. The field of developmental and reproductive toxicology (DART) in particular aims to protect our progeny from harmful chemicals. Certain incidents in the 1950s highlighted deficits in evaluating chemicals for potential DART effects and were the impetus for triggering improved testing strategies. For example, thalidomide was prescribed as a drug to morning sickness and was often used early during pregnancy and caused human foetal death and malformations [1]. However, these abnormalities were not observed in the developmental toxicity studies in the offspring of rats that were available at that time. After the thalidomide incident, foetal death was observed in rat developmental toxicity studies and similar effects were detected in the rabbit including embryofoetal malformations and triggered the requirement for evaluation in a second species. Another incident related to developmental defects in new-borns, was related to environmental pollution. During the Minamata tragedy, leakage of methylmercury from a factory nearby the Japanese Minamata bay resulted in human health effects on the central nervous system in adults eating contaminated fish, which also caused developmental defects in new-borns [2]. Therefore, this tragedy provided insight into differences in sensitivities at different life stages. Ever since, safety assessment regulations have been improved and reinforced. In the DART field, animal testing protocols have been extended to inclusively cover the reproduction period, the lactation phase and effects on F1 and F2 generations. However, the increase in vertebrate animal testing also came with ethical, economical and biological issues.

From the ethical perspective, conflicts arose between on the one hand the benefits of successful animal experiments and on the other hand the principle of potential inhumane treatments of animals. As experimentations and therefore the use of animals increased, the ethical framework for animal experimentation in the form of the Three R's principles was proposed by Russel and Burch in 1959: Replacement, Reduction, Refinement [3]. This paradigm aimed for removal of inhumanity in animal testing. The Replacement of animal tests should occur in case alternative non-animal test systems are available. The Reduction of the number of animals

within an experimental design should be such that a minimum number of animals is used, while still meeting the objectives of the research. The Refinement of the animal living conditions should be such that the suffering from pain or distress are reduced as much as possible.

In spite of the implementation of this paradigm, we still encounter the issue of a tremendous use in animals which obviously also comes with economic expenses. Under European legislations, 65% of the animals were estimated to be used in the DART field in the year 2004 [4, 5]. This amount was hypothetically re-evaluated in 2009, a few years after the new and current regulations for animal testing were implemented by the European Commission (REACH Regulation No. 1907/2006) [6, 7]. The impact of these new regulations on the necessary numbers of animals were hypothetically estimated. Based on 68.000-100.000 substances that should be registered according to the newly implemented European regulations, the number of animals would encounter an overall estimation of 90% of all animals (48.648.236) and 70% (€691.214.700) of the required costs for registration in the DART field [6].

Animal testing also raises the question to what extent it can actually represent and predict human biology [8]. The biology in terms of kinetics and physiology differs between animals and humans [9, 10]. Additionally, animal test systems are not always able to predict all aspects of human health including the detection of long-term effects like behavioural (e.g. autism, Alzheimer's disease) and disease predisposition due to a limited mechanistic understanding [11]. Such limitations may possibly explain similarities and differences between the animal and human biology [11]. The mechanistic understanding can be enhanced using alternatives to animal testing such as *in vitro* cell-based models.

Given the ethical, economical, and biological issues associated with laboratory animal use as mentioned, it becomes clear that the field of DART is particularly in urgent need of alternative approaches through innovation. In the last five years, multiple incentives were announced to move away from animal testing. In 2016, the Dutch government announced to be world leader in animal free innovations by 2025 [12]. The United States Environmental Protection Agency (US EPA) even announced to eliminate requests for, and funding of, mammal studies completely by 2035 [13]. Multiple efforts and approaches towards animal replacements have been made already, but a paradigm shift away from the default of *in vivo* models is required in order to completely replace animal testing. The National Research Council (NRC)

of the US presented '*toxicity testing in the 21st century*', promoting the use of a new toxicity-testing system relying on understanding toxicity mechanisms that can result in adverse health effects [14]. In order to understand these mechanisms, multiple efforts have been made to identify molecular pathways that are affected by chemicals and could function as examples for further development in animal alternative testing [15-19].

Embryo development and birth defects

Human pregnancy begins with fusion of female and male gametes, an egg and a sperm. After fertilization the embryo is formed, starting with just one single cell which will be cleaved into multiple cells within the first week of conception forming the blastocyst (fig. 1) [20]. Early cleavage occurs while the embryo is transported to the uterus where the blastocyst is implanted around day 7. In the next 3 weeks, important processes take place: germ layer formation and gastrulation will start forming the basic body plan with formation of the neural tube, somites, first primitive functional heart and vessels, tubular gut and rudiments of most of the major organ systems. By 8 weeks after fertilization, the embryo transforms into a foetus with all organs present, which will continue to mature until birth around 38 weeks after fertilization. At any time, the complex developmental biology processes may fail, resulting in sub-optimal development. The precise developmental stage when the damage occurs and the chemical potency will dictate the severity of any resulting defect.

The study of birth defects is also called teratology, literally meaning "the study of monsters". Birth defects can have a genetic cause, but also environmental effects can perturb normal embryo development. Globally, approximately 2-3% of living new-borns are born with a birth defect [20]. The causes of only 30% of these birth defects are somewhat understood, leaving the possibility that environmental factors could be playing a significant role [21]. The most extreme pregnancy outcomes are miscarriages during the first trimester of pregnancy with maximal susceptibility between 3 and 8 weeks, whereas in late pregnancy this would result in still birth [20]. All parts of pregnancy are important to lead to a successful outcome, but the earlier stages are perhaps more vulnerable to chemical damage as any effects are typically irreversible and maybe more severe. Nevertheless, organ maturation in the foetal period can also be affected by chemical exposure and should also be protected.

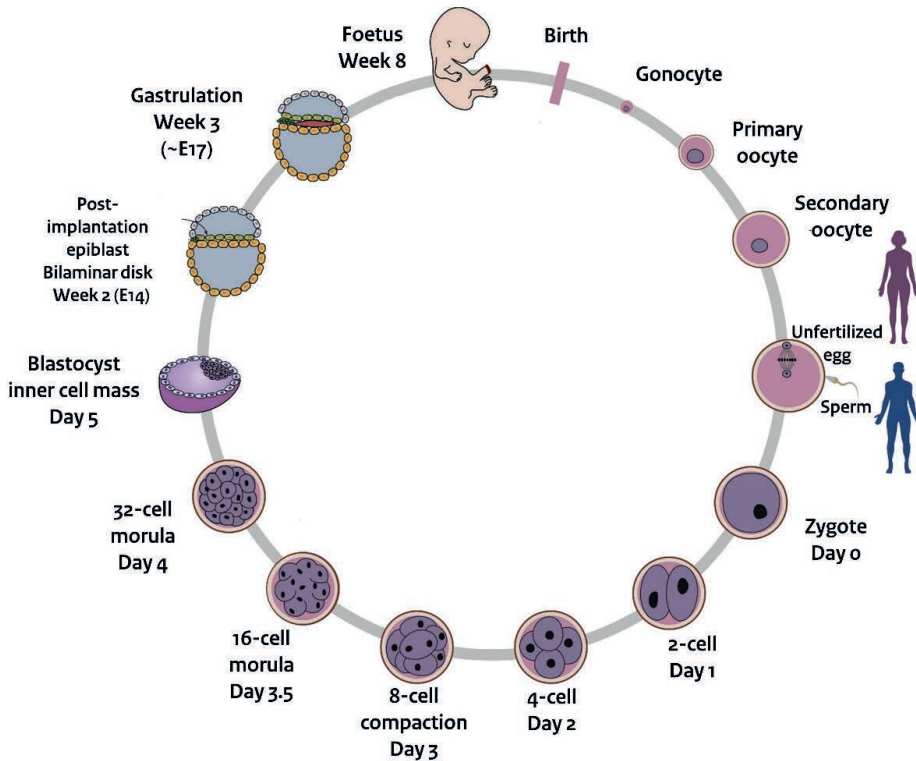


Figure 1: Human life cycle starting with the development of the oocyte which gets fertilized by a sperm cell, forming the zygote. Cell cleavage transforms the embryo into a blastocyst. The blastocyst contains the inner cell mass, which will transform into the bilaminar disk and consequently the three germ layers from which each cell within the body is formed. The embryo will transform into a foetus in week 8. Adjusted from: [22]

Basic principles in toxicology

The field of toxicology studies potential harmful effects of chemicals on biological systems. Generally in toxicology, an identified adverse effect defines the hazard profile of a chemical, whereas exposure identifies whether or not the chemical poses a health risk by reaching the organism or organ and in what magnitude (dose or concentration) or duration (time) [23]. The relation between a chemical and an adverse effect is generally assessed by identifying dose-response relationships from laboratory studies, where the quantifiable effect is dependent on the dose of the chemical administered to the test system. From these relationships,

threshold values can be extracted based on statistically significant differences compared to controls. The no observed adverse effect level (NOAEL) is the highest non-statistically significant dose tested for toxicity, whereas the lowest observed adverse effect level (LOAEL) is the lowest dose tested with a statistically significant effect. Traditionally, the NOAEL from animal studies is used for risk assessment calculations to determine estimates for safe daily exposure. To correct for interspecies (animal-to-human) and intraspecies (human-to-human) the NOAEL is generally divided by a safety factor of 100 (10x10) [24]. Another approach to identify the point of departure from the dose-response slope is to calculate the benchmark dose (BMD) obtained from animal studies. This approach has advantages since it takes the full dose-response curve into account, includes the variability of all the relevant datapoints and additionally determines whether the specified response level (e.g. 10%) is consistent across studies [25-27].

Developmental and Reproductive Toxicology (DART)

The DART field aims to protect human reproduction and development which is a continuum as visualised in figure 1 and can be divided into the branches of reproduction and development. Reproductive toxicology considers the influence of external exposures on the development of a healthy oocyte or sperm cell and the capacity of fertilisation throughout generations. Developmental toxicology considers a healthy embryo and foetal development and perturbations thereof from the zygote until birth, during lactation and also during the F1 and F2 generations. In risk assessment of birth defects, the health risk of chemicals is predicted by assessing the probability on the development of birth defects by identifying the hazard a chemical can cause in case the mother is exposed during pregnancy.

DART regulatory testing frameworks

The European Union amended its regulations to improve the protection of human health and the environment from chemical risks in the legislation of 'Registration, Evaluation, Authorisation and Restriction of Chemicals' (REACH), which came into force in 2007 [5, 28]. REACH demands additional safety testing data for all chemicals produced or marketed amounting over one tonne per year [7]. This legislation is implemented by the European Chemical Agency (ECHA) which is an agency of the

European Union. Another European agency is the European Food Safety Authority (EFSA) guiding EU legislation for pesticides and food safety.

The current regulatory frameworks for developmental safety testing for toxicity are described by the Organisation for Economic Co-operation and Development (OECD) and the International Council for Harmonisation (ICH). The OECD guidelines encompass environmental and industrial chemicals whereas the ICH embodies guidelines for pharmaceuticals. An overview of OECD test guidelines for DART studies is given in figure 2 [29]. These test guidelines include: one and two generation reproductive toxicity studies: OECD 415 [30] OECD 416 [31], DART Screening Tests OECD 421 [32] and OECD 422 [33], Developmental Neurotoxicity (DNT) studies OECD 426 [34], and lastly the OECD 414 which is a Prenatal Developmental Toxicity Study [35]. The ICH guideline ICH S5(R3) describes testing for detection of DART for human pharmaceuticals [36]. Under the auspices of classification, labelling and packaging (CLP) chemicals identified as inducing DART effects can be classified according to the categories R1A (known human DART toxicant based largely on human evidence), R1B (presumed human DART toxicant based mainly on animal evidence) or R2 (suspected human DART toxicant based only on animal evidence) of the Regulation (EC) No 1272/2008 on the of substances and mixtures (CLP Regulation) [37].

Regulatory safety assessment is thus still based on animal studies, but advances are being made in relation to the 3R-paradigm. For instance, the Extended One-Generation Reproductive Toxicity Study (EOGRTS) (OECD TG 443) was implemented in 2018, which can replace the two-generation studies (e.g. OED TG 416) and reduces the number of animals [38]. Also, questions arise in the need for a second species in the developmental toxicity studies which is currently demanded to correct for interspecies differences [39]. The use of a second species for developmental toxicity assessments showed a reproducibility error because of the scatter in the correlation plots when comparing rat and rabbit developmental toxicity studies (OECD TG 414) N(L)OAELs [40]. These questions about the second species were taken into consideration in the EOGRTS test guideline will help in the reduction in animal testing in DART. Despite this great effort towards the 3R paradigm by animal test reduction, replacement will need to take place in order to downsize the vast amount of animal testing [41].

Table 1: Summary of test guidelines for DART-testing (obtained from: [29])

Test	Exposure period	Endpoints in parental and/or offspring	Guideline(s)
Generation studies	Continuously over one, two or several generations	Growth, development and viability. Pregnancy length and birth outcome Histopathology of sex organs and target organs Oestrus cyclicity and sperm quality in TG 416	TG 415: One-generation study TG 416: Two-generation study
Prenatal Developmental Toxicity Study (Teratology study)	From implantation to the day before birth	Litter composition (e.g. resorptions, live, dead foetuses) Embryonic development Foetal growth Morphological variations and malformations	TG 414: Prenatal Developmental Study
Developmental Neurotoxicity study	During pregnancy and lactation	Pregnancy length and birth outcome Physical and functional maturation Behavioural changes due to CNS and PNS effects Brain weights and neuropathology	TG 426: Developmental Neurotoxicity Study
Reproduction/ Developmental toxicity screening test	From 2 weeks prior to mating until day 4 post-natal	Fertility Pregnancy length and birth outcome Histopathology of sex organs and target organs (and brain in TG 422) Foetal and pup growth and survival until day 3	TG 421 and 422

Alternatives to animals for developmental toxicity testing

Alternatives to animals in developmental toxicity testing investigate hazards by testing chemicals on biological systems outside of the organism and *in vitro* (latin: 'in glass'). Since the complete and intact organism (*in vivo*) is not assessed, *in vitro* models are relatively simplistic and have limitations such as a reduced number of endpoints or available mechanisms [11]. Additionally, the chemical distribution in

the body and chemical breakdown (metabolism and excretion) can't be assessed *in vitro* and culture conditions may influence the test readout [11]. These limitations including reproducibility, sensitivity, and transferability highlight the need to validate these *in vitro* systems to achieve regulatory acceptance, while maintaining or even improving the ability to support safety assessment requirements. It is not anticipated that a single *in vitro* assay will replace 1:1 the *in vivo* models. It is more likely that a collection of several assays will be needed, where each one might answer a specific question and together an assessment of developmental and reproductive toxicity can be made. Encouragingly, multiple promising advances in test systems have been made for alternative testing for developmental toxicants: zebrafish embryotoxicity test (ZET) [42], the frog embryo teratogenesis assay (FETAX) [43], *in vitro* rat micromass (MM) test, the rat whole-embryo culture assay (WEC), and the cardiac mouse embryonic stem cell test (mESTc) [44, 45]. The ZET, FETAX, MM, and WEC are alternative test systems that benefit from studying the complete embryo, whereas the mESTc benefits from being almost completely animal free [4].

Embryonic stem cells as an alternative model

The mESTc makes use of cultured embryonic stem cells which are originally derived from the inner cell mass from mouse blastocysts (Fig. 1) [46]. These stem cells have the potential to become every cell type present in developing mammalian the body. The development to the various cell types starts with the formation of the germ layers during gastrulation: the ectoderm, endoderm, and mesoderm [47, 48]. The ectoderm gives rise to the epidermis (skin) and neuronal tissues, the endoderm to the gastrointestinal tract, the lungs, urinary tract and pancreas, and the mesoderm to the blood, skeleton, cartilage, kidneys, connective tissue, notochord and striated muscles [49].

The classical mESTc method is one of the most commonly studied alternative test methods for developmental toxicity and a protocol has previously been validated by ECVAM (European Centre for the Validation of Alternative Methods) in 2004 [50]. This test uses the hanging-drop method in order to form aggregates on study day zero and consequently form embryoid bodies (EBs) on day three. The EBs are then plated out using tissue culture techniques to adhere, grow and differentiate to give rise to cardiac cells on day five [51]. These cardiac cells are scored for beating

using the microscope on day ten [51]. The effects of chemicals on differentiation of beating cardiomyocytes are studied in the differentiation window between day three and day ten (fig. 2).

However, this readout of microscopic scoring is limited since it precludes the use of the assay as a high-throughput screening (HTS) tool [52, 53]. The scoring is performed by human-eye and is a time-consuming process that is rather subjective. Additionally, the differentiation process to beating cardiomyocytes takes ten days. Therefore, a shorter test duration and more objective quantification of the test readout would open up the possibility for potential use as an HTS tool. To shorten the test duration demands shifting to other readout parameters than scoring of beating cardiomyocytes, which also gives the opportunity to improve the quantification of the readout. This increase in throughput would increase the utility of the mESTc as a hazard assessment tool for developmental toxicity testing. Additionally, a quantitative readout would also open up the possibility for potential use as a new approach method (NAM) when interested in cellular effect levels in interplay with a collection several assays for regulatory decision making.

Ever since this test method was validated in 2004, alternative readout parameters were proposed to shorten the test duration and improve quantification based on: luciferase assays measuring gene expression, embryoid body (EB) size measurement, and amino acid-based approaches. Luciferase assays were developed to quantify the assay readout for *Hand1* and *Cmya1*, which both play a role in cardiomyocyte development [54, 55]. Although these assays could replace the readout of beating cardiomyocytes scoring since the expressed luciferase is better quantifiable and gives mechanistic insight of differentiated cells, the specific mechanistic insight of the differentiation process is limited. Insight into the mechanism of toxicity would contribute to the vision of toxicity testing in the 21st century to use a new toxicity-testing system relying on understanding toxicity mechanisms [14, 16, 56]. Slightly more mechanistic insight in the differentiation process is addressed in reporter assays related to monitor embryogenesis pathway activities such as pathways for Wnt/ β -catenin, TGF- β , Notch, Hedgehog, tyrosine kinase receptor/Ras, or cytokine receptors. An example is the ReProGlo assay that uses a Wnt luciferase reporter as an indicator for embryotoxicity after toxicant exposure [57, 58]. However, in this case only one gene is assessed and not all chemicals interfere with the same pathways and therefore the ReProGlo assay is prone to high false-negative rates. Another way to quantify the mESTc's readout, is by EB size measurements that

look at the correlation of beating cardiomyocyte formation and the EB size [59-61]. However, EB size measurement is likely to be impacted by the effect of reduced viability that is causing the EBs to be smaller which is therefore not specific to differentiation. Other stem cell assays are using an amino acid based approach to quantify the test readout. For instance the commercially available method from Stemina (www.stemina.com) uses human stem cells and determines the ornithine/cysteine (O/C) ratio as readout measured after a three-day compound exposure in a concentration-response manner [62, 63]. A reduction in the O/C ratio is indicative of developmental toxicity. This method identified potential developmental toxicants with 77% accuracy, with 100% in specificity but only a low overall sensitivity of 57% [62].

In order to give more insight into the mechanism of toxicity, evaluating the expression levels of a selection of multiple genes that are commonly regulated by developmental toxicants, defined as gene transcript biomarkers, could be of added value to the mESTc. For example, assessment of 12 developmentally regulated genes and 65 chemicals reduced the assay time from 10 to 4 days, and had a similar degree of accuracy (72%–83%) as the original mESTc [64].

Improving the sensitivity of biomarkers to compounds could further improve the accuracy and therefore the predictability of the mESTc. Therefore, a robust test system with optimal culture conditions would be of added value to limit variations. Culture conditions that may affect the robustness are e.g. O_2 or medium constituents. The sensitivity to compounds in relation to O_2 culture conditions has only slightly been studied in stem cell differentiation [65]. However, the effects of low O_2 levels on stem cell maintenance are known to be beneficial for pluripotency, cell survival and colony expansion [66-68].

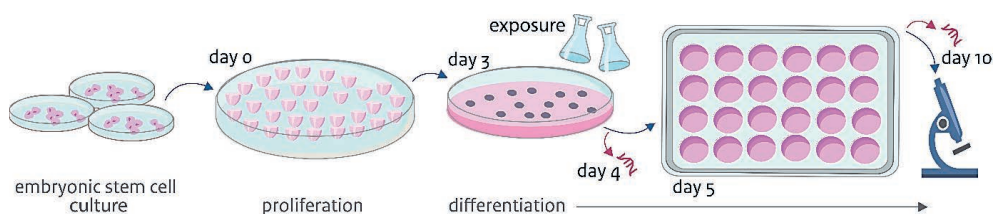


Figure 2: Overview of the mESTc protocol

Mechanistic understanding and prediction of developmental toxicity

Ever since the development of the first cardiomyocyte differentiation-based EST (mESTc) method, the alternative differentiation routes of neural (mESTn) and osteogenic (mESTo) differentiation have been further developed and investigated for use in the DART field [69-73]. These alternative differentiation routes have had added value to the applicability of EST methods since previously misclassified chemicals by the mESTc were detected by employing these additional differentiation routes. For example, the dioxin TCDD was detected using the mESTo but not by the mESTc [74]. These additional variations on the original mESTc protocol thus add to the predictivity of EST test systems in general.

Knowledge of the biological specificity and sensitivity ranges within a test system can also add to the predictivity of the test and can add to a mechanism based understanding of observed embryotoxicity [75, 76]. The stem cells within the mESTc differentiate into cells of all three germ layers, from which all tissues are formed [77]. The mESTc is using cardiomyocyte contraction as readout, but not all stem cells differentiate into cardiomyocytes in the mESTc and therefore also other differentiation routes are present [78, 79]. In fact, other cell types are necessary for the formation of cardiomyocytes, exemplified by the homogenous mesenchymal stem cells that can't form beating EBs [80, 81]. Different sub-populations in the same test might provide improved sensitivity because of different sub-type specific outcomes when assessing gene based biomarkers. In addition to characterising differentiation routes within the mESTc, also important pathways in embryo development may add to the predictivity of the test. The all-trans retinoic acid pathway is active within the mESTc and can be a useful readout system as it is important in multiple processes including patterning of the body plan within the developing embryo [82, 83]. These differentiation routes and relevant pathways within the mESTc represent a part of the available biology defined as the biological domain of the assay.

The applicability domain of this assay is defined as the range of chemical structures that can be correctly scored within the ESTc as their structure-activity relationship (SAR) is revealed within the ESTc [84]. Regulations by chemicals on a mechanistic level using omics technologies (e.g. proteomics, metabolomics, transcriptomics) are studied in the field of toxicogenomics and transcriptomics assesses the

expression of RNA transcribed from DNA [85-87]. Monitoring gene transcript biomarkers could further improve the chemical predictivity of this test. Examples of chemicals that were correctly scored as developmental toxicants using the mESTc are the azole class of fungicides and the phthalate family of polyvinylchloride (PVC) plasticisers [88, 89]. These two chemical classes were successfully discriminated from each other within the mESTc based on differential regulation of gene expression [90]. Already over 50 studies have been published on molecular based readouts by transcriptomics within the mESTc, as reviewed by *van Dartel et al.* [91]. The accuracy of the mESTc using transcriptomics, depends on the level of false positives and false negatives in relation to the real situation. A low accuracy may be due to the fact that the chemical-induced mechanism of action is not represented by the biological domain of the test causing false negative results [50, 92, 93]. False positive results may be indicated in case a mechanism is triggered *in vitro* that is not relevant *in vivo* or in case the concentration of effect is physiologically not realistic [92].

Objectives and outline of this thesis

The aim of this thesis was to explore the biological domain of the mESTc and to discriminate between compounds of the same chemical class by selecting biomarker profiles beyond cardiac differentiation. This aim was divided into four objectives:

1. To expand our knowledge on the biological domain of the mESTc.
2. To make progress towards setting a biomarker profile related to mechanisms important in developmental toxicity.
3. To explore whether this biomarker profile can distinguish between similar chemical structures within the same chemical class.
4. To enhance the sensitivity of the assay for detecting biomarkers.

These objectives were assessed according to two approaches for selecting gene transcript biomarkers. Approach 1 makes use of a hypothesis-driven targeted approach of biomarker selection based on existing knowledge of mechanisms involved in embryo development. Approach 2 makes use of a hypothesis-generating data driven approach of biomarker selection based on genome-wide expression screening.

Approach 1 for selecting biomarkers – targeted biomarker selection

The stem cells in the cardiac Embryonic Stem cell Test (ESTc) differentiate into a heterogeneous cell population with cardiomyocytes and non-cardiomyocyte cells including neural crest (NC) cells. *In vivo*, NC cells contribute critically to heart formation. Furthermore, the all-trans retinoic acid (ATRA) pathway contributes to normal heart development and to defining the morphogenetic route of NC cell migration and differentiation. The use of molecular biomarkers from different mechanistic pathways can refine quantitative embryotoxicity assessment. Gene expression levels representing different signalling pathways that could relate to beating cardiomyocyte formation were analysed at different time-points in **chapter 2**. Immunocytochemistry and RT-qPCR were performed to discover the added value of NC cell differentiation as additional readout to cardiomyocyte differentiation in the ESTc at multiple time-points. Markers related to pluripotency, cardiomyocytes, ATRA balance, and NC cells were examined for regulation by valproic acid and two structural analogues 2-ethylhexanoic acid (EHA) and 2-ethylhexanol (EHOL).

Molecular markers for NC cells were investigated in **chapter 3** to explore if their differential expression improved discrimination between three structurally related organophosphates (OP): chlorpyrifos (CPF), malathion (MLT), and triphenyl phosphate (TPP). Molecular markers as the readout of the ESTc were assessed to improve the objective quantification of the assay results. To decrease the test duration, gene transcript biomarkers were measured on study day 4 instead of the traditional cardiomyocyte beating assessment at day 10. Cell proliferation was also assessed by measurements of embryoid body (EB) size and total protein quantification (day 7). Gene expression profiling and immunocytochemistry were performed using markers for pluripotency, proliferation and cardiomyocyte and NC differentiation.

In **chapter 4**, the effects of representative compounds from two chemical classes were explored within the mESTc: morpholines (tridemorph; fenpropimorph) and piperidines (fenpropidin; spiroxamine). These compounds can cause embryotoxicity in rat such as cleft palate. This malformation can be linked to interference with retinoic acid balance, neural crest (NC) cell migration, and cholesterol biosynthesis. Potential effects on neural differentiation within the mESTc were explored in relation to these compounds. Gene transcript expression of related biomarkers was measured at low and high concentrations on differentiation day 4 (DD4) and DD10.

Approach 2 for selecting biomarkers – genome-wide biomarker screening

In **chapter 5**, next generation sequencing (NGS) was applied as a hypothesis-generating data driven approach to gain more insight into the biological domain of the ESTc and for biomarker selection. In this chapter we again tested the morpholines and piperidines with flusilazole as a positive control compound, in order to investigate whether the explored biological domain was sensitive to these compounds.

Understanding the biomarker sensitivity of the assay

The importance of oxygen tension in *in vitro* cultures and its effect on embryonic stem cell (ESC) differentiation has been widely acknowledged. Research has mainly focussed on ESC maintenance or on single lines of differentiation and only few studies have examined the potential relationship between oxygen tension during these two phases of the study design. In **chapter 6** we investigated the influence of atmospheric (20%) versus physiologic (5%) oxygen tension in ESC cultures and their impact on the differentiation within the cardiac and neural embryonic stem cell tests (mESTc, mESTn) including gene transcript regulations. Oxygen tension was set at 5% or 20% and cells were kept in these conditions from starting up cell culture until use for differentiation. Differentiation was either performed in the same or in the alternative oxygen tension compared to ESC culture creating four different experimental conditions.

In **chapter 7**, the potential impact of oxygen tension on chemical sensitivity was investigated by carrying out the mESTc under 20% O₂, using embryonic stem cells (ESC) cultured under either 20% O₂ or 5% O₂. Valproic acid and flusilazole were tested for interference with ESC viability, development of beating cardiomyocytes, and gene expression regulation was monitored on differentiation day 4 and day 10.

Chapter 8 provides an inventory of achievements in mesodermal and endodermal differentiation from embryonic stem cells *in vitro*, with a view to possibilities for their use in non-animal test systems in developmental toxicology. This includes murine and human stem cell differentiation models, and also gains information from the field of stem cell use in regenerative medicine. Endodermal stem cell derivatives produced *in vitro* include hepatocytes, pancreatic cells, lung epithelium, and intestinal epithelium, and mesodermal derivatives include besides cardiac muscle, osteogenic, vascular and hemopoietic cells. This inventory provides an overview of studies on the different cell types together with cell type-specific biomarkers and culture conditions that stimulate their differentiation from embryonic stem cells.

References

1. Lenz, W., *A short history of thalidomide embryopathy*. *Teratology*, 1988. **38**(3): p. 203-15.
2. Harada, M., *Minamata disease: methylmercury poisoning in Japan caused by environmental pollution*. *Crit Rev Toxicol*, 1995. **25**(1): p. 1-24.
3. Russell, W.M.S., Burch, R.L., Hume, C.W., *The principles of human experimental technique*. Methuen London, 1959.
4. Piersma, A.H., *Alternative methods for developmental toxicity testing*. *Basic Clin Pharmacol Toxicol*, 2006. **98**(5): p. 427-31.
5. van der Jagt, K., Munn, S., Torslov, J., de Bruijn, J., *Alternative Approaches Can Reduce the Use of Test Animals under REACH*. 2004, EC Joint Research Centre.
6. Rovida, C. and T. Hartung, *Re-evaluation of animal numbers and costs for in vivo tests to accomplish REACH legislation requirements for chemicals - a report by the transatlantic think tank for toxicology (t(4))*. *Altex*, 2009. **26**(3): p. 187-208.
7. *Regulation (EC) No 1907/2006 of the European Parliament and of the Council of 18 December 2006 concerning the Registration, Evaluation, Authorisation and Restriction of Chemicals (REACH), establishing a European Chemicals Agency, amending Directive 1999/45/EC and repealing Council Regulation (EEC) No 793/93 and Commission Regulation (EC) No 1488/94 as well as Council Directive 76/769/EEC and Commission Directives 91/155/EEC, 93/67/EEC, 93/105/EC and 2000/21/EC*.
8. Olson, H., et al., *Concordance of the toxicity of pharmaceuticals in humans and in animals*. *Regulatory Toxicology and Pharmacology*, 2000. **32**(1): p. 56-67.
9. Poggesi, I., *Predicting human pharmacokinetics from preclinical data*. *Current opinion in drug discovery & development*, 2004. **7**(1): p. 100-111.
10. Davies, B. and T. Morris, *Physiological parameters in laboratory animals and humans*. *Pharmaceutical research*, 1993. **10**(7): p. 1093-1095.
11. Kugler, J., et al., *Embryonic stem cells and the next generation of developmental toxicity testing*. *Expert Opin Drug Metab Toxicol*, 2017. **13**(8): p. 833-841.
12. (NCad), N.C.a.d., *Transitie naar proefdiervrij onderzoek*. 2016.
13. (USEPA), U.S.E.P.A., *Memo Directive to Prioritize Efforts to Reduce Animal Testing*. 2019.
14. Gibb, S., *Toxicity testing in the 21st century: A vision and a strategy*. *Reproductive Toxicology*, 2008. **25**(1): p. 136-138.
15. Andersen, M.E., et al., *Can case study approaches speed implementation of the NRC report: "toxicity testing in the 21st century: a vision and a strategy?"*. *Altex*, 2011. **28**(3): p. 175-82.
16. Rovida, C., et al., *Toxicity testing in the 21st century beyond environmental chemicals*. *Altex*, 2015. **32**(3): p. 171-81.
17. Buesen, R., et al., *Applying 'omics technologies in chemicals risk assessment: Report of an ECETOC workshop*. *Regul Toxicol Pharmacol*, 2017. **91 Suppl 1**(Suppl 1): p. S3-s13.
18. Craig, E., et al., *Reducing the need for animal testing while increasing efficiency in a pesticide regulatory setting: Lessons from the EPA Office of Pesticide Programs' Hazard and Science Policy Council*. *Regul Toxicol Pharmacol*, 2019. **108**: p. 104481.
19. Mahony, C., et al., *New ideas for non-animal approaches to predict repeated-dose systemic toxicity: Report from an EPAA Blue Sky Workshop*. *Regul Toxicol Pharmacol*, 2020. **114**: p. 104668.

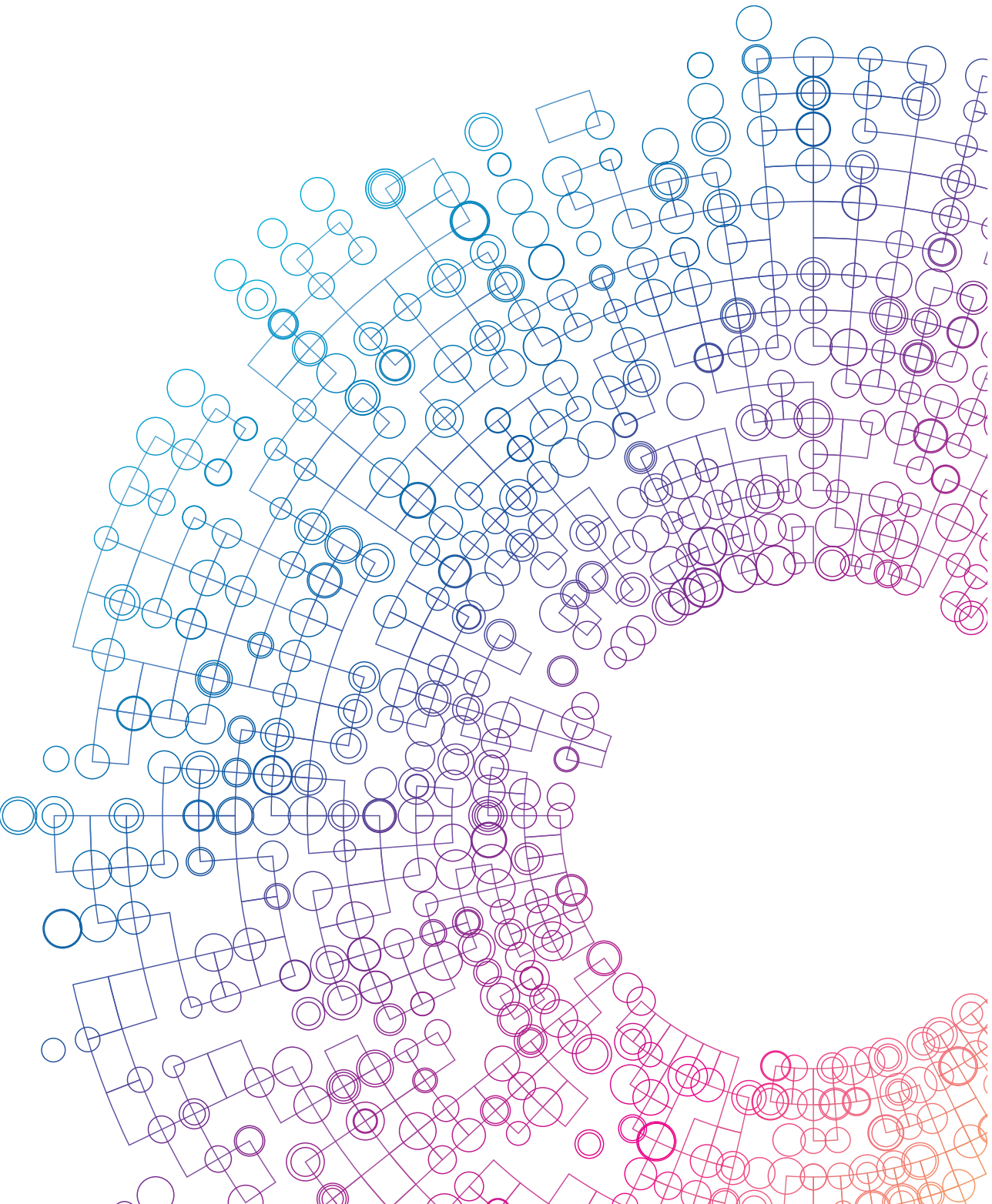
20. Carlson, B.M., *Human Embryology and Developmental biology E-book*. 2018: Elsevier Health Sciences.
21. Weinhold, B., *Environmental Factors in Birth Defects: What We Need to Know*. Environmental Health Perspectives, 2009. **117**(10): p. A440-A447.
22. Liu, J., *The "life code": A theory that unifies the human life cycle and the origin of human tumors*. Seminars in Cancer Biology, 2020. **60**: p. 380-397.
23. Klaassen, C.D., *Casarett and Doull's toxicology: the basic science of poisons*. Vol. 1236. 2013: McGraw-Hill New York.
24. Dorne, J.L.C.M. and A.G. Renwick, *The Refinement of Uncertainty/Safety Factors in Risk Assessment by the Incorporation of Data on Toxicokinetic Variability in Humans*. Toxicological Sciences, 2005. **86**(1): p. 20-26.
25. Slob, W., *Dose-response modeling of continuous endpoints*. Toxicol Sci, 2002. **66**(2): p. 298-312.
26. Slob, W., et al., *A Statistical Evaluation of Toxicity Study Designs for the Estimation of the Benchmark Dose in Continuous Endpoints*. Toxicological Sciences, 2004. **84**(1): p. 167-185.
27. Slob, W. and R.W. Setzer, *Shape and steepness of toxicological dose-response relationships of continuous endpoints*. Critical Reviews in Toxicology, 2014. **44**(3): p. 270-297.
28. Taylor, K., *Ten years of REACH - An animal protection perspective*. Altern Lab Anim, 2018. **46**(6): p. 347-373.
29. OECD, *Guidance Document on Mammalian Reproductive Toxicity Testing and Assessment*. 2008.
30. OECD, *Test No. 415: One-Generation Reproduction Toxicity Study*. 1983.
31. OECD, *Test No. 416: Two-Generation Reproduction Toxicity*. 2001.
32. OECD, *Test No. 421: Reproduction/Developmental Toxicity Screening Test*. 2016.
33. OECD, *Test No. 422: Combined Repeated Dose Toxicity Study with the Reproduction/Developmental Toxicity Screening Test*. 2015.
34. OECD, *Test No. 426: Developmental Neurotoxicity Study*. 2007.
35. OECD, *Test No. 414: Prenatal Developmental Toxicity Study*. 2018.
36. ICH, *Detection of reproductive and developmental toxicity for human pharmaceuticals S5(R3)*. 2020.
37. *Regulation (EC) No 1272/2008 of the European Parliament and of the Council of 16 December 2008 on classification, labelling and packaging of substances and mixtures, amending and repealing Directives 67/548/EEC and 1999/45/EC, and amending Regulation (EC) No 1907/2006 (Text with EEA relevance)Text with EEA relevance*.
38. OECD, *Test No. 443: Extended One-Generation Reproductive Toxicity Study*. 2018.
39. Moore, N.P., et al., *Guidance on the selection of cohorts for the extended one-generation reproduction toxicity study (OECD test guideline 443)*. Regul Toxicol Pharmacol, 2016. **80**: p. 32-40.
40. Braakhuis, H.M., et al., *Testing developmental toxicity in a second species: are the differences due to species or replication error?* Regul Toxicol Pharmacol, 2019. **107**: p. 104410.
41. Beekhuijzen, M., *The era of 3Rs implementation in developmental and reproductive toxicity (DART) testing: Current overview and future perspectives*. Reproductive Toxicology, 2017. **72**: p. 86-96.

42. Chapin, R., et al., *State of the art in developmental toxicity screening methods and a way forward: a meeting report addressing embryonic stem cells, whole embryo culture, and zebrafish*. Birth Defects Research Part B: Developmental and Reproductive Toxicology, 2008. **83**(4): p. 446-456.
43. Bantle, J.A., D.J. Fort, and B.L. James. *Identification of developmental toxicants using the Frog Embryo Teratogenesis Assay-Xenopus (FETAX)*. 1989. Dordrecht: Springer Netherlands.
44. Genschow, E., et al., *The ECVAM International Validation Study on In Vitro Embryotoxicity Tests: Results of the Definitive Phase and Evaluation of Prediction Models*. Alternatives to Laboratory Animals, 2002. **30**(2): p. 151-176.
45. McNERNEY, M., et al., *Concordance of 3 alternative teratogenicity assays with results from corresponding in vivo embryo-fetal development studies: Final report from the International Consortium for Innovation and Quality in Pharmaceutical Development (IQ) DruSafe working group 2*. Regulatory Toxicology and Pharmacology, 2021. **124**: p. 104984.
46. Kim, P.T. and C.J. Ong, *Differentiation of definitive endoderm from mouse embryonic stem cells*. Results Probl Cell Differ, 2012. **55**: p. 303-19.
47. Chan, M.M., et al., *Molecular recording of mammalian embryogenesis*. Nature, 2019. **570**(7759): p. 77-82.
48. Pijuan-Sala, B., et al., *A single-cell molecular map of mouse gastrulation and early organogenesis*. Nature, 2019. **566**(7745): p. 490-495.
49. Marikawa, Y. and V.B. Alarcón, *Establishment of trophectoderm and inner cell mass lineages in the mouse embryo*. Mol Reprod Dev, 2009. **76**(11): p. 1019-32.
50. Genschow, E., et al., *Validation of the embryonic stem cell test in the international ECVAM validation study on three in vitro embryotoxicity tests*. Altern Lab Anim, 2004. **32**(3): p. 209-44.
51. Spielmann, H., et al., *The Embryonic Stem Cell Test, an In Vitro Embryotoxicity Test Using Two Permanent Mouse Cell Lines: 3T3 Fibroblasts and Embryonic Stem Cells*. In Vitro Toxicology, 1997. **10**: p. 119-127.
52. Kameoka, S., et al., *A high-throughput screen for teratogens using human pluripotent stem cells*. Toxicol Sci, 2014. **137**(1): p. 76-90.
53. Kobayashi, K., et al., *Editor's Highlight: Development of Novel Neural Embryonic Stem Cell Tests for High-Throughput Screening of Embryotoxic Chemicals*. Toxicol Sci, 2017. **159**(1): p. 238-250.
54. Le Coz, F., et al., *Hand1-Luc embryonic stem cell test (Hand1-Luc EST): a novel rapid and highly reproducible in vitro test for embryotoxicity by measuring cytotoxicity and differentiation toxicity using engineered mouse ES cells*. J Toxicol Sci, 2015. **40**(2): p. 251-61.
55. Suzuki, N., et al., *Evaluation of novel high-throughput embryonic stem cell tests with new molecular markers for screening embryotoxic chemicals in vitro*. Toxicol Sci, 2011. **124**(2): p. 460-71.
56. Anderson, J.P. and K.H. Domsch, *Influence of selected pesticides on the microbial degradation of ¹⁴C-triallate and ¹⁴C-diallate in soil*. Arch Environ Contam Toxicol, 1980. **9**(1): p. 115-23.
57. Uibel, F., et al., *ReProGlo: A new stem cell-based reporter assay aimed to predict embryotoxic potential of drugs and chemicals*. Reproductive Toxicology, 2010. **30**(1): p. 103-112.

58. Uibel, F. and M. Schwarz, *Prediction of embryotoxic potential using the ReProGlo stem cell-based Wnt reporter assay*. Reproductive Toxicology, 2015. **55**: p. 30-49.
59. Flamier, A., S. Singh, and T.P. Rasmussen, *A standardized human embryoid body platform for the detection and analysis of teratogens*. PLOS ONE, 2017. **12**(2): p. e0171101.
60. Kang, H.Y., et al., *Advanced developmental toxicity test method based on embryoid body's area*. Reproductive Toxicology, 2017. **72**: p. 74-85.
61. Warkus, E.L.L. and Y. Marikawa, *Exposure-Based Validation of an In Vitro Gastrulation Model for Developmental Toxicity Assays*. Toxicological Sciences, 2017. **157**(1): p. 235-245.
62. Palmer, J.A., et al., *Establishment and assessment of a new human embryonic stem cell-based biomarker assay for developmental toxicity screening*. Birth Defects Res B Dev Reprod Toxicol, 2013. **98**(4): p. 343-63.
63. Palmer, J.A., et al., *A human induced pluripotent stem cell-based in vitro assay predicts developmental toxicity through a retinoic acid receptor-mediated pathway for a series of related retinoid analogues*. Reproductive Toxicology, 2017. **73**: p. 350-361.
64. Panzica-Kelly, J.M., et al., *Establishment of a molecular embryonic stem cell developmental toxicity assay*. Toxicol Sci, 2013. **131**(2): p. 447-57.
65. Koutsouraki, E., S. Pells, and P.A. De Sousa, *Sufficiency of hypoxia-inducible 2-oxoglutarate dioxygenases to block chemical oxidative stress-induced differentiation of human embryonic stem cells*. Stem Cell Res, 2019. **34**: p. 101358.
66. Ezashi, T., P. Das, and R.M. Roberts, *Low O2 tensions and the prevention of differentiation of hES cells*. Proc Natl Acad Sci U S A, 2005. **102**(13): p. 4783-8.
67. Forristal, C.E., et al., *Hypoxia inducible factors regulate pluripotency and proliferation in human embryonic stem cells cultured at reduced oxygen tensions*. Reproduction, 2010. **139**(1): p. 85-97.
68. Gustafsson, M.V., et al., *Hypoxia requires notch signaling to maintain the undifferentiated cell state*. Dev Cell, 2005. **9**(5): p. 617-28.
69. Bibel, M., et al., *Differentiation of mouse embryonic stem cells into a defined neuronal lineage*. Nat Neurosci, 2004. **7**(9): p. 1003-9.
70. Okabe, S., et al., *Development of neuronal precursor cells and functional postmitotic neurons from embryonic stem cells in vitro*. Mechanisms of Development, 1996. **59**(1): p. 89-102.
71. zur Nieden, N.I. and L. Baumgartner, *Assessing developmental osteotoxicity of chlorides in the embryonic stem cell test*. Reprod Toxicol, 2010. **30**(2): p. 277-83.
72. de Jong, E., L. van Beek, and A.H. Piersma, *Osteoblast differentiation of murine embryonic stem cells as a model to study the embryotoxic effect of compounds*. Toxicol In Vitro, 2012. **26**(6): p. 970-8.
73. Fritsche, E., et al., *Current Availability of Stem Cell-Based In Vitro Methods for Developmental Neurotoxicity (DNT) Testing*. Toxicological Sciences, 2018. **165**(1): p. 21-30.
74. de Jong, E., L. van Beek, and A.H. Piersma, *Comparison of osteoblast and cardiomyocyte differentiation in the embryonic stem cell test for predicting embryotoxicity in vivo*. Reprod Toxicol, 2014. **48**: p. 62-71.
75. Merrick, B.A., *Next generation sequencing data for use in risk assessment*. Curr Opin Toxicol, 2019. **18**: p. 18-26.
76. Verheijen, M., et al., *Towards the development of an omics data analysis framework*. Regul Toxicol Pharmacol, 2020. **112**: p. 104621.

77. Machado, R., A. Sachinidis, and M.E. Futschik, *Detection of Novel Potential Regulators of Stem Cell Differentiation and Cardiogenesis through Combined Genome-Wide Profiling of Protein-Coding Transcripts and microRNAs*. *Cells*, 2021. **10**(9).
78. Yang, Y., et al., *Endogenous IGF Signaling Directs Heterogeneous Mesoderm Differentiation in Human Embryonic Stem Cells*. *Cell Rep*, 2019. **29**(11): p. 3374-3384.e5.
79. Seiler, A., et al., *Improvement of an in vitro stem cell assay for developmental toxicity: the use of molecular endpoints in the embryonic stem cell test*. *Reprod Toxicol*, 2004. **18**(2): p. 231-40.
80. Miskon, A., et al., *A suspension induction for myocardial differentiation of rat mesenchymal stem cells on various extracellular matrix proteins*. *Tissue Eng Part C Methods*, 2010. **16**(5): p. 979-87.
81. Tong, S., et al., *Development of functional If channels in mMSCs after transfection with mHcN4: effects on cell morphology and mechanical activity in vitro*. *Cardiology*, 2009. **112**(2): p. 114-21.
82. Tonk, E.C., J.L. Pennings, and A.H. Piersma, *An adverse outcome pathway framework for neural tube and axial defects mediated by modulation of retinoic acid homeostasis*. *Reprod Toxicol*, 2015. **55**: p. 104-13.
83. Tonk, E.C., et al., *Valproic acid-induced gene expression responses in rat whole embryo culture and comparison across in vitro developmental and non-developmental models*. *Reprod Toxicol*, 2013. **41**: p. 57-66.
84. Hessel, E.V., Y.C. Staal, and A.H. Piersma, *Design and validation of an ontology-driven animal-free testing strategy for developmental neurotoxicity testing*. *Toxicology and applied pharmacology*, 2018. **354**: p. 136-152.
85. Nuwaysir, E.F., et al., *Microarrays and toxicology: the advent of toxicogenomics*. *Molecular Carcinogenesis: Published in cooperation with the University of Texas MD Anderson Cancer Center*, 1999. **24**(3): p. 153-159.
86. Robinson, J.F. and A.H. Piersma, *Toxicogenomic approaches in developmental toxicology testing*. *Teratogenicity Testing*, 2013: p. 451-473.
87. Wilson, V.S., et al., *Utilizing toxicogenomic data to understand chemical mechanism of action in risk assessment*. *Toxicology and applied pharmacology*, 2013. **271**(3): p. 299-308.
88. Dimopoulou, M., et al., *A comparison of the embryonic stem cell test and whole embryo culture assay combined with the BeWo placental passage model for predicting the embryotoxicity of azoles*. *Toxicol Lett*, 2018. **286**: p. 10-21.
89. Schulpen, S.H., et al., *Dose response analysis of monophthalates in the murine embryonic stem cell test assessed by cardiomyocyte differentiation and gene expression*. *Reprod Toxicol*, 2013. **35**: p. 81-8.
90. van Dartel, D.A., et al., *Discriminating classes of developmental toxicants using gene expression profiling in the embryonic stem cell test*. *Toxicol Lett*, 2011. **201**(2): p. 143-51.
91. van Dartel, D.A. and A.H. Piersma, *The embryonic stem cell test combined with toxicogenomics as an alternative testing model for the assessment of developmental toxicity*. *Reprod Toxicol*, 2011. **32**(2): p. 235-44.
92. Piersma, A.H., et al., *A critical appraisal of the process of regulatory implementation of novel in vivo and in vitro methods for chemical hazard and risk assessment*. *Critical reviews in toxicology*, 2014. **44**(10): p. 876-894.

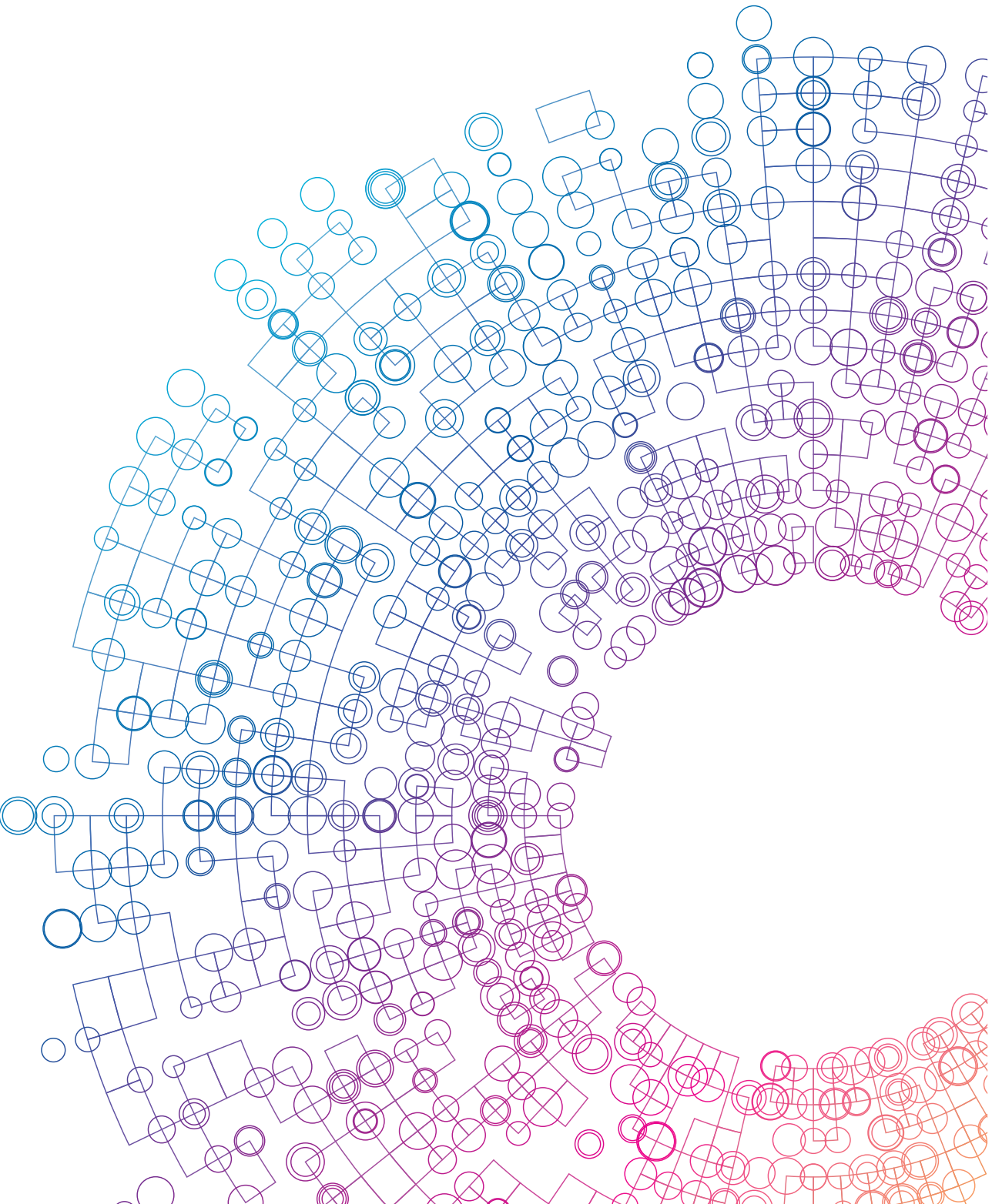
93. Marx-Stoelting, P., et al., *A review of the implementation of the embryonic stem cell test (EST). The report and recommendations of an ECVAM/ReProTect Workshop*. *Altern Lab Anim*, 2009. **37**(3): p. 313-28.



SECTION

A hypothesis-driven literature
based approach for biomarker
selection





2

CHAPTER

Neural crest related gene
transcript regulation by
valproic acid analogues in the
cardiac embryonic stem cell
test

R.H. Mennen, J.L.A. Pennings, A.H. Piersma

Reproductive Toxicology, 2019 Dec; 90: 44-52

DOI: 10.1016/j.reprotox.2019.08.013

Abstract

In vivo, neural crest (NC) cells contribute critically to heart formation. The embryonic stem cells in the cardiac Embryonic Stem cell Test (ESTc) differentiate into a heterogeneous cell population including non-cardiomyocyte cells. The use of molecular biomarkers from different mechanistic pathways can refine quantitative embryotoxicity assessment. Gene expression levels representing different signalling pathways that could relate to beating cardiomyocyte formation were analysed at different time-points. Immunocytochemistry showed NC cells were present in the ESTc and RT-qPCR showed upregulation of NC related gene expression levels in a time-dependent manner. NC related genes were sensitive to VPA and its analogues 2-ethylhexanoic acid (EHA) and 2-ethylhexanol (EHOL) and indicated VPA as the most potent one. STITCH ('search tool for interactions of chemicals') analysis showed relationships between the examined signalling pathways and suggested additional candidate marker genes. Biomarkers from dedicated mechanistic pathways, e.g. NC differentiation, provide promising tools for monitoring specific effects in ESTc.

Key words: embryonic stem cell test, cardiomyocytes, neural crest, network regulations

Introduction

The cardiac Embryonic Stem cell Test (ESTc) is one of several alternatives for animal testing and is designed to detect embryotoxic compounds by their interference with the differentiation of beating cardiomyocytes [1]. An estimated 65% of experimental animals is required for the field of reproductive and developmental toxicity testing [2, 3]. For this complex field in toxicology it is particularly demanding to develop and implement alternative test methods, like the ESTc, providing equal if not more information for use in obligatory regulatory assessments. The classical ESTc method is one of the most commonly studied alternative test methods for developmental toxicity and a protocol has previously been validated by ECVAM (European Centre for the Validation of Alternative Methods) [1]. However, this protocol is limited to microscopic scoring of beating cardiomyocytes, which is not only a time-consuming process, but also a rather subjective endpoint. Additionally, the differentiation process to beating cardiomyocytes takes 10 days. To shorten the test duration demands shifting to other endpoints than scoring of beating cardiomyocytes. This would increase the utility of the ESTc as a hazard assessment tool for developmental toxicity testing. Molecular biomarkers of effect could render embryotoxicity assessment in ESTc objective and quantitative. The embryonic stem cells in the ESTc differentiate into a heterogeneous cell population including non-cardiomyocyte cells [4]. In previous toxicogenomic studies, the use of a wide array of genomic biomarkers of differentiation was studied comprising all potential cell populations present in the ESTc [5, 6]. Therefore, analysis of cell type-specific RNAs would allow refined description of the biological domain of ESTc to compensate for the heterogeneity, and may improve potency rankings of compounds within structural chemical classes.

Valproic acid (VPA) is a potent teratogen in the rat with defects including hydronephrosis, cardiovascular defects, malformed tails, and limb defects [7]. In humans, when prescribed as an antiepileptic drug in early pregnancy, VPA was associated with congenital malformations related to neural tube defects [8, 9]. Neural tube defects are characterised by a primary failure in closure of the neural tube, that would involve abnormalities of neuroepithelial-mesenchymal interactions [8], accompanied by e.g. changes in neural crest cell migration and retinoic acid balance [10]. VPA has been proposed to act through the inhibition of HDAC (histone deacetylase) as its primary molecular effect [11, 12]. HDAC consequently can have epigenetic effects on multiple genes [13]. Previous studies

showed *Mycn* and *Hlf0* were regulated HDAC target genes after VPA exposure in the embryos of treated mice (all gene names are fully defined in Table S1) [11]. These genes are involved in organ morphogenesis and chromosome organisation, respectively. VPA also influences the apoptosis pathway via *Gsk3 β* [8]. Additionally, early (*Anxa2*, *Myl7*) and late (*Myh6*, *Nkx2-5*) cardiomyocyte markers were affected [5, 14]. Other molecular effects of VPA related to the neural tube defects likely involve neural crest cell differentiation and retinoid signalling as retinoic acid homeostasis plays an important role in embryo development.

The retinoic acid (RA) pathway is also likely to be affected by VPA as indicated by Jergil *et al.* [12]. For example, HDAC influences *Cyp26a1* expression levels, from which the enzyme catabolises retinoic acid (RA) into inactive metabolites [15]. Other enzymes involved in the RA pathway are ADH1 and RDH10 that transform retinol (vitamin A) into retinaldehyde as well as ALDH1A1 and ALDH1A2 that produce RA out of retinaldehyde [15]. RA also influences neural crest (NC) cell migration, which is essential for normal heart formation [16]. The NC cells, also called the fourth germ layer, are of great importance during embryogenesis and contribute to both neuronal and mesenchymal structures [17, 18]. After neural tube closure, neural crest cells separate from the neural tube and migrate into different parts of the embryo to contribute to the peripheral nervous system, pigment cells, cartilage and bones of the craniofacial part of the embryo, and cardiac structures [17, 19, 20]. Cardiac neural crest contributes to the cardiac outflow tract, smooth muscles in great arteries, and the septum between the aorta and pulmonary veins [19]. They even contribute to the formation of cardiomyocytes [21, 22].

It is known that VPA inhibits development of beating cardiomyocytes at non-cytotoxic levels in the ESTc [23-25]. Since NC cells are progenitors of multiple cell lineages and can be affected by teratogens, they are a relevant target in developmental toxicity screening methods such as ESTc. Different genes contribute to NC cell differentiation depending on their developmental stage, be it non-neural ectoderm, the neural plate border, premigratory NC, or migratory NC [26]. These genes can be expressed in different stages, from early (non-neural ectoderm, neural plate border; *Msx2*, *Pax3*, *Ap2a*) to late (pre migratory and migratory NC; *Sox9*, *Snail* (*Snai1*), *Slug* (*Snai2*), *Twist*) [17, 26]. *P75* (Nerve growth factor receptor; *Ngfr*) is expressed in migratory NC stem cells, and has been used in FACS to isolate NC cells [27].

In this study, we explore the presence of a RA-sensitive NC subpopulation of cells in the ESTc at different time-points. In addition, we study gene regulations in time related to cardiomyocyte differentiation, retinoic acid homeostasis, and neural crest in cardiac related stem cell differentiation to study the most relevant time-points within the ESTc related to these signaling pathways. Furthermore, we explore the effect of the NC toxin VPA and the potency ranking possibilities among VPA and two structural analogues as a proof of concept using the regulation of these genes. Lastly, gene interactions were predicted and time and exposure dependent gene expression changes were visualised in a network in order to understand these interactions and to look for gene transcript biomarkers. This study aims at expanding the understanding of the biological domain and at potentially shortening the duration of the ESTc by studying the NC as a potential new endpoint.

Methods

Test compounds

Valproic acid (VPA, CAS# 99-66-1), 2-ethylhexanoic acid (EHA, CAS# 149-57-5), and 2-ethylhexanol (EHOL, CAS# 104-76-7) were purchased from Sigma-Aldrich (Zwijndrecht, The Netherlands). The compounds were tested in the cell differentiation and viability test at concentrations up to 1 mM with 0.25% dimethyl sulfoxide (DMSO, Sigma-Aldrich) final solvent concentration in the medium.

Stem cell culture

The embryonic stem cells (ES-D3 (D3)) were purchased from ATCC® (Manassas, VA, USA) and cultured according to the protocol described by Spielmann *et al.* [28]. The cells were cultured in 35 mm culture dishes (Corning, New York, NY, USA) in a humidified atmosphere of 37°C with 5% CO₂. The cells were routinely cultured every 2-3 days in complete medium containing Dulbecco's Modified Eagle's Medium (DMEM; Gibco, Waltham, MA, USA), 20% Fetal Bovine Serum (FBS; Greiner Bio-One, Kremsmünster, Austria); 1% Non-Essential Amino Acids (NEAA; Gibco); 2 mM L-Glutamine (Gibco); 1% 5000 IU/ml Penicillin/5000 µg/ml Streptomycin (Gibco); 0.1 mM β-mercaptoethanol (Gibco). 1000 units/ml leukemia inhibitory factor (LIF; ESGRO®, Millipore, Burlington, MA, USA) was added to the medium to keep the cells in an undifferentiated state. These cultured cells were used for all subsequent experiments.

Cell viability assay

Non-differentiated cells were plated in a 96-wells plate (Greiner Bio-One) to a concentration of 500 cells per well. After two hours of incubation at 37°C and 5% CO₂, the compounds were added to the plate in seven concentrations (1, 0.33, 0.1, 0.033, 0.01, 0.0033, 0.001 and 0 mM) together with the generally used controls DMSO (0.25%; solvent control; Sigma-Aldrich), 5-fluoruracil (0.1 µg/ml; positive control; Sigma-Aldrich), and penicillin G (500 µg/ml; negative control; Sigma-Aldrich). All conditions were performed in six technical replicates. The wells contained 200 µl medium per well with an end-concentration of 5 µl/ml LIF. After three days of incubation (37°C and 5% CO₂) the exposure concentrations were completely refreshed by 200 µl of the same compositions and were incubated for another two days. On day 5, 100 µl of solution was removed from each well and 20 µl of CellTiter-Blue reagent (Promega, Leiden, The Netherlands) was added to each well. Fluorescence was measured after 2-4 hours of incubation at 544_{Ex}/590_{Em} nm on the SpectraMax® M2 spectrofluorometer (Molecular Devices, Berkshire, United Kingdom). Cell viability levels were expressed in percentages relative to the solvent control. Three independent experiments were done for each test compound.

Cell differentiation assay

Cardiac differentiation of the ES-D3 cells during the ESTc assay was done according to a protocol previously described [1, 28]. At differentiation day 0 a cell suspension of 15·10⁴ cells/ml was put on ice and further diluted to a suspension of 3.75·10⁴ cells/ml. For the formation of Embryoid Bodies (EBs), hanging drops were made by putting 56 20 µl droplets of the cell suspension to the inside of the lid of a 100/20 mm CELLSTAR® cell culture dish (Greiner Bio-One). The culture dish contained 5 ml of ice-cold phosphate buffered saline (PBS; Ca²⁺, Mg²⁺ free; Gibco). The hanging drops were incubated for 3 days at 37°C and 5% CO₂, after which they were transferred in 5 ml complete medium without LIF to a 60 mm bacterial petri dish (Greiner Bio-One). This complete medium contained the desired concentration of the test compounds or controls. This EB solution was incubated for 2 days. At differentiation day 5, the EBs were transferred to a 24-wells plate (TPP, Trasadingen, Switzerland) containing one EB per well and 1 ml of complete medium (without LIF) with the desired concentration of the test compounds or controls. Each plate contained 24 replicates per concentration and two plates per concentration were tested. After 5 days of incubation at differentiation day 10, the EBs were scored for presence or absence of beating cardiomyocytes. The number of beating EBs were calculated

as fraction of the total EBs per 24-wells plate. All three compounds were tested in duplicate at concentrations of 1, 0.33, 0.1, 0.033, 0.01, 0.0033, 0.001 and 0 mM. The differentiation assay was performed by using a 0.25% DMSO control and an untreated control (2 times 24-wells plate per test compound per control). The test was considered as being successful when the fraction of the number of beating EBs to the total EBs per 24-wells plate is equal to 1 in both control conditions. Three independent experiments were done for each test compound.

Immunocytochemistry

EBs were transferred to 35mm culture dishes at differentiation day 5 and were stained at differentiation day 7 and 10 using immunocytochemistry. First, the EBs were rinsed with pre-warmed PBS and fixed for 10-30 minutes with 4% formaldehyde at differentiation day 7 and 10 (Electron Microscopy Sciences, Hatfield, PA, USA). The fixed cells were stored at 4°C up to one week until the staining was done. The cells were rinsed three times for 5 minutes with PBS before and after storage and in between each step of the process. The cells were permeabilised with 0.2% Triton X-100 in PBS (0.5% for TWIST; T9284, Sigma-Aldrich) for 5 minutes. Then, the samples were blocked with blocking buffer for 1 hour (1% bovine serum albumin (BSA, Sigma-Aldrich), 0.5% Tween-20 (Sigma-Aldrich) in PBS (Twist staining: 5% BSA in PBS)). The rinsed cells were incubated with the primary antibody (AP2 α : Activating Enhancer-Binding Protein 2 Alpha; early NC marker, (1:100, sc-12726, Santa-Cruz), TWIST: Twist Family basic helix-loop-helix Transcription Factor: late NC marker, (1:500, ab50887, Abcam), Myosin Heavy Chain (1:65, MF20, MAB4470, R&D Systems) at 4°C overnight. After incubation, the cells were rinsed again and incubated with the secondary antibody (1:200, goat-anti-mouse, TRITC, AP503R, Millipore) for 1 hour in dilution buffer (0.5% BSA, 0.5% Tween-20 in PBS). For TWIST: 5% normal goat serum (NGS, G9023, Sigma-Aldrich), 0.5% Tween-20 in PBS). DAPI stock (Sigma-Aldrich) was diluted to 1 μ g/ml in dilution buffer and was incubated for 10 minutes. The cells were rinsed once with PBS for 10 minutes and the EBs were covered with mounting medium (Thermo Fisher) and a cover glass. The stainings were visualised on an Olympus BX51 light microscope (Shinjuku, Japan).

Gene expression analysis

Following the cell differentiation protocol and previously published methods [29], sample collection was done for all three compounds (1 mM: highest concentration tested during differentiation and viability tests) and DMSO control (0.25%) at

differentiation day 4, day 7, and day 10 of the test. The samples were collected in RNeasy Protect (Qiagen, Cat # 76526) and stored at -80°C prior to RNA isolation. All exposure groups contained 6 to 10 samples collected from two independent experiments. Control plates were additionally tested for beating on day 10 of the test. RNA isolation was done using the RNeasy Mini-kit (Qiagen, Cat. # 74104) according to manufacturer's protocol. The samples were spun down and the RNeasy Protect was removed from the pellet. The samples were lysed by RLT buffer containing 10 $\mu\text{l/ml}$ β -mercaptoethanol and were homogenized using QIAshredder columns (Qiagen, Cat. # 79654). A DNase step was done using a RNase-Free DNase set (Qiagen, Cat # 79254). The samples were examined for quantity and quality using the Nanodrop (Nanodrop Technologies Inc., Wilmington, Delaware) and 2100 Bioanalyzer (Agilent Technologies, Amstelveen, The Netherlands). The 260 nm/280 nm absorbance ratios were between 1.9 and 2.2 and the RIN (RNA Integrity Number) scores were >7 . cDNA was formed using the Fluidigm® Reverse Transcription Master Mix according to manufacturer's recommendations. The next step was a pre-amplification step of 18 cycles with Fluidigm® PreAmp Master Mix and TaqMan® Assays. The TaqMan® Assays used, were provided by Thermo Fisher Scientific and are listed with the genes that were tested in table S1. The gene expression levels were measured by RT-qPCR with the 192.24 IFC of Fluidigm® and the data were collected using the BioMark (Fluidigm®, CA, USA). The expression levels were normalised against the average expression level of the housekeeping genes *Polr2a*, *B2m*, and *Gusb* (Table S1). For each condition, the median value of the DMSO control group was used as the reference sample. The expression levels of the compound groups were compared to the DMSO control groups for the different genes for significant regulations by a Student's T-Test ($p < 0.001$). Fold change was calculated for the time-graphs by using the $2^{-\text{ddCt}}$ method. The exposed data were presented as -ddCt.

Gene interaction mapping

A network with gene interactions was obtained from the STITCH ('search tool for interactions of chemicals') web tool ([30]; <http://stitch.embl.de/>). The inputs used were the gene symbols tested in the RT-qPCR test using the *Mus musculus* as organism. This resulted in a network containing the input genes and additional genes that could be associated with the input set, using default settings for information sources and the confidence level (moderate (0.4); the probability that a predicted link is present between two genes or proteins in the database). The obtained data of gene interaction strengths were separated for text mining and

other experimental evidence and exported as tab-delimited files. Together with tables containing functional and gene expression data, these were imported in Cytoscape (version 3.4.0) [31] to visualise the gene interactions and to combine the networks with the gene expression data. The RT-qPCR -ddCt values were visualised in the network generated for both control samples in time and exposure to the compounds relative to the control per time point.

Statistics

Cell viability and differentiation data were fitted using the PROAST software version 65.5 according to the exponential method [32]. ID₁₀ values were determined from the differentiation curve with 95% confidence interval (CI). Zero values were visualised using a dummy value. Gene expression data were compared to the control samples using a Student's T-Test and differences of $p < 0.001$ were marked in order to look for the statistically highly significant regulated genes. This low p-value was chosen a priori to ensure sufficient statistical stringency. Based on all the statistical comparisons included in this manuscript, this p-value would correspond to a false discovery value (FDR) of $< 1\%$.

Results

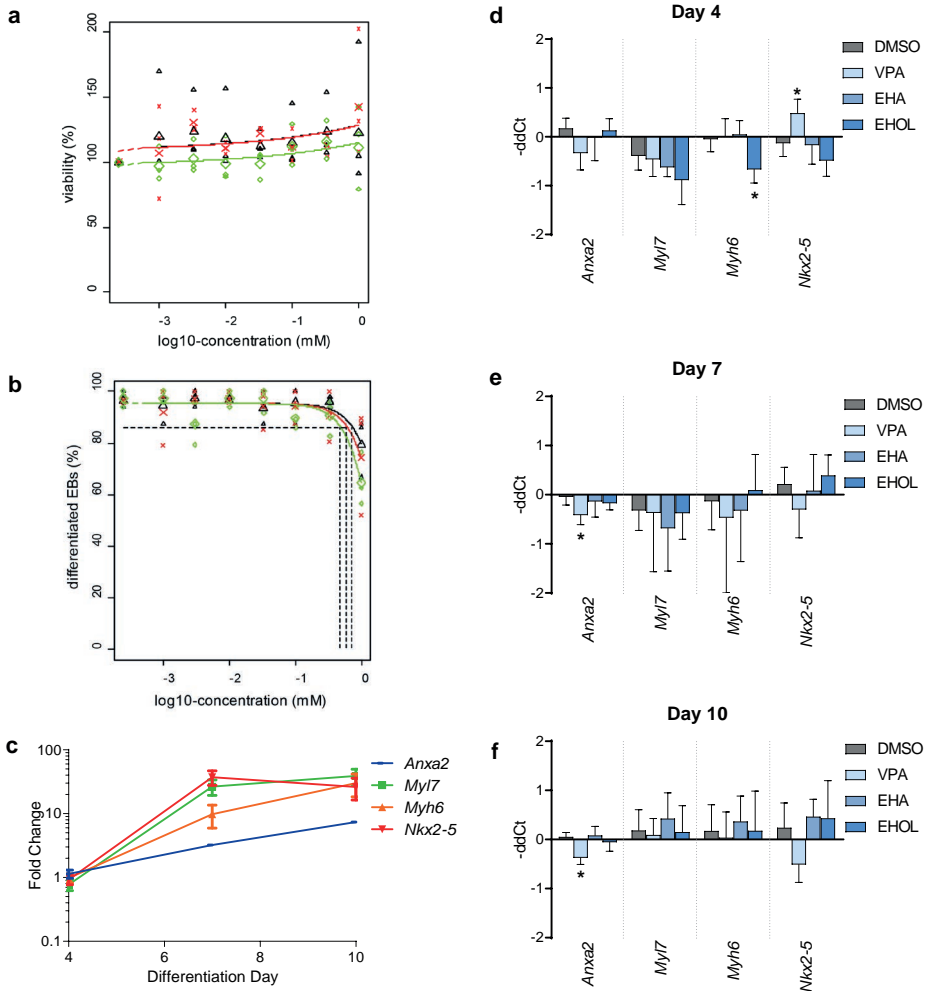


Figure 1: Cardiomyocyte differentiation effects on the classical viability and differentiation ESTc endpoints and on RNA expression level in time and after exposure. a) Cell viability and b) cardiomyocyte differentiation dose-responses of valproic acid (VPA; \diamond), 2-ethylhexanoic acid (EHA; Δ), and 2-ethylhexanol (EHOL; \times) in percentage of beating embryoid bodies (EBs). ID10 values indicated by the dotted lines were determined from the curves using PROAST. c) Expression levels of cardiomyocyte markers Anxa2, Myl7, Myh6, and Nkx2-5 at differentiation day 4, 7, and 10 relative to the median value at differentiation day 4 analysed by RT-qPCR in non-exposed embryoid body differentiation cultures. d-f) Expression levels of cardiomyocyte markers Anxa2, Myl7, Myh6, and Nkx2-5 after 1 mM VPA, EHA, and EHOL exposure relative to the DMSO control at different time points. Error bars indicate the standard deviation. N=2 with in total 6 to 10 samples. *p < 0.001

Effects on cardiomyocyte differentiation

VPA, EHA, and EHOL were tested for their effects on cardiomyocyte differentiation in the ESTc by scoring beating cardiomyocytes and by measuring cardiomyocyte marker gene expression levels (fig. 1). The percentage of beating EBs was reduced to 65-80% at the highest concentration tested at 100% cell viability for all three compounds (fig. 1a,b). The ID_{10} values for EB differentiation were 0.50 mM (CI 0.30-0.75 mM) for VPA, 0.76 mM (CI 0.56-0.95 mM) for EHA, and 0.63 mM (CI 0.40-0.89 mM) for EHOL and showed no significant differences since the 95% CI of the ID_{10} values overlap. The expression levels of the cardiomyocyte marker genes in control samples (0.25% DMSO) increased up to 30 fold between differentiation day 4 and 10 (fig. 1c). Cardiomyocyte differentiation markers showed downregulations after VPA exposure for *Anxa2* at differentiation day 7 and day 10 and after EHOL exposure for *Myh6* at day 4 (fig1d-f). The *Nkx2-5* gene expression level was upregulated by VPA exposure at day 4.

NC cell presence in the ESTc and the effects of VPA, EHA, and EHOL on NC gene expression levels

The presence of NC cells was studied with the rationale to explore the use of NC related transcript markers as a new ESTc endpoint for potency ranking between related chemicals based on chemical structures. NC cells were stained for the NC markers AP2 α and TWIST and appeared as colonies throughout the cultures from differentiation day 7 onwards (fig. 2a). The expression levels of NC related genes increased with time for both early NC markers (fig. 2b; up to 10/20-fold) and NC specifiers (fig. 2c; up to 200-fold). At differentiation day 4 of the test, several NC markers were significantly upregulated (*Ngfr*, *Msx2*, *Pax3*, *Snai2*) by VPA and sometimes by EHOL (*Msx2*, *Snai2*) (fig. 2d). At differentiation day 7 upregulations persisted but *Pax3* and *Sox9* were downregulated by VPA (fig. 2e). At differentiation day 10 *Msx2*, *Snai2*, *Twist1* were upregulated after VPA exposure and *Ap2 α* was downregulated (fig. 2f). In contrast to VPA, gene expression changes induced by EHOL were limited to upregulation of *Msx2* and *Snai2* at differentiation day 4 and *Snai1* and *Twist1* at differentiation day 7, whereas EHA did not result in any significant changes in expression among the genes studied.

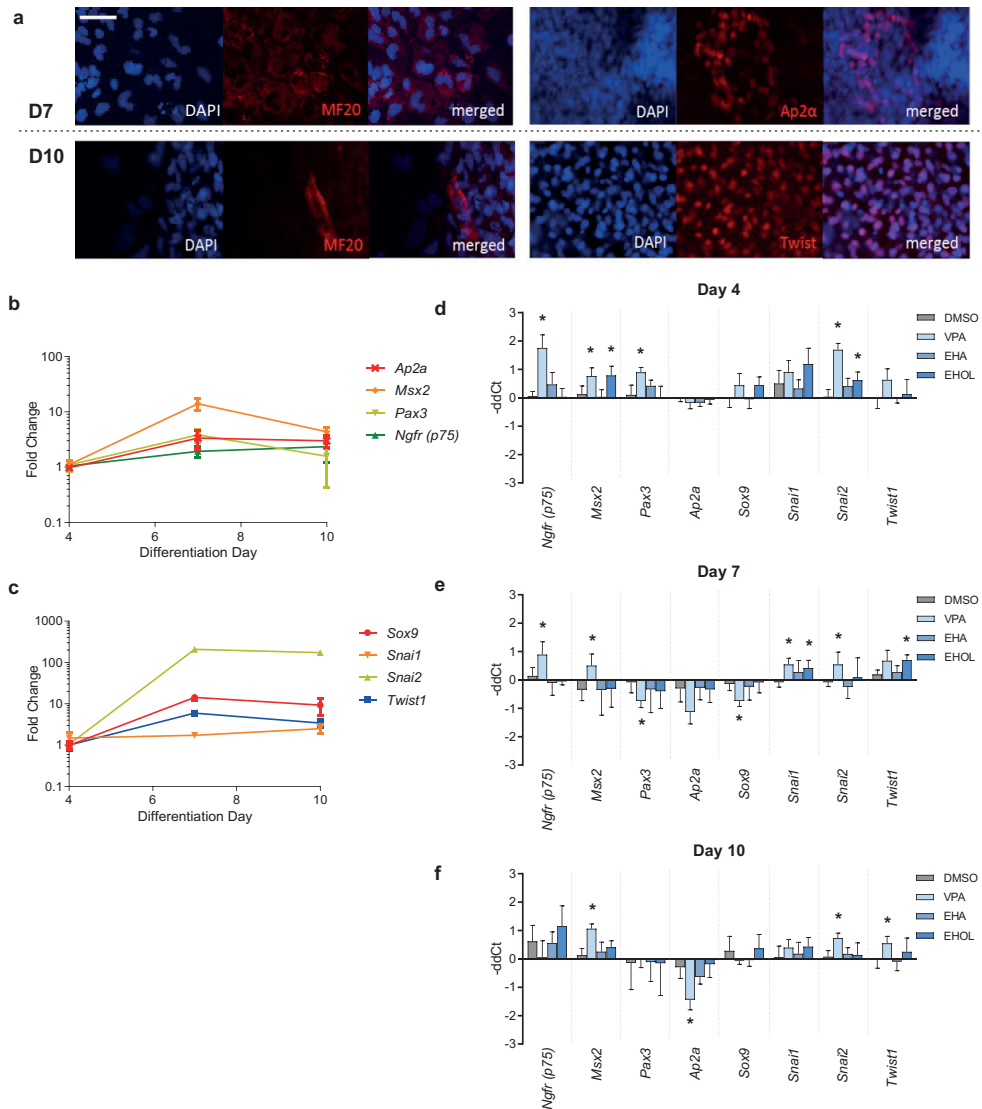


Figure 2: Neural crest (NC) cells in the ESTc and gene expression levels of NC markers. a) Immunocytochemistry staining of DAPI, myosin heavy chain marker MF20 (differentiation day 7 and day 10, 1:65), and NC cell markers AP2α (differentiation day 7, 1:100) and TWIST (differentiation day 10, 1:500). Scale bar indicates 20 μm, Magnification 40x. b) Early NC marker gene expression and c) NC specifier gene expression with time relative to differentiation day 4. d-f) Gene expression levels of NC related genes at differentiation day 4, 7, and 10 of the EST after exposure to VPA, EHA, and EHOL at exposure levels of 1mM. Error bars indicate the standard deviation. N=2 with in total 6 to 10 samples. *p < 0.001

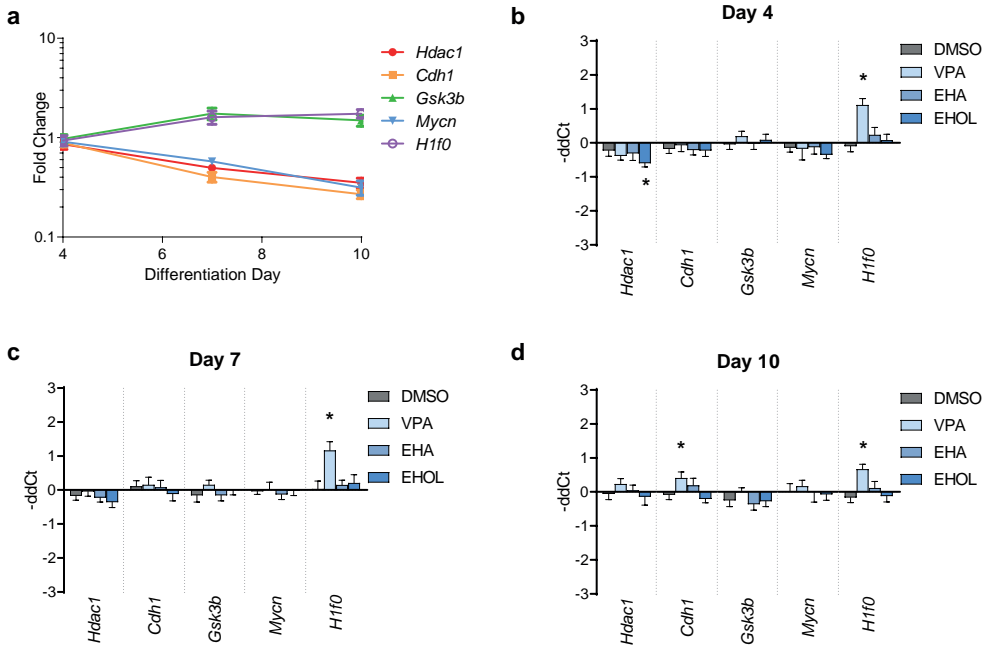


Figure 3: RNA expression levels in time and after exposure, related to previously proposed mechanisms of VPA: HDAC inhibition and Gsk3 β . a) RNA expression levels of *Hdac1*, *Cdh1*, *Gsk3 β* , *Mycn*, and *H1f0* with time in the unexposed EST depicted as Fold Change after RT-qPCR analysis. b-d) Expression levels at differentiation days 4, 7, and 10 at VPA, EHA, and EHOL exposure levels of 1 mM relative to the DMSO control (0.25%). Error bars indicate the standard deviation. N=2 with in total 6 to 10 samples. *p < 0.001

Effects on expression levels of genes related to HDAC inhibition

Genes related to previously proposed mechanisms of VPA were studied with the rationale to confirm the proposed primary molecular effect of VPA, being HDAC inhibition, and to compare these effects with the two structural analogues to study the possibility of using these transcripts as possible biomarkers for potency ranking within the ESTc. While expression levels of *Hdac1*, *Cdh1*, and *Mycn* went down in with time up to a 3 fold change, the expression levels of *Gsk3 β* and *H1f0* went up with time to an almost 2 fold change compared to differentiation day 4 (fig. 3a). EBs exposed to VPA had upregulated *H1f0* gene expression levels for all three time points (fig. 3b-d).

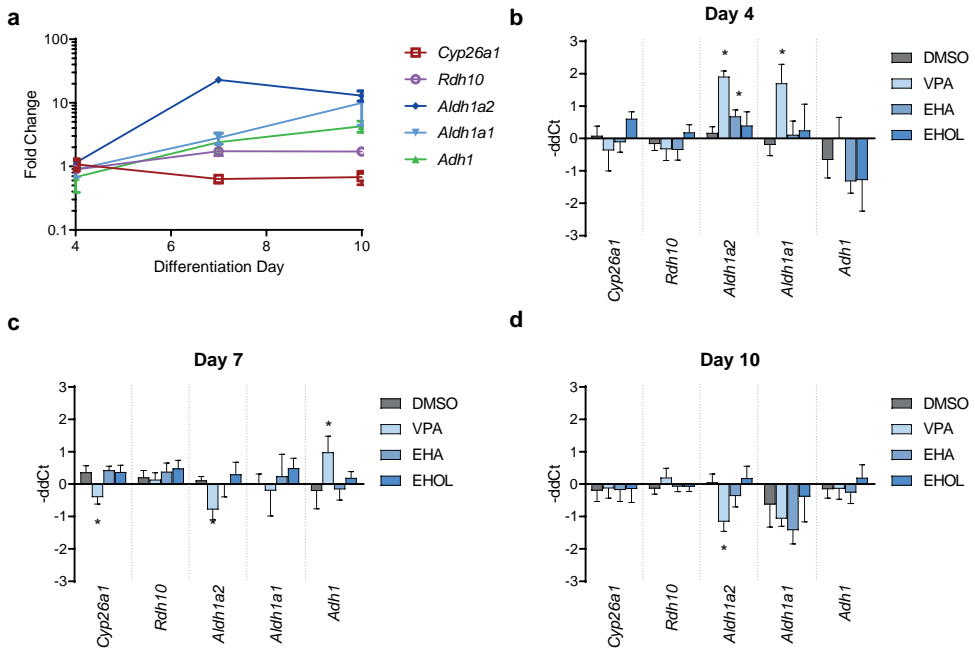


Figure 4: Expression levels of retinoic acid (RA) homeostasis related genes in time and after exposure. a) Gene expression levels of RA related genes in the ESTc and depicted as Fold Change after RT-qPCR analysis. b-d) Gene expression levels at differentiation day 4, 7, and 10 of the EST after exposure to 1 mM VPA, EHA, or EHOL. Error bars indicate the standard deviation. N=2 with in total 6 to 10 samples. *p < 0.001

Effects on the gene expression levels of the Retinoic Acid homeostasis enzymes

As VPA also likely affects the RA pathway, the effects of time and exposure to RNA transcripts related to RA homeostasis were studied in order to explore the possibility of their use in potency ranking within the ESTc. The expression levels of RA related genes between differentiation day 4 and 10 all increased with time from a 4-fold to a 25-fold induction, except for *Rdh10* and *Cyp26a1*, which were reduced to a 3-fold change with time (fig. 4a). *Aldh1a2* and *Aldh1a1* were upregulated at differentiation day 4, after 24 hours of VPA and EHA exposure (fig. 4b). *Adh1* was significantly upregulated by VPA at differentiation day 7 (fig. 4c). VPA-induced downregulations were observed for *Aldh1a2* at differentiation day 7 and 10 and for *Cyp26a1* at differentiation day 7 (fig. 4c, d).

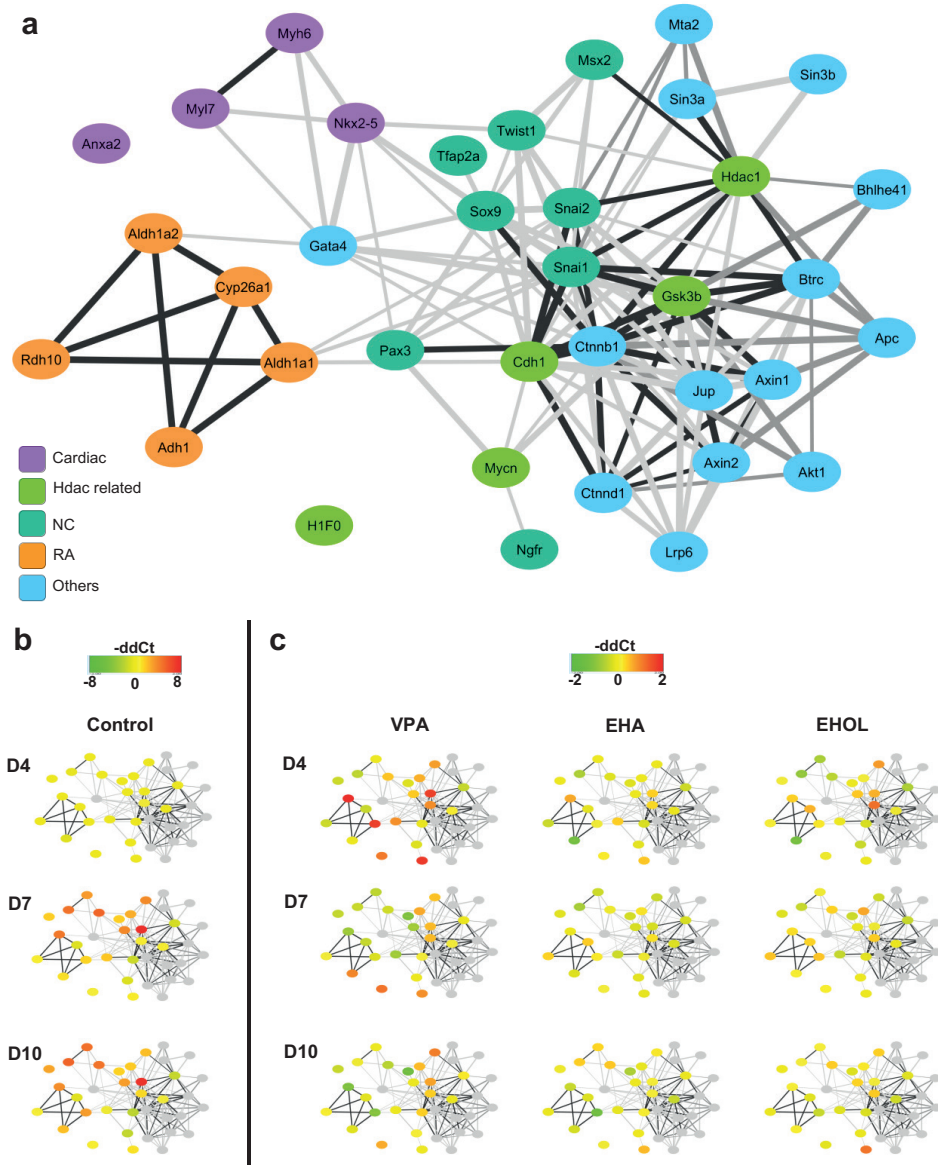


Figure 5: Gene expression networks including cardiomyocyte differentiation, HDAC effector, RA homeostasis, and neural crest related genes. a) Relation between the different genes tested, including additional genes in blue, proposed by STITCH. Gene edges are depicted in black for relations that were experimentally determined and found by textmining as well, dark grey when the relations were experimentally determined only, and light grey when the relations were found by textmining only. The thickness of the edges is proportional to the level of evidence. b,c) RT-qPCR data (-ddCt) of control, VPA, EHA, and EHOL exposure effects on gene expression at differentiation day 4, 7, and 10.

Gene interaction analysis of the functional gene groups of cardiomyocyte differentiation, HDAC inhibition, RA homeostasis, and NC.

The coregulations of the tested gene groups for cardiomyocyte differentiation, the NC, HDAC inhibition, and RA homeostasis were analysed using STITCH (figure 5a), a search tool for gene interactions based on text mining and experimental evidence. NC associated genes appeared associated with all other functional gene groups tested. RA homeostasis and cardiomyocyte markers show less direct relations in this network. Other genes (in blue in figure 5a) were added by STITCH analysis by default on the basis of strength of evidence of network relations. Figure 5b shows the up- and downregulation of all the genes measured of the control samples compared to differentiation day 4. The colours show an overall upregulation of cardiomyocyte differentiation and NC associated genes with time. In addition, most of the RA homeostasis related gene expression levels went up with time. The HDAC effector genes were up- or downregulated. Exposure to VPA, EHA, and EHOL resulted in changes in expression levels relative to the control samples of the corresponding differentiation day (fig. 5c). Most upregulations were visible after VPA exposure in the RA and NC associated genes at differentiation day 4. These upregulations diminished or became downregulated later with time. EHA and EHOL showed less strong effects compared to VPA.

Discussion

In this study, NC markers showed presence of NC cells in ESTc at the protein level (fig. 2a). The AP2 α staining indicated the specification of NC cells within ESTc (differentiation day 7), followed by epithelial to mesenchymal transition (EMT) shown by TWIST staining (differentiation day 10). In mice, the neural crest cells develop and migrate from embryonic day E9.0 onwards [33]. As differentiation day 4, 5, and 6 of the ESTc have been shown to compare to embryonic days E5.5, E6.5, and E7.5 in mice, respectively [34], embryonic day E9.0 in mice should compare to differentiation day 7 or 8 in the ESTc when NC cells are developing in mice, which is in concordance with our immunocytochemistry results.

Gene expression analysis confirmed the upregulation of NC marker transcripts in time (fig. 2b,c). This study showed an increase of neural plate border specifiers/ NC precursor genes (*Msx2*, *Pax3*), NC specifiers (*Sox9*, *Ap2a*), NC related genes

responsible for its migration and differentiation (*p75*, *Sox9*), and epithelial to mesenchymal transition (EMT) genes (*Snail*, *Snai2*, *Twist1*) between differentiation days 4 and 10 (fig. 2b,c). Although all NC related genes increased with time, the increase of the EMT genes was most evident, suggesting the transformation of epithelial cells towards mesenchymal cells during the differentiation process of the ESTc. *Sox9* interacts with *Snail/2* to drive EMT [26]. The increase of *Sox9* and *Snail/2* expression with time (fig. 2c), was accompanied by a decrease of *Cdh1* expression with time (fig. 3). Subsequently a downregulation of type 1 cadherins takes place by the functional repressors *Snail/2* in order for the NC cells to delaminate from the neural tube [26]. The ESTc EBs are not as neatly structured as the embryo and the present NC cells will not delaminate and migrate to a specific place as they do in an embryo. However, it seems these gene expression levels in the ESTc behave in the same way as in embryos, as indicated by the upregulated NC specifier *Sox9* and EMT genes *Snail/2* and downregulation of the cadherin gene *Cdh1*.

VPA exposure resulted in multiple significant gene regulations at different stages of NC development (Fig. 4). Especially at differentiation day 4 upregulation occurred for the neural plate border specifiers (*Msx2*, *Pax3*), NC migration related (*p75*), and EMT (*Snai2*) related genes. The stimulation of neural plate border specifiers could suggest an increase in NC precursor cells and the stimulation of *p75* and *Snai2* could suggest NC migration and EMT, respectively. Other studies also showed VPA as a NC cell toxicant by means of VPA inhibiting the NC migration after NC isolation of human embryonic stem cells [35-38]. Together these data suggest that VPA may affect both migration and differentiation of NC cells. *In vivo*, the effects of VPA on NC and its migration have never been examined to our knowledge. VPA causes developmental effects both in the brain and in the heart [7]. Neural crest cells are involved developmental processes of both these organs [17]. Our observation that VPA affects NC cell differentiation in ESTc supports the suggestion that VPA affects NC development in both these organ systems.

To be able to test potency ranking between structurally related chemicals, EHA and EHOL exposures were tested next to VPA exposure. Of the three compounds tested, VPA appeared the most potent molecule in the ESTc based on our NC related gene expression results showing most significant changes for VPA (fig. 2). This correlates with *in vivo* rat data indicating VPA as most potent, followed by EHA and EHOL as roughly equipotent compounds as to effective dose levels [7]. This *in vivo* finding was confirmed by the classical ESTc endpoint of beating cardiomyocytes, since

the 95% CI of the ID_{10} values overlapped (fig. 1b). Neither the cardiomyocyte nor the neural crest endpoint showed only few differences between EHA and EHOL on the gene expression level. The use of NC cell markers in the ESTc might be a promising additional tool for distinguishing potency of structurally closely related chemicals within the same compound class and should be further explored by testing additional compound classes in relation to NC marker expression.

The previously proposed primary molecular effect of VPA is HDAC inhibition [13], from which the effector genes are amongst others related to neural crest formation. *Hdac* and the effector genes tested in the ESTc were regulated with time (fig. 3a). In the EBs the *Hdac* gene expression level gradually decreased with time (fig. 3a). This corresponds to HDAC being necessary for pluripotency that decreases as the cells differentiate [39-42]. *Cdh1* and *Mycn* expression levels also decreased with time, which can be explained since HDAC is in the promoting complex with and of MYCN and *Cdh1*, respectively [43, 44]. Neither of the compounds tested had an effect on these expression levels. The expression levels of *H1f0* went up with time and is likely to be required in later stages of embryogenesis [45]. *Hdac* downregulation is associated with *H1f0* upregulation [11, 46]. This explains the upregulation of *H1f0* after VPA exposure. It is estimated that a loss of HDAC1 or HDAC2 activity would cause a deregulation of 2000 genes [42]. As we tested only a small selection of HDAC effector genes, it is possible, therefore, that many other different genes would also be affected. For example, HDAC inhibits the level of transcription of the cardiomyocyte differentiation marker *Nkx2-5* [39]. This explains the upregulation of *Nkx2-5* by VPA. Furthermore, HDAC would induce the expression of the neural plate border specifier *Pax3* by binding and activating its promotor [47]. An inhibition of HDAC would suggest an inhibition of *Pax3*. Our results show an increase in *Pax3* expression after VPA exposure at differentiation day 4, but an inhibition at differentiation day 7. The exact pathway of VPA increasing the *Pax3* expression at differentiation day 4 is not clear. The effect on differentiation day 7, probably due to HDAC inhibition, indicates timing is very important and that the time needed to cause an effect differs per pathway.

The RA homeostasis pathway was regulated with time and by exposure to VPA (fig. 4). RA homeostasis is important in embryo development including cardiogenesis as perturbed RA signalling disrupts NC migration from the neural tube into the pharynx and eventually the heart [10, 48] [16]. We observed an upregulation with time of the RA synthesising genes and a small downregulation of the RA metabolising gene *Cyp26a1*. RA is synthesised by the expression of enzymes like

RDH10, ADH1, and ALDH1A2 or metabolised by the level of e.g. CYP26A1 [10, 15]. Exposure to VPA caused an upregulation of *Aldh1a1* and *Aldh1a2* at differentiation day 4 (24 hours after exposure). The inhibition of *Cyp26a1* gene expression by VPA at differentiation day 7 (72 hours of exposure) directs towards a reduction in the RA metabolising enzyme. These effects of VPA are in concordance with previous findings in literature [11, 12]. HDAC influences. The *Cyp26a1* expression levels, as a direct effector of HDAC regulation [49], were affected by VPA (fig. 4c). However, other genes important for RA homeostasis were affected to a larger extent, from which *Aldh1a2* was affected most (fig. 4b,c,d). This gives the impression that VPA may have another mode of action in addition to inhibition of HDAC.

The different functional gene groups studied showed relations by STITCH analysis (fig. 5a) and were all regulated in time (fig. 5b). The NC gene group showed multiple relations within the network, visualised by the edges showing connections between the different nodes. Although VPA, EHA, and EHOL all affected gene expression compared to control samples, VPA was most effective, especially at differentiation day 4 (fig. 5c). At later differentiation days the effects were smaller, indicating the importance of timing for observing highest gene expression changes. Most coregulated genes suggested by STITCH were related to *Hdac* an RA associated genes. These additional genes are involved in the regulation of gene expression and transcription (*Mta2*, *Sin3a*, *Sin3b*), *Wnt* signalling and its regulation (*Apc*, *Axin1*, *Axin2*, *Ctnnb1*, *Ctnnd1*, *Lrp6*), cell adhesion and cell junctions (*Ctnnb1*, *Ctnnd1*, *Jup*) and cell survival or apoptosis (*Akt1*, *Axin1*, *Btrc*). All these processes are important key players in embryogenesis that warrant further investigation as possible biomarkers of embryotoxicity in ESTc.

In summary, we have confirmed the presence of NC cells in the ESTc and demonstrated that gene markers for these cells are more sensitive than those for cardiomyocytes to VPA exposure. Additionally, the sensitivity to exposure of the VPA analogues tested differed depending on time. The presence of NC in the ESTc and the relations between the different functional gene groups contribute to expanding our understanding of the biological domain of the ESTc. This increases the possibilities for wider exploitation of the biological domain of the ESTc beyond cardiomyocyte differentiation and assists in mechanistic explanation of compound effects in ESTc. Further studies using chemicals from different chemical domains with developmental toxicity characteristics (CLP registered) are needed to explore the predictivity of these mRNA networks for developmental toxicity screenings.

Acknowledgements

We gratefully thank Helen Tinwell, Nina Hallmark, and Marc Pallardy for their helpful suggestions and useful discussions and ideas.

References

1. Genschow, E., et al., *Validation of the embryonic stem cell test in the international ECVAM validation study on three in vitro embryotoxicity tests*. *Altern Lab Anim*, 2004. **32**(3): p. 209-44.
2. Piersma, A.H., *Alternative methods for developmental toxicity testing*. *Basic Clin Pharmacol Toxicol*, 2006. **98**(5): p. 427-31.
3. van der Jagt, K., Munn, S., Torslov, J., de Bruijn, J., *Alternative Approaches Can Reduce the Use of Test Animals under REACH*. 2004, EC Joint Research Centre.
4. Seiler, A., et al., *Improvement of an in vitro stem cell assay for developmental toxicity: the use of molecular endpoints in the embryonic stem cell test*. *Reprod Toxicol*, 2004. **18**(2): p. 231-40.
5. Pennings, J.L., et al., *Gene set assembly for quantitative prediction of developmental toxicity in the embryonic stem cell test*. *Toxicology*, 2011. **284**(1-3): p. 63-71.
6. van Dartel, D.A., et al., *Discriminating classes of developmental toxicants using gene expression profiling in the embryonic stem cell test*. *Toxicol Lett*, 2011. **201**(2): p. 143-51.
7. Ritter, E.J., et al., *Teratogenicity of di(2-ethylhexyl) phthalate, 2-ethylhexanol, 2-ethylhexanoic acid, and valproic acid, and potentiation by caffeine*. *Teratology*, 1987. **35**(1): p. 41-6.
8. Blaheta, R.A., et al., *Valproate and valproate-analogues: potent tools to fight against cancer*. *Curr Med Chem*, 2002. **9**(15): p. 1417-33.
9. Robert, E. and P. Guibaud, *Maternal valproic acid and congenital neural tube defects*. *Lancet*, 1982. **2**(8304): p. 937.
10. Piersma, A.H., E.V. Hessel, and Y.C. Staal, *Retinoic acid in developmental toxicology: Teratogen, morphogen and biomarker*. *Reprod Toxicol*, 2017. **72**: p. 53-61.
11. Kultima, K., et al., *Early transcriptional responses in mouse embryos as a basis for selection of molecular markers predictive of valproic acid teratogenicity*. *Reprod Toxicol*, 2010. **30**(3): p. 457-68.
12. Jergil, M., et al., *Short-time gene expression response to valproic acid and valproic acid analogs in mouse embryonic stem cells*. *Toxicol Sci*, 2011. **121**(2): p. 328-42.
13. Eikel, D., A. Lampen, and H. Nau, *Teratogenic effects mediated by inhibition of histone deacetylases: evidence from quantitative structure activity relationships of 20 valproic acid derivatives*. *Chem Res Toxicol*, 2006. **19**(2): p. 272-8.
14. van Dartel, D.A. and A.H. Piersma, *The embryonic stem cell test combined with toxicogenomics as an alternative testing model for the assessment of developmental toxicity*. *Reprod Toxicol*, 2011. **32**(2): p. 235-44.
15. Tonk, E.C., J.L. Pennings, and A.H. Piersma, *An adverse outcome pathway framework for neural tube and axial defects mediated by modulation of retinoic acid homeostasis*. *Reprod Toxicol*, 2015. **55**: p. 104-13.
16. Keyte, A. and M.R. Hutson, *The neural crest in cardiac congenital anomalies*. *Differentiation*, 2012. **84**(1): p. 25-40.
17. Simoes-Costa, M. and M.E. Bronner, *Insights into neural crest development and evolution from genomic analysis*. *Genome Res*, 2013. **23**(7): p. 1069-80.

18. Achilleos, A. and P.A. Trainor, *Neural crest stem cells: discovery, properties and potential for therapy*. Cell Res, 2012. **22**(2): p. 288-304.
19. Monsoro-Burq, A.H., *PAX transcription factors in neural crest development*. Semin Cell Dev Biol, 2015. **44**: p. 87-96.
20. Rada-Iglesias, A., et al., *Epigenomic annotation of enhancers predicts transcriptional regulators of human neural crest*. Cell Stem Cell, 2012. **11**(5): p. 633-48.
21. Tamura, Y., et al., *Neural crest-derived stem cells migrate and differentiate into cardiomyocytes after myocardial infarction*. Arterioscler Thromb Vasc Biol, 2011. **31**(3): p. 582-9.
22. Cavanaugh, A.M., J. Huang, and J.N. Chen, *Two developmentally distinct populations of neural crest cells contribute to the zebrafish heart*. Dev Biol, 2015. **404**(2): p. 103-12.
23. van Dartel, D.A., et al., *Monitoring developmental toxicity in the embryonic stem cell test using differential gene expression of differentiation-related genes*. Toxicol Sci, 2010. **116**(1): p. 130-9.
24. Peters, A.K., et al., *Automated analysis of contractility in the embryonic stem cell test, a novel approach to assess embryotoxicity*. Toxicol In Vitro, 2008. **22**(8): p. 1948-56.
25. de Jong, E., et al., *Potency ranking of valproic acid analogues as to inhibition of cardiac differentiation of embryonic stem cells in comparison to their in vivo embryotoxicity*. Reprod Toxicol, 2011. **31**(4): p. 375-82.
26. Simoes-Costa, M. and M.E. Bronner, *Establishing neural crest identity: a gene regulatory recipe*. Development, 2015. **142**(2): p. 242-57.
27. Jiang, X., et al., *Isolation and characterization of neural crest stem cells derived from in vitro-differentiated human embryonic stem cells*. Stem Cells Dev, 2009. **18**(7): p. 1059-70.
28. Spielmann, H., et al., *The Embryonic Stem Cell Test, an In Vitro Embryotoxicity Test Using Two Permanent Mouse Cell Lines: 3T3 Fibroblasts and Embryonic Stem Cells*. In Vitro Toxicology, 1997. **10**: p. 119-127.
29. Dimopoulou, M., et al., *A comparison of the embryonic stem cell test and whole embryo culture assay combined with the BeWo placental passage model for predicting the embryotoxicity of azoles*. Toxicol Lett, 2018. **286**: p. 10-21.
30. Szklarczyk, D., et al., *STRING v10: protein-protein interaction networks, integrated over the tree of life*. Nucleic Acids Res, 2015. **43**(Database issue): p. D447-52.
31. Shannon, P., et al., *Cytoscape: a software environment for integrated models of biomolecular interaction networks*. Genome Res, 2003. **13**(11): p. 2498-504.
32. Slob, W., *Dose-response modeling of continuous endpoints*. Toxicol Sci, 2002. **66**(2): p. 298-312.
33. Baggiolini, A., et al., *Premigratory and migratory neural crest cells are multipotent in vivo*. Cell Stem Cell, 2015. **16**(3): p. 314-22.
34. Yu, R., et al., *A Modified Murine Embryonic Stem Cell Test for Evaluating the Teratogenic Effects of Drugs on Early Embryogenesis*. PLoS One, 2015. **10**(12): p. e0145286.
35. Zimmer, B., et al., *Evaluation of developmental toxicants and signaling pathways in a functional test based on the migration of human neural crest cells*. Environ Health Perspect, 2012. **120**(8): p. 1116-22.
36. Dreser, N., et al., *Grouping of histone deacetylase inhibitors and other toxicants disturbing neural crest migration by transcriptional profiling*. Neurotoxicology, 2015. **50**: p. 56-70.

37. Colleoni, S., et al., *A comparative transcriptomic study on the effects of valproic acid on two different hESCs lines in a neural teratogenicity test system*. *Toxicol Lett*, 2014. **231**(1): p. 38-44.
38. Fuller, L.C., et al., *Neural crest cell motility in valproic acid*. *Reprod Toxicol*, 2002. **16**(6): p. 825-39.
39. Lv, W., et al., *Histone deacetylase 1 and 3 regulate the mesodermal lineage commitment of mouse embryonic stem cells*. *PLoS One*, 2014. **9**(11): p. e113262.
40. Kidder, B.L. and S. Palmer, *HDAC1 regulates pluripotency and lineage specific transcriptional networks in embryonic and trophoblast stem cells*. *Nucleic Acids Res*, 2012. **40**(7): p. 2925-39.
41. Dovey, O.M., C.T. Foster, and S.M. Cowley, *Histone deacetylase 1 (HDAC1), but not HDAC2, controls embryonic stem cell differentiation*. *Proc Natl Acad Sci U S A*, 2010. **107**(18): p. 8242-7.
42. Jamaladdin, S., et al., *Histone deacetylase (HDAC) 1 and 2 are essential for accurate cell division and the pluripotency of embryonic stem cells*. *Proc Natl Acad Sci U S A*, 2014. **111**(27): p. 9840-5.
43. Iraci, N., et al., *A SP1/MIZ1/MYCN repression complex recruits HDAC1 at the TRKA and p75NTR promoters and affects neuroblastoma malignancy by inhibiting the cell response to NGF*. *Cancer Res*, 2011. **71**(2): p. 404-12.
44. Aghdassi, A., et al., *Recruitment of histone deacetylases HDAC1 and HDAC2 by the transcriptional repressor ZEB1 downregulates E-cadherin expression in pancreatic cancer*. *Gut*, 2012. **61**(3): p. 439-48.
45. Ichihara-Tanaka, K., K. Kadomatsu, and S. Kishida, *Temporally and Spatially Regulated Expression of the Linker Histone H1fx During Mouse Development*. *J Histochem Cytochem*, 2017. **65**(9): p. 513-530.
46. Wade, M.G., et al., *Methoxyacetic acid-induced spermatocyte death is associated with histone hyperacetylation in rats*. *Biol Reprod*, 2008. **78**(5): p. 822-31.
47. Jacob, C., et al., *HDAC1 and HDAC2 control the specification of neural crest cells into peripheral glia*. *J Neurosci*, 2014. **34**(17): p. 6112-22.
48. Stefanovic, S. and S. Zaffran, *Mechanisms of retinoic acid signaling during cardiogenesis*. *Mech Dev*, 2017. **143**: p. 9-19.
49. Urvalek, A.M. and L.J. Gudas, *Retinoic acid and histone deacetylases regulate epigenetic changes in embryonic stem cells*. *J Biol Chem*, 2014. **289**(28): p. 19519-30.

Supplementary

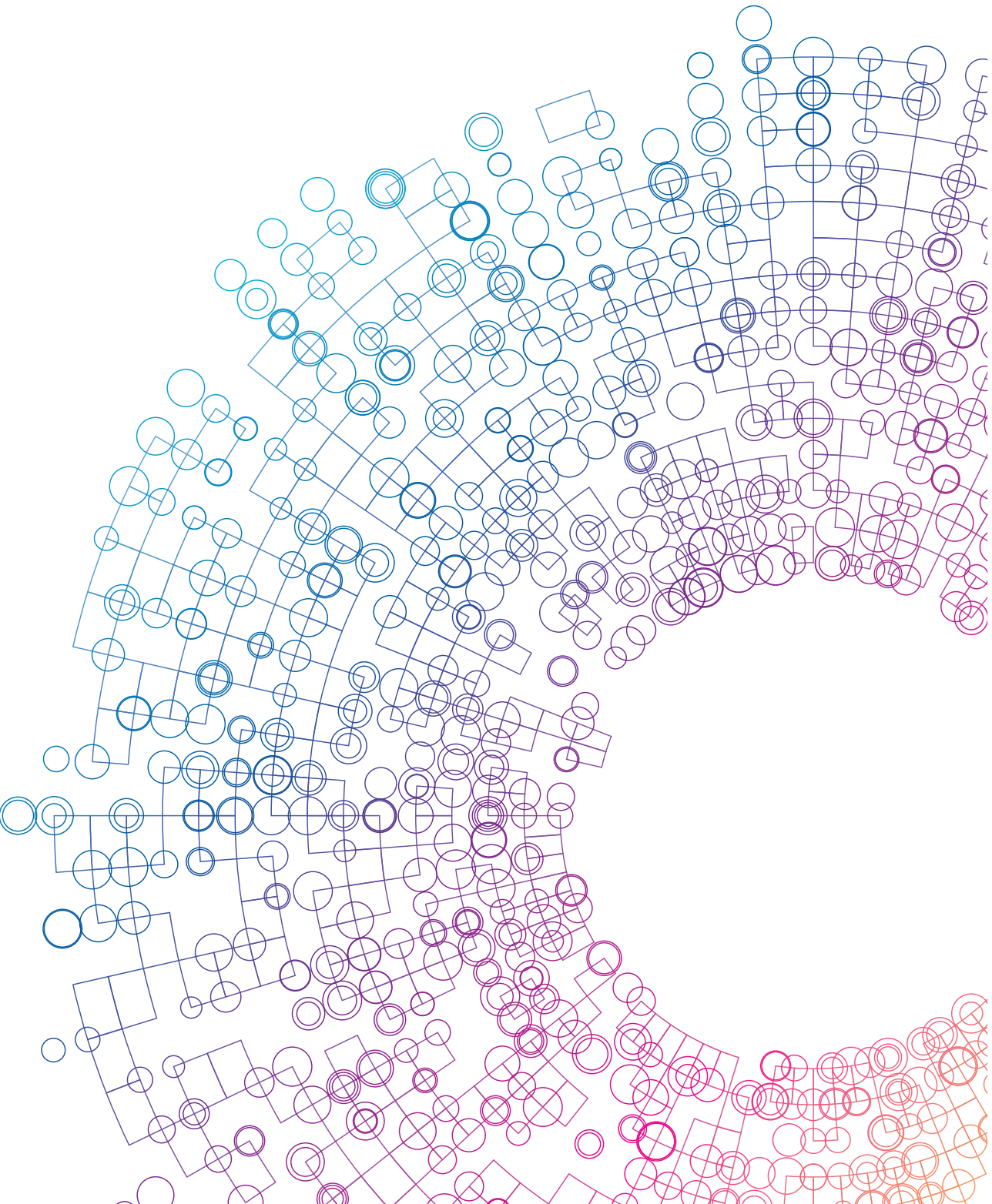
Table S1: Assays used for the RT-qPCR experiments and gene function

Cardiomyocyte differentiation	Assay used	Function
MyI7	Mm00491655_m1	Myosin light chain 7 [1].
Myh6	Mm00440359_m1	Myosin heavy chain 6 [1].
Nkx2-5	Mm01309813_s1	NK2 transcription factor related locus 5 is a homeobox-containing transcription factor functioning in heart formation and development [1].
Anxa2	Mm01150673_m1	Annexin A2 calcium-dependent phospholipid binding protein [2].
Retinoic acid homeostasis		
Cyp26a1	Mm00514486_m1	Cytochrome P450 Family 26 Subfamily A member 1 is an enzyme involved in metabolising retinoic acid into its inactive metabolites [3].
Rdh10	Mm004467150_m1	Retinol dehydrogenase 10 synthesises retinaldehyde [3].
Aldh1a2	Mm00501306_m1	Aldehyde Dehydrogenase 1 Family Member A2 is a retinaldehyde dehydrogenase responsible for retinoic acid synthesis [3].
Aldh1a1	Mm00657317_m1	Aldehyde Dehydrogenase 1 Family Member A1 is a retinaldehyde dehydrogenase responsible for retinoic acid synthesis [3].
Adh1	Mm00507711_m1	Alcohol dehydrogenase 1 stimulates the oxidation of retinol into retinaldehyde [3].
Neural crest cells		
Ap2α (Tfap2a)	Mm00495574_m1	Activating Enhancer-Binding Protein 2 Alpha causes defects in derivatives of NC in mutant mice and acts at the non-neural ectoderm, neural plate border, neural folds, and in the NC cells [4, 5].
Msx2	Mm00442992_m1	Msh Homeobox 2 is a transcriptional repressor present in the neural folds [4].
Sox9	Mm00448840_m1	SRY (Sex-Determining Region Y)-Box 9 stimulates non-histone proteins involved in gene regulation and chromatin structure [4].
Ngfr (p75)	Mm00446296_m1	P75 neurotrophin receptor (P75), also called Nerve Growth Factor Receptor (Ngfr) is mainly present in migrating NC stem cells [6].
Snail (Snail)	Mm00441533_g1	Snail Family Transcriptional Repressor 1 is involved in EMT at the phase where the NC cells separate from the neural tube. Snail (Snail) and Snai2 (Slug) are functionally equivalent and act as transcriptional repressors and an overexpression would stimulate NC migration while a block would inhibit the specification and migration of NC [4, 5].

Cardiomyocyte differentiation	Assay used	Function
Snai2 (Slug)	Mm00441531_m1	Snail Family Transcriptional Repressor 2 is involved in EMT at the phase where the NC cells separate from the neural tube. Snai1 (Snail) and Snai2 (Slug) are functionally equivalent and act as transcriptional repressors and an overexpression would stimulate NC migration while a block would inhibit the specification and migration of NC [4, 5].
Twist1	Mm00442036_m1	Twist Family basic helix-loop-helix Transcription Factor 1 is involved in EMT at the phase where the NC cells separate from the neural tube [4, 5].
Pax3	Mm00435493_m1	Paired Box 3 is a transcriptional activator both in NC and at the neural plate border and its perturbation causes NC defects in mutant mice [4].
HDAC inhibition related genes		
Hdac1	Mm02745760_g1	Histone deacetylase 1 regulates chromatin structure in order to assist in modulating gene expression levels [7].
Cdh1	Mm01247357_m1	Cadherin 1 is a protein providing intercellular contacts between adjacent cells [8].
Gsk3 β	Mm00444911_m1	Glycogen synthase kinase-3 β is a component of the WNT signalling pathway and is involved in apoptosis [9].
Mycn	Mm00476449_m1	V-myc myelocytomatosis viral related oncogene neuroblastoma derived is a transcription factor related to cell cycle control mostly active in neurodevelopment [10, 11]
H1f0	Mm00515079_s1	H1 histone family, member 0 has been proposed to play a role in cell differentiation and to be a candidate marker for VPA teratogenicity [12].
Housekeeping genes		
Polr2a	Mm00839502_m1	RNA polymerase II subunit A
Gusb	Mm0.1197698_m1	β -D-glucuronidase
B2m	Mm00437762_m1	β -2-microglobulin

References

1. Radaszkiewicz, K.A., et al., *The acceleration of cardiomyogenesis in embryonic stem cells in vitro by serum depletion does not increase the number of developed cardiomyocytes*. PLoS One, 2017. **12**(3): p. e0173140.
2. Camors, E., D. Monceau V Fau - Charlemagne, and D. Charlemagne, *Annexins and Ca²⁺ handling in the heart*. 2005(0008-6363 (Print)).
3. Tonk, E.C., J.L. Pennings, and A.H. Piersma, *An adverse outcome pathway framework for neural tube and axial defects mediated by modulation of retinoic acid homeostasis*. Reprod Toxicol, 2015. **55**: p. 104-13.
4. Gammill, L.S. and M. Bronner-Fraser, *Neural crest specification: migrating into genomics*. Nat Rev Neurosci, 2003. **4**(10): p. 795-805.
5. Simoes-Costa, M. and M.E. Bronner, *Establishing neural crest identity: a gene regulatory recipe*. Development, 2015. **142**(2): p. 242-57.
6. Betters, E., et al., *Analysis of early human neural crest development*. Dev Biol, 2010. **344**(2): p. 578-92.
7. Dovey, O.M., C.T. Foster, and S.M. Cowley, *Histone deacetylase 1 (HDAC1), but not HDAC2, controls embryonic stem cell differentiation*. Proc Natl Acad Sci U S A, 2010. **107**(18): p. 8242-7.
8. Aghdassi, A., et al., *Recruitment of histone deacetylases HDAC1 and HDAC2 by the transcriptional repressor ZEB1 downregulates E-cadherin expression in pancreatic cancer*. Gut, 2012. **61**(3): p. 439-48.
9. Blaheta, R.A., et al., *Valproate and valproate-analogues: potent tools to fight against cancer*. Curr Med Chem, 2002. **9**(15): p. 1417-33.
10. Gan, L. and B. Denecke, *Co-regulation of microRNAs and transcription factors in cardiomyocyte specific differentiation of murine embryonic stem cells: An aspect from transcriptome analysis*. Biochim Biophys Acta, 2017. **1860**(9): p. 983-1001.
11. Iraci, N., et al., *A SPI/MIZ1/MYCN repression complex recruits HDAC1 at the TRKA and p75NTR promoters and affects neuroblastoma malignancy by inhibiting the cell response to NGF*. Cancer Res, 2011. **71**(2): p. 404-12.
12. Kultima, K., et al., *Early transcriptional responses in mouse embryos as a basis for selection of molecular markers predictive of valproic acid teratogenicity*. Reprod Toxicol, 2010. **30**(3): p. 457-68.



CHAPTER

Molecular neural crest cell
markers enable discrimination
of organophosphates in the
murine cardiac embryonic
stem cell test

R.H. Mennen, N. Hallmark, M. Pallardy, R. Bars,
H. Tinwell, A.H. Piersma

Toxicology Reports. 2021 Jul 31; 8: 1513-1520

DOI: [10.1016/j.toxrep.2021.07.017](https://doi.org/10.1016/j.toxrep.2021.07.017)

Abstract

The cardiac embryonic stem cell test (ESTc) originally used the differentiation of beating cardiomyocytes for embryotoxicity screenings of compounds. However, the ESTc consists of a heterogeneous cell population, including neural crest (NC) cells, which are important contributors to heart development *in vivo*. Molecular markers for NC cells were investigated to explore if this approach improved discrimination between structurally related chemicals, using the three organophosphates (OP): chlorpyrifos (CPF), malathion (MLT), and triphenyl phosphate (TPP). To decrease the test duration and to improve the objective quantification of the assay read-out, gene transcript biomarkers were measured on study day 4 instead of the traditional cardiomyocyte beating assessment at day 10. Gene expression profiling and immunocytochemistry were performed using markers for pluripotency, proliferation and cardiomyocyte and NC differentiation. Cell proliferation was also assessed by measurements of embryoid body (EB) size and total protein quantification (day 7). Exposure to the OPs resulted in similar patterns of inhibition of beating cardiomyocyte differentiation and of myosin protein expression on day 10. However, these three chemically related compounds induced distinctive effects on NC cell differentiation, indicated by changes in expression levels of the NC precursor (*Msx2*), NC marker (*Ap2a*), and epithelial to mesenchymal transition (EMT; *Snai2*) gene transcripts. This study shows that investigating NC markers can provide added value for ESTc outcome profiling and may enhance the applicability of this assay for the screening of structurally related test chemicals.

Key words: cardiac embryonic stem cell test, neural crest, developmental toxicology, organophosphates

Introduction

European legislation for chemical safety necessitates extensive *in vivo* toxicity testing requiring large amounts of laboratory animals. The field of developmental toxicology has been estimated to demand a large part (approximately 65%) of all test animals in Registration, Evaluation, Authorisation and Restriction of Chemicals (REACH) and therefore is a focal area for the development of alternatives to animals [1, 2]. The cardiac Embryonic Stem cell Test (ESTc) is an often studied animal-free model in developmental toxicology. Originally the ESTc uses the differentiation to beating cardiomyocytes as a screening tool to identify embryotoxic compounds and has been validated by the European Centre for the Validation of Alternative Methods (ECVAM) [3]. However, this assay is known to be limited in various aspects. Therefore, refining this assay could make it more useful as part of a chemical hazard testing and profiling paradigm.

One of the limitations is the 10-day duration of the test restricting the possibility to use it as a high-throughput screening tool. In addition, the read-out of the test is rather subjective i.e. scoring embryoid bodies (EBs) for beating cardiomyocytes by human eye, using a light microscope. To reduce test duration and to improve the objective quantification of the test results, it is necessary to incorporate alternative and more accurate technologies, such as quantification of the expression of a pre-determined gene transcript set. Quantifying the read-out can improve effect assessment and provide potency rankings between similar chemical structures within the same compound class.

A second limitation is that the standard ESTc protocol only considers beating cardiomyocyte differentiation, effectively ignoring potential effects on any other cell types also present. Neural crest (NC) cell presence in the heterogenous ESTc population has been demonstrated previously in our laboratory, using specific NC markers [4]. By extending the investigations into this cell population within the ESTc, the biological domain of this assay can be better defined and employed. This may enhance the detection of potential embryo-toxicants that do not affect cardiomyocyte differentiation in the ESTc.

This added value of NC cell differentiation related gene expression readouts in the ESTc was explored by testing Organophosphates (OPs), a chemical family with pesticide and flame-retardant applications. Some OPs cause differential developmentally toxic effects in animal models [5]. The mechanism through which

the OPs would cause developmental toxicity was long thought to be by specifically inhibiting neuropathy target esterase (NTE) and acetylcholinesterase (AChE) [6]. However, differences in developmental effects observed in rats suggested different mechanisms of action among OPs [6]. Some OPs interact with muscarinic receptors in rats in the nanomolar range as agonists of the m_2 subtype, involved in cardiac contraction [6, 7]. Direct effects of some OPs with rat cardiac muscarinic receptors *in vitro* would suggest a potential contribution to cardiac toxicity [7]. The most extensively used OP pesticide is chlorpyrifos (CPF) and acts on cell signalling cascades involved in cardiac and hepatic homeostasis in rats [8].

Exposure of pregnant rats to CPF showed increased degenerated neurons in the cerebellum of the offspring, but also a reduced numbers of Purkinje cells [9]. In neonatal rats, a dose-dependent decrease in muscarinic receptors and reductions in acetylcholine esterase (AChE) were reported [9]. Other studies reported a delay in psychobiological development in neonatal rats when dams were exposed to 1 mg/kg per os [10]. *Farag et al.* [11] described multiple malformations at maternally toxic doses of 25 mg/kg per day, including anophthalmia and ectrodactyly, cleft soft palate, liver haemorrhage, cranial retardation, retardation of pelvic bones, and absence of phalanges. The maternal effects included reduction in body weight and AChE activity [11]. Malathion (MLT) and the flame retardant triphenyl phosphate (TPP) were neither fetotoxic nor teratogenic in rabbits (for MLT) and rats (for TPP) [12, 13].

These differences in effect may be attributed to the metabolism of the compounds *in vivo*. CPF and MLT are metabolised to reactive oxon metabolites by hepatic microsomal enzymes [9, 14-16]. These oxon metabolites are more potent inhibitors of the AChE enzyme, although there is significant evidence that also other targets are affected by both the parent compounds and metabolites [17-21]. For TPP the parent compound is more reactive and is degraded by hydrolysis into its metabolites diphenyl and monophenyl phosphates by CYP450 enzymes [22, 23]. In zebrafish, CPF, MLT and TPP did show a range of teratogenic effects, including cardiac-related developmental defects [20, 24-26]. CPF induced pericardial oedema, MLT induced bradycardia and a reduced heart rate [20, 25], and TPP impaired cardiac looping and function in the zebrafish model [26]. The variety of developmental effects observed and the proposed mechanisms in different models warrant further investigations within this chemical class.

We studied the OPs CPF, MLT and TPP in the ESTc, specifically for their interference with proliferation, cardiac differentiation, and NC cell development in order to explore the benefit of additional molecular parameters for assessing differential developmental toxicity of structurally related chemicals.

Methods

Test compounds

Chlorpyrifos (CPF, CAS# 2921-88-2), malathion (MLT, CAS# 121-75-5), and triphenyl phosphate (TPP, CAS# 115-86-6) were obtained from Sigma-Aldrich (Zwijndrecht, The Netherlands) and were tested in the subsequent described assays at concentrations up to 330 μM in order to obtain sigmoid-shaped concentration-response curves. 0.25% dimethyl sulfoxide (DMSO, CAS# 67-68-5, Sigma-Aldrich) was used as a solvent.

Stem cell culture

Murine embryonic stem cells (ES-D3 (D3), ATCC®, Manassas, VA, USA) were cultured as previously described [4, 27]. In short, the cells were cultured every 2-3 days in a humidified atmosphere of 37°C with 5% CO_2 by using culture dishes (35 mm, Corning, New York, NY, USA). The culture medium consisted of Dulbecco's Modified Eagle's Medium (DMEM; Gibco, Waltham, MA, USA) enriched with 20% Fetal Bovine Serum (FBS; Greiner Bio-One, Kremsmünster, Austria); 2 mM L-Glutamin (Gibco); 1% Non-Essential Amino Acids (NEAA; Gibco); 1% 5000 IU/ml Penicillin/5000 $\mu\text{g}/\text{ml}$ Streptomycin (Gibco); and 0.1 mM β -mercaptoethanol (Gibco). 1000 units/ml leukemia inhibitory factor (LIF; ESGRO®, Millipore, Burlington, MA, USA) was added to the medium to maintain the ES-D3 cells in a pluripotent state.

Cell viability assay

Cell viability of the ES-D3 cells was executed as before [28]. 500 cells per well were plated in a 96-wells plate (Greiner Bio-One) and were kept warm at 37°C and 5% CO_2 for two hours. Cells were exposed in six replicates to 200 μl of LIF-containing medium including the OPs in concentrations ranging from 330 μM to 0,33 μM or 0 μM or including the negative control penicillin G (500 $\mu\text{g}/\text{ml}$; Sigma-Aldrich), the positive control 5-fluoruracil (0.1 $\mu\text{g}/\text{ml}$; Sigma-Aldrich), or the vehicle control

DMSO (0.25%; Sigma-Aldrich). The exposure medium was refreshed at identical final concentrations after three days of exposure under 37°C and 5% CO₂. Following incubation for a further two days, the exposed plates were prepared for the viability fluorescence measurements by replacing 100 µl of solution by 20 µl of CellTiter-Blue reagent (Promega, Leiden, The Netherlands) per well [29]. After 2 hours of incubation the extinction values were determined at 544_{Ex}/590_{Em} nm on the SpectraMax® M2 spectrofluorometer (Molecular Devices, Berkshire, United Kingdom). Viability levels were calculated relative to the DMSO control (in %). For each test compound the average and standard deviation of the six replicates of each experiment (n=3) were analysed using PROAST v67.0 as described in the statistics section. This was used to determine the concentration for which 50% of the cells were viable (IC₅₀ values).

Cell differentiation assay

A previously described protocol was used to differentiate the ES-D3 cells into cardiomyocytes during the ESTc assay [3, 27]. A similar medium composition was used as for stem cell culture and viability testing except LIF was no longer provided, to enable differentiation. At differentiation day 0, hanging drops were formed by plating a 3.75·10⁴ cells/ml suspension in 56 droplets of 20 µl to the lid of a 100/20 mm CELLSTAR® cell culture dish (Greiner Bio-One), which itself held 5 ml of ice-cold phosphate buffered saline (PBS; Ca²⁺, Mg²⁺ free; Gibco). The hanging drops were kept warm at 37°C and 5% CO₂ for 3 days and were relocated to a 60 mm bacterial petri dish (Greiner Bio-One) with 5 ml of exposure medium. This exposure medium contained concentrations between 330 µM to 0,33 µM of CPF, MLT, TPP or contained controls. After two days of consequent incubation, each embryonic body (EB) was transferred to a well of a culture plate (24-wells, Greiner Bio-One) with 1 ml of exposure medium or controls. Within one experiment, each plate consisted of one condition (=24 replicates) and was performed in duplicate. On differentiation day 10, after exposing the EBs for an additional 5 days, the EBs were scored for beating cardiomyocytes using a bright field microscope (Olympus BX51, Shinjuku, Japan). The number of beating EBs was divided by the total number of EBs per 24-wells plate. These data were pragmatically used for protein and gene expression analysis in order to determine a concentration at which an effect was measured. To determine such a concentration, two independent experiments were performed for each test compound. The dose for which beating cardiomyocyte differentiation was inhibited at 50% (ID₅₀) was determined for each compound as described in the statistics section.

Embryoid body (EB) size measurements

To measure effects on proliferation, EB size and total protein were measured as surrogates for proliferation success. The differentiation test was performed as described in the previous paragraph with the same exposure concentrations for the three compounds. To be able to capture one EB with a 4x magnification, EB sizes were measured at differentiation day 7. The EB sizes were captured using a bright field microscope (Olympus BX51, Shinjuku, Japan) and the software CellSens Standard version 2.3 (Olympus Life Science). Measurements were executed by indicating the EB borders using ImageJ 1.51n, which computed the EB area. The average area of 24 EBs per condition was calculated and the 50% effect concentrations (EC_{50} values) were determined as described in the statistics section.

Total protein measurements

The differentiation test was performed with the same exposure concentrations for CPF, MLT, and TPP. At differentiation day 7, 24 EBs per condition were incubated in cell dissociation buffer (Gibco) at 37°C for 3 minutes. The EBs were collected and after precipitation they were washed with PBS (Ca^{2+} , Mg^{2+} free; Gibco). The EBs were permeabilised in 1ml of 1% Triton X-100 for 5 minutes (T9284, Sigma-Aldrich) and protein levels were measured in triplicate using the Micro BCA™ Protein Assay Kit (Thermo Fisher) according to manufacturer's protocol [30]. EC_{50} values were determined as described in the statistics section.

Protein expression analysis

The differentiation test was performed with exposure to ID_{50} values of each compound or with a 0.25% DMSO control. Immunocytochemistry was performed according to a previously described protocol [4]. On differentiation day 5, EBs were collected in 35mm culture dishes for further differentiation and were later stained using immunocytochemistry on differentiation day 10. The samples were washed with PBS (37°C, Ca^{2+} , Mg^{2+} free; Gibco) and were fixed with 4% formaldehyde (Electron Microscopy Sciences, Hatfield, PA, USA) for 30 minutes at differentiation day 10. For up to 7 days, the fixed cells were kept at 4°C until the moment of staining. The cells were washed for 3x5 minutes with PBS (Ca^{2+} , Mg^{2+} free; Gibco) in between each step of the protocol and before and after storage. The EBs were incubated at room-temperature with 0.2% Triton X-100 (T9284, Sigma-Aldrich) in PBS (Ca^{2+} , Mg^{2+} free; Gibco) for 5 minutes to permeabilise the cells. To minimise non-specific

protein binding, samples were incubated with 1% bovine serum albumin (BSA, Sigma-Aldrich) with 0.5% Tween-20 (Sigma-Aldrich) in PBS (Ca^{2+} , Mg^{2+} free; Gibco) for 1 hour. The following primary antibodies were added to the EBs in dilution buffer (0.5% BSA, 0.5% Tween-20 in PBS (Ca^{2+} , Mg^{2+} free; Gibco)) at 4°C overnight: Activating Enhancer-Binding Protein 2 Alpha (AP2 α , early NC marker, sc-12726, Santa-Cruz, 1:100), Myosin Heavy Chain (MF20, MAB4470, R&D Systems, 1:100), proliferation marker (Ki67, MA5-14520, Thermo Fisher, 1:500), E-cadherin (ECAD, ECCD-2, 13-1900, Thermo Fisher, 1:1000). The next day, the following secondary antibodies in dilution buffer were added for 1 hour: goat-anti-mouse A647 (1:500, A21236, Thermo Fisher), goat-anti-rabbit A488 (1:1000, A11034, Thermo Fisher) or goat-anti-rat A555 (1:500, A21434, Thermo Fisher). A concentration of 1 $\mu\text{g}/\text{ml}$ DAPI (Sigma-Aldrich) in dilution buffer was added to the EBs and incubated for 10 minutes. The EBs were washed with PBS (Ca^{2+} , Mg^{2+} free; Gibco) for 10 minutes and were covered with a cover glass and mounting medium (Thermo Fisher). The EBs were visualised with a 4x magnification DMI8 microscope (Leica, Germany) with a Leica DFC7000 GT camera (Leica, Germany).

Gene expression analysis

The stem cells were differentiated until day 4 (24 hours of exposure) of the protocol and samples were collected from EBs exposed to ID_{50} concentrations for each compounds determined as described in the statistics section or to the DMSO control (0.25%). 7 to 8 EB samples in RNAlater (Qiagen, Cat # 76526) from two independent experiments ($n=2$) were stored at -80°C . Parallel to this, beating was scored of control plates on differentiation day 10. The stored samples were used for RNA isolation (RNeasy Mini-kit, Qiagen, Cat. # 74104) according to manufacturer's protocol [31]. QIAshredder columns (Qiagen, Cat. # 79654) homogenised the samples and a DNase step (RNase-Free DNase set, Qiagen, Cat # 79254) was added to the RNA isolation protocol. RNA quantity and quality was assessed using the Nanodrop (Nanodrop Technologies Inc., Wilmington, Delaware) and the 2100 Bioanalyzer (Agilent Technologies, Amstelveen, The Netherlands). Quality control results contained 260 nm/280 nm absorbance ratios between 1.9 and 2.2. RIN (RNA Integrity Number) scores were evaluated >8.2 . cDNA was synthesised using a cDNA synthesis kit (Applied Biosystems, Foster City, CA, USA) according to manufacturer's prescriptions. The cDNA was quantified using the thermal cycling conditions: 95°C for 20s, followed by 40 cycles of 95°C for 3s and 60°C for 30s using a 7500 Fast Real-Time PCR system (Applied Biosystems). The used TaqMan® Assays (Thermo

Fisher Scientific) are listed in table S1. The relative differences were calculated using the $-\Delta\Delta\text{Ct}$ method [32], and were normalised against the mean expression levels of the *Hprt1*, *Gusb*, and *Polr2a* housekeeping genes (Table S1). The expression levels for each experiment separately, are provided as supplementary material in figure S1 for experiment 1 and in figure S2 for experiment 2.

Statistics

The obtained data on cell viability, differentiation, EB size, and protein levels were fitted and statistically analysed using PROAST v67.0 using the exponential method [33]. IC_{50} , ID_{50} , and EC_{50} values were obtained from the concentration-response curves with 90% confidence lower and upper benchmark concentration limit values (BMCL-BMCU). Control values were added to the graphs using a dummy value. An one-way ANOVA test with a post-hoc Sidak's multiple comparisons test ($p < 0.05$) was performed to compare gene expression data to the control samples.

Results

Effects on EB proliferation

The effects of OPs on EB size and total protein content were used as surrogates to determine the *in vitro* concentration provoking a 50% reduction (EC_{50}) in EB proliferation. The EB area (fig. 1a) and total protein content (fig. 1b) were reduced by all three OPs in a concentration-dependent manner. For the EB area measurements (fig. 1a), comparable EC_{50} levels were found, except for MLT which resulted in a lower EC_{50} value where confidence limits did not overlap the values of CPF and TPP (fig. 1a, table 1). The total protein measurements resulted in comparable EC_{50} values for all treated groups (fig. 1b, table 1).

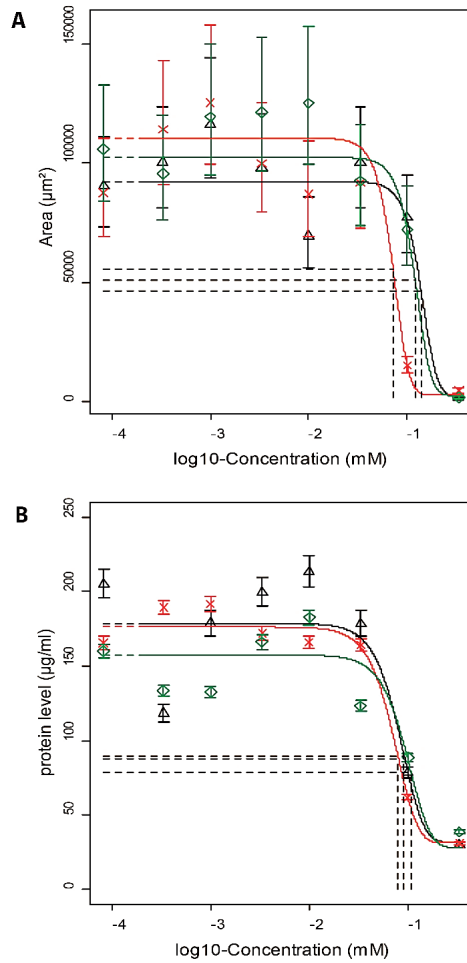


Figure 1: Concentration-response relationships of CPF, MLT, and TPP on a) EB area and b) total protein content on differentiation day 7. a) EB area expressed in μm^2 for concentrations tested up to 330 μM during differentiation until day 7. The datapoints show the size average of 24 EBs per condition, b) Total protein level expressed in $\mu\text{g/ml}$ for each sample, which consisted of 24 EBs. The datapoints indicate the average of three measurements per sample. Black Δ = CPF, red \times = MLT, green \diamond = TPP. Control values were indicated at the starting point of each graph and were connected by dotted (coloured) lines to the exposure measurements. Error bars indicate standard deviation. Dotted lines specify the EC₅₀ values obtained through statistical analysis using the exponential method of PROAST v67.0 in R.

Table 1: Summary of inhibitory and effective concentrations for the tested endpoints after exposure to CPF, MLT, and TPP. EC_{50} , IC_{50} , and ID_{50} values are indicated in μM with lower and upper BMC confidence limits (BMCL – BMCU).

	Chlorpyrifos	Malathion	Triphenyl phosphite
EB area (EC_{50}); day 7	139 μM (117-162)	72.0 μM (65.3-75.1)	120 μM (106-145)
Protein level (EC_{50}); day 7	92.0 μM (81.6-105)	80.2 μM (75.0-86.1)	108 μM (94.7-129)
Viability (IC_{50})	85.7 μM (42.5-118)	49.4 μM (22.8-105)	61.4 μM (29.9-139)
Differentiation (ID_{50}); day 10	117 μM (74.2-189)	73.2 μM (60.3-73.8)	143 μM (121-168)

Effects on cell viability and functional cardiomyocyte differentiation

The classical ESTc measures of cell viability and cardiomyocyte differentiation were assessed and compared between the three compounds. Viability was reduced with IC_{50} concentrations for CPF, MLT, and TPP of 85.7 μM , 49.4 μM , and 61.4 μM , respectively (fig. 2a, b, c, table 1). CPF, MLT, and TPP reduced the development of beating cardiomyocytes with ID_{50} levels of 117 μM , 73.2 μM , and 143 μM , respectively (fig. 2d, e, f, table 1). The overlapping BMC confidence limits of the three compounds indicated no differences in ID_{50} for inhibition of beating cardiomyocytes or IC_{50} values for cell viability.

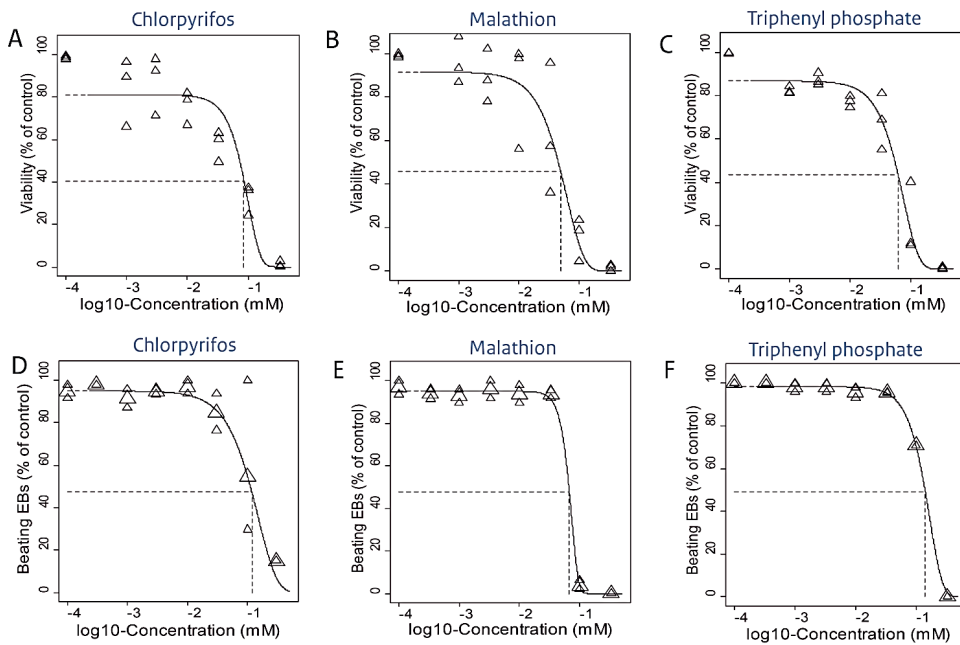


Figure 2: Cell viability and cardiomyocyte differentiation effects after exposure to CPF, MLT, and TPP. Viability was depicted as relative to the control for a) CPF, b) MLT, and c) TPP and datapoints represent six replicates. Three independent experiments were conducted. The dotted lines specify the IC₅₀ values. Effects on differentiation of cardiomyocytes for d) CPF, e) MLT, and f) TPP are expressed in percentage of beating embryoid bodies (EBs) on differentiation day 10 with small triangles as data points and large triangles as average from two independent experiments. The dotted lines specify the ID₅₀ values obtained through statistical analysis using the exponential method of PROAST v67.0 in R.

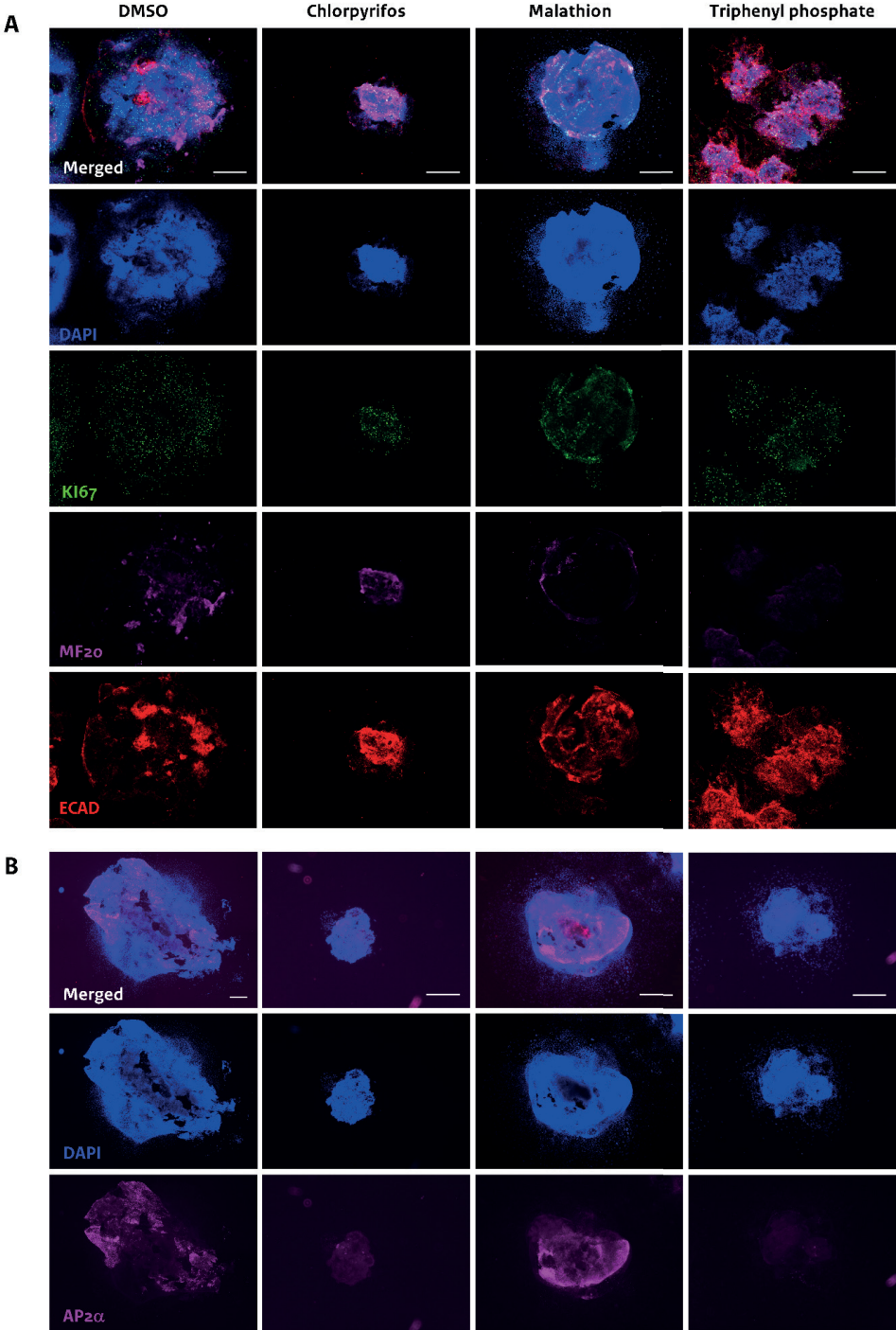
Effects of OPs on protein and gene expression levels

As the classical readouts didn't show differences between the compounds, we needed to zoom in on specific protein and gene expression levels. Effects on proliferation and differentiation were studied with markers for pluripotency, proliferation, cardiomyocyte differentiation, and neural crest cell differentiation. Fig. 3a shows immunostainings for proliferation (Ki67), the cardiomyocyte marker myosin heavy chain (MF20), and pluripotency (ECAD) markers after exposure to ID₅₀ concentrations of CPF, MLT, TPP (for concentrations used see table 1) and DMSO (vehicle control). DAPI was used to stain cell nuclei. CPF and MLT exposure showed a more solid DAPI staining within the EBs than controls, whereas TPP exposure

affected the round shape of the EBs. Ki67 staining appeared evenly distributed through the EB relative to total amount of cells for all conditions, except for MLT exposure. Staining of MF20 showed clear presence of myosin in all EBs except for the TPP exposed EBs. ECAD staining for pluripotency was present in all exposure groups with staining areas located at different positions within the EB. Fig. 3b indicates presence of the neural crest marker AP2 α with clear expression in the MLT and DMSO groups. CPF and TPP exposure did not show a clear AP2 α staining.

To assess if the differences between control and treated EBs observed qualitatively at the protein level were also present at the gene transcript level, gene expression analysis was performed for markers of acetylcholine esterase (Ache), cell death, pluripotency, proliferation, cardiomyocyte differentiation and neural crest cell differentiation (fig. 3c,d). Expression for Ache seemed to be augmented by CPF and TPP but not by MLT compared to controls, as the two performed experiments showed opposite results in Ache expression for MLT as shown in figures S1 and S2. Regarding cell death, the pro-apoptotic marker Casp3 was statistically significantly downregulated by CPF, but not by TPP and MLT. The expression levels for the necrosis marker Parp1 were not affected in any of the exposures groups. The pluripotency marker Ssea-1 showed an upregulated trend in the TPP exposed group and Cdh1 (=Ecad) was statistically significantly upregulated by all three exposure groups. Ki67 for proliferation showed a downregulated trend in the TPP exposed group and the cardiomyocyte marker Nkx2-5 showed an upregulated trend in the TPP exposed group. MLT exposure resulted in opposite expression levels in up- or downregulation of Nkx2-5 when comparing the two experiments, as shown in the supplementary figures S1 and S2.

As to NC markers, Msx2 showed a downregulated trend in all three exposure groups and the epithelial-to-mesenchymal transition (EMT) marker Snai2 for NC was statistically significantly upregulated in the CPF and TPP exposed groups when compared to the control.



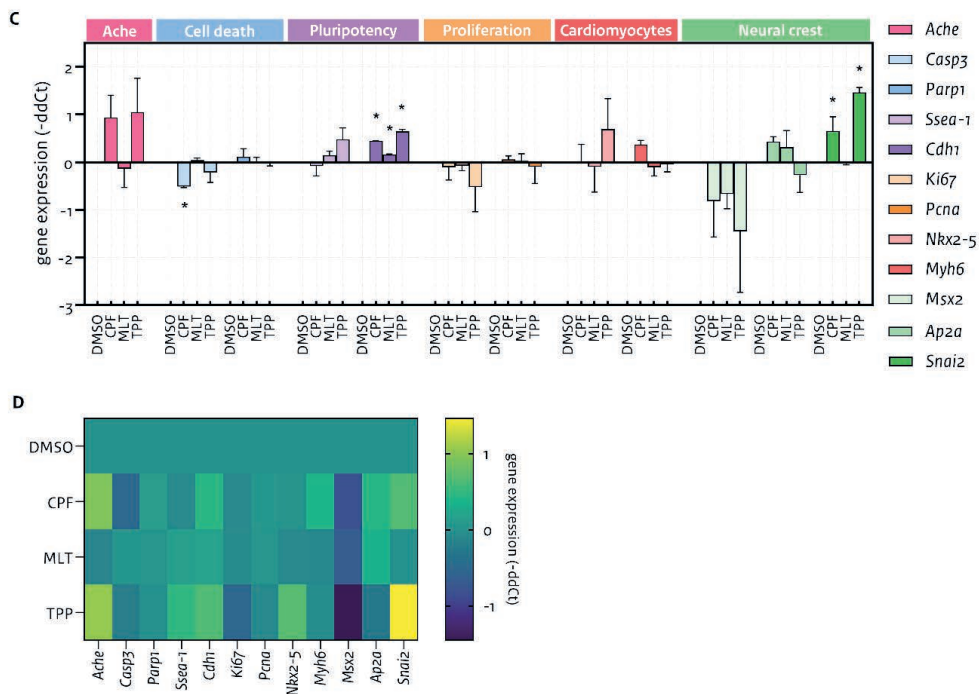


Figure 3: Effects of CPF, MLT or TPP on the expression levels of markers for Ache, cell death, pluripotency, proliferation, cardiomyocyte differentiation, and neural crest cell differentiation in the ESTc assay. a) Immunocytochemistry staining of the nuclei (DAPI), proliferation marker Ki67 (1:500), myosin heavy chain marker MF20 (1:100), and pluripotency marker ECAD (1:1000) after exposure to 0.25% DMSO or ID50 concentrations of CPF, MLT and TPP at differentiation day 10 (7 days of exposure). Scale bar indicates 500 μ m, magnification 4x. b) Immunocytochemistry staining of the nuclei (DAPI) and neural crest marker AP2 α (1:100) after exposure of 0.25% DMSO or ID50 concentrations of CPF, MLT and TPP at differentiation day 10 (7 days of exposure). Scale bar indicates 500 μ m, notice the smaller scale bar for the DMSO control for which the image was stitched. magnification 4x. c) Expression levels of Ache, cell death, pluripotency, proliferation, cardiomyocyte and neural crest cell related genes after exposure to the ID50 concentrations at differentiation day 4 (24 hours of exposure). Gene expression was measured using real-time PCR. Error bars indicate the standard deviation. Two independent experiments with in total 7-8 samples. Asterisks indicate a significant difference compared to the DMSO control (one-way ANOVA; Sidak's multiple comparisons post-hoc test). * $p < 0.05$. d) Mean gene expression levels expressed as -ddCt in a heatmap with scale bar ranging from yellow (upregulation) to blue (downregulation).

Discussion

The objectives of the experiments conducted in this work were to investigate the added value of molecular gene and protein markers for cell proliferation, cardiomyocyte differentiation, and neural crest (NC) cell development to distinguish between structurally related compounds using the ESTc. Using the organophosphates CPF, MLT, and TPP as model compounds, distinctive effects on gene expression were observed, while effects on cell proliferation and differentiation were not distinctive. At differentiation day 4 (24 hours of exposure), gene expression regulation of NC cell markers revealed clear differences between the compounds. Therefore, NC marker gene expression profiles provide specific developmental toxicity information in addition to the cardiomyocyte beating read-out of the standard ESTc, and so may contribute to the screening and prioritisation of new chemicals for further commercial development.

In particular, the three NC cell specific genes tested did show clear and distinct responses after 24 hours of exposure (*Msx2*, *Ap2 α* and *Snai2*, fig 3). All three compounds showed a downregulated trend of *Msx2* gene expression. *Msx2* is a neural plate border specifier and a NC precursor gene present in the neural folds [34]. The expression levels of *Ap2 α* were upregulated by CPF and MLT (fig. 3c). *AP2 α* is a NC specifier and alterations in its gene or protein expression affect the non-neural ectoderm, neural plate border, neural folds and in derivatives of the NC cells. These alterations cause defects in NC derivatives in mutant mice [34, 35]. Additionally, exposure to TPP and CPF showed a statistically significantly *Snai2* gene transcript upregulation compared to the control. *SNAI2* acts as a transcriptional repressor of e.g. E-cadherin and a *Snai2* overexpression would stimulate NC cell delamination and migration by activating epithelial to mesenchymal transition (EMT) when the NC cells separate from the neural tube [34, 35]. Although neural tube closure and NC migration akin to *in vivo* morphogenesis cannot occur in the *in vitro* ESTc assay, alterations were observed in the expression levels of NC cell markers after 24 hours of exposure (differentiation day 4) to the tested OPs. The presence of NC cells in the ESTc has been investigated in previous research and also showed compound specific effects when testing valproic acid analogues [4]. These previous and current findings confirm the utility of assessing gene expression profiling at an early time-point as part of the toxicity screening with the ESTc [36-38].

The use of a short exposure duration of 24 hours for gene expression analysis may also benefit distinguishing developmental effects from possible effects on viability

that may arise after longer exposures as shown in figure 1 and 2. After 24 hours of exposure, the expression levels of Casp3, which is a pro-apoptotic gene, were statistically significantly down-regulated following CPF exposure, whereas TPP and MLT did not affect its expression (fig3c). This suggests that the apoptotic pathway is not activated yet at this time-point. The downregulation of pro-apoptotic Casp3 expression levels was accompanied by an upregulation of the pluripotency marker Cdh1. This latter observation illustrates the relationship between increases of highly proliferating pluripotent cells and a relatively lower level of apoptosis. Therefore, monitoring effects on gene expression levels is of added value to the ESTc.

Additionally, a short exposure duration of 24 hours benefits NC cell gene expression over cardiomyocyte gene expression. After 24 hours TPP exposure, the early cardiomyocyte differentiation marker Nkx2-5 seemed to be differently expressed, but the late differentiation marker Myh6 was not expressed yet. In the ESTc, myosin structures start to form on differentiation day 7 [4]. Also on the gene expression level, Myh6 for myosin is expressed later during development and was most evidently expressed on differentiation day 14 of the embryonic stem cell line HMI [39].

The effects of the OPs CPF, MLT or TPP specifically on NC cell differentiation have been previously studied to a limited extent. Tussellino et al. (2016) showed developmental defects caused by CPF on anatomical NC derived cranial structures and NC gene expression levels in *Xenopus laevis* [40]. In the chick (*Gallus domesticus*), exposure to a mixture of CPF and cypermethrin (50%; 5%) during embryo development affected the cranial NC cells and resulted in craniofacial dysmorphism [41]. In zebrafish, impairments in cardiac looping and function defects were observed after exposure to TPP [42-47]. Defects in neural crest cell differentiation and migration can cause cardiac deficiencies during embryogenesis, like defective outflow tract septation, abnormal patterning of the aortic arch and great arteries and abnormal cardiac tube looping [48, 49].

In contrast to the effects of OPs on NC cell differentiation, the effects on acetylcholine esterase (AChE) have been more extensively studied. OPs inhibit the activity of this enzyme [6, 9, 11]. In this study, Ache gene expression levels seemed to be augmented by CPF and TPP (fig. 3c). Although an inhibition of Ache would be expected, the opposing upregulation of gene expression levels after exposure to CPF has been measured before in embryonic stem cells in conditions where

the enzymatic activity was inhibited [15]. Based on the gene expression results in general, TPP seems to be more potent and this may be explained by the lack of metabolic activation within the ESTc. TPP is degraded by hydrolysis into less reactive metabolites diphenyl and monophenyl phosphates by CYP450 enzymes [22, 23]. CPF and MLT are metabolised *in vivo* by hepatic microsomal enzymes, belonging to the CYP450 family, to their reactive oxons [9, 14-16] [50-53]. These metabolites have a higher affinity for AChE in fungicides, although there is significant evidence also other targets are affected that cause adverse effects *in vivo* by both the parent compounds and metabolites [17-21]. In line with most *in vitro* cellular assays, the ESTc has limited xenobiotic metabolic capacity [54, 55]. This should be taken into account in *in vitro-in vivo* extrapolations for which the mechanistic boundaries should be further explored [55].

Taken together, our results indicate that adding parameters specific to the neural crest (NC) cell population and gene expression analysis allows discrimination between the tested compounds that is not observable with classical readout parameters usually monitored in the ESTc. Therefore, molecular markers for neural crest differentiation provide a benefit for the detection and discrimination of putative developmental toxicants in the ESTc. In general, this study illustrates the usefulness of more fully exploring and exploiting the biological domain of *in vitro* assays for toxicity screening.

Acknowledgements

Gina Mennen was supported through a CIFRE PhD grant no. 2018-0682 by the French National Association for Research and Technology (ANRT), which was co-supervised by Aldert Piersma, Marc Pallardy, Nina Hallmark, Helen Tinwell, and Remi Bars. Aldert Piersma was supported by the Dutch Ministry of Health, Welfare and Sports. A special thank you to Harm Heusinkveld who critically reviewed the manuscript.

References

1. Piersma, A.H., *Alternative methods for developmental toxicity testing*. Basic Clin Pharmacol Toxicol, 2006. **98**(5): p. 427-31.
2. van der Jagt, K., Munn, S., Torslov, J., de Bruijn, J., *Alternative Approaches Can Reduce the Use of Test Animals under REACH*. 2004, EC Joint Research Centre.
3. Genschow, E., et al., *Validation of the embryonic stem cell test in the international ECVAM validation study on three in vitro embryotoxicity tests*. Altern Lab Anim, 2004. **32**(3): p. 209-44.
4. Mennen, R.H.G., J.L.A.J. Pennings, and A.H.A. Piersma, *Neural crest related gene transcript regulation by valproic acid analogues in the cardiac embryonic stem cell test*. Reproductive toxicology (Elmsford, N.Y.), 2019. **90**: p. 44-52.
5. Nurulain, S. and M. Shafiullah, *Teratogenicity and embryotoxicity of organophosphorus compounds in animal models-a short review*. Mil. Med. Sci. Lett. (Voj. Zdrav. Listy) 2012, vol. 81(1), p. 16-26, 2012. **81**: p. 16-26.
6. Costa, L.G., *Current issues in organophosphate toxicology*. Clin Chim Acta, 2006. **366**(1-2): p. 1-13.
7. Howard, M.D. and C.N. Pope, *In vitro effects of chlorpyrifos, parathion, methyl parathion and their oxons on cardiac muscarinic receptor binding in neonatal and adult rats*. Toxicology, 2002. **170**(1-2): p. 1-10.
8. Meyer, A., F.J. Seidler, and T.A. Slotkin, *Developmental effects of chlorpyrifos extend beyond neurotoxicity: critical periods for immediate and delayed-onset effects on cardiac and hepatic cell signaling*. Environmental health perspectives, 2004. **112**(2): p. 170-178.
9. Commission, E., *Draft Renwal Assessment Report prepared according to the Commission Regulation (EU) No 1107/2009, in Chlorpyrifos*. 2017.
10. Laporte, B., et al., *Developmental neurotoxicity in the progeny after maternal gavage with chlorpyrifos*. Food Chem Toxicol, 2018. **113**: p. 66-72.
11. Farag, A.T., A.M. El Okazy, and A.F. El-Aswed, *Developmental toxicity study of chlorpyrifos in rats*. Reprod Toxicol, 2003. **17**(2): p. 203-8.
12. Welsh, J.J., et al., *Teratogenic potential of triphenyl phosphate in Sprague-Dawley (Spartan) rats*. Toxicology and industrial health, 1987. **3**(3): p. 357-369.
13. Machin, M.G. and W.G. McBride, *Teratological study of malathion in the rabbit*. Journal of toxicology and environmental health, 1989. **26**(3): p. 249-253.
14. Commission, E., *Draft Assessment Report (DAR), in Malathion*. 2004.
15. Estevan, C., E. Vilanova, and M.A. Sogorb, *Chlorpyrifos and its metabolites alter gene expression at non-cytotoxic concentrations in D3 mouse embryonic stem cells under in vitro differentiation: considerations for embryotoxic risk assessment*. Toxicol Lett, 2013. **217**(1): p. 14-22.
16. Lu, X.T., et al., *Cytotoxicity and DNA damage of five organophosphorus pesticides mediated by oxidative stress in PC12 cells and protection by vitamin E*. J Environ Sci Health B, 2012. **47**(5): p. 445-54.
17. Gao, J., et al., *Chlorpyrifos and chlorpyrifos oxon impair the transport of membrane bound organelles in rat cortical axons*. Neurotoxicology, 2017. **62**: p. 111-123.

18. Sogorb, M.A., et al., *Effects of mipafox, paraoxon, chlorpyrifos and its metabolite chlorpyrifos-oxon on the expression of biomarker genes of differentiation in D3 mouse embryonic stem cells*. Chem Biol Interact, 2016. **259**(Pt B): p. 368-373.
19. Estevan, C., et al., *Organophosphorus pesticide chlorpyrifos and its metabolites alter the expression of biomarker genes of differentiation in D3 mouse embryonic stem cells in a comparable way to other model neurodevelopmental toxicants*. Chem Res Toxicol, 2014. **27**(9): p. 1487-95.
20. Dishaw, L.V., et al., *Developmental exposure to organophosphate flame retardants elicits overt toxicity and alters behavior in early life stage zebrafish (Danio rerio)*. Toxicological sciences : an official journal of the Society of Toxicology, 2014. **142**(2): p. 445-454.
21. Eaton, D.L., et al., *Review of the toxicology of chlorpyrifos with an emphasis on human exposure and neurodevelopment*. Crit Rev Toxicol, 2008. **38 Suppl 2**: p. 1-125.
22. Zhang, Q., et al., *Metabolic Mechanism of Aryl Phosphorus Flame Retardants by Cytochromes P450: A Combined Experimental and Computational Study on Triphenyl Phosphate*. Environ Sci Technol, 2018. **52**(24): p. 14411-14421.
23. Tsugoshi, Y., et al., *Inhibitory effects of organophosphate esters on carboxylesterase activity of rat liver microsomes*. Chem Biol Interact, 2020. **327**: p. 109148.
24. Ducharme, N.A., et al., *Comparison of toxicity values across zebrafish early life stages and mammalian studies: Implications for chemical testing*. Reproductive toxicology (Elmsford, N.Y.), 2015. **55**: p. 3-10.
25. Simoneschi, D., F. Simoneschi, and N.E. Todd, *Assessment of cardiotoxicity and effects of malathion on the early development of zebrafish (Danio rerio) using computer vision for heart rate quantification*. Zebrafish, 2014. **11**(3): p. 275-80.
26. McGee, S.P., et al., *Aryl phosphate esters within a major PentaBDE replacement product induce cardiotoxicity in developing zebrafish embryos: potential role of the aryl hydrocarbon receptor*. Toxicol Sci, 2013. **133**(1): p. 144-56.
27. Spielmann, H., et al., *The Embryonic Stem Cell Test, an In Vitro Embryotoxicity Test Using Two Permanent Mouse Cell Lines: 3T3 Fibroblasts and Embryonic Stem Cells*. In Vitro Toxicology, 1997. **10**: p. 119-127.
28. de Jong, E., et al., *Potency ranking of valproic acid analogues as to inhibition of cardiac differentiation of embryonic stem cells in comparison to their in vivo embryotoxicity*. Reprod Toxicol, 2011. **31**(4): p. 375-82.
29. *CellTiter-Blue Cell Viability Assay technical bulletin #TB317*. Promega Corporation.
30. Smith, P.K., et al., *Measurement of protein using bicinchoninic acid*. Anal Biochem, 1985. **150**(1): p. 76-85.
31. *RNeasy Mini Handbook*. Qiagen, 2019.
32. Pfaffl, M.W., *A new mathematical model for relative quantification in real-time RT-PCR*. Nucleic Acids Res, 2001. **29**(9): p. e45.
33. Slob, W., *Dose-response modeling of continuous endpoints*. Toxicol Sci, 2002. **66**(2): p. 298-312.
34. Gammill, L.S. and M. Bronner-Fraser, *Neural crest specification: migrating into genomics*. Nat Rev Neurosci, 2003. **4**(10): p. 795-805.
35. Simoes-Costa, M. and M.E. Bronner, *Insights into neural crest development and evolution from genomic analysis*. Genome Res, 2013. **23**(7): p. 1069-80.

36. van Dartel, D.A., et al., *Evaluation of developmental toxicant identification using gene expression profiling in embryonic stem cell differentiation cultures*. *Toxicol Sci*, 2011. **119**(1): p. 126-34.
37. van Dartel, D.A., et al., *Discriminating classes of developmental toxicants using gene expression profiling in the embryonic stem cell test*. *Toxicol Lett*, 2011. **201**(2): p. 143-51.
38. Schulpen, S.H., et al., *Dose response analysis of monophthalates in the murine embryonic stem cell test assessed by cardiomyocyte differentiation and gene expression*. *Reprod Toxicol*, 2013. **35**: p. 81-8.
39. Rungarunlert, S., et al., *Enhanced cardiac differentiation of mouse embryonic stem cells by use of the slow-turning, lateral vessel (STLV) bioreactor*. *Biotechnol Lett*, 2011. **33**(8): p. 1565-73.
40. Tussellino, M., et al., *Chlorpyrifos exposure affects fgf8, sox9, and bmp4 expression required for cranial neural crest morphogenesis and chondrogenesis in Xenopus laevis embryos*. *Environmental and molecular mutagenesis*, 2016. **57**(8): p. 630-640.
41. Sharma, S., et al., *A combination insecticide at sub-lethal dose debilitated the expression pattern of crucial signalling molecules that facilitate craniofacial patterning in domestic chick Gallus domesticus*. *Neurotoxicology and teratology*, 2019. **76**: p. 106836-106836.
42. Reddam, A., et al., *mRNA-Sequencing Identifies Liver as a Potential Target Organ for Triphenyl Phosphate in Embryonic Zebrafish*. *Toxicological sciences : an official journal of the Society of Toxicology*, 2019. **172**(1): p. 51-62.
43. Mitchell, C.A., et al., *Disruption of Nuclear Receptor Signaling Alters Triphenyl Phosphate-Induced Cardiotoxicity in Zebrafish Embryos*. *Toxicological sciences : an official journal of the Society of Toxicology*, 2018. **163**(1): p. 307-318.
44. Shi, Q., et al., *Developmental neurotoxicity of triphenyl phosphate in zebrafish larvae*. *Aquatic toxicology (Amsterdam, Netherlands)*, 2018. **203**: p. 80-87.
45. Isales, G.M., et al., *Triphenyl phosphate-induced developmental toxicity in zebrafish: potential role of the retinoic acid receptor*. *Aquatic toxicology (Amsterdam, Netherlands)*, 2015. **161**: p. 221-230.
46. Du, Z., et al., *Aryl organophosphate flame retardants induced cardiotoxicity during zebrafish embryogenesis: by disturbing expression of the transcriptional regulators*. *Aquatic toxicology (Amsterdam, Netherlands)*, 2015. **161**: p. 25-32.
47. McGee, S.P., et al., *Aryl phosphate esters within a major PentaBDE replacement product induce cardiotoxicity in developing zebrafish embryos: potential role of the aryl hydrocarbon receptor*. *Toxicological sciences : an official journal of the Society of Toxicology*, 2013. **133**(1): p. 144-156.
48. Keyte, A. and M.R. Hutson, *The neural crest in cardiac congenital anomalies*. *Differentiation*, 2012. **84**(1): p. 25-40.
49. Yelbuz, T.M., et al., *Shortened outflow tract leads to altered cardiac looping after neural crest ablation*. *Circulation*, 2002. **106**(4): p. 504-510.
50. Wu, X., et al., *From the Cover: Astrocytes Are Protective Against Chlorpyrifos Developmental Neurotoxicity in Human Pluripotent Stem Cell-Derived Astrocyte-Neuron Cocultures*. *Toxicol Sci*, 2017. **157**(2): p. 410-420.
51. Foxenberg, R.J., et al., *Human hepatic cytochrome p450-specific metabolism of parathion and chlorpyrifos*. *Drug Metab Dispos*, 2007. **35**(2): p. 189-93.

52. Khokhar, J.Y. and R.F. Tyndale, *Rat brain CYP2B-enzymatic activation of chlorpyrifos to the oxon mediates cholinergic neurotoxicity*. *Toxicol Sci*, 2012. **126**(2): p. 325-35.
53. Mutch, E. and F.M. Williams, *Diazinon, chlorpyrifos and parathion are metabolised by multiple cytochromes P450 in human liver*. *Toxicology*, 2006. **224**(1-2): p. 22-32.
54. Bremer, S., et al., *Detection of the embryotoxic potential of cyclophosphamide by using a combined system of metabolic competent cells and embryonic stem cells*. *Altern Lab Anim*, 2002. **30**(1): p. 77-85.
55. Sogorb, M.A., et al., *An integrated approach for detecting embryotoxicity and developmental toxicity of environmental contaminants using in vitro alternative methods*. *Toxicol Lett*, 2014. **230**(2): p. 356-67.

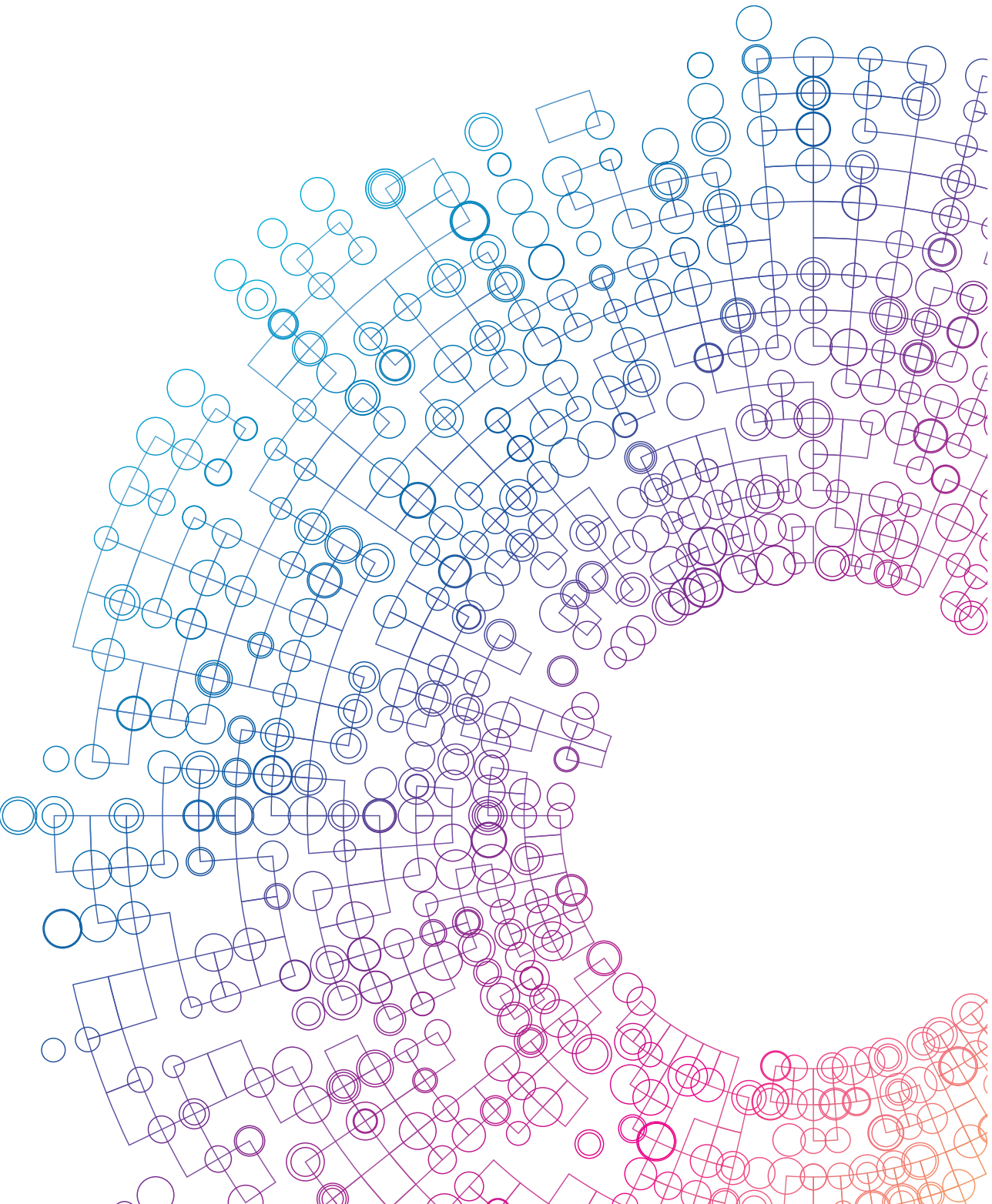
Supplementary

Table S1: Assays used for the RT-qPCR experiments and gene function

Pluripotency	Assay used	Function
Ssea-1 (Fut4)	Mm00487448_s1	Stage Specific Embryonic Antigen-1 (Fucosyltransferase 4)
Cdh1	Mm01247357_m1	Cadherin 1 is a protein providing intercellular contacts between adjacent cells [1].
Proliferation		
Ki67	Mm01278617_m1	The Ki-67 protein is present during all active phases of the cell cycle (G1,S,G2, and mitosis) [2].
Pcna	Mm00448100_g1	Proliferating cell nuclear antigen is essential in nucleic acid metabolism and part of the replication and repair machinery [3].
Cardiomyocyte differentiation		
Myh6	Mm00440359_m1	Myosin heavy chain 6 [4].
Nkx2-5	Mm01309813_s1	NK2 transcription factor related locus 5 is a homeobox-containing transcription factor functioning in heart formation and development [4].
Neural Crest cells		
Ap2α (Tfap2a)	Mm00495574_m1	Activating Enhancer-Binding Protein 2 Alpha causes defects in derivatives of NC in mutant mice and acts at the non-neural ectoderm, neural plate border, neural folds, and in the NC cells [5, 6].
Msx2	Mm00442992_m1	Msh Homeobox 2 is a transcriptional repressor present in the neural folds [5].
Snai2 (Slug)	Mm00441531_m1	Snail Family Transcriptional Repressor 2 is involved in EMT at the phase where the NC cells separate from the neural tube. Snai1 (Snail) and Snai2 (Slug) are functionally equivalent and act as transcriptional repressors and an overexpression would stimulate NC migration while a block would inhibit the specification and migration of NC [5, 6].
Housekeeping genes		
Polr2a	Mm00839502_m1	RNA polymerase II subunit A
Gusb	Mm0.1197698_m1	β-D-glucuronidase
Hprt	Mm03024075_m1	Hypoxanthine Phosphoribosyltransferase 1

References

1. Aghdassi, A., et al., *Recruitment of histone deacetylases HDAC1 and HDAC2 by the transcriptional repressor ZEB1 downregulates E-cadherin expression in pancreatic cancer*. *Gut*, 2012. **61**(3): p. 439-48.
2. Scholzen, T. and J. Gerdes, *The Ki-67 protein: from the known and the unknown*. *J Cell Physiol*, 2000. **182**(3): p. 311-22.
3. Kelman, Z., *PCNA: structure, functions and interactions*. *Oncogene*, 1997. **14**(6): p. 629-40.
4. Radaszkiewicz, K.A., et al., *The acceleration of cardiomyogenesis in embryonic stem cells in vitro by serum depletion does not increase the number of developed cardiomyocytes*. *PLoS One*, 2017. **12**(3): p. e0173140.
5. Gammill, L.S. and M. Bronner-Fraser, *Neural crest specification: migrating into genomics*. *Nat Rev Neurosci*, 2003. **4**(10): p. 795-805.
6. Simoes-Costa, M. and M.E. Bronner, *Establishing neural crest identity: a gene regulatory recipe*. *Development*, 2015. **142**(2): p. 242-57.



4

CHAPTER

Gene regulation by
morpholines and piperidines
in the cardiac embryonic stem
cell test

R.H. Mennen, N. Hallmark, M. Pallardy, R. Bars,
H. Tinwell, A.H. Piersma

Toxicology and Applied Pharmacology. 2021 Dec
15; 433: 115781

DOI: 10.1016/j.taap.2021.115781

Abstract

The cardiac embryonic stem cell test (ESTc) is an *in vitro* embryotoxicity screen which uses cardiomyocyte formation as the main differentiation route. Studies are ongoing into whether an improved specification of the biological domain can broaden the applicability of the test, e.g. to discriminate between structurally similar chemicals by measuring expression of dedicated gene transcript biomarkers. We explored this with two chemical classes: morpholines (tridemorph; fenpropimorph) and piperidines (fenpropidin; spiroxamine). These compounds cause embryotoxicity in rat such as cleft palate. This malformation can be linked to interference with retinoic acid balance, neural crest (NC) cell migration, or cholesterol biosynthesis. Also neural differentiation within the ESTc was explored in relation to these compounds. Gene transcript expression of related biomarkers were measured at low and high concentrations on differentiation day 4 (DD4) and DD10. All compounds showed stimulating effects on the cholesterol biosynthesis related marker *Msmo1* after 24h exposure and tridemorph showed inhibition of *Cyp26a1* which codes for one of the enzymes that metabolises retinoic acid. A longer exposure duration enhanced expression levels for differentiation markers for cardiomyocytes (*Nkx2-5*; *Myh6*) and neural cells (*Tubb3*) on DD10. This readout gave additional mechanistic insight which enabled previously unavailable *in vitro* discrimination between the compounds, showing the practical utility of specifying the biological domain of the ESTc.

Key words: embryonic stem cell test, morpholines, piperidines, gene transcript biomarkers

Introduction

Due to ethical concerns, there is an increasing societal urge to reduce laboratory animal testing and change to non-animal alternatives methods when and as soon as possible [1]. To protect human and environmental health, regulations such as the European REACH legislation (Registration, Evaluation, Authorisation and Restriction of Chemicals) requires testing on laboratory animals for human safety predictions as part of regulatory chemical hazard and risk assessment [1, 2]. The highest number of test animals is used to assess potential reproductive and developmental toxicity. Therefore this area of toxicology has a critical need for non-animal screening methods that can reliably predict reproductive or developmental toxicity so that the least toxic chemicals within the same class can be identified and prioritised for further development [3].

To understand and predict chemical toxicity in animals or humans, multiple promising alternatives to animal studies are under investigation. An important example is the cardiac embryonic stem cell test (ESTc) which tests for chemically induced inhibition of the differentiation of pluripotent murine stem cells into beating cardiomyocytes as the assay output. The variety of differentiating cell types and the biological processes leading to their formation in the ESTc, defining its biological domain, still remains largely uninvestigated. However, we have shown that apart from cardiomyocyte differentiation, neural crest (NC) cells are formed as well [4]. Additionally, *Tubb3* as a marker for neuron development, has been found to be present within the ESTc as well and was regulated by the oxygen level [5]. Based on a deeper understanding of the biological domain of this assay, beyond the time-consuming process of counting beating cardiomyocytes by eye, the readout could be expanded to increase the sensitivity of the ESTc. In this respect, the use of gene transcript biomarkers for different cell types could be beneficial in the ESTc, since it would provide a wider spectrum of mechanistic information which is useful for the application of the ESTc. In addition, this might allow to determine quantifiable differences in the detailed effects between related chemical structures.

The possibility to study the biological applicability domain while obtaining mechanistic information was tested using the chemical classes of morpholines and piperidines. These chemicals were primarily designed for agricultural use to protect crops from fungi by interfering with fungal sterol formation. In animal studies exposure to these chemicals resulted in developmental toxicity with multiple

foetal malformations (table 1). An example of a morpholine is tridemorph (TDM) which primarily caused malformations with cleft lip or palate in rats at doses that were not toxic to the pregnant animal [6]. The interference with steroidogenesis, the fungicidal mode of action of the morpholines and piperidines is shared by flusilazole, a structurally unrelated chemical which has been extensively studied separately in the ESTc and can be useful for comparison [7-9].

Embryonic formation depends on multiple and diverse factors including all-trans retinoic acid (ATRA) balance, the cholesterol biosynthesis pathway, and also the development of neural crest (NC) cells [10-13]. We have focused a priori on these major developmentally relevant pathways for the present study as their perturbation can result in teratogenic outcomes as e.g. craniofacial, limb patterning, or heart formation defects [10-15]. These pathways can also be identified in the ESTc [4, 7]. Furthermore, the ATRA and NC pathways are interrelated. ATRA plays a major role in early development and is also a regulator of NC cell development through regulation of histone acetylation of genes involved in NC cell initiation, as studied in avian embryos [13, 16]. Both an overload or a shortage of ATRA influences the development of NC cells [13, 17]. The NC cells contribute to both neuronal and mesodermal structures during embryogenesis, such as pigment cells, the peripheral nervous system, and cartilage, cardiac structures and craniofacial bones [18-22]. Important regulatory genes in the ATRA pathway are *Aldh1a2* coding for the enzyme synthesising ATRA from retinaldehyde, and *Cyp26a1*, coding for the enzyme metabolising ATRA into inactive metabolites [23]. Genes related to NC cell development include early differentiation markers at the stage of the neural plate border and non-neural ectoderm *Msx2* and *Ap2a*, and the late differentiation markers for migratory NC include *Snai2* (Slug) expression [20, 24]. In the cholesterol biosynthesis pathway, *CYP51* (sterol 14 α -demethylase cytochrome P450) and *SC4MOL* (*MSMO1*) were found to be critical during embryogenesis (skeletal and heart formation in case of *CYP51*) in mouse knockout studies [25, 26]. *CYP51* is important in demethylation of lanosterol, whereas *MSMO1* is important in demethylation of 4,4-dimethyl and 4 α -monomethyl sterols [25, 27]. These two genes have been shown to be regulated in the ESTc by azoles [25, 28]. Azoles have also shown to regulate neural differentiation within the neural EST (ESTn) [29], and the neuron marker *Tubb3* seemed to be present in the ESTc as well [5].

In this study we examined gene transcript expression of biomarkers linked to NC cell development, ATRA balance, cholesterol biosynthesis, and neural

differentiation in the ESTc, after exposure to morpholines and piperidines. In addition, we examined whether gene expression signatures related to these pathways provide possible biomarkers for developmental toxicity predictions and whether these potential biomarkers are able to distinguish the piperidines from the morpholines. These findings may contribute to a more complete mechanistic insight of potential compound-induced effects detectable in the ESTc. This could lead to the incorporation of the ESTc in hazard prediction strategies.

Table 1: In vivo data for the tested compounds including CLP registration, foetal NOAEL and LOAEL, and the main foetal observations

	CLP registration	Foetal NOAEL	Foetal LOAEL	Maternal toxicity at foetal LOAEL	Main foetal observations	literature
Tridemorph (TDM, CAS# 24602-86-6)	R.1B (H360D)	Not observed (rat) 5 mg/kg bw/day (rabbit)	10 mg/kg bw/day (rat) 15 mg/kg bw/day (rabbit)	No	Rat: cleft palate, irregular sternebrae, bipartite thoracic vertebrae Rabbit: increased resorptions	[6]
Fenpropimorph (FPM, CAS# 67564-91-4)	R.2 (H361D)	40 mg/kg bw/day (rat) 15 mg/kg bw/day (rabbit)	160 mg/kg bw/day (rat) 30 mg/kg bw/day (rabbit)	Yes	Rat: reduced foetal weight and length, increased placental weight, cleft palate Rabbit: shortened fore and hind limbs, cleft palate	[30, 31]
Fenpropidin (FPD, CAS# 67306-00-7)	-	90 mg/kg bw/day (rat) 12 mg/kg bw/day (rabbit)	Not observed	Not observed	Not observed	[32]
Spiroxamine (SPX, CAS# 118134-30-8)	R.2 (H361D)	30 mg/kg bw/day (rat) 20 mg/kg bw/day (rabbit)	100 mg/kg bw/day (rat) 80 mg/kg bw/day (rabbit)	Yes	Rat: delayed ossification, reduced body weight, cleft palate Rabbit: skeletal malformations	[33, 34]

CLP registration	Foetal NOAEL	Foetal LOAEL	Maternal toxicity at foetal LOAEL	Main foetal observations	literature
Flusilazole (FLU, R. 1B CAS# 85509-19-9) (H360D)	2 mg/kg bw/day (rat) 7 mg/kg bw/day (rabbit)	10 mg/kg bw/day (rat) 15 mg/kg bw/day (rabbit)	Yes	Rat: cleft palate, nares atresia, absent renal papillae, extra cervical ribs and patent ductus arteriosis. Rabbit: clinical signs of toxicity, increased incidence of abortion and total resorption	[35]

Methods

Test compounds

The tested compounds were: two morpholines tridemorph (TDM, CAS# 24602-86-6) and fenpropimorph (FPM, CAS# 67564-91-4), and two piperidines fenpropidin (FPD, CAS# 67306-00-7) and spiroxamine (SPX, CAS# 118134-30-8). Flusilazole (FLU, CAS# 85509-19-9), was included as a known positive control. The compounds were obtained from Sigma-Aldrich (Zwijndrecht, The Netherlands) and were tested in the various assays at concentrations up to 1 mM for TDM and FPM and up to 330 μ M for FPD, SPX and FLU. All experimental conditions contained 0.25% dimethyl sulfoxide (DMSO, CAS# 67-68-5, Sigma-Aldrich).

Stem cell culture

Murine embryonic stem cells (ES-D3 (D3)) were purchased from ATCC® (Manassas, VA, USA) and cultured according to the previously described protocol [4, 36]. The cells were plated in 35 mm culture dishes (Corning, New York, NY, USA) and were stimulated to multiply in a humidified atmosphere at 37°C with 5% CO₂. Every 2-3 days, cells were replated in fresh medium. The culture medium consisted of Dulbecco's Modified Eagle's Medium (DMEM; Gibco, Waltham, MA, USA), 20% Fetal Bovine Serum (FBS; Greiner Bio-One, Kremsmünster, Austria); 1% 5000 IU/ml Penicillin/5000 μ g/ml Streptomycin (Gibco); 2 mM L-Glutamin (Gibco); 1% Non-

Essential Amino Acids (NEAA; Gibco); and 0.1 mM β -mercaptoethanol (Gibco). The cells in culture medium were enriched with 1000 units/ml leukemia inhibitory factor (LIF; ESGRO®, Millipore, Burlington, MA, USA) to maintain pluripotency. These cultured stem cells were used in the cell viability and differentiation assays.

Cell viability assay

Upon exposure to the described chemicals, cell viability was tested as previously described [37]. Cells were grown at a density of 500 cells per well in a 96-wells plate (Greiner Bio-One) and were incubated at 37°C and 5% CO₂ for two hours. Cells were grown in a pluripotent state using LIF-containing culture medium. These pluripotent cells were exposed to the morpholines and piperidines in concentrations ranges as described in the test compounds section. The following controls were included: DMSO (0.25%; solvent control; Sigma-Aldrich), 5-fluoruracil (0.1 μ g/ml; positive control; Sigma-Aldrich), and penicillin G (500 μ g/ml; negative control; Sigma-Aldrich). All exposure conditions were performed in six replicates. The exposure medium was refreshed after three days of incubation (37°C and 5% CO₂). After an additional two days of incubation, the exposed plates were prepared for fluorescence measurements using CellTiter-Blue reagent according to manufacturer's protocol (Promega, Leiden, The Netherlands) [38]. After the incubation step, extinction coefficients were determined using the SpectraMax® M2 spectrofluorometer (Molecular Devices, Berkshire, United Kingdom) at 544_{Ex}/590_{Em} nm. Relative cell viability levels were expressed in percentages compared to the solvent control. The average and standard deviation of the six replicates of three independent experiments were analysed using PROAST v67.0 in R to determine the IC₅₀ = 50% inhibition in cell viability concentration.

Cell differentiation assay

To differentiate ES-D3 cells into cardiomyocytes, a previously described protocol was used [36, 39]. The culture medium was used without the addition of LIF to enable differentiation. The formation of hanging drops is key to form aggregates called embryonic bodies (EBs) from a 3.75·10⁴ cells/ml cell suspension to the inside of the lid of a 100/20 mm CELLSTAR® cell culture dish (Greiner Bio-One) at differentiation day 0 (DD0). 5 ml of ice-cold phosphate buffered saline (PBS; Ca²⁺, Mg²⁺ free; Gibco) was added to the culture dish. Subsequently, these dishes were incubated for 3 days at 37°C and 5% CO₂. The EBs were collected in 5 ml of

exposure medium and were added to a 60 mm bacterial petri dish (Greiner Bio-One). At differentiation day 5 (DD5), the EBs were transferred to a 24-wells plate (Greiner Bio-One) containing one EB per well in 1 ml of exposure medium and were cultured without further medium changes until differentiation day 10 (DD10). Each condition contained 24 replicates and was performed in duplicate. At DD10, the beating of cardiomyocytes was evaluated by the presence or absence of it within the EBs using a bright field microscope (Olympus BX51, Shinjuku, Japan) and the percentage of beating EBs relative to the total EBs per 24-wells plate was calculated. Two independent experiments were performed and the data were analysed to determine the ID_{50} (= 50% differentiation inhibition concentration) and ID_{10} (= 10% differentiation inhibition concentration) for further protein and gene expression analysis.

Protein expression analysis

Protein expression was visualised by immunocytochemistry with differentiating EBs exposed to ID_{50} concentrations or a 0.25% DMSO control. To facilitate staining, the EBs are moved into 35mm dishes instead of 24 well plates on DD5 to continue normal differentiation until the experiment was concluded and the EBs were stained on DD10. The EBs were washed with 37°C pre-warmed PBS and fixed with 4% formaldehyde (Electron Microscopy Sciences, Hatfield, PA, USA) for 30 minutes. The fixed cells were kept at 4°C for up to 7 days until the staining was performed. In between each step of the protocol the cells were washed three times for 5 minutes with PBS. The EBs were permeabilised with 0.2% Triton X-100 in PBS (T9284, Sigma-Aldrich) for 5 minutes. Samples were incubated with 1% bovine serum albumin (BSA, Sigma-Aldrich) with 0.5% Tween-20 (Sigma-Aldrich) in PBS for 1 hour, to minimise non-specific protein binding. The primary antibodies were added to the EBs in dilution buffer (0.5% BSA, 0.5% Tween-20 in PBS) at 4°C overnight: MF20 (Myosin Heavy Chain, cardiomyocyte marker, 1:100, MAB4470, R&D Systems), AP2 α (Activating Enhancer-Binding Protein 2 Alpha, early NC marker, 1:100, sc-12726, Santa-Cruz), , TUBB3 (β (III) Tubulin, neuron marker, 1:1000, 302302, Bio-connect). The following secondary antibodies were dissolved in dilution buffer for a 1 hour incubation of the EBs: goat-anti-mouse A647 (1:500, A21236, Thermo Fisher) and goat-anti-rabbit A488 (1:1000, A11034, Thermo Fisher). A concentration of 1 μ g/ml DAPI (Sigma-Aldrich) in dilution buffer was added to the EBs and incubated for 10 minutes. Following the last 10 minute washing step, stained EBs were covered with mounting medium (ThermoFisher) and sealed with a cover glass. The EBs were

visualised with a Dmi8 microscope (Leica, Germany) at 4x magnification, with a Leica DFC7000 GT camera (Leica, Germany).

Gene expression analysis

For gene expression analysis we used the RT-qPCR method. The samples contained differentiating EBs exposed to ID₁₀ or ID₅₀ concentrations (determined from concentration-response curves of beating cardiomyocyte differentiation inhibition) and the vehicle control (0.25% DMSO) of differentiation day 4 (DD4) and DD10. These differentiation days correspond to 24 hours and 7 days of compound exposure, respectively. DD4 sample collections contained ~56 EBs from one 60 mm plate per sample. DD10 sample collections contained 24 EBs (one from each well) from one 24-wells plate per sample. Per condition 3-4 samples per timepoint and condition were collected from each of two independent experiments. Samples were transferred into Qiazol (Qiagen, Cat # 79306), and were stored at -80°C prior to RNA isolation (RNeasy Mini-kit (Qiagen, Cat. # 74104) according to manufacturer's protocol). Two additional steps to this protocol were added. The samples were homogenised using QIAshredder columns (Qiagen, Cat. # 79654) and a DNase step was implemented using a RNase-Free DNase set (Qiagen, Cat # 79254). RNA quantity and quality were assessed using the Nanodrop (Nanodrop Technologies Inc., Wilmington, Delaware) and the 2100 Bioanalyzer (Aligent Technologies, Amstelveen, The Netherlands). The 260/280 nm absorbance ratios were between 1.7 and 2.2 and the RIN (RNA Integrity Number) scores were >8.6. From the RNA obtained, cDNA was formed according to manufacturer's prescriptions (cDNA synthesis kit, Applied Biosystems, Foster City, CA, USA). The cDNA was quantified using a 7500 Fast Real-Time PCR system (Applied Biosystems) with the thermal cycling conditions: 95°C for 20s, followed by 40 cycles of 95°C for 3s and 60°C for 30s. The tested genes with the respective TaqMan® Assay IDs (Thermo Fisher Scientific) are listed in table 2.

Gene network analysis

A gene interaction network was built using the STITCH ('search tool for interactions of chemicals') web tool ([40]; <http://stitch.embl.de/>). The tested gene symbols of the RT-qPCR experiment were used as input with the *Mus musculus* as organism. The generated network consisted of the input genes and additional genes with potential associations to the tested genes. This was generated using default

settings at a moderate confidence level (0.4); the probability that a predicted link is present between two genes or proteins in the database. The obtained strengths of gene interaction were separated for text mining and other experimental evidence and exported as tab-delimited files, which were used for visualisation in Cytoscape (version 3.4.0; [41]).

Statistics

The obtained concentration-response data on cell viability and differentiation were fitted and statistically analysed using the PROAST software version 67.0 according to the exponential method [42]. IC_{50} (cell viability) and ID_{50} (differentiation) levels for 50% inhibition in cell viability and differentiation inhibition were determined. In addition, 90% confidence lower and upper bench mark dose values (BMDL-BMDU) were calculated. Control values were visualised using a dummy value. For gene expression analysis, the $-\Delta\Delta Ct$ method was used [43]. Ct values were normalised against the average expression levels of the *Hprt1*, *Gusb*, and *Polr2a* housekeeping genes (table 2). The mean values per experiment of gene expression data were compared to the control samples using a one-way ANOVA test with Sidak's multiple comparisons post-hoc test ($p < 0.05$).

Table 2: Primers used for RT-qPCR procedure

Gene name	Abbreviation	Marker for	Assay ID/primer sequence
POU domain, class 5, transcription factor 1	Pou5f1	Stem cell	Mm03053917_g1
Cadherin 1	Cdh1	Stem cell	Mm01247357_m1
Bone morphogenetic protein 4	Bmp4	Mesoderm	Mm00432087_m1
Nestin	Nes	Ectoderm/Neural progenitor	Mm00450205_m1
GATA binding protein 4	Gata4	Endoderm	Mm00484689_m1
NK2 transcription factor related, locus 5	Nkx2.5	Early cardiomyocyte	Mm01309813_s1
myosin, heavy polypeptide 6, cardiac muscle, alpha	Myh6	Cardiomyocyte	Mm00440359_m1
β -tubulin	Tubb3	Neuron	Mm00727586_s1
Transcription factor AP-2 alpha	Ap2a	Early neural crest cell marker	Mm00495574_m1

Gene name	Abbreviation	Marker for	Assay ID/primer sequence
Msh homeobox 2	Msx2	Early neural crest cell marker	Mm00442992_m1
Snail family zinc finger 2	Snai2	Epithelial-Mesenchymal Transition	Mm00441531_m1
Cytochrome P450 26A1	Cyp26a1	ATRA homeostasis	Mm00514486_m1
Aldehyde dehydrogenase 1 family member A2	Aldh1a2	ATRA homeostasis	Mm00501306_m1
Methylsterol monooxygenase 1	Msmo1 (Sc4mol)	Cholesterol biosynthesis	Mm00499390_m1
Lanosterol 14 α -demethylase	Cyp51	Cholesterol biosynthesis	Mm00490968_m1
Glucuronidase beta	Gusb	Housekeeping gene	Mm01197698_m1
Hypoxanthine phosphoribosyltransferase 1	Hprt1	Housekeeping gene	Mm03024075_m1
RNA Polymerase II Subunit A	Polr2a	Housekeeping gene	Mm00839502_m1

Results

The test compounds showed different potencies in inhibition of beating cardiomyocyte differentiation

Viability and differentiation results showed dose-response relationships for flusilazole (FLU) as a reference and for the morpholines (TDM, FPM) and piperidines (FPD, SPX) (fig. 1). For FLU, the ID_{50} obtained from the differentiation experiments was higher compared to the IC_{50} obtained from the viability measurements, indicating the presence of cell death at ID_{50} levels, which should be kept in mind when interpreting results of the following experiments in this manuscript. Differentiation was affected at lower concentrations than viability for both the morpholines and piperidines (table 3), resulting in the following ranking of highest to lowest viability IC_{50} for the five chemicals: TDM>FPM>FPD=SPX=FLU. The piperidines (FPD, SPX) inhibited differentiation of beating cardiomyocytes at lower concentrations compared to the morpholines (TDM, FPM), resulting in the following ranking of highest to lowest differentiation (ID_{50}) for the five chemicals: TDM >FLU>FPM>SPX>FPD.

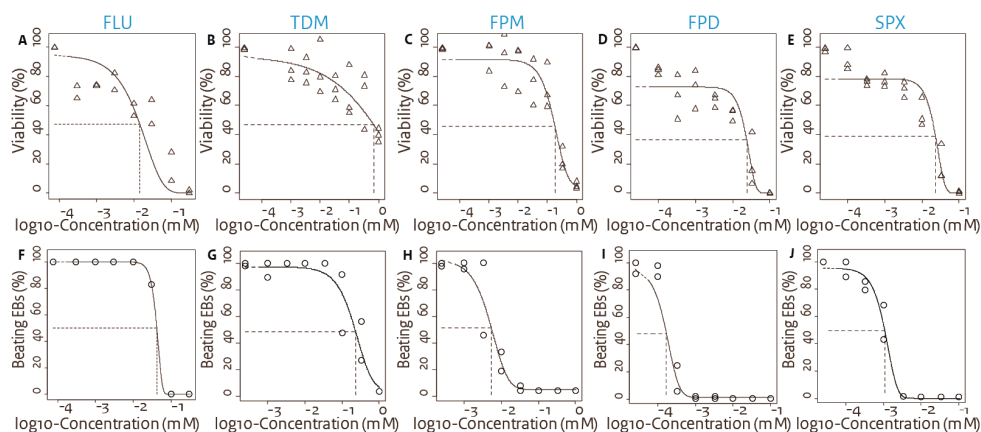


Figure 1: Concentration-response curves for viability and cardiomyocyte differentiation inhibition for flusilazole, the morpholines and the piperidines. Viability effects (A- E) expressed in % of control. Each datapoint shows the average within one experiment, $n=3$ experiments, flusilazole $n=2$. Differentiation effects (F-J) were expressed in % beating EBs compared to the control. Each datapoint shows the average within one experiment, $n=2$ experiments. Concentrations were tested up to 1 mM for TDM and FPM, 330 μM for FLU, and up to 100 μM for FPD and SPX. Curves were fitted to the datapoints using PROAST v67.0 in R. Dotted lines indicate the IC_{50} or ID_{50} levels.

Table 3: 50% inhibition levels with 90% confidence intervals in brackets for viability (IC_{50}) and beating cardiomyocyte differentiation (ID_{50}) after compound exposure.

	FLU	TDM	FPM	FPD	SPX
Viability IC_{50}	14 μM (11-19)	680 μM (430-980)	180 μM (150-220)	24 μM (15-34)	23 μM (14-43)
Differentiation ID_{50}	42 μM (41-43)	230 μM (150-320)	5.5 μM (3.8-7.4)	0.21 μM (0.17-0.28)	1.1 μM (0.99-1.3)

Protein expression levels based on immunocytochemistry showed diverse differentiation effects

In order to map protein expression of the selected biomarkers to the subsequent gene expression data, immunostainings were conducted. The cardiomyocyte structure was assessed using *immunocytochemistry* staining for the structural protein marker MF20 (myosin formation) (fig. 2). Images of the protein staining showed myofilaments (magenta) in the DMSO control EBs, however myosin

formation appears blocked by compound exposure, seen as the absence of formed myofilaments and appearance of 'spots'.

Compound exposure also influenced the differentiation of NC cells and neurons in the ESTc, to different extents. Exposure to all tested compounds except for TDM (fig. 3H) induced an increase in staining intensity of the NC cell marker AP2 α compared to the DMSO control at DD10. Changes in the pattern of TUBB3 staining for neurons (green) in the formation of axon-like structures were observed following compound exposure. These structures were visible when the EBs were exposed to the DMSO control, FLU, and FPD (fig 3C, F, O) and were less clear when exposed to FPM and SPX (fig. 3L, R). TDM exposure resulted in the least evident visible formation of these axon-like structures (fig. 3I).

Gene networks visualise pathway relationships

In order to illustrate interrelationships among the genes of interest, they were visualised in a network using STITCH, as shown in figure 4. The gene appearing with most connections for both functional and textual links was the endodermal germ cell marker *Gata4*. This gene was connected based on a functional relationship and on text-mining to the pluripotency marker *Pou5f1*, the mesodermal marker *Bmp4* and to the early cardiomyocyte marker *Nkx2-5*. Related genes suggested by STITCH include markers for pluripotency (*Zfpm2*, *Sox2*, *Nanog*) and cell adhesion (*Ctnnb1* and *Ctnnd1*).

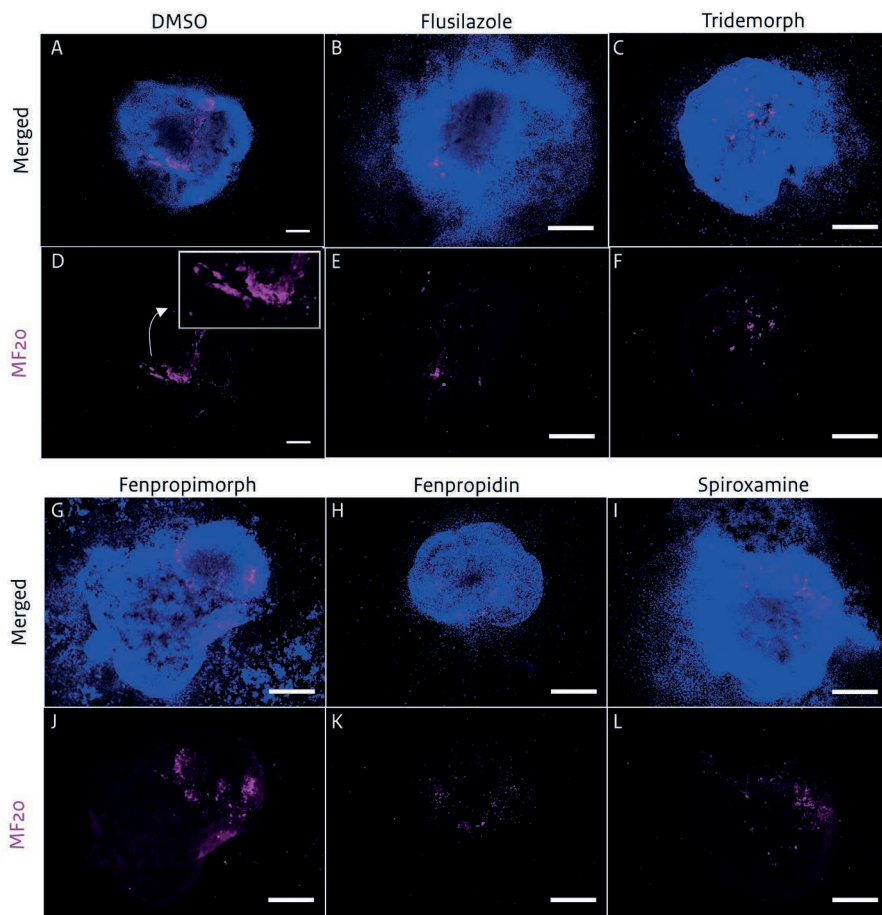


Figure 2: Cardiomyocyte myosin expression in EBs exposed to compound specific ID50 values at DD10. Cell nuclei were stained with DAPI in blue and myosin was stained using a MF20 staining in magenta. DMSO control shows myofilaments (magnified insert in D), whereas exposure to FLU, TDM, FPM, PFD, or SPX didn't show myosin structures. Scale bar indicates 500 μm .

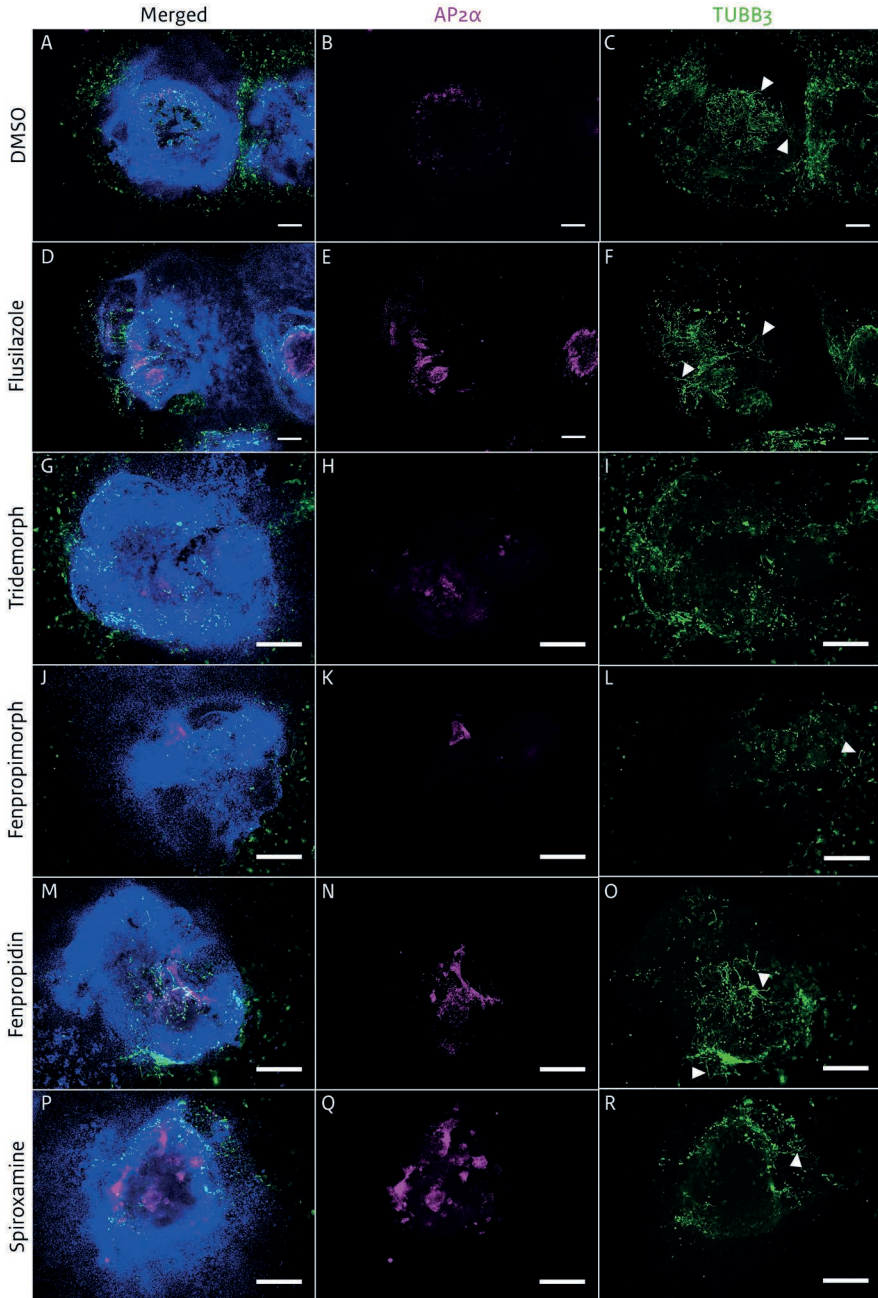


Figure 3: Neural crest cell (AP2a) and neural cell (TUBB3) presence in EBs at DD10 to ID50 values of indicated compounds. Cell nuclei were stained with DAPI in blue, AP2a in magenta and TUBB3 in green. Scale bar indicates 500 μm. White arrows indicate axon-like structures.

Gene expression regulations showed differences in mechanism

At DD4, the effects of compound exposure on all pathways assessed, showed limited changes in gene expression at ID₁₀ or ID₅₀ exposure levels (fig. 5). The effects of compound exposure on pluripotency and germ layer differentiation showed small to no effects (fig. 5). ATRA homeostasis and cholesterol synthesis related markers showed statistically significant effects ($p < 0.05$). The ATRA homeostasis related marker Cyp26a1 was downregulated by TDM (fig. 5). Cyp26a1 transforms ATRA into its inactive metabolites. Msmo1 and Cyp51 are both involved in the intermediate steps towards cholesterol formation out of lanosterol. Cyp51 only showed an upregulated trend (ns) at high concentrations of FLU exposure (fig. 5). Msmo1 was significantly upregulated by all compounds ($p < 0.05$), although ID₅₀ concentrations of TDM and SPX didn't show statistically significant differences compared to control.

By DD10, the effects of compound exposure on gene expression levels were more obvious for all the pathways investigated and chemical specific profiles were evident as summarised in table 4. ID₅₀ levels of TDM upregulated the expression levels of the pluripotency marker *Pou5f1* (=Oct4) (fig. 6). The ectodermal marker *Nes* was upregulated by ID₅₀ concentrations of FLU, TDM, and FPD and by ID₁₀ concentrations of FPM. The endodermal marker *Gata4* was upregulated after exposure to ID₁₀ levels of TDM (fig. 6). All compounds downregulated the expression levels of cardiomyocyte markers *Nkx2-5* and *Myh6* except for FLU and SPX. FLU ID₅₀ levels upregulated the early NC marker *Ap2a*. At this timepoint also the expression levels of the neural marker *Tubb3* were affected by all compounds, with the exception of TDM exposure and ID₁₀ levels of FPD and SPX. All compounds clearly stimulated the expression levels of Cyp26a1 (ATRA inactivation) except for FLU and ID₁₀ levels of FPD and SPX. *Aldh1a2*, which is involved in ATRA formation, was induced by ID₁₀ levels of FPM and FPD and by ID₅₀ levels of SPX. The marker Cyp51, involved in cholesterol synthesis, was upregulated by exposure to ID₅₀ levels of FLU and ID₁₀ levels of FPM.

To summarise, when comparing the gene expression results between DD4 and DD10, gene expression characteristic of both pluripotency and germ layer differentiation were observed on DD10, but not on DD4. Quantification of the differentiation markers for cardiomyocytes, neural crest cells, and neural cells

showed small cell lineage specific differences in sensitivity between compounds at DD10. And lastly, quantification of retinoic acid homeostasis and cholesterol synthesis related markers showed clear exposure related effects on both differentiation days.

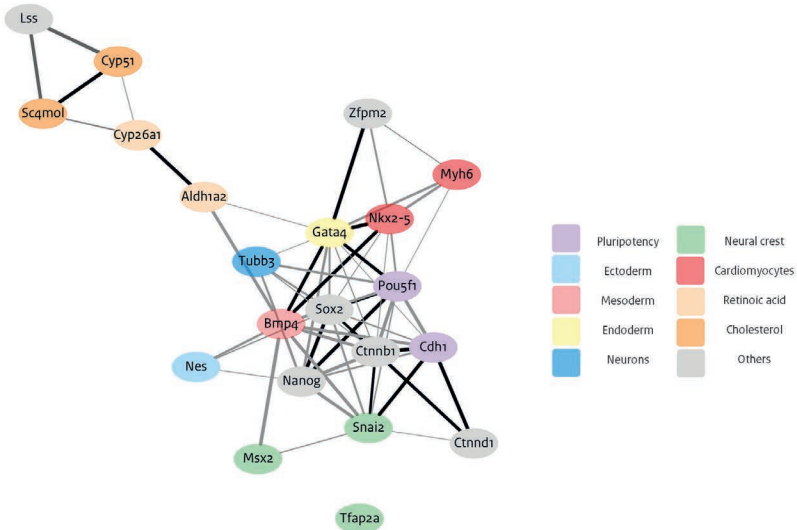


Figure 4: Gene network of genes studied, created using STITCH and visualised using Cytoscape. A) Gene colours relate to tissue specificity as indicated in the legend. Grey genes were proposed by STITCH as associated to the genes of interest. The thickness of the gene edges (i.e. connecting lines) is proportional to the level of evidence of relationship. Black gene edges represent relations that were both experimentally determined and found by text-mining. Dark grey edges show relations that were experimentally determined and light grey edges were found by text-mining only.

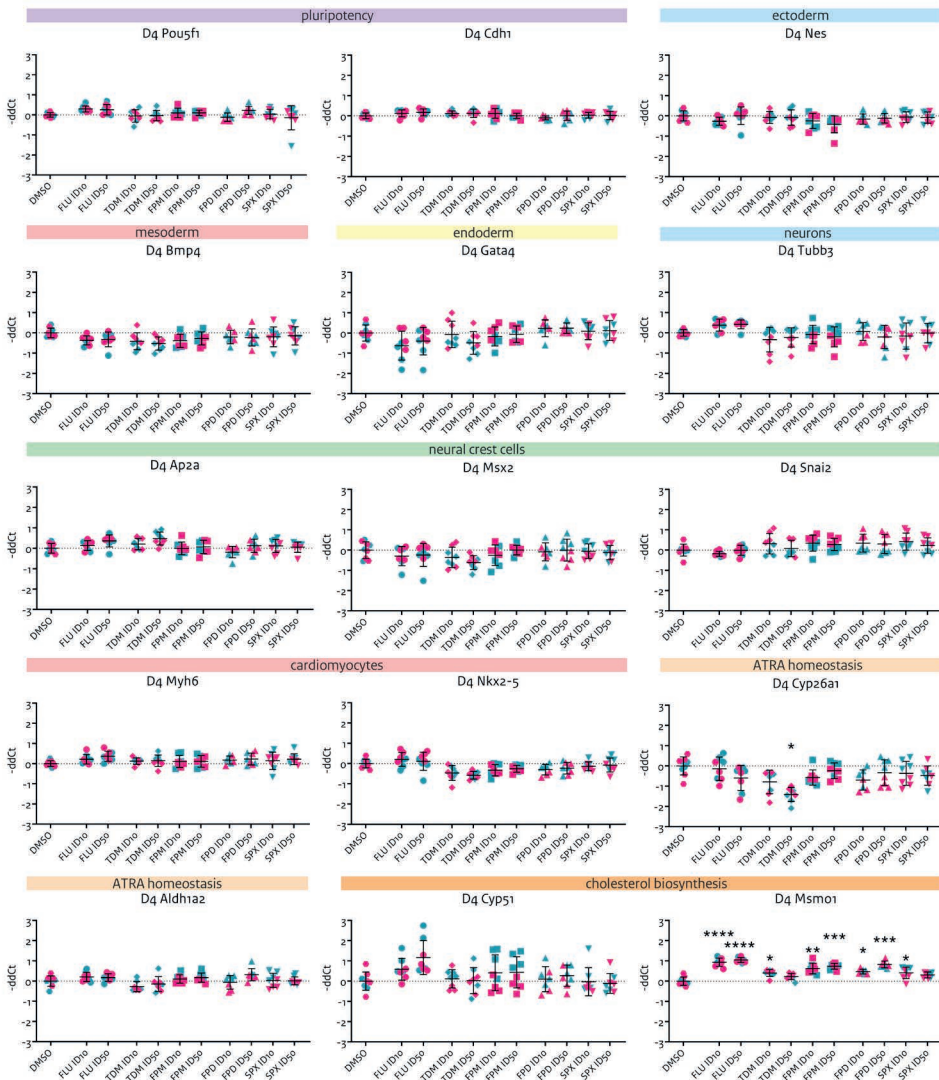


Figure 5: Gene expression levels of selected genes after exposure to ID10 or ID50 levels of FLU, TDM, FPM, FPD, or SPX at DD4. Gene expression levels are expressed as $-ddCt$, relative to the DMSO control. Coloured bars indicate the gene specificity for pluripotency, ectoderm and neurons, mesoderm and cardiomyocytes, endoderm, neural crest cells, retinoic acid homeostasis, cholesterol biosynthesis. Gene expression was measured using real-time PCR. Error bars indicate the standard deviation. Two independent experiments with each 3-4 samples. Blue data points indicate samples of experiment 1, magenta data points indicate samples of experiment 2. Asterisks indicate a significant difference compared to the DMSO control (one-way ANOVA; Sidak's multiple comparisons post-hoc test). * $p < 0.05$, ** $p < 0.01$, *** $p < 0.001$, **** $p < 0.0001$.

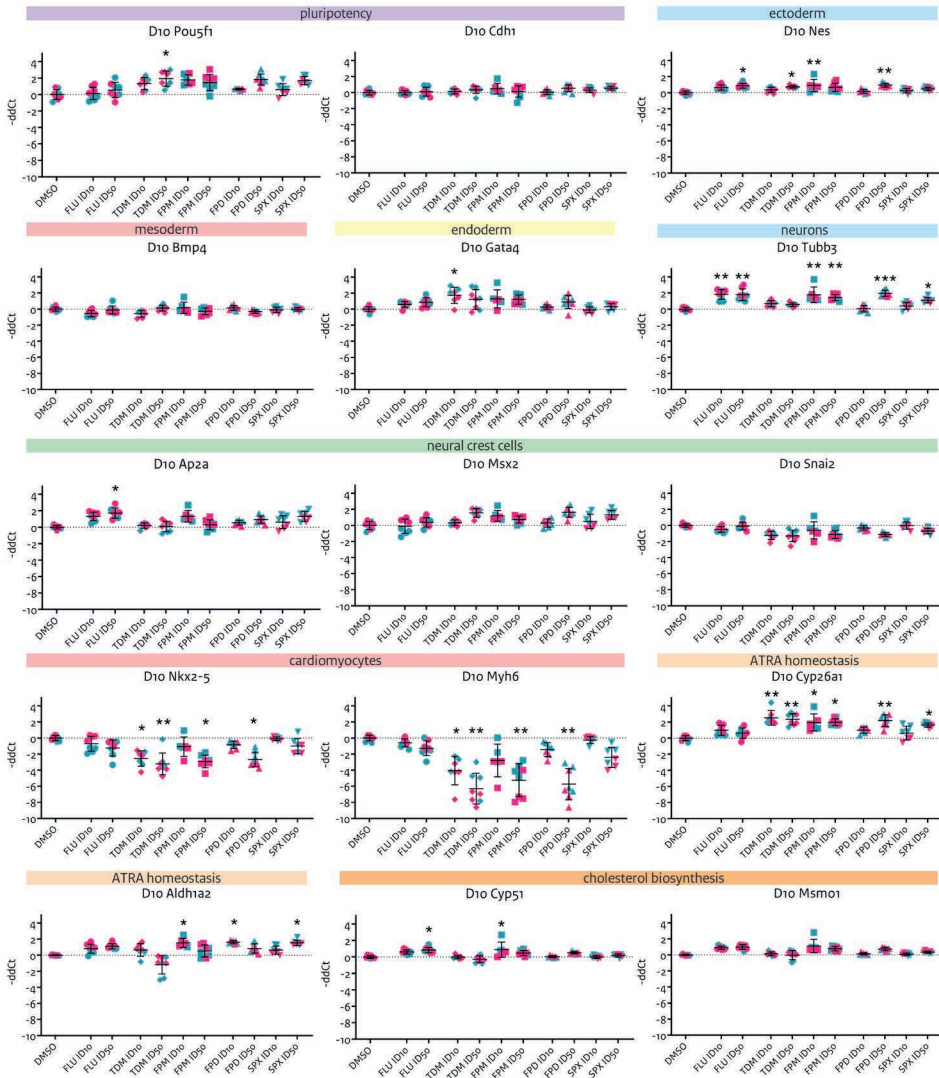


Figure 6: Gene expression levels of selected genes after exposure to ID10 or ID50 levels of FLU, TDM, FPM, FPD, or SPX at DD10. Gene expression levels are expressed as -ddCt, which were compared to the DMSO control. Coloured bars indicate the gene specificity for pluripotency, ectoderm and neurons, mesoderm and cardiomyocytes, endoderm, neural crest cells, retinoic acid homeostasis, cholesterol biosynthesis. Gene expression was measured using real-time PCR. Error bars indicate the standard deviation. Two independent experiments with each 3-4 samples. Blue data points indicate samples of experiment 1, magenta data points indicate samples of experiment 2. Asterisks indicate a statistically significant difference compared to the DMSO control (one-way ANOVA; Sidak's multiple comparisons post-hoc test). * p < 0.05, ** p < 0.01, *** p < 0.001, **** p < 0.0001.

Table 4: Summary of gene expression results after exposure to TDM, FPM, FPD, or SPX at DD10. For each of the test compounds the expression levels were summarised for each group of genes by an upward arrow for upregulation, a downward arrow for downregulation, or a dash in case the gene groups were not regulated.

	Pluripotency	Ectoderm	Mesoderm	Endoderm	Neurons	NC cells	Cardiomyocytes	ATRA homeostasis	Cholesterol biosynthesis
TDM	↑	↑	-	↑	-	-	↓	↑	-
FPM	-	↑	-	-	↑	-	↓	↑	↑
FPD	-	↑	-	-	↑	-	↓	↑	-
SPX	-	-	-	-	↑	-	-	↑	-

Discussion

In order to explore the mechanisms affected by chemical exposure underlying the effects on cell differentiation in the ESTc, expanding the readout of the test is helpful, for instance by investigating effects on known molecular pathways important in developmental biology such as cholesterol synthesis and ATRA homeostasis. The additional monitoring of neural cell development within the ESTc provided additional molecular mechanistic insight and this further specification

of the biological domain might enable more sensitive embryotoxicity predictions. The gene network gave insight into interrelationships between genes of known mechanistic pathways as well as of specific cellular differentiation routes, which reveal differences in the influence of the four chemicals tested, which would otherwise have remained obscure.

The additional readout of neural cell differentiation added to the complete picture of the biological domain of the ESTc. Such readout could enhance the insight in the mechanistic basis underlying the ESTc as a model for embryotoxicity assessment and its power of discriminating between compounds. This is illustrated e.g. by both protein (TUBB3), gene expression levels (Tubb3) and axon-like structures, that were affected by all tested compounds but not TDM. In studies with the neural embryonic stem cell test (ESTn), neural cell differentiation was also regulated by FLU [29]. Like FLU, the test compounds have been studied in vitro as to structure affinity studies related to the $\sigma 1$ receptor, which is a potential therapeutic target for a variety of neurological disorders [44-46]. This receptor acts as a chaperone and although the complete signal transduction pathway remains unclear, it is involved in cell survival but also in functional neurological processes like Ca^{2+} signalling, neurotransmitter release, and inhibition of voltage-dependent K^+ channels [47]. Although Moebius et al. state that the sterol isomerase isoenzymes between fungi and vertebrates are completely unrelated, the mammalian σ receptor subtype 1 has structural similarities with yeast sterol isomerases [46], the intended mechanism of action of the test compounds involved in cholesterol biosynthesis [48]. FPM and TDM appear to have a high affinity for the mammalian $\sigma 1$ receptor [44-46], which may have a relation to the aberrant effects on neurons present in the ESTc compared to controls. However, a direct comparison between the affinities of the various mammalian $\sigma 1$ receptors has not been made. TDM is slightly more effective against fungal sterol isomerase compared to FPM [48]. The differences in affinity to fungicidal sterol isomerase cannot directly be translated to the mammalian $\sigma 1$ receptor. Additional research is needed to explore a possible relationship between the $\sigma 1$ receptor and the effects observed within the ESTc.

The target common mode of action of the test compounds is inhibition of sterol synthesis in fungi, although interfering at different levels in sterol biosynthesis pathway. Morpholines primarily inhibit sterol $\Delta 14$ -reductase and sterol $\Delta 8, \Delta 7$ -isomerase in the formation of 4,4-dimethylzymosterol or ergosterol, respectively [49]. Azoles inhibit the sterol 14 α -demethylase cytochrome P450 (CYP51), important

in demethylation of lanosterol [25, 28]. More downstream within this pathway, also MSMO1 (SC4MOL) is regulated by azoles and is important in demethylation of 4,4-dimethyl and 4 α -monomethyl sterols [25, 27]. In mouse gene knockout studies *In vivo*, CYP51 and SC4MOL were found to be critical during embryogenesis [25, 26]. On DD4 of the ESTc, all tested compounds upregulated Msmo1 and an upregulating trend of Cyp51 was observed after exposure to FLU. FLU and FPM, upregulated Cyp51 on DD10. These results indicate that mammalian systems are also susceptible to change via this pesticidal MOA. The effects of FLU on cholesterol-related expression levels were measured in previous ESTc studies, showing an upregulation of the expression levels of Cyp51 and Msmo1, with Msmo1 indicating its potential as being a sensitive biomarker for interruptions in differentiation [7, 8]. In the whole embryo culture model, FLU regulated expression of multiple key genes within the cholesterol metabolism pathway, including induction of Cyp51 and Sc4mol (= Msmo1) [50]. The accumulation of sterol intermediates in the cholesterol biosynthesis pathway were measured in several *in vitro* tests upon exposure to morpholines and/or piperidines. These accumulations were seen in hiPSCs after exposure to FPM and SPX [51], in 3T3 fibroblasts after exposure to FPM which repressed cell growth [52], and in rat liver homogenates after FPM exposure which inhibited the $\Delta 8$ - $\Delta 7$ isomerase [53]. Exposure to the piperidine YM9429 induced cleft palate in the presence of a reduction of maternal plasma phospholipids at the time when foetal palate formation should occur [54]. These *in vitro* and *in vivo* effects show that the mechanistic effects on cholesterol biosynthesis observed in the ESTc are of relevance for the prediction of *in vivo* mechanistic effects and related adversities.

Also mechanistic effects on the level of ATRA homeostasis *in vitro* can predict related adverse effects *in vivo*. Previous studies have shown that monitoring perturbation of ATRA homeostasis is useful in predicting developmental toxicants *in vivo* [4, 7]. On DD4 in our study, we observed a downregulating trend by FLU of Cyp26a1 and a statistically significant downregulation of Cyp26a1 by TDM. Previous exposures in the ESTc with ID₅₀ levels of FLU tended to suppress Cyp26a1 expression on DD4 [7], which is consistent with our results. Based on the various *in vitro* studies published in ToxCast, Cyp26 was identified as the molecular initiating event (MIE) towards cleft palate formation by triazole exposure including FLU [55]. In the WEC, FLU was predicted as an embryotoxicant because of time-dependent significant upregulations in gene expression of Cyp26a1 [27]. As FLU and TDM

caused a (trend in) downregulation of Cyp26a1 on DD4, comparable regulation of Cyp26a1 by TDM was seen on DD10. The tested morpholines and piperidines have hardly been studied in relation to regulation of ATRA homeostasis before. However, the differences in gene expression regulation in the ESTc between these compounds and FLU, indicate differences in mechanisms of action. Therefore, the ATRA metabolic pathway in the ESTc may be useful in discriminating compounds within one chemical class and in mechanism based embryotoxicity predictions.

The upregulation of the NC cell differentiation marker Ap2a by FLU discriminated this compound from among those tested. Both other NC markers showed no difference between compounds. *In line with the Ap2a effect, Menegola et al. exposed rat embryos in culture to teratogenic concentrations of triazoles including FLU, which resulted in a delay in neuropore development, branchial arch alterations, cleft palate formation, but also in alterations in NC cell migration [56, 57].*

The gene expression regulations were also dependent on the timing of exposure and the time-point of measurement. Although in toxicology the paradigm of Paracelsus “the dose makes the poison” for a long time dictated current regulations of threshold measures, the paradigm of “timing makes the poison” receives more and more attention in the field of developmental toxicology [58-60]. In these experiments both dimensions of exposure concentration and timing were investigated. Most clear differences were seen among both time points of gene expression assessment. As DD10 showed more pronounced effects on differentiation markers, in line with the progression of cell differentiation with time, DD4 showed more pronounced effects on mechanistic markers related to cholesterol biosynthesis and ATRA metabolism, as has been observed before [4]. This illustrates that mechanistic effects precede morphological effects, and informs about optimal time points for assessments of either readout.

It was not the purpose of this study to translate readouts in the ESTc to compound potencies in vivo. It is hard to actually translate the differences observed as effective concentrations in the ESTc to NOAELs in in vivo studies. The effects seen in the in vivo studies (table 1) based on NOAELs and LOAELs are within the same orders of magnitude and can not necessarily be discriminated by effective concentrations in the ESTc. Kinetic characteristics in vivo such as the distribution of compounds between maternal and foetal compartments can also affect relative in

vivo compound potency. The effective concentrations in the ESTc should therefore be complemented with data on compound kinetics in vivo to predict adversity in the human situation. Studies in adult rats show that both TDM and FPM do not accumulate in the body and are excreted at around the same pace with half-lives of 15.6 hours for TDM and 16-24 hours for FPM [61, 62]. As TDM gets equally excreted in urine and faeces, FPM gets mainly excreted through the urine [32, 61]. Information on kinetics in pregnancy is often not available for non-pharmaceutical chemicals, which hampers kinetic extrapolation of in vitro effective concentrations to in vivo LOAELs.

Overall, in addition to predicting adverse effects on cell differentiation, the ESTc provides mechanistic information underlying adversity, which provides added information as compared to existing data of in vivo testing in the rat. Given the conserved mechanisms of vertebrate embryonic cell differentiation represented in the ESTc, these findings are likely relevant for humans as well. The ESTc, together with other in vitro and in silico test systems and combined with kinetic modelling, can be instrumental in the context of test batteries for developmental hazard and risk assessment.

Acknowledgements

Gina Mennen was supported by the French National Association for Research and Technology (ANRT) through a CIFRE PhD grant no. 2018-0682, which was co-supervised by Aldert Piersma, Nina Hallmark, Marc Pallardy, Remi Bars, and Helen Tinwell. Aldert Piersma was funded by the Dutch Ministry of Health, Welfare and Sports. We would like to thank Harm Heusinkveld for a critical review of the manuscript.

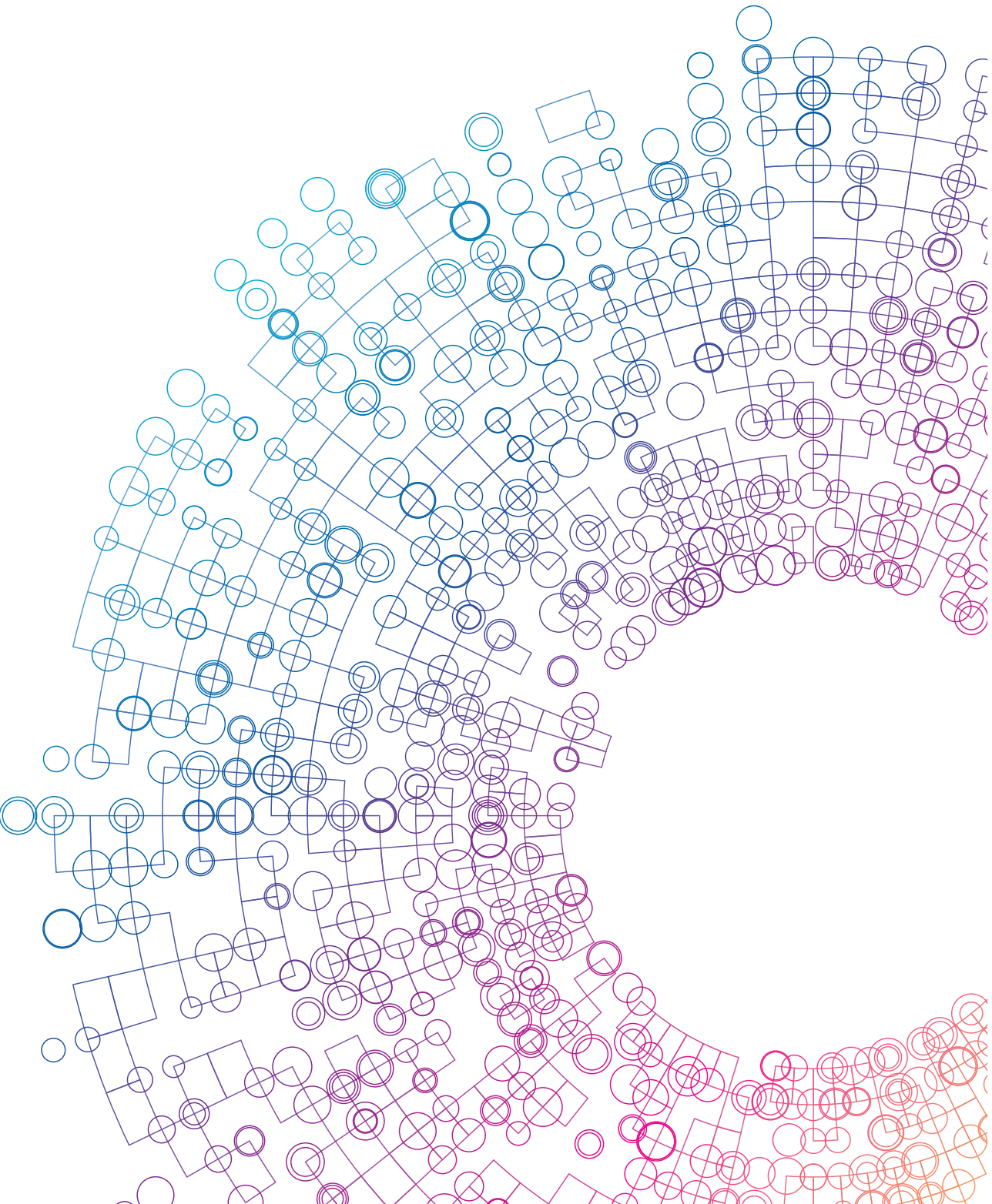
References

1. van der Jagt, K., Munn, S., Torslov, J., de Bruijn, J., *Alternative Approaches Can Reduce the Use of Test Animals under REACH*. 2004, EC Joint Research Centre.
2. Taylor, K., *Ten years of REACH - An animal protection perspective*. *Altern Lab Anim*, 2018. **46**(6): p. 347-373.
3. Piersma, A.H., *Alternative methods for developmental toxicity testing*. *Basic Clin Pharmacol Toxicol*, 2006. **98**(5): p. 427-31.
4. Mennen, R.H.G., J.L.A.J. Pennings, and A.H.A. Piersma, *Neural crest related gene transcript regulation by valproic acid analogues in the cardiac embryonic stem cell test*. *Reproductive toxicology* (Elmsford, N.Y.), 2019. **90**: p. 44-52.
5. Mennen, R.H., V.C. de Leeuw, and A.H. Piersma, *Oxygen tension influences embryonic stem cell maintenance and has lineage specific effects on neural and cardiac differentiation*. *Differentiation*, 2020. **115**: p. 1-10.
6. Act, F.a.E.P., *Review of tridemorph*. 1999.
7. Dimopoulou, M., et al., *A comparison of the embryonic stem cell test and whole embryo culture assay combined with the BeWo placental passage model for predicting the embryotoxicity of azoles*. *Toxicol Lett*, 2018. **286**: p. 10-21.
8. van Dartel, D.A., et al., *Concentration-dependent gene expression responses to flusilazole in embryonic stem cell differentiation cultures*. *Toxicol Appl Pharmacol*, 2011. **251**(2): p. 110-8.
9. de Jong, E., et al., *Comparison of the mouse Embryonic Stem cell Test, the rat Whole Embryo Culture and the Zebrafish Embryotoxicity Test as alternative methods for developmental toxicity testing of six 1,2,4-triazoles*. *Toxicol Appl Pharmacol*, 2011. **253**(2): p. 103-11.
10. Krakowiak, P.A., et al., *Lathosterolosis: an inborn error of human and murine cholesterol synthesis due to lathosterol 5-desaturase deficiency*. *Hum Mol Genet*, 2003. **12**(13): p. 1631-41.
11. Engelking, L.J., et al., *Severe facial clefting in Insig-deficient mouse embryos caused by sterol accumulation and reversed by lovastatin*. *J Clin Invest*, 2006. **116**(9): p. 2356-65.
12. Porter, F.D., *Cholesterol precursors and facial clefting*. *J Clin Invest*, 2006. **116**(9): p. 2322-5.
13. Cerrizuela, S., G.A. Vega-Lopez, and M.J. Aybar, *The role of teratogens in neural crest development*. *Birth Defects Res*, 2020. **112**(8): p. 584-632.
14. Niederreither, K., et al., *Embryonic retinoic acid synthesis is essential for heart morphogenesis in the mouse*. *Development*, 2001. **128**(7): p. 1019-31.
15. El Robrini, N., et al., *Cardiac outflow morphogenesis depends on effects of retinoic acid signaling on multiple cell lineages*. *Dev Dyn*, 2016. **245**(3): p. 388-401.
16. Simkin, J.E., et al., *Retinoic acid upregulates ret and induces chain migration and population expansion in vagal neural crest cells to colonise the embryonic gut*. *PLoS One*, 2013. **8**(5): p. e64077.
17. van Gelder, M.M., et al., *Teratogenic mechanisms of medical drugs*. *Hum Reprod Update*, 2010. **16**(4): p. 378-94.
18. Keyte, A. and M.R. Hutson, *The neural crest in cardiac congenital anomalies*. *Differentiation*, 2012. **84**(1): p. 25-40.

19. Achilleos, A. and P.A. Trainor, *Neural crest stem cells: discovery, properties and potential for therapy*. Cell Res, 2012. **22**(2): p. 288-304.
20. Simoes-Costa, M. and M.E. Bronner, *Insights into neural crest development and evolution from genomic analysis*. Genome Res, 2013. **23**(7): p. 1069-80.
21. Monsoro-Burq, A.H., *PAX transcription factors in neural crest development*. Semin Cell Dev Biol, 2015. **44**: p. 87-96.
22. Rada-Iglesias, A., et al., *Epigenomic annotation of enhancers predicts transcriptional regulators of human neural crest*. Cell Stem Cell, 2012. **11**(5): p. 633-48.
23. Tonk, E.C., J.L. Pennings, and A.H. Piersma, *An adverse outcome pathway framework for neural tube and axial defects mediated by modulation of retinoic acid homeostasis*. Reprod Toxicol, 2015. **55**: p. 104-13.
24. Simoes-Costa, M. and M.E. Bronner, *Establishing neural crest identity: a gene regulatory recipe*. Development, 2015. **142**(2): p. 242-57.
25. He, M., et al., *Mutations in the human SC4MOL gene encoding a methyl sterol oxidase cause psoriasiform dermatitis, microcephaly, and developmental delay*. J Clin Invest, 2011. **121**(3): p. 976-84.
26. Keber, R., et al., *Mouse knockout of the cholesterologenic cytochrome P450 lanosterol 14alpha-demethylase (Cyp51) resembles Antley-Bixler syndrome*. J Biol Chem, 2011. **286**(33): p. 29086-97.
27. Dimopoulou, M., et al., *Flusilazole induces spatio-temporal expression patterns of retinoic acid-, differentiation- and sterol biosynthesis-related genes in the rat Whole Embryo Culture*. Reprod Toxicol, 2016. **64**: p. 77-85.
28. Pan, J., C. Hu, and J.H. Yu, *Lipid Biosynthesis as an Antifungal Target*. J Fungi (Basel), 2018. **4**(2).
29. Theunissen, P.T., et al., *Compound-specific effects of diverse neurodevelopmental toxicants on global gene expression in the neural embryonic stem cell test (ESTn)*. Toxicol Appl Pharmacol, 2012. **262**(3): p. 330-40.
30. Pfeil, R., *Fenpropimorph 27-34 JMPR*, B. Federal Institute for Risk Assessment, Germany, Editor. 2004.
31. EFSA, *Conclusion regarding the peer review of the pesticide risk assessment of the active substance fenpropimorph*. 2008.
32. Report, E.S., *Conclusion regarding the peer review of the pesticide risk assessment of the active substance fenpropiadin*. 2007, EFSA. p. 1-84.
33. EFSA, *Outcome of the consultation with Member States, the applicant and EFSA on the pesticide risk assessment for spiroxamine in light of confirmatory data*. 2017.
34. ECHA, *Background document to the Opinion proposing harmonised classification and labelling at EU level of Spiroxamine*, C.f.R.A. RAC, Editor. 2015.
35. Adcock, C., Tasheva, M., *Flusilazole 317-347 JMPR*. 2007, Health Evaluation Directorate, Pest Management Regulatory Agency, Health Canada, Canada; and National Center of Public Health Protection, Sofia, Bulgaria.
36. Spielmann, H., et al., *The Embryonic Stem Cell Test, an In Vitro Embryotoxicity Test Using Two Permanent Mouse Cell Lines: 3T3 Fibroblasts and Embryonic Stem Cells*. In Vitro Toxicology, 1997. **10**: p. 119-127.

37. de Jong, E., et al., *Potency ranking of valproic acid analogues as to inhibition of cardiac differentiation of embryonic stem cells in comparison to their in vivo embryotoxicity*. *Reprod Toxicol*, 2011. **31**(4): p. 375-82.
38. *CellTiter-Blue Cell Viability Assay technical bulletin #TB317*. Promega Corporation.
39. Genschow, E., et al., *Validation of the embryonic stem cell test in the international ECVAM validation study on three in vitro embryotoxicity tests*. *Altern Lab Anim*, 2004. **32**(3): p. 209-44.
40. Szklarczyk, D., et al., *STRING v10: protein-protein interaction networks, integrated over the tree of life*. *Nucleic Acids Res*, 2015. **43**(Database issue): p. D447-52.
41. Shannon, P., et al., *Cytoscape: a software environment for integrated models of biomolecular interaction networks*. *Genome Res*, 2003. **13**(11): p. 2498-504.
42. Slob, W., *Dose-response modeling of continuous endpoints*. *Toxicol Sci*, 2002. **66**(2): p. 298-312.
43. Pfaffl, M.W., *A new mathematical model for relative quantification in real-time RT-PCR*. *Nucleic Acids Res*, 2001. **29**(9): p. e45.
44. Sguazzini, E., et al., *Reevaluation of fenpropimorph as a sigma receptor ligand: Structure-affinity relationship studies at human sigma1 receptors*. *Bioorg Med Chem Lett*, 2017. **27**(13): p. 2912-2919.
45. Hajipour, A.R., et al., *Synthesis and characterization of N,N-dialkyl and N-alkyl-N-arylalkyl fenpropimorph-derived compounds as high affinity ligands for sigma receptors*. *Bioorg Med Chem*, 2010. **18**(12): p. 4397-404.
46. Moebius, F.F., et al., *Pharmacological analysis of sterol delta8-delta7 isomerase proteins with [3H]ifenprodil*. *Mol Pharmacol*, 1998. **54**(3): p. 591-8.
47. Penke, B., et al., *The Role of Sigma-1 Receptor, an Intracellular Chaperone in Neurodegenerative Diseases*. *Curr Neuropharmacol*, 2018. **16**(1): p. 97-116.
48. Paul, R., et al., *Both the immunosuppressant SR31747 and the antiestrogen tamoxifen bind to an emopamil-insensitive site of mammalian Delta8-Delta7 sterol isomerase*. *J Pharmacol Exp Ther*, 1998. **285**(3): p. 1296-302.
49. Pan, J., C. Hu, and J.-H. Yu, *Lipid Biosynthesis as an Antifungal Target*. *Journal of Fungi*, 2018. **4**(2): p. 50.
50. Robinson, J.F., et al., *Triazole induced concentration-related gene signatures in rat whole embryo culture*. *Reprod Toxicol*, 2012. **34**(2): p. 275-83.
51. Wages, P.A., et al., *Screening ToxCast™ for Chemicals That Affect Cholesterol Biosynthesis: Studies in Cell Culture and Human Induced Pluripotent Stem Cell-Derived Neuroprogenitors*. *Environ Health Perspect*, 2020. **128**(1): p. 17014.
52. Corio-Costet, M.F., et al., *Inhibition by the fungicide fenpropimorph of cholesterol biosynthesis in 3T3 fibroblasts*. *Biochem J*, 1988. **256**(3): p. 829-34.
53. Ruan, B., et al., *Aberrant pathways in the late stages of cholesterol biosynthesis in the rat. Origin and metabolic fate of unsaturated sterols relevant to the Smith-Lemli-Opitz syndrome*. *J Lipid Res*, 2000. **41**(11): p. 1772-82.
54. Shibata, M., *A new potent teratogen in CD rats inducing cleft palate*. *J Toxicol Sci*, 1993. **18**(3): p. 171-8.

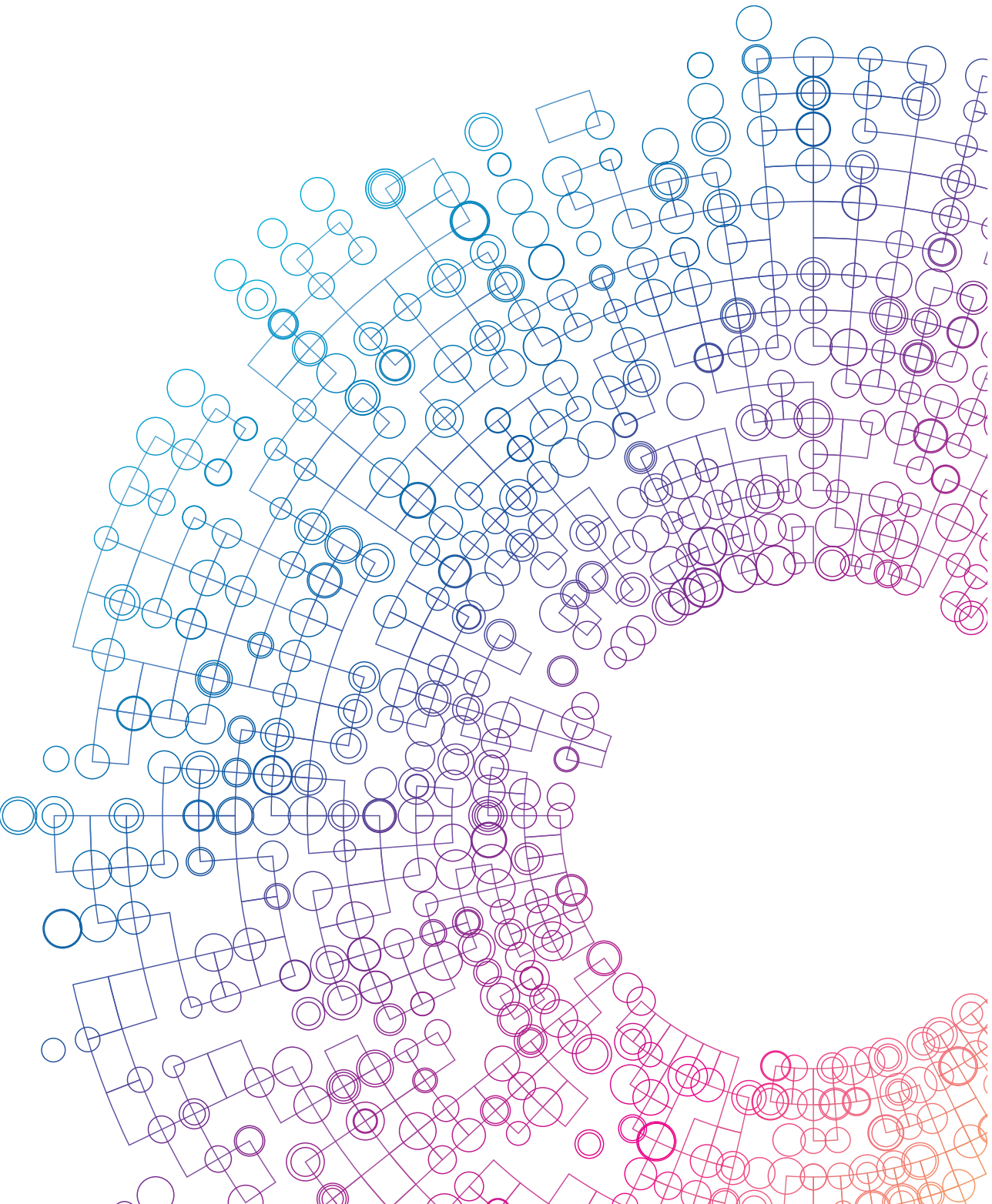
55. Baker, N.C., et al., *Characterizing cleft palate toxicants using ToxCast data, chemical structure, and the biomedical literature*. Birth Defects Res, 2020. **112**(1): p. 19-39.
56. Menegola, E., et al., *Study on the common teratogenic pathway elicited by the fungicides triazole-derivatives*. Toxicol In Vitro, 2005. **19**(6): p. 737-48.
57. Menegola, E., et al., *Antifungal triazoles induce malformations in vitro*. Reprod Toxicol, 2001. **15**(4): p. 421-7.
58. Grandjean, P., *Paracelsus Revisited: The Dose Concept in a Complex World*. Basic & Clinical Pharmacology & Toxicology, 2016. **119**(2): p. 126-132.
59. Grandjean, P., et al., *The faroes statement: human health effects of developmental exposure to chemicals in our environment*. Basic Clin Pharmacol Toxicol, 2008. **102**(2): p. 73-5.
60. Vogel, S.A., *From 'The Dose Makes the Poison' to 'The Timing Makes the Poison': Conceptualizing Risk in the Synthetic Age*. Environmental History, 2008. **13**(4): p. 667-673.
61. Hawkins, D.R., et al., *The metabolic fate of tridemorph in rats*. Pesticide Science, 1974. **5**(5): p. 535-542.
62. EC, *Directive 98/8/EC concerning the placing of biocidal products on the market. Assessment report Fenpropimorph*. 2009.



SECTION

A hypothesis-generating data-driven approach for biomarker selection





5

CHAPTER

Genome-wide expression
screening in the cardiac
embryonic stem cell test shows
additional differentiation
routes that are regulated by
morpholines and piperidines

R.H. Mennen, N. Hallmark, M. Pallardy, R. Bars,
H. Tinwell, A.H. Piersma

Submitted to Current Research in Toxicology

Abstract

The cardiac embryonic stem cell test (ESTc) is a well-studied non-animal alternative test method based on cardiac cell differentiation inhibition as a measure for developmental toxicity of tested chemicals. In the ESTc, a heterogenic cell population is generated besides cardiomyocytes. Using the full biological domain of ESTc may improve the sensitivity of the test system, possibly broadening the range of chemicals for which developmental effects can be detected in the test. In order to improve our knowledge of the biological and chemical applicability domains of the ESTc, we applied a hypothesis-generating data-driven approach on control samples as follows. A genome-wide expression screening was performed, using Next Generation Sequencing (NGS), to map the range of developmental pathways in the ESTc and to search for a predictive embryotoxicity biomarker profile, instead of the conventional read-out of beating cardiomyocytes. The detected developmental pathways included circulatory system development, skeletal system development, heart development, muscle and organ tissue development, and nervous system and cell development. Two pesticidal chemical classes, the morpholines and piperidines, were assessed for perturbation of differentiation in the ESTc using NGS. In addition to the anticipated impact on cardiomyocyte differentiation, the other developmental pathways were also regulated, in a concentration-response fashion. Despite the structural differences between the morpholine and piperidine pairs, their gene expression effect patterns were largely comparable. In addition, some chemical-specific gene regulation was also observed, which may help with future mechanistic understanding of specific effects with individual test compounds. These similar and unique regulations of gene expression profiles by the test compounds, adds to our knowledge of the chemical applicability domain, specificity and sensitivity of the ESTc. Knowledge of both the biological and chemical applicability domain contributes to the optimal placement of ESTc in test batteries and in Integrated Approaches to Testing and Assessment (IATA).

Key words: cardiac embryonic stem cell test, biological domain, applicability domain, genome-wide expression screening, morpholines, piperidines

Introduction

The extensive use of animals under current international regulations for human chemical safety testing is increasingly conflicting with ethical and scientific principles. This is especially relevant in the field of developmental and reproductive toxicology (DART), as it uses relatively large numbers of animals partially because effects on multiple generations are assessed [1-3]. To move away from animal-model based 'black box' testing and to focus more directly on human biology, alternative methods should preferably be mechanism based as this would increase comparability between perturbation of developmental pathways between species and would facilitate extrapolation of laboratory test methods to human individuals [4].

The cardiac embryonic stem cell test (ESTc) is a well-studied *in vitro* assay for developmental toxicity testing. It determines chemical-induced perturbations of the differentiation of pluripotent stem cells into beating cardiomyocytes [5]. Within the ESTc, a heterogenic cell population is generated with mixed cell types besides cardiomyocytes. For example, neural crest cells and neurons are also present within the ESTc [6, 7]. However, a complete inventory of the cell type composition generated by stem cell differentiation within the ESTc has not been mapped so far. Such an understanding of the complete biological domain of the ESTc could improve our mechanistic understanding of cell differentiation in the ESTc and provide more information on which mechanisms within the ESTc can be perturbed, aiding the specificity and the sensitivity of this *in vitro* tool for the assessment of chemically induced developmental toxicity.

It is already known that not all developmental toxicants that show an *in vivo* response in laboratory mammals also show a response in the ESTc. While this difference in assay sensitivity is not yet well understood, it is logical given that the stem cells cannot fully mimic the biological complexity and diversity in whole organisms. The reason for these differences is becoming better understood using the growing knowledge of toxicity mechanisms at the sub-cellular level e.g. using gene expression profiling. This would explain why the original ESTc method by scoring beating cardiomyocytes has a limit to its biological applicability domain which is at the cellular level. By changing the endpoint of the assay from subjective observation of beating cardiomyocyte inhibition to gene expression profiles of the differentiation route, it may become possible to improve the predictability of this assay. This will result in a better understanding of its biological applicability domain and therefore the knowledge of the limits and scope of its chemical applicability domain will

increase. For example, the developmental toxicant 2,3,7,8-Tetrachlorodibenzo-p-dioxin (TCDD) is not detected by the cardiomyocyte readout of the ESTc, but can be predicted a developmental toxicant by an additional EST test in which osteogenesis is stimulated [8]. Defining the biological and chemical applicability domains of *in vitro* test systems such as the ESTc could facilitate test assay selection for chemical screening strategies or Integrated Approaches to Testing and Assessment (IATA) and with that improve toxicity predictions.

The ESTc has been shown to be an appropriate screening tool for triazoles by their interference with beating cardiomyocyte differentiation [9]. Triazoles are designed to interfere with fungal cholesterol biosynthesis by inhibiting sterol 14 α -demethylase cytochrome P450 (CYP51), which demethylates lanosterol in the cholesterol biosynthesis pathway [10, 11]. Like triazoles, morpholines and piperidines are classes of fungicides but which are less well studied including within the ESTc. They are also designed and shown to interfere with fungal cholesterol (= ergosterol) biosynthesis, but are structurally different from triazoles. Within the ergosterol biosynthesis pathway the morpholines and piperidines inhibit sterol Δ 14-reductase and sterol Δ 8, Δ 7-isomerase which are important in the formation of 4,4-dimethylzymosterol or ergosterol, respectively (Fig 1) [11, 12]. Morpholines and piperidines can cause foetal malformations in rats, such as cleft palate formation after oral exposure to tridemorph at doses not toxic to the dams [13].

In order to apply a mechanism based ESTc readout, previous studies have involved gene transcript analysis using a hypothesis-driven targeted approach by preselecting gene transcript biomarkers based on existing literature [6, 14-16]. This approach has been successful for chemicals with known adverse effects for which it is possible to generate such hypotheses. However, unknown effects not supported by existing literature can be missed. Therefore, a comprehensive genome-wide expression screening could help improve our mechanistic understanding of chemical perturbations. Such an approach can be used to generate reasonable hypotheses by linking regulated pathways to phenotypic changes [17], and may ultimately improve hazard and risk assessment [18, 19]. This may potentially avoid future confirmatory *in vivo* testing.

The objective of the present investigations was to derive an inclusive predictive biomarker profile for embryotoxicity, using a hypothesis-generating data-driven approach using genome-wide gene expression screening 'NGS', that would be able to eventually distinguish compounds within and between chemical classes.

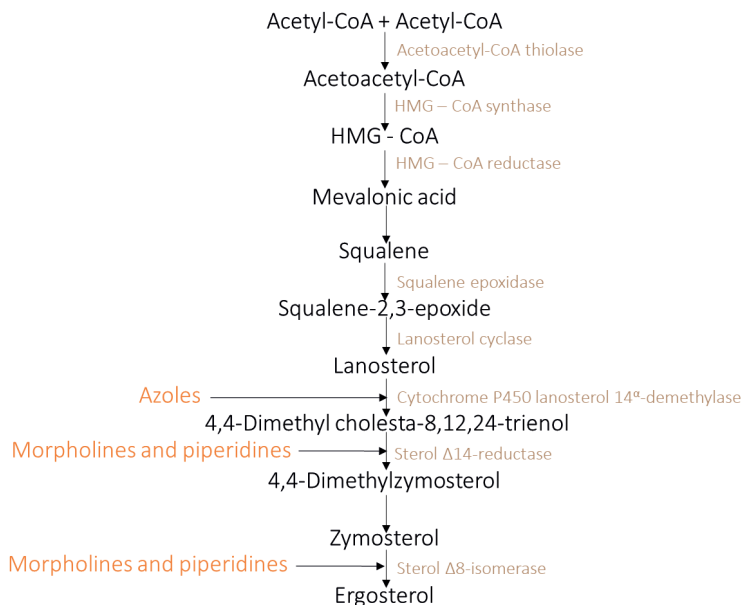


Figure 1: Ergosterol biosynthesis interference by azoles, morpholines and piperidines. Adapted and modified from [11]. HMG-CoA = β -Hydroxy- β -methylglutaryl-CoA.

This approach was used to describe which differentiation routes appear during embryonic stem cell differentiation in the ESTc, comparing immature early stage (day four) and mature late stage (day ten) differentiation timepoints. The effects of the morpholines and piperidines on the ESTc biological domain were studied, by investigating differences in gene expression level changes between the structurally similar compounds within compound groups.

Methods

Stem cell culture

Murine embryonic stem cells (ES-D3 (D3), ATCC® (Manassas, VA, USA)) were maintained according to the previously described protocol [6, 20]. The embryonic stem cells (ESCs) were maintained in 35 mm culture dishes (Corning, New York, NY, USA) in a humidified atmosphere at 37°C with 5% CO₂ for stimulation of cell proliferation. ESCs were replated in fresh medium every 2-3 days. The culture medium (CM) consisted of Dulbecco's Modified Eagle's Medium (DMEM; Gibco, Waltham,

MA, USA), 20% Foetal Bovine Serum (FBS; Greiner Bio-One, Kremsmünster, Austria); 2 mM L-Glutamine (Gibco); 1% Non-Essential Amino Acids (NEAA; Gibco); 1% 5000 IU/ml Penicillin/5000 µg/ml Streptomycin (Gibco); and 0.1 mM β-mercaptoethanol (Gibco). In order to preserve pluripotency, the ESCs in CM were supplemented with 1000 units/ml leukemia inhibitory factor (LIF; ESGRO®, Millipore, Burlington, MA, USA). These pluripotent ESCs were used in the differentiation assays.

Cell differentiation assay

A previously described protocol was used to differentiate ESCs into cardiomyocytes [5, 20]. To enable differentiation, the CM as described for stem cell-culture was used without the addition of LIF. The differentiation protocol started with the hanging-drop method to form cell-aggregates called embryoid bodies (EBs) at differentiation day 0 (DD0). For this method, a $3.75 \cdot 10^4$ cells/ml cell suspension was added in droplets to the inside of the lid of a 100/20 mm CELLSTAR® cell culture dish (Greiner Bio-One). 5 ml of ice-cold phosphate buffered saline (PBS; Ca²⁺, Mg²⁺ free; Gibco) was added within the base of the culture dish and then lids were added after which the complete dishes were incubated for 3 days at 37°C and 5% CO₂. At differentiation day 3 (DD3), the EBs were collected in 5 ml of exposure medium containing test compound (see section test compounds) and were added to a 60 mm bacterial petri dish (Greiner Bio-One) to prevent attachment to the bottom of the dish. At differentiation day 5 (DD5), one EBs per well of a 24-wells plate (Greiner Bio-One) was transferred, each containing 1 ml of exposure medium. These EBs were cultured without further medium changes until differentiation day 10 (DD10). Four to five independent experiments were performed and EB samples were collected for gene expression analysis.

Test compounds

Two morpholines, tridemorph (TDM, CAS# 24602-86-6) and fenpropimorph (FPM, CAS# 67564-91-4), and two piperidines, fenpropidin (FPD, CAS# 67306-00-7) and spiroxamine (SPX, CAS# 118134-30-8) were tested. The triazole flusilazole (FLU, CAS# 85509-19-9), was included as a known positive control. The compounds were obtained from Sigma-Aldrich (Zwijndrecht, The Netherlands) and were tested in concentrations previously determined from concentration-response curves for inhibition in beating cardiomyocyte development [7]. The tested ID₁₀ (= inhibitory concentration at which 10% beating inhibition occurs) and ID₅₀ (= inhibitory concentration at which 50% beating inhibition occurs) values are depicted in table 1. All experimental conditions contained 0.25% dimethyl sulfoxide (DMSO, CAS# 67-68-5, Sigma-Aldrich).

Table 1: The tested ID₁₀ (= inhibitory concentration at which 10% beating inhibition occurs) and ID₅₀ (= inhibitory concentration at which 50% beating inhibition occurs) values for the positive control FLU and the test compounds TDM, FPM, FPD, and SPX (obtained from: [7]).

	FLU	TDM	FPM	FPD	SPX
Differentiation ID ₁₀	26 μM	57 μM	1.3 μM	0.1 μM	0.54 μM
Differentiation ID ₅₀	42 μM	230 μM	5.5 μM	0.21 μM	1.2 μM

Next Generation Sequencing (NGS)

RNA collection and quality control

The samples comprised of collected EBs exposed to ID₁₀ or ID₅₀ compound concentrations or the vehicle control (0.25% DMSO) at differentiation day 4 (DD4) and DD10. These days correspond to exposure periods of 24 hours and 7 days in the ESTc, respectively. DD4 samples consisted of ~56 EBs from one 60 mm plate per sample. The larger DD10 samples consisted of 24 EBs (one from each well) from one 24-wells plate per sample. Four to five samples per condition (five for all controls and the ID₅₀ samples of DD10, four for all other samples) were collected from independent experiments and were transferred into Qiazol (Qiagen, Cat # 79306). The collected samples were stored at -80°C prior to RNA isolation (RNeasy Mini-kit (Qiagen, Cat. # 74104) according to manufacturer's protocol). Two additional steps were added to the RNA isolation protocol: a homogenisation step using QIAshredder columns (Qiagen, Cat. # 79654) and a DNase step using a RNase-Free DNase set (Qiagen, Cat # 79254). RNA quantity and quality were assessed using the Qubit3 (Invitrogen, Carlsbad, CA, USA) and the 2100 Bioanalyzer (Agilent Technologies, Amstelveen, The Netherlands).

RNA sequencing

The collected RNA samples were processed and sequenced by GenomeScan (Leiden, The Netherlands) using NGS which can sequence millions of fragments simultaneously per run and therefore can sequence hundreds to thousands of genes at one time. The NEBNext Ultra II Directional RNA Library Prep Kit for Illumina was used to process the samples. The sample preparation was performed according to the protocol "NEBNext Ultra II Directional RNA Library Prep Kit for Illumina" (NEB #E7760S/L). Briefly, mRNA was isolated from total RNA by polyA affinity purification using oligo-dT magnetic beads. After fragmentation of the mRNA, a cDNA synthesis

was performed. This was used for ligation with the sequencing adapters and PCR amplification of the resulting product. The quality and yield after sample preparation was measured with the Fragment Analyzer. The size of the resulting products was consistent with the expected size distribution (a broad peak between 300-500 bp). Clustering and DNA sequencing using the NovaSeq6000 v1.5 was performed according to the manufacturer's protocols including a concentration of 1.1 nM of DNA, two flow cells, and NovaSeq control software NCS v1.7. Image analysis, base calling, and quality check was performed with the Illumina data analysis pipeline RTA3.4.4 and Bcl2fastq v2.20. Expression levels of the transcripts (20 million paired end reads per sample) were quantified against the mouse reference genome (Ensembl GRCm38.p6, containing 22,519 coding genes) using TopHat version 2.0.14.

RNA sequencing analysis

The obtained count-tables were used for further differential gene expression analysis using Rstudio statistical software (version 4.1.0). Control samples for DD4 and DD10 were compared by differential gene expression using DESeq2 (version 1.30.0), adjusting for the sampling day per individual independent experiment to extract log₂FC values of genes with at least one count in the analysis (=20,335). Differentially Expressed Genes (DEGs) were obtained by filtering results for $p < 0.001$ and $\log_2FC > 1.5$. Functional enrichment analysis of genes in Gene Ontologies (GO) terms (biological processes GO BP5) was performed using Database for Annotation, Visualization and Integrated Discovery (DAVID; <https://david.ncifcrf.gov/> consulted in September 2021, version 6.8) as a gene list with genes of at least one count in the analysis. GO-terms were clustered using the 'functional annotation clustering' tool and summary names (see supplementary material) were obtained with help of <http://amigo.geneontology.org/amigo> based on their tree-view.

The compound treated samples were analysed in a similar manner. First, for visualisation, principal component analysis (PCA) was performed on count data after filtering out the 0 values and applying a Variance Stabilizing Transformation (VST). Additionally, data was corrected for differences between experiments. Determination of DEGs was performed using DESeq2 after filtering results for $p < 0.001$ and $\log_2FC > 0.5$ and the number of up and downregulated genes per condition were determined compared to the control (DMSO) values. PCA plots and heatmaps were generated in RStudio (version 4.0.0), Venn diagrams were assembled using Venny (version 2.1.0), and the remaining graphs were visualised using GraphPad Prism (version 8.1.2, www.graphpad.com).

Results

Gene expression changes in unexposed control cultures

To investigate cell types developing within the ESTc, we compared DD4 and DD10 gene expression in controls relative to each other by DESeq analysis. Results showed that 1255 / 20335 genes were upregulated on DD4 and 2987 / 20335 genes were upregulated on DD10 (Fig 2A). These DEGs were organised into GO-clusters and the enrichment scores were given (Fig 2B, 3C). Six GO-term clusters were regulated on DD4 were mainly related to general cell processes and mechanisms. These clusters included RNA metabolic process, small molecule metabolic process, primary metabolic process, meiotic cell cycle process, embryonic morphogenesis, and synaptic signalling (Fig 2B). At DD10, cell differentiation related GO-term clusters were significantly higher regulated as

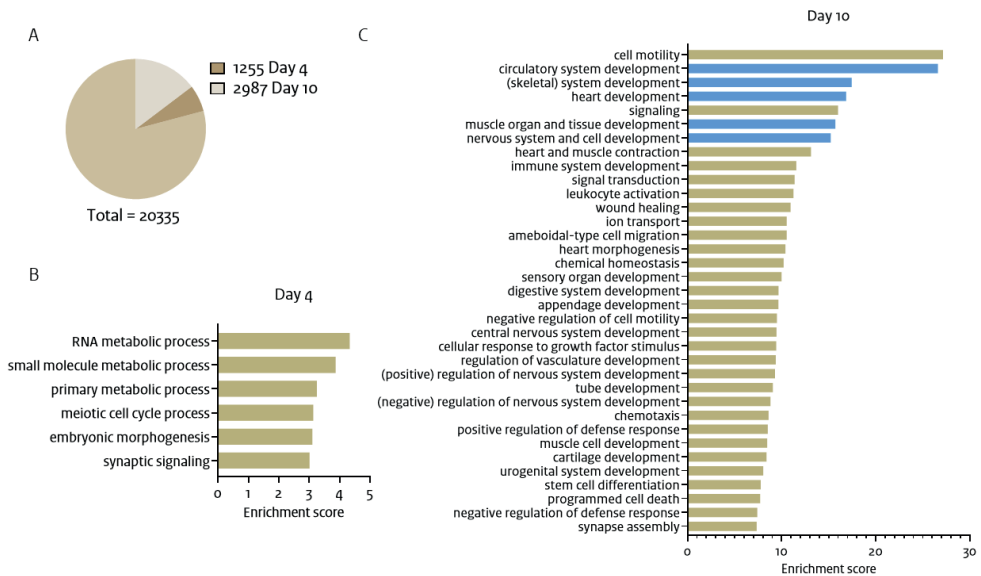


Figure 2: Genome-wide specific gene expression changes in controls per differentiation day. A) The number of Differentially Expressed Genes (DEGs) after comparison between day 4 and day 10 as part of the total number of assessed genes. B) Enrichment scores per enriched cluster of GO-terms related to the 1255 genes specific to day 4, or C) 2987 genes specific to day 10. The top 5 enriched clusters related to specific differentiation routes are depicted in blue and were selected for further analysis. Enrichment score = $-\log(p\text{-value})$ for which the p-value is the mean/median of GO-terms belonging to each cluster. $P < 0.001$, $\log_2FC > 1.5$.

compared to DD4. The top five differentiation related clusters, according to enrichment score, were circulatory system development, (skeletal) system development, heart development, muscle and organ tissue development, and nervous system and cell development. In line with the experimental purpose of understanding the differentiation occurring in this test system, these top five clusters (in blue, Fig 2C) were used for the selection of related GO-terms which were examined on DD10 for their perturbation by the test compounds.

Gene expression changes after compound exposures

To study the extent that the morpholines and piperidines perturbed normal cell differentiation in the ESTc, effects of exposure to ID₁₀ and ID₅₀ concentrations of test compounds were assessed on DD4 or DD10, corresponding to 24 hrs or 7 days exposure duration, respectively. Using a PCA plot of DD4 data, individual exposure and control samples per experiment showed a scattered pattern with low PC1 and PC2 values of 14.9% and 12%, respectively (fig. 3A). DEGs count on DD4 was highest after exposure to FLU, resulting in >20 regulated DEGs per exposure condition (fig. 3B). On DD10, the PCA plot showed more clear distinctions between samples exposed to the vehicle, FLU or the test compounds with higher PC values: PC1 53.6% and PC2 8.9% (fig. 3C). There was a clear difference in the PC2 related direction of FLU versus the PC1 related shift of the other test compounds relative to the position of the vehicle control. As anticipated, concentration responses were apparent for all compounds with ID₁₀ samples closer to the vehicle controls as compared to the ID₅₀ sample responses. The TDM ID₅₀ showed the largest distance from the vehicle controls, followed by FPD. Also, TDM ID₁₀ levels showed a relatively large distance from the vehicle controls as compared to the ID₁₀ concentrations of the other test compounds. These differences between test groups in the PCA plots were also reflected in the DESeq analysis and DEGs showed most regulated genes in the samples exposed with TDM ID₅₀ or FPD ID₅₀ (fig. 3D).

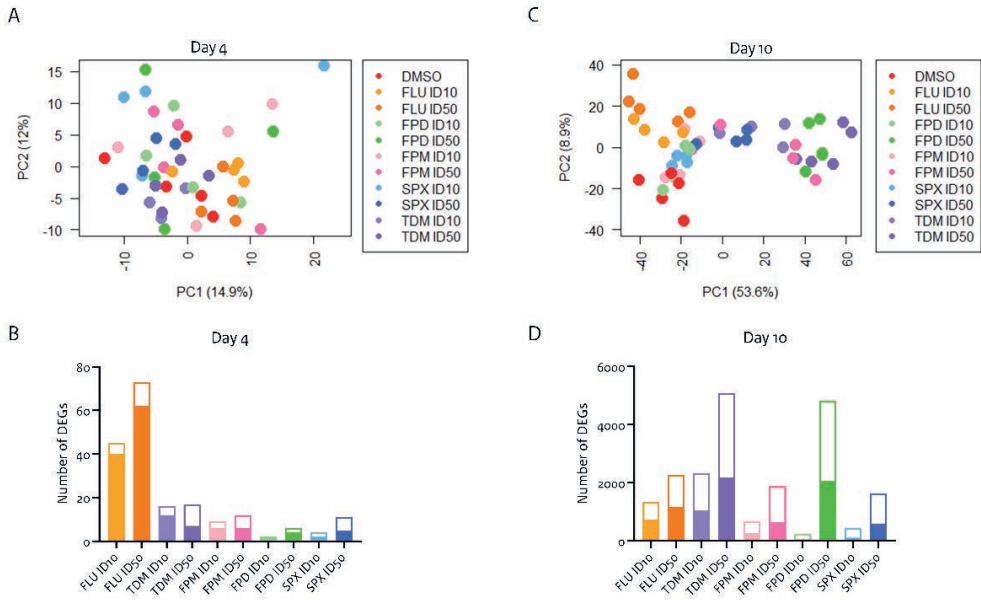


Figure 3: Genome-wide gene expression regulations in exposure groups on days 4 and 10. A) Principal Component Analysis (PCA) of all experimental groups on day 4. B) Number of DEGs per exposure group with $P < 0.001$ and $\log_2FC > 0.5$; solid coloured bars indicating upregulated genes and the white bars indicate downregulated genes. C) PCA and D) DEGs per exposure group on day 10.

Differentiation day 4 gene expression analysis

The expression of regulated genes on DD4 was compared between exposures using Venny and a heatmap (fig. 4). Commonly regulated genes by at least two compounds at ID₁₀ (fig. 4A) and ID₅₀ levels (fig. 4B) were extracted from the Venny diagrams. The 9 commonly regulated genes exhibited some overlap between the ID₁₀ and ID₅₀ levels and resulted in 6 unique genes: *Tgfr3*, *Slc38a3*, *Acta2*, *Msmo1*, *Actc1*, and *Smc1b*. All conditions resulted in upregulations of these genes with \log_2FC s up to 1.1 (Fig. 4C). The conditions clustered pairwise per compound, except for the SPX conditions. *Smc1b* showed most diversity in expression levels among the test conditions.

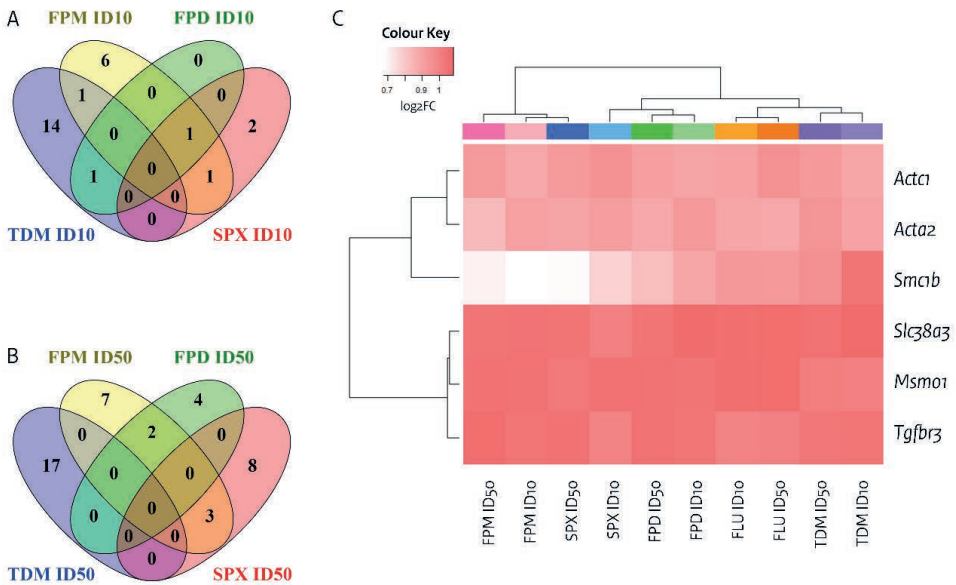


Figure 4: Common and unique DEGs per test group at day 4. A) Venny diagram for ID10 concentrations and B) ID50 concentrations. C) Heatmap of genes commonly regulated by at least two test compounds. Colour key indicates the log₂FC.

Differentiation day 10 gene expression analysis

Test conditions were examined for their interferences with the top five differentiation routes regulated in control cultures, based on GO-terms and on individual gene expression related to these GO-terms.

Analysis of effects on GO-terms

Within each of the five GO-terms, the enrichment value and number of regulated genes by each condition were assessed (fig.5). ID₁₀ and ID₅₀ showed clear concentration-responses for all compounds and GO-terms analysed. The enrichment values of GO-terms differed in magnitude between test compounds. TDM and FPD ID₅₀ conditions showed highest enrichment for the GO-term circulatory system development. FLU conditions showed highest enrichment for skeletal system development and nervous system development. Smaller differences in enrichment values were found for the GO-terms heart development and muscle organ development. Although the ESTc was designed to detect cardiomyocyte differentiation effects, the largest effects of the test compounds were found on nervous system development.

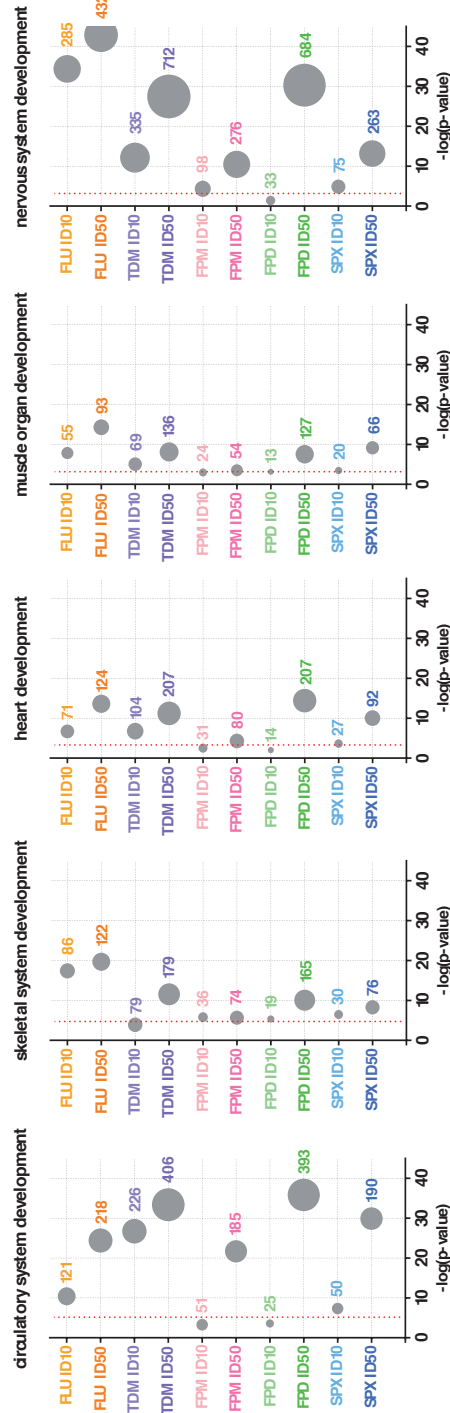


Figure 5: GO-term enrichment per exposure group. The -log(p-value) displays the significance of enrichment. Circle size indicates the number of regulated genes (as indicated) by each condition. The red dotted line indicates a P-value of 0.001. All values to the right of this line are $P < 0.001$.

Analysis of effects on individual gene expression

Shared and unique genes per GO-term regulated between test compounds were visualised in the Venn-diagrams (fig. 6). Shared regulated genes per GO-term were assessed for overlap of DEGs between GO-terms of the genes that were commonly regulated by the morpholines and piperidines (fig. 7). The genes responsive in the GO-term heart development were all shared by the GO-term circulatory system development. The GO-terms circulatory system development, skeletal system development, muscle organ development, and nervous system development also showed overlap between commonly regulated DEGs, but also contained uniquely regulated genes. Chemical regulation of the common DEGs per GO-term obtained from figure 6 were evaluated and visualised in heatmaps (fig. 8-12). Generally, the heatmaps separated FLU and ID₁₀ conditions of FPM, SPX, and FPD from the remaining ID₅₀ test compounds and TDM ID₁₀. For all the test compounds except FLU, genes were always regulated in the same direction of up- or down-regulation. Therefore, no distinction as to specific gene up- or down-regulation could be made between the morpholine and piperidine group, nor within these structural groups. However, in some cases FLU regulated genes in an opposite direction (fig 8-12, Table 2). These genes were related to multiple GO-terms and were not unique to one of the GO-terms.

Uniquely regulated genes by the test compounds within ID₅₀ levels are listed per GO-term in Supplementary table 1. TDM generally showed the most uniquely regulated genes, whereas FPM showed the least uniquely regulated genes. Also, in this case, the listed genes were not always unique to each GO-term.

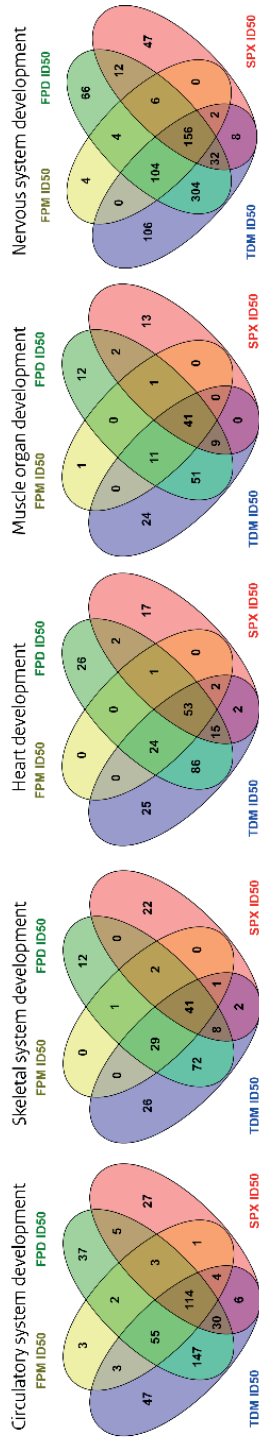


Figure 6: Venn-diagrams of common and specific Differentially Expressed Genes (DEGs) per GO-term of ID₅₀ test groups at day 10.

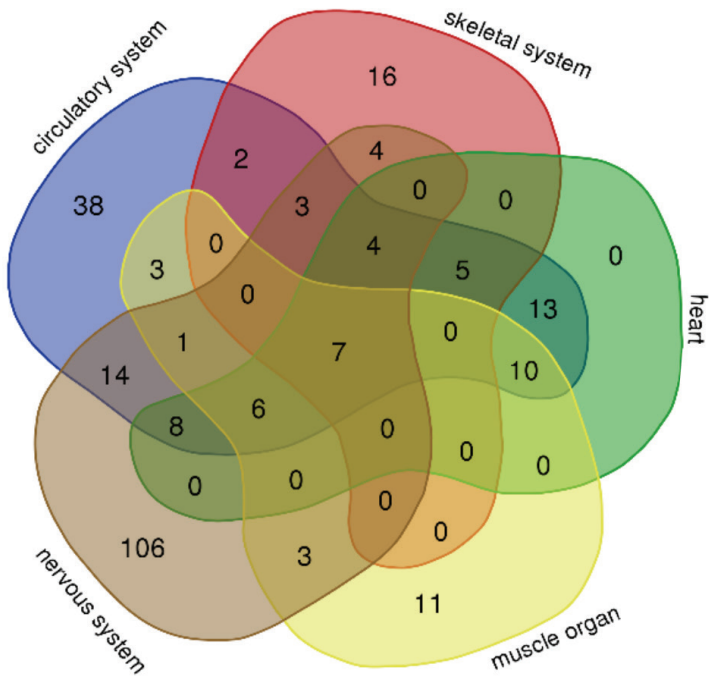
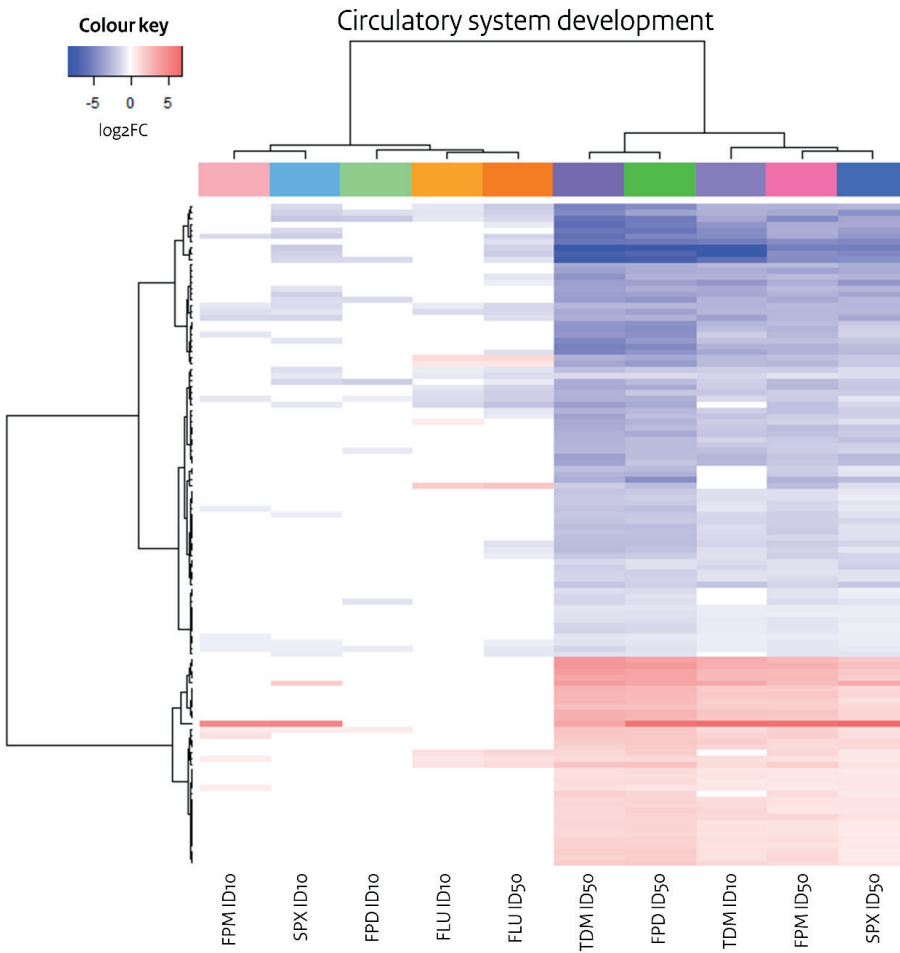


Figure 7: Venn-diagram of common chemical regulated DEGs per development related GO-term of ID50 test groups at day 10.



5

Figure 8: Heatmap of common DEGs between test compounds for the GO-term Circulatory system development. The red-blue colour key indicates the log₂FC.

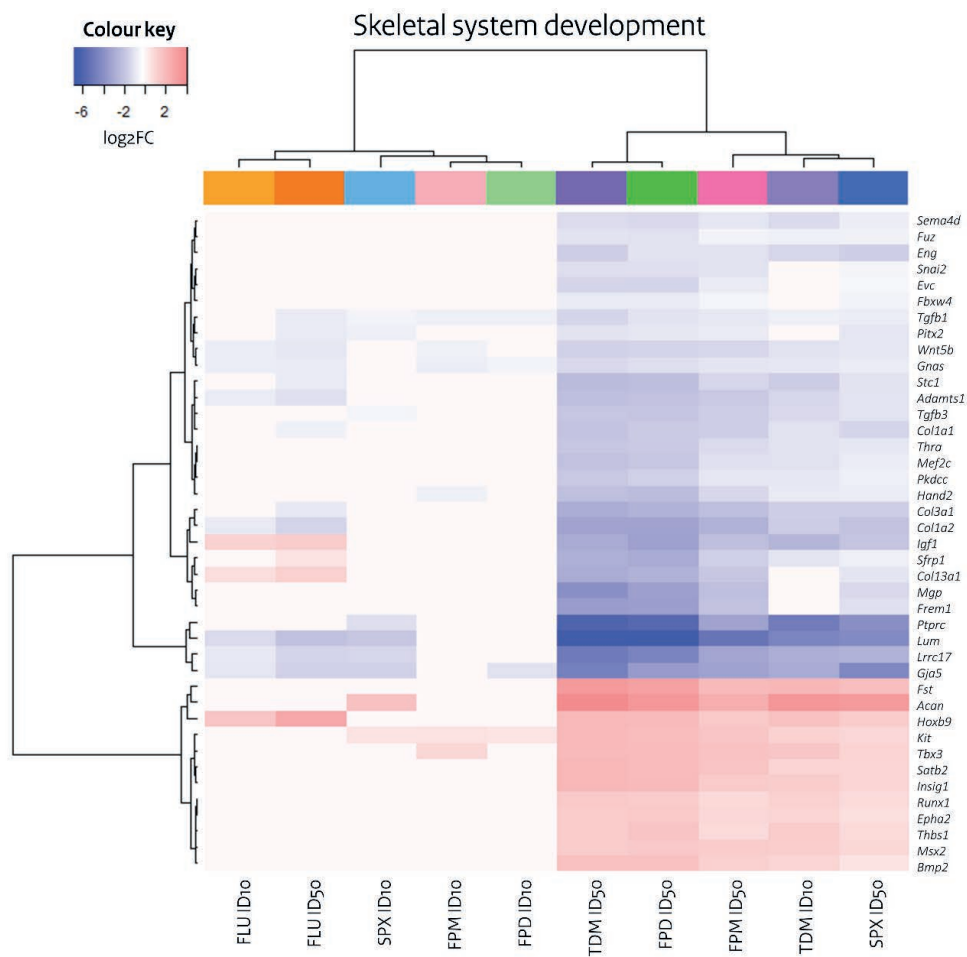


Figure 9: Heatmap of common DEGs between test compounds for the GO-term Skeletal system development. The red-blue colour key indicates the log₂FC.

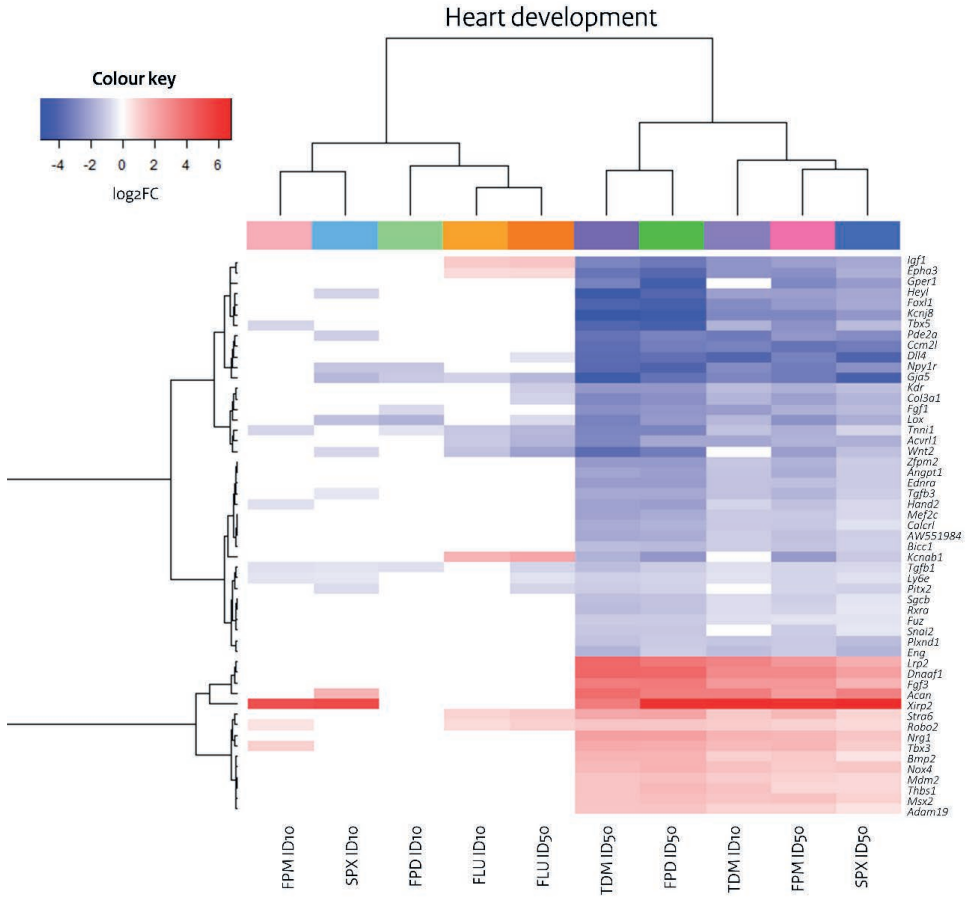


Figure 10: Heatmap of common DEGs between test compounds for the GO-term Heart development. The red-blue colour key indicates the log₂FC.

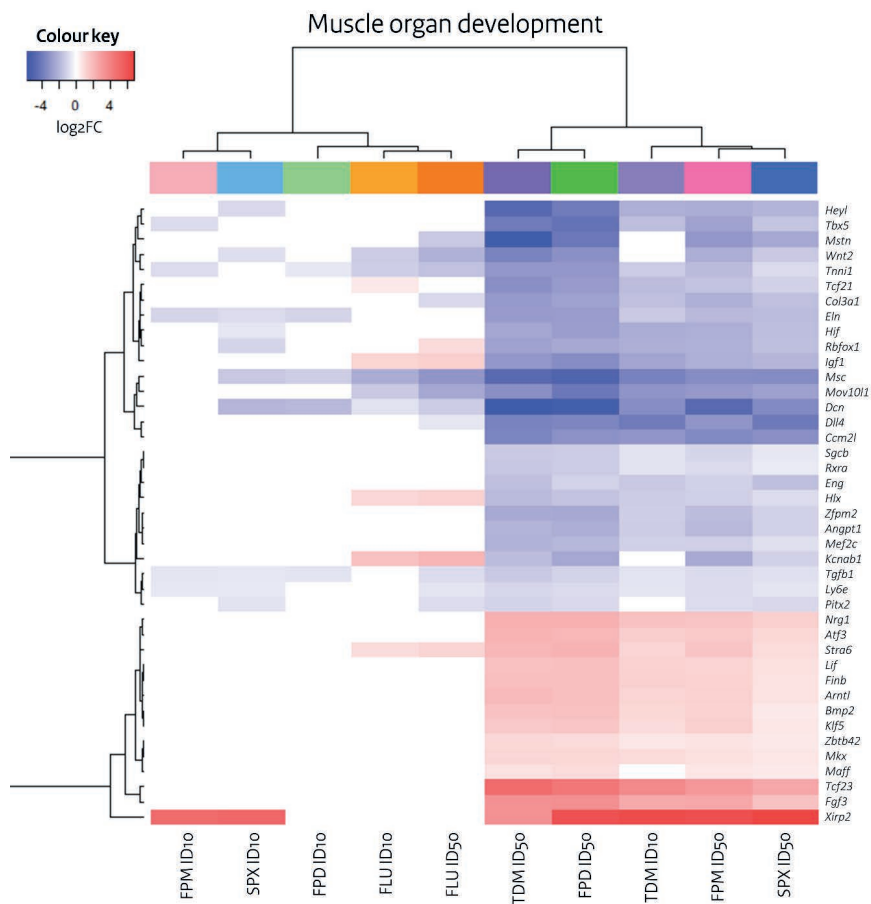


Figure 11: Heatmap of common DEGs between test compounds for the GO-term Muscle organ development. The red-blue colour key indicates the log₂FC.

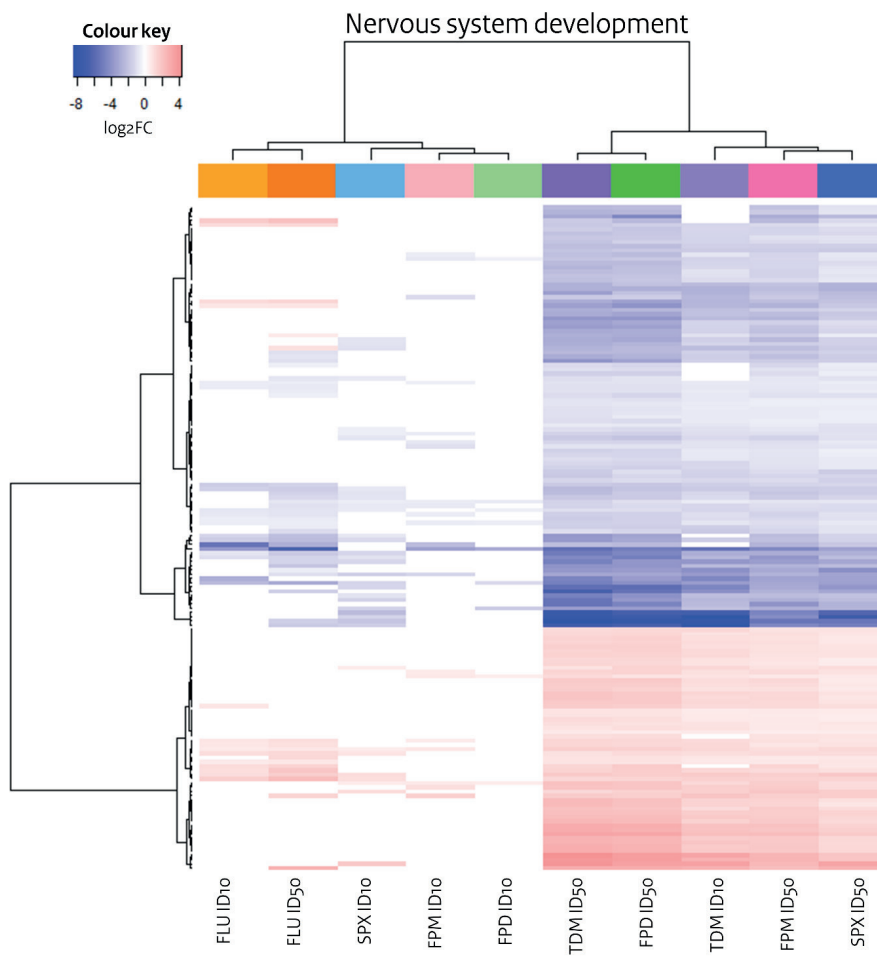


Figure 12: Heatmap of common DEGs between test compounds for the GO-term Nervous system development. The red-blue colour key indicates the log₂FC.

Table 2: List of genes that were upregulated by FLU, but downregulated by the other test compounds relative to the DMSO control. Crosses indicate these genes and the GO-terms in which they appear.

	Circulatory system development	Skeletal system development	Heart development	Muscle organ development	Nervous system development
Epha3	X		X		X
Igf1	X	X	X	X	X
Kcnab1	X		X	X	X
Tcf21	X				
Sfrp1		X			X
Coll3a1		X			
Hlx				X	X

Discussion

This study has advanced the understanding of the biological domain within the ESTc. This has been possible through mapping the biological domain in terms of emerging cell differentiation routes within the ESTc by applying a hypothesis-generating data-driven approach using a genome-wide gene expression screen (NGS). This tool has the advantage to sequence millions of fragments simultaneously per run and therefore can sequence hundreds to thousands of genes at one time. A comparison between an early and a late time-point within the ESTc protocol confirmed cardiomyocyte differentiation and also revealed the presence of additional differentiation routes as was shown by cell type specific GO-term analysis. These GO-terms were regulated by all compounds and thus gave mechanistic insight into the perturbations by morpholines and piperidines on multiple stem cell differentiation routes.

Compared to existing literature describing the use of transcriptomics with the ESTc [21-26], the current study used a more comprehensive approach for gene expression analysis as there was no 'a priori' selection of a subset of genes to be measured and instead the expression level of all expressed genes (>20k) was determined and then organised into GO-terms. This approach revealed that the GO-cluster for nervous system development in particular represented the highest number of regulated genes that were unique to this GO-term as illustrated in figure 7. The presence of a

sub-population of neuronal cells within the ESTc has been previously investigated. Using a different study approach, the presence of TUBB3 positive cells, indicative of neuronal differentiation, has been shown in the ESTc [7]. Also, neural crest cells have been observed within the ESTc [6, 15], but this differentiation route is relatively less represented in the current study (Fig 2; supplementary material).

On DD4, genes specific to basic cell processes and mechanisms were mainly expressed and chemical treatments showed regulation of six common genes between the test compounds. These genes had mixed functions with half of them (Msmo1, Actc1, Acta2) being related to the intended mode of action of the test compounds or to the original readout of the ESTc. Interestingly, Methylsterol Monooxygenase 1 (Msmo1) has previously been found to be commonly regulated by the test compounds within the ESTc [7]. The selection of this gene was based on existing literature, whereas in this genome-wide analysis it was one of the significant genome-wide regulated genes on DD4. FLU also induces Msmo1 in the rat whole embryo culture [27]. The test compounds affect the sterol biosynthesis pathway by accumulation of sterol intermediates upon FPM and SPX exposure in hiPSCs [28] and by inhibition of $\Delta 8$ - $\Delta 7$ isomerase by exposure to FPM in rat liver homogenates [29]. Our results confirm Msmo1 is a useful gene for early developmental toxicity screening for compounds with similar modes of action. The genes Actc1 (actin alpha cardiac muscle 1) and Acta2 (α -smooth muscle actin) are both markers for early heart development and have been studied in relation to perturbations of murine embryonic stem cell differentiation before [30-32]. The other three genes (Smc1b, Tgfbr3, Slc38a3) were studied in cell differentiation in different contexts. Smc1b (Structural maintenance of chromosome 1b) has been studied in relation to the formation of germ cells from embryonic stem cells and meiosis and was influenced by BMP4 (bone morphogenetic protein 4) [33]. Tgfbr3 (transforming growth factor beta receptor 3) has been studied in relation to osteogenic differentiation [34-36]. Lastly, the amino acid transporter Slc38a3 (Solute carrier family 38 member 3) has been studied in relation to lung cancer development [37,38]. Although the differences in regulation of these six genes by the test compounds were small, especially the genes Msmo1, Actc1, and Acta2 related to cardiac muscle cell differentiation and chemical mode of action (MOA) may be relevant biomarker genes when studying differentiation perturbations on DD4.

On DD10, the test compounds also regulated other differentiation routes in addition to the original readout of the ESTc. The morpholines and piperidines have

been tested before in the ESTc in relation to neuron differentiation and regulated gene expression of *Tubb3* [7]. The effects of FPM and SPX have also been tested in several human cell lines and developing human neural tissue [28]. In these cells, FPM and SPX increased levels of 7- and 8-dehydrocholesterol and reduced levels of desmosterol and cholesterol. Therefore, the authors concluded these compounds may be developmental neurotoxicants as cholesterol is an essential lipid in the central nervous system and its metabolism is affected in many neurodevelopmental disorders [28]. FPM has also been assessed with regard to craniofacial malformations in zebrafish embryos where a set of marker genes were selected that gave insight into the mode of action associated with skeletal mal-development [39].

At equipotent concentrations, as measured by inhibition of cardiac differentiation, TDM and FPD regulated ~5000 DEGs while the other compounds regulated ~2000 DEGs (fig. 2D). Large differences in gene expression regulation by equipotent concentrations of compounds have been observed before, e.g. in ESTn, in which carbamazepine regulated far fewer genes as compared to valproic acid, which are both anti-epileptic drugs [40]. This indicates that gene expression analysis offers a very different perspective on compound effects and potency, in particular providing additional information on molecular regulation, that can inform about mechanism of action.

The test compounds regulated genes within all prioritized GO-terms. The commonly affected genes were all regulated in the same direction when comparing test compounds and therefore discriminate between compounds. However, uniquely regulated genes were also found for each test compound within each GO-term that may help in the identification of compound specific effects when comparing the morpholines and piperidines (supplementary table 1). These dozens of genes should be verified for their uniqueness and functional properties in additional experiments. These findings are indicative of common and unique mechanisms of toxicity induced by the selection of the test compounds in these experiments. The presence of such potential differences in mechanisms were not observed or studied in *in vivo* studies [13, 41-46]. Apart from mechanistic comparisons of dynamic effects, differences in potency, kinetics and metabolism *in vivo* may affect embryotoxicity. Studies in adult rats show clearance of FPM, TDM, and FLU from the body into urine and faeces [46-48], while information on kinetics in pregnancy is often not available for non-pharmaceutical chemicals. This hampers the estimation of relative potency.

The expression changes of commonly affected genes occurred in some cases in the opposite direction for the test compounds as compared to FLU, which is indicative of the perturbations of different mechanisms. Seven genes were differently regulated: *Epha3*, *Igf1*, *Kcnab1*, *Tcf21*, *Sfrp1*, *Col13a1*, and *Hlx* and were all upregulated by FLU. These genes were not unique to the related GO-terms (Table 2), but are involved in embryo development. Genes *Igf1*, *Epha3*, and *Tcf21* all play a role in heart development. *Igf1* (insulin growth factor 1) is involved in expanding the developing mesoderm and promoting cardiac differentiation [49], which would hold true for FLU since it upregulated *Igf1* expression, but not for the test compounds. A repression of *Igf1* by bisphenol A in human ESC (hESC) EBs is correlated with a decreased neural cell differentiation [50]. hESC maintenance by the addition of IGF to Activin containing medium supported pluripotency through PI3K/mTOR signalling [51]. *Epha3* (Ephrin type-A receptor 3) is a receptor kinase necessary for the fusion of the ventricular septum and atrioventricular cushions during heart development [52]. *Tcf21* (transcription factor 21) is an epicardial marker in heart development and a progenitor of ventricular cardiomyocyte and pharyngeal muscle [53-55]. *Tcf21* is also involved in the mesenchyme of developing organs like the kidney, lung and gut [56]. *Col13a1* and *Hlx* are also involved in mesenchyme cells and organ development. *Col13a1* (collagen type XIII alpha 1 chain) is a collagen involved in the mesenchymal subtype in the lungs and causes congenital myasthenic syndrome type 19 [57, 58]. This collagen is also important in the basal lamina of neuromuscular junctions and mice lacking *Col13a1* show immature nerve terminals and reduced neurotransmission [59]. *Hlx* (H2.0 like homeobox) enhanced the appearance of premature reprogramming cells in hiPSCs and interfered with pluripotency [60]. During embryogenesis, *Hlx* is prominently expressed in visceral mesenchyme of the developing liver, gall bladder and gut [61]. *Sfrp1* (Secreted frizzled related protein 1) is the counter-acting molecule of Wnt and seems to have a role in rostral- and caudal regulation of ESC-derived neuroectoderm [62], and in differentiation of stem cells to dopaminergic neurons [63]. *Kcnab1* (potassium voltage-gated channel subfamily A regulatory beta subunit 1) has not been studied in relation to stem cells or embryo development, except for its association with elevated birth weight, which may have been attributed to gestational duration [64]. In summary, these differently regulated genes between FLU and the test compounds are involved in multiple differentiation routes.

Overall, this hypothesis-generating data-driven approach provided a valuable and additional perspective on the biological domain of the ESTc, through the novel

mechanistic information from the large quantity of gene expression analysis compared to methods with a priori gene selection. Given the conserved nature of the developmental mechanisms of vertebrate embryonic cell differentiation represented in the mouse-derived ESTc, these mechanisms are likely to be relevant for human safety prediction and protection as well. The overlapping and unique gene regulations of the tested compounds advances our knowledge of the chemical applicability domain of the ESTc. This progressive understanding and knowledge of both the biological and chemical applicability domains for this assay could contribute to future toxicity predictions by facilitating selection of reliable and relevant test assays for effective chemical screening strategies, themselves part of Integrated Approaches to Testing and Assessment (IATA). This refined ESTc method, together with other *in vitro* and *in silico* test systems in combination with kinetic modelling, can be instrumental for the contextualisation of such test batteries for improved prediction and protection of human development, enabling hazard and risk assessment with reduced dependence on *in vivo* animal models.

Acknowledgements

Gina Mennen was supported by the French National Association for Research and Technology (ANRT) through a CIFRE PhD grant no. 2018-0682, which was co-supervised by Aldert Piersma, Nina Hallmark, Marc Pallardy, Remi Bars, and Helen Tinwell. Aldert Piersma was funded by the Dutch Ministry of Health, Welfare and Sports. We would like to thank Jeroen Pennings for a critical review of the manuscript.

References

1. van der Jagt, K., Munn, S., Torslov, J., de Bruijn, J., *Alternative Approaches Can Reduce the Use of Test Animals under REACH*. 2004, EC Joint Research Centre.
2. Rovida, C. and T. Hartung, *Re-evaluation of animal numbers and costs for in vivo tests to accomplish REACH legislation requirements for chemicals - a report by the transatlantic think tank for toxicology (t(4))*. *Altex*, 2009. **26**(3): p. 187-208.
3. Beekhuijzen, M., *The era of 3Rs implementation in developmental and reproductive toxicity (DART) testing: Current overview and future perspectives*. *Reproductive Toxicology*, 2017. **72**: p. 86-96.
4. Gibb, S., *Toxicity testing in the 21st century: A vision and a strategy*. *Reproductive Toxicology*, 2008. **25**(1): p. 136-138.
5. Genschow, E., et al., *Validation of the embryonic stem cell test in the international ECVAM validation study on three in vitro embryotoxicity tests*. *Altern Lab Anim*, 2004. **32**(3): p. 209-44.
6. Mennen, R.H.G., J.L.A.J. Pennings, and A.H.A. Piersma, *Neural crest related gene transcript regulation by valproic acid analogues in the cardiac embryonic stem cell test*. *Reproductive toxicology* (Elmsford, N.Y.), 2019. **90**: p. 44-52.
7. Mennen, R.H., et al., *Gene regulation by morpholines and piperidines in the cardiac embryonic stem cell test*. *Toxicol Appl Pharmacol*, 2021. **433**: p. 115781.
8. de Jong, E., L. van Beek, and A.H. Piersma, *Comparison of osteoblast and cardiomyocyte differentiation in the embryonic stem cell test for predicting embryotoxicity in vivo*. *Reprod Toxicol*, 2014. **48**: p. 62-71.
9. Dimopoulou, M., et al., *A comparison of the embryonic stem cell test and whole embryo culture assay combined with the BeWo placental passage model for predicting the embryotoxicity of azoles*. *Toxicol Lett*, 2018. **286**: p. 10-21.
10. He, M., et al., *Mutations in the human SC4MOL gene encoding a methyl sterol oxidase cause psoriasiform dermatitis, microcephaly, and developmental delay*. *J Clin Invest*, 2011. **121**(3): p. 976-84.
11. Pan, J., C. Hu, and J.H. Yu, *Lipid Biosynthesis as an Antifungal Target*. *J Fungi (Basel)*, 2018. **4**(2).
12. FRAC, *FRAC Classification of Fungicides*. 2021: Fungicide Resistance Action Committee.
13. Act, F.a.E.P., *Review of tridemorph*. 1999.
14. Mennen, R.H., V.C. de Leeuw, and A.H. Piersma, *Oxygen tension influences embryonic stem cell maintenance and has lineage specific effects on neural and cardiac differentiation*. *Differentiation*, 2020. **115**: p. 1-10.
15. Mennen, R.H., et al., *Molecular neural crest cell markers enable discrimination of organophosphates in the murine cardiac embryonic stem cell test*. *Toxicology Reports*, 2021. **8**: p. 1513-1520.
16. Mennen, R.H., V.C. de Leeuw, and A.H. Piersma, *Cell differentiation in the cardiac embryonic stem cell test (ESTc) is influenced by the oxygen tension in its underlying embryonic stem cell culture*. *Toxicol In Vitro*, 2021: p. 105247.
17. Currie, R.A., *Toxicogenomics: the challenges and opportunities to identify biomarkers, signatures and thresholds to support mode-of-action*. *Mutat Res*, 2012. **746**(2): p. 97-103.

18. Liu, Z., et al., *Toxicogenomics: A 2020 Vision*. Trends Pharmacol Sci, 2019. **40**(2): p. 92-103.
19. Merrick, B.A., *Next generation sequencing data for use in risk assessment*. Curr Opin Toxicol, 2019. **18**: p. 18-26.
20. Spielmann, H., et al., *The Embryonic Stem Cell Test, an In Vitro Embryotoxicity Test Using Two Permanent Mouse Cell Lines: 3T3 Fibroblasts and Embryonic Stem Cells*. In Vitro Toxicology, 1997. **10**: p. 119-127.
21. Pennings, J.L., et al., *Gene set assembly for quantitative prediction of developmental toxicity in the embryonic stem cell test*. Toxicology, 2011. **284**(1-3): p. 63-71.
22. Schulpen, S.H., et al., *A statistical approach towards the derivation of predictive gene sets for potency ranking of chemicals in the mouse embryonic stem cell test*. Toxicol Lett, 2014. **225**(3): p. 342-9.
23. van Dartel, D.A., et al., *Early gene expression changes during embryonic stem cell differentiation into cardiomyocytes and their modulation by monobutyl phthalate*. Reprod Toxicol, 2009. **27**(2): p. 93-102.
24. van Dartel, D.A., et al., *Transcriptomics-based identification of developmental toxicants through their interference with cardiomyocyte differentiation of embryonic stem cells*. Toxicol Appl Pharmacol, 2010. **243**(3): p. 420-8.
25. van Dartel, D.A. and A.H. Piersma, *The embryonic stem cell test combined with toxicogenomics as an alternative testing model for the assessment of developmental toxicity*. Reprod Toxicol, 2011. **32**(2): p. 235-44.
26. van Dartel, D.A., et al., *Dynamic changes in energy metabolism upon embryonic stem cell differentiation support developmental toxicant identification*. Toxicology, 2014. **324**: p. 76-87.
27. Robinson, J.F., et al., *Triazole induced concentration-related gene signatures in rat whole embryo culture*. Reprod Toxicol, 2012. **34**(2): p. 275-83.
28. Wages, P.A., et al., *Screening ToxCast™ for Chemicals That Affect Cholesterol Biosynthesis: Studies in Cell Culture and Human Induced Pluripotent Stem Cell-Derived Neuroprogenitors*. Environ Health Perspect, 2020. **128**(1): p. 17014.
29. Ruan, B., et al., *Aberrant pathways in the late stages of cholesterol biosynthesis in the rat. Origin and metabolic fate of unsaturated sterols relevant to the Smith-Lemli-Opitz syndrome*. J Lipid Res, 2000. **41**(11): p. 1772-82.
30. KalantarMotamedi, Y., et al., *Systematic selection of small molecules to promote differentiation of embryonic stem cells and experimental validation for generating cardiomyocytes*. Cell Death Discov, 2016. **2**: p. 16007.
31. Potta, S.P., et al., *Isolation and functional characterization of alpha-smooth muscle actin expressing cardiomyocytes from embryonic stem cells*. Cell Physiol Biochem, 2010. **25**(6): p. 595-604.
32. Smirnova, L., et al., *MicroRNA profiling as tool for in vitro developmental neurotoxicity testing: the case of sodium valproate*. PLoS One, 2014. **9**(6): p. e98892.
33. Esfandiari, F., et al., *Microparticle-Mediated Delivery of BMP4 for Generation of Meiosis-Competent Germ Cells from Embryonic Stem Cells*. Macromolecular Bioscience, 2017. **17**(3): p. 1600284.
34. Atala, A., *Re: Betaglycan Drives the Mesenchymal Stromal Cell Osteogenic Program and Prostate Cancer-Induced Osteogenesis*. J Urol, 2020. **203**(3): p. 465-466.

35. Cook, L.M., et al., *Betaglycan drives the mesenchymal stromal cell osteogenic program and prostate cancer-induced osteogenesis*. *Oncogene*, 2019. **38**(44): p. 6959-6969.
36. Shojaee, A., et al., *Equine adipose mesenchymal stem cells (eq-ASCs) appear to have higher potential for migration and musculoskeletal differentiation*. *Res Vet Sci*, 2019. **125**: p. 235-243.
37. Wang, Y., et al., *Amino acid transporter SLC38A3 promotes metastasis of non-small cell lung cancer cells by activating PDK1*. *Cancer Lett*, 2017. **393**: p. 8-15.
38. Person, R.J., et al., *Chronic inorganic arsenic exposure in vitro induces a cancer cell phenotype in human peripheral lung epithelial cells*. *Toxicol Appl Pharmacol*, 2015. **286**(1): p. 36-43.
39. Heusinkveld, H.J., et al., *Distinguishing mode of action of compounds inducing craniofacial malformations in zebrafish embryos to support dose-response modeling in combined exposures*. *Reprod Toxicol*, 2020. **96**: p. 114-127.
40. Schulpen, S.H., J.L. Pennings, and A.H. Piersma, *Gene Expression Regulation and Pathway Analysis After Valproic Acid and Carbamazepine Exposure in a Human Embryonic Stem Cell-Based Neurodevelopmental Toxicity Assay*. *Toxicol Sci*, 2015. **146**(2): p. 311-20.
41. EFSA, *Conclusion regarding the peer review of the pesticide risk assessment of the active substance fenpropimorph*. 2008.
42. Pfeil, R., *Fenpropimorph 27-34 JMPR*, B. Federal Institute for Risk Assessment, Germany, Editor. 2004.
43. Report, E.S., *Conclusion regarding the peer review of the pesticide risk assessment of the active substance fenpropidin*. 2007, EFSA. p. 1-84.
44. ECHA, *Background document to the Opinion proposing harmonised classification and labelling at EU level of Spiroxamine*, C.f.R.A. RAC, Editor. 2015.
45. EFSA, *Outcome of the consultation with Member States, the applicant and EFSA on the pesticide risk assessment for spiroxamine in light of confirmatory data*. 2017.
46. Adcock, C., Tasheva, M., *Flusilazole 317-347 JMPR*. 2007, Health Evaluation Directorate, Pest Management Regulatory Agency, Health Canada, Canada; and National Center of Public Health Protection, Sofia, Bulgaria.
47. EC, *Directive 98/8/EC concerning the placing of biocidal products on the market. Assessment report Fenpropimorph*. 2009.
48. Hawkins, D.R., et al., *The metabolic fate of tridemorph in rats*. *Pesticide Science*, 1974. **5**(5): p. 535-542.
49. Engels, M.C., et al., *Insulin-Like Growth Factor Promotes Cardiac Lineage Induction In Vitro by Selective Expansion of Early Mesoderm*. *STEM CELLS*, 2014. **32**(6): p. 1493-1502.
50. Huang, B., et al., *Bisphenol A Represses Dopaminergic Neuron Differentiation from Human Embryonic Stem Cells through Downregulating the Expression of Insulin-like Growth Factor 1*. *Mol Neurobiol*, 2017. **54**(5): p. 3798-3812.
51. Wamaitha, S.E., et al., *IGF1-mediated human embryonic stem cell self-renewal recapitulates the embryonic niche*. *Nature Communications*, 2020. **11**(1): p. 764.
52. Dilg, D., et al., *HIRA Is Required for Heart Development and Directly Regulates Tnni2 and Tnnt3*. *PLoS One*, 2016. **11**(8): p. e0161096.
53. upu, I.E., A.N. Redpath, and N. Smart, *Spatiotemporal Analysis Reveals Overlap of Key Proepicardial Markers in the Developing Murine Heart*. *Stem Cell Reports*, 2020. **14**(5): p. 770-787.

54. Braitsch, C.M., et al., *Differential expression of embryonic epicardial progenitor markers and localization of cardiac fibrosis in adult ischemic injury and hypertensive heart disease*. J Mol Cell Cardiol, 2013. **65**: p. 108-19.
55. Dohn, T.E., et al., *Nr2f-dependent allocation of ventricular cardiomyocyte and pharyngeal muscle progenitors*. PLoS Genet, 2019. **15**(2): p. e1007962.
56. Cui, S., L. Schwartz, and S.E. Quaggin, *Pod1 is required in stromal cells for glomerulogenesis*. Dev Dyn, 2003. **226**(3): p. 512-22.
57. uan, Y., et al., *Deconvolution of RNA-Seq Analysis of Hyperbaric Oxygen-Treated Mice Lungs Reveals Mesenchymal Cell Subtype Changes*. Int J Mol Sci, 2020. **21**(4).
58. Logan, C.V., et al., *Congenital Myasthenic Syndrome Type 19 Is Caused by Mutations in COL13A1, Encoding the Atypical Non-fibrillar Collagen Type XIII α 1 Chain*. Am J Hum Genet, 2015. **97**(6): p. 878-85.
59. Maselli, R.A., et al., *Synaptic basal lamina-associated congenital myasthenic syndromes*. Ann N Y Acad Sci, 2012. **1275**: p. 36-48.
60. Yamakawa, T., et al., *Screening of Human cDNA Library Reveals Two differentiation-Related Genes, HHEX and HLX, as Promoters of Early Phase Reprogramming toward Pluripotency*. Stem Cells, 2016. **34**(11): p. 2661-2669.
61. Hentsch, B., et al., *Hlx homeo box gene is essential for an inductive tissue interaction that drives expansion of embryonic liver and gut*. Genes Dev, 1996. **10**(1): p. 70-9.
62. Takata, N., et al., *Self-patterning of rostral-caudal neuroectoderm requires dual role of Fgf signaling for localized Wnt antagonism*. Nature Communications, 2017. **8**(1): p. 1339.
63. Kwon, Y.W., et al., *Comparative study of efficacy of dopaminergic neuron differentiation between embryonic stem cell and protein-based induced pluripotent stem cell*. PLoS One, 2014. **9**(1): p. e85736.
64. Beaumont, R.N., et al., *Genome-wide association study of offspring birth weight in 86577 women identifies five novel loci and highlights maternal genetic effects that are independent of fetal genetics*. Human Molecular Genetics, 2018. **27**(4): p. 742-756.

Supplementary

Supplementary table 1: Genes that were uniquely regulated for each test compound per selected GO-term.

	TDM	FPM	FPD	SPX
Circulatory system development	<i>Dhcr7</i>	<i>Cav1</i>	<i>B9d1</i>	<i>Adap2</i>
	<i>Cd59a</i>	<i>Cxcr2</i>	<i>Bax</i>	<i>Egfl7</i>
	<i>Gata1</i>	<i>Hoxb13</i>	<i>Fat4</i>	<i>Gata3</i>
	<i>Hopx</i>		<i>Slitrk5</i>	<i>Rb1cc1</i>
	<i>Isl1</i>		<i>Smad2</i>	<i>Sox11</i>
	<i>Nsdhl</i>		<i>Tead1</i>	<i>Adam8</i>
	<i>Tal1</i>		<i>Anp32b</i>	<i>Adra1b</i>
	<i>Adgrg6</i>		<i>Cela1</i>	<i>Bmpr2</i>
	<i>Adra2b</i>		<i>Cluap1</i>	<i>Cdh5</i>
	<i>Adm2</i>		<i>Col11a1</i>	<i>Col2a1</i>
	<i>Anpep</i>		<i>C3</i>	<i>Dkk1</i>
	<i>ApoE</i>		<i>Cdk1</i>	<i>Enpp2</i>
	<i>Atm</i>		<i>Dlc1</i>	<i>Erap1</i>
	<i>Becn1</i>		<i>Fgf9</i>	<i>Id1</i>
	<i>Bcas3</i>		<i>Foxh1</i>	<i>Id3</i>
	<i>Cdx2</i>		<i>Grem1</i>	<i>Prrx1</i>
	<i>Chil1</i>		<i>Hspb1</i>	<i>Pr17d1</i>
	<i>Dnaaf3</i>		<i>Hoxa13</i>	<i>Ptgis</i>
	<i>Dnah11</i>		<i>Junb</i>	<i>Sema3c</i>
	<i>Eomes</i>		<i>Kif7</i>	<i>Six1</i>
	<i>Epor</i>		<i>Lrrc10</i>	<i>Shh</i>
	<i>Epo</i>		<i>Met</i>	<i>S1pr1</i>
	<i>Fdps</i>		<i>Mb</i>	<i>Sulf1</i>
	<i>Flrt3</i>		<i>My12</i>	<i>Tfap2a</i>
	<i>Gjc1</i>		<i>My13</i>	<i>Tgfa</i>
	<i>Gaa</i>		<i>Neb1</i>	<i>Tgfb2</i>
	<i>Grhl2</i>		<i>Noto</i>	<i>Tgfb3</i>
	<i>Hdac5</i>		<i>Nfatc1</i>	
	<i>Hoxa5</i>		<i>Pln</i>	
	<i>Ism1</i>		<i>Pkd1</i>	
	<i>Lef1</i>		<i>Pkd11</i>	

	TDM	FPM	FPD	SPX
	<i>Mmp2</i>		<i>Rgcc</i>	
	<i>Med1</i>		<i>Sirt1</i>	
	<i>Meox2</i>		<i>Sorbs2</i>	
	<i>Map2k1</i>		<i>Shb</i>	
	<i>Nog</i>		<i>Tnnt2</i>	
	<i>Olfm1</i>		<i>Zc3h12a</i>	
	<i>Pgf</i>			
	<i>Synj2bp</i>			
	<i>Tert</i>			
	<i>Tspan12</i>			
	<i>Thy1</i>			
	<i>Uty</i>			
	<i>Vcam1</i>			
	<i>Wnt5a</i>			
	<i>Xdh</i>			
	<i>Zic3</i>			
Skeletal system development	<i>Cd44</i>	No uniquely regulated genes	<i>Papss2</i>	<i>Barx2</i>
	<i>Fli1</i>		<i>Fat4</i>	<i>Sox11</i>
	<i>Tal1</i>		<i>Smad2</i>	<i>Bmpr2</i>
	<i>Tbx15</i>		<i>Bmpr1b</i>	<i>Cadm1</i>
	<i>Acp5</i>		<i>Col9a1</i>	<i>Col2a1</i>
	<i>Alpl</i>		<i>Col11a1</i>	<i>Dlx2</i>
	<i>Csgalnact1</i>		<i>Fgf9</i>	<i>Dlx5</i>
	<i>Carm1</i>		<i>Grem1</i>	<i>Fgfr3</i>
	<i>Grhl2</i>		<i>Hspb11</i>	<i>Gdf11</i>
	<i>Hoxa11</i>		<i>Ift80</i>	<i>Hmga2</i>
	<i>Hoxa2</i>		<i>Pkd1</i>	<i>Hoxb2</i>
	<i>Hoxa5</i>		<i>Wnt9a</i>	<i>Hapln1</i>
	<i>Hoxb6</i>			<i>Prrx1</i>
	<i>Hoxb8</i>			<i>Ptpn6</i>
	<i>Itgb8</i>			<i>Six1</i>
	<i>Mmp2</i>			<i>Six4</i>
	<i>Med1</i>			<i>Shh</i>
	<i>Mia3</i>			<i>Sulf1</i>
	<i>Nog</i>			<i>Tfap2a</i>
	<i>Osr2</i>			<i>Tgfb2</i>

	TDM	FPM	FPD	SPX
	<i>Otor</i>			<i>Vkorc1</i>
	<i>Rarg</i>			<i>Wnt9b</i>
	<i>Ripply1</i>			
	<i>Serpinh1</i>			
	<i>Wnt1</i>			
	<i>Wnt5a</i>			
Heart development	<i>Gata1</i>	No uniquely regulated genes	<i>Fat4</i>	<i>Adap2</i>
	<i>Hopx</i>		<i>Smad2</i>	<i>Gata3</i>
	<i>Isl1</i>		<i>Tead1</i>	<i>Rb1cc1</i>
	<i>Adgrg6</i>		<i>Cluap1</i>	<i>Sox11</i>
	<i>Atm</i>		<i>Col11a1</i>	<i>Adra1b</i>
	<i>Dnaaf3</i>		<i>Cdkl1</i>	<i>Bmpr2</i>
	<i>Dnah11</i>		<i>Dlc1</i>	<i>Col2a1</i>
	<i>Eomes</i>		<i>Fgf9</i>	<i>Dkk1</i>
	<i>Epor</i>		<i>Foxh1</i>	<i>Id1</i>
	<i>Epo</i>		<i>Grem1</i>	<i>Id3</i>
	<i>Fdps</i>		<i>Hspb11</i>	<i>Sema3c</i>
	<i>Flrt3</i>		<i>Hoxa13</i>	<i>Six1</i>
	<i>Gjc1</i>		<i>Kif7</i>	<i>Shh</i>
	<i>Gaa</i>		<i>Lrrc10</i>	<i>S1pr1</i>
	<i>Grhl2</i>		<i>Met</i>	<i>Tfap2a</i>
	<i>Hdac5</i>		<i>Mb</i>	<i>Tgfb2</i>
	<i>Mmp2</i>		<i>My12</i>	<i>Tgfbr3</i>
	<i>Med1</i>		<i>My13</i>	
	<i>Map2k1</i>		<i>Neb1</i>	
	<i>Nog</i>		<i>Noto</i>	
	<i>Olfm1</i>		<i>Nfatc1</i>	
	<i>Uty</i>		<i>Pln</i>	
	<i>Vcam1</i>		<i>Pkd1</i>	
	<i>Wnt5a</i>		<i>Pkd111</i>	
	<i>Zic3</i>		<i>Sorbs2</i>	
			<i>Tnnt2</i>	
Muscle organ development	<i>Fbxo22</i>	<i>Cav1</i>	<i>Fos</i>	<i>Hmgcr</i>
	<i>Isl1</i>		<i>Col11a1</i>	<i>Sox11</i>
	<i>Kel</i>		<i>Fgf9</i>	<i>Col19a1</i>

	TDM	FPM	FPD	SPX
	<i>Sfmbt1</i>		<i>Foxh1</i>	
	<i>Eomes</i>		<i>Grem1</i>	<i>Dkk1</i>
	<i>Epor</i>		<i>Met</i>	<i>Etv1</i>
	<i>Epo</i>		<i>Myl2</i>	<i>Id3</i>
	<i>Fdps</i>		<i>Myl3</i>	<i>Myh14</i>
	<i>Gtf3c5</i>		<i>Rb1</i>	<i>Six1</i>
	<i>Gpc1</i>		<i>Sirt1</i>	<i>Six4</i>
	<i>Hdac5</i>		<i>Tnnt2</i>	<i>Shh</i>
	<i>Hivep3</i>		<i>Uqcc2</i>	<i>Slpr1</i>
	<i>Lef1</i>			<i>Tgfb2</i>
	<i>Med1</i>			<i>Tgfr3</i>
	<i>Meox2</i>			
	<i>Neurl1a</i>			
	<i>Nog</i>			
	<i>Nr1d2</i>			
	<i>Sirt2</i>			
	<i>Scn8a</i>			
	<i>Svil</i>			
	<i>Usp2</i>			
	<i>Wnt5a</i>			
	<i>Zfp689</i>			
Nervous system development	<i>Bok</i>	<i>Cav1</i>	<i>Bax</i>	<i>Hmgcs1</i>
	<i>Btbd6</i>	<i>Cxcr2</i>	<i>Braf</i>	<i>Barhl1</i>
	<i>Cd44</i>	<i>Grin2a</i>	<i>Dpf1</i>	<i>Gata3</i>
	<i>Ctdsp1</i>	<i>Sim1</i>	<i>Fat4</i>	<i>Klf7</i>
	<i>Fkbp4</i>		<i>Fos</i>	<i>Ndr1</i>
	<i>Fry</i>		<i>Fkbp1b</i>	<i>Skil</i>
	<i>Gpsm1</i>		<i>Gpr173</i>	<i>Sox11</i>
	<i>Ikzf1</i>		<i>Nkx2-1</i>	<i>Apcdd1</i>
	<i>Isl1</i>		<i>Pou3f2</i>	<i>Bmpr2</i>
	<i>Irx3</i>		<i>Slitrk5</i>	<i>Cadm1</i>
	<i>Kel</i>		<i>Srcin1</i>	<i>Crabp2</i>
	<i>Klf15</i>		<i>Tal2</i>	<i>Col2a1</i>
	<i>Mycbp2</i>		<i>Tlx3</i>	<i>Cdkn2c</i>
	<i>Pou3f4</i>		<i>Wasf3</i>	<i>Dkk1</i>

TDM	FPM	FPD	SPX
<i>Rab13</i>		<i>Anp32b</i>	<i>Dpysl5</i>
<i>Rasa1</i>		<i>Alcam</i>	<i>Dab1</i>
<i>Rbfox2</i>		<i>App</i>	<i>Dlx2</i>
<i>Shank1</i>		<i>Anxa1</i>	<i>Dlx5</i>
<i>Smarcb1</i>		<i>Rere</i>	<i>Enpp2</i>
<i>Tal1</i>		<i>Bmpr1b</i>	<i>Emx2</i>
<i>Tnik</i>		<i>Cacna1a</i>	<i>Etv1</i>
<i>Xrcc2</i>		<i>Ccr4</i>	<i>Fgfr3</i>
<i>Adgrg6</i>		<i>Cluap1</i>	<i>Gdf11</i>
<i>Adgrl1</i>		<i>Col25a1</i>	<i>Hmga2</i>
<i>Amigo1</i>		<i>Cntn3</i>	<i>Hoxb2</i>
<i>Adra2b</i>		<i>Cntn6</i>	<i>Hapln1</i>
<i>Apoe</i>		<i>Gak</i>	<i>Id1</i>
<i>Artn</i>		<i>Cdkn2b</i>	<i>Id3</i>
<i>Arnt2</i>		<i>Dlc1</i>	<i>Id4</i>
<i>Atm</i>		<i>Drd1</i>	<i>Igflr</i>
<i>Becn1</i>		<i>Fgf14</i>	<i>Mt2</i>
<i>B4gat1</i>		<i>Fgf9</i>	<i>Prrx1</i>
<i>Bloc1s5</i>		<i>Flrt1</i>	<i>Rims2</i>
<i>Cdh4</i>		<i>Fut10</i>	<i>Sema3c</i>
<i>Clstn1</i>		<i>Gas6</i>	<i>Sema3g</i>
<i>Clstn3</i>		<i>Gfi1</i>	<i>Six1</i>
<i>Cend1</i>		<i>Hap1</i>	<i>Six4</i>
<i>Cbln2</i>		<i>Kif5a</i>	<i>Sstr2</i>
<i>Carm1</i>		<i>Lrfn2</i>	<i>Shh</i>
<i>F2</i>		<i>Lrrc7</i>	<i>S1pr1</i>
<i>Dpysl2</i>		<i>Lrrn3</i>	<i>Sulf1</i>
<i>Dab2</i>		<i>Lpar1</i>	<i>Timp4</i>
<i>Eed</i>		<i>Met</i>	<i>Tfap2a</i>
<i>Ezh1</i>		<i>Map6</i>	<i>Tgfb2</i>
<i>Eomes</i>		<i>Myt1l</i>	<i>Unc13b</i>
<i>Epor</i>		<i>Numb</i>	<i>Vps13a</i>
<i>Epo</i>		<i>Plxna2</i>	<i>Wnt9b</i>
<i>Flrt3</i>		<i>Pkd1</i>	
<i>Gabrb2</i>		<i>Kcnma1</i>	
<i>Gpc1</i>		<i>Ptprd</i>	

TDM	FPM	FPD	SPX
<i>Grhl2</i>		<i>Rb1</i>	
<i>Hspa5</i>		<i>Robo3</i>	
<i>Hdac5</i>		<i>Sez6l2</i>	
<i>Hoxa2</i>		<i>Sirt1</i>	
<i>Hoxb8</i>		<i>Scn2a</i>	
<i>Htt</i>		<i>Stmn2</i>	
<i>Irs2</i>		<i>Ttc26</i>	
<i>Itga1</i>		<i>Tle6</i>	
<i>Kif13b</i>		<i>Trpc6</i>	
<i>Lgals1</i>		<i>Trpm1</i>	
<i>Lgl1</i>		<i>Tmem223</i>	
<i>Lig4</i>		<i>Vax2</i>	
<i>Lef1</i>		<i>Vldlr</i>	
<i>Mmp2</i>		<i>Vcl</i>	
<i>Med1</i>		<i>Wnt9a</i>	
<i>Map2k1</i>		<i>Zc3h12a</i>	
<i>Maob</i>			
<i>Myo6</i>			
<i>Myo7a</i>			
<i>Neur11a</i>			
<i>Nyap1</i>			
<i>Nog</i>			
<i>Olfm1</i>			
<i>Ophn1</i>			
<i>Phox2a</i>			
<i>Prx</i>			
<i>Plxnb2</i>			
<i>Penk</i>			
<i>Psen2</i>			
<i>Prkcsh</i>			
<i>Prkcz</i>			
<i>Ppp3cc</i>			
<i>Ptpro</i>			
<i>P2ry1</i>			
<i>Reln</i>			
<i>Rarg</i>			

TDM	FPM	FPD	SPX
<i>Stk36</i>			
<i>Sirt2</i>			
<i>Slit3</i>			
<i>Slc32a1</i>			
<i>Slc7a11</i>			
<i>Slc9a3r1</i>			
<i>Spry3</i>			
<i>Syngap1</i>			
<i>Sdc4</i>			
<i>Tert</i>			
<i>Thy1</i>			
<i>Tg</i>			
<i>Tlr4</i>			
<i>Tcf12</i>			
<i>Tmem126a</i>			
<i>Wnt1</i>			
<i>Wnt5a</i>			
<i>Zic3</i>			
<i>Zfyve27</i>			
<i>Zmynd8</i>			

Cluster annotation controls day 4

Annotation Cluster 1	RNA metabolic process	Enrichment Score: 4.33	Count	P_Value	FDR
	GOTERM_BP_5	rRNA processing	27	3.10E-07	1.10E-03
	GOTERM_BP_5	ncRNA metabolic process	45	1.20E-06	2.00E-03
	GOTERM_BP_5	RNA processing	40	2.90E-01	9.80E-01
Annotation Cluster 2	small molecule metabolic process	Enrichment Score: 3.87	Count	P_Value	FDR
	GOTERM_BP_5	alpha-amino acid metabolic process	26	1.70E-06	2.00E-03
	GOTERM_BP_5	aspartate family amino acid metabolic process	12	6.20E-06	3.30E-03
	GOTERM_BP_5	alpha-amino acid catabolic process	14	6.40E-06	3.30E-03
	GOTERM_BP_5	cellular amino acid catabolic process	11	1.00E-03	6.80E-02
	GOTERM_BP_5	organic acid catabolic process	19	3.60E-03	1.50E-01
	GOTERM_BP_5	carboxylic acid catabolic process	15	2.70E-02	5.10E-01
Annotation Cluster 3	primary metabolic process	Enrichment Score: 3.25	Count	P_Value	FDR
	GOTERM_BP_5	aspartate family amino acid metabolic process	12	6.20E-06	3.30E-03
	GOTERM_BP_5	methionine metabolic process	5	4.20E-03	1.60E-01
	GOTERM_BP_5	S-adenosylmethionine metabolic process	5	6.80E-03	2.10E-01
Annotation Cluster 4	meiotic cell cycle process	Enrichment Score: 3.13	Count	P_Value	FDR
	GOTERM_BP_5	Synapsis	12	7.80E-06	3.40E-03
	GOTERM_BP_5	homologous chromosome segregation	13	2.00E-05	5.00E-03
	GOTERM_BP_5	meiotic cell cycle process	24	4.00E-05	8.90E-03
	GOTERM_BP_5	meiosis I	17	4.40E-05	8.90E-03
	GOTERM_BP_5	meiotic nuclear division	23	4.40E-05	8.90E-03

GOTERM_BP_5	chromosome organization involved in meiotic cell cycle	13	7.30E-05	1.10E-02
GOTERM_BP_5	synaptonemal complex assembly	7	3.00E-04	3.10E-02
GOTERM_BP_5	synaptonemal complex organization	7	6.60E-04	5.30E-02
GOTERM_BP_5	meiotic chromosome segregation	13	8.40E-04	5.90E-02
GOTERM_BP_5	reciprocal meiotic recombination	8	4.50E-03	1.60E-01
GOTERM_BP_5	chiasma assembly	4	4.70E-03	1.70E-01
GOTERM_BP_5	nuclear chromosome segregation	17	8.60E-02	9.80E-01
GOTERM_BP_5	nuclear division	33	1.70E-01	9.80E-01
GOTERM_BP_5	DNA recombination	13	3.60E-01	9.80E-01
Annotation Cluster 5 embryonic morphogenesis				
Enrichment Score: 3.1				
GOTERM_BP_5	embryonic morphogenesis	57	6.20E-06	3.30E-03
GOTERM_BP_5	tube morphogenesis	39	5.30E-05	9.10E-03
GOTERM_BP_5	epithelial tube morphogenesis	35	1.30E-04	1.60E-02
GOTERM_BP_5	embryonic organ morphogenesis	30	5.50E-04	4.70E-02
GOTERM_BP_5	morphogenesis of an epithelium	42	1.40E-03	8.30E-02
GOTERM_BP_5	embryo development ending in birth or egg hatching	53	2.00E-03	9.90E-02
GOTERM_BP_5	organ morphogenesis	68	4.10E-03	1.60E-01
GOTERM_BP_5	embryonic organ development	37	5.50E-03	1.90E-01
GOTERM_BP_5	branching morphogenesis of an epithelial tube	18	5.60E-03	1.90E-01
GOTERM_BP_5	morphogenesis of a branching epithelium	19	1.30E-02	3.20E-01
Annotation Cluster 6 synaptic signaling				
Enrichment Score: 3.01				
GOTERM_BP_5	synaptic signaling	47	2.10E-04	2.20E-02
GOTERM_BP_5	trans-synaptic signaling	47	2.10E-04	2.20E-02
GOTERM_BP_5	modulation of synaptic transmission	25	2.20E-02	4.60E-01

Cluster annotation controls day 10

Annotation Cluster 1	cell motility	Enrichment Score: 27.15	Count	P_Value	FDR
	GOTERM_BP_5	cell migration	315	2.90E-43	2.70E-40
	GOTERM_BP_5	regulation of cell migration	207	6.50E-32	2.90E-29
	GOTERM_BP_5	regulation of cell motility	213	3.00E-31	1.20E-28
	GOTERM_BP_5	positive regulation of cell migration	128	5.00E-21	8.90E-19
	GOTERM_BP_5	positive regulation of cell motility	129	3.70E-20	5.50E-18
	GOTERM_BP_5	positive regulation of cellular component movement	130	1.10E-19	1.40E-17
Annotation Cluster 2	circulatory system development	Enrichment Score: 26.6	Count	P_Value	FDR
	GOTERM_BP_5	cardiovascular system development	303	1.90E-49	3.10E-46
	GOTERM_BP_5	circulatory system development	303	1.90E-49	3.10E-46
	GOTERM_BP_5	blood vessel development	193	1.60E-34	8.70E-32
	GOTERM_BP_5	vasculature development	200	1.60E-34	8.70E-32
	GOTERM_BP_5	Angiogenesis	136	3.50E-25	1.10E-22
	GOTERM_BP_5	regulation of vasculature development	81	7.50E-16	6.30E-14
	GOTERM_BP_5	regulation of angiogenesis	73	3.30E-14	1.90E-12
	GOTERM_BP_5	positive regulation of vasculature development	51	1.80E-11	6.60E-10
	GOTERM_BP_5	positive regulation of angiogenesis	47	2.90E-11	1.00E-09
Annotation Cluster 3	(skeletal) system development	Enrichment Score: 17.44	Count	P_Value	FDR
	GOTERM_BP_5	embryonic organ development	137	5.50E-21	9.40E-19
	GOTERM_BP_5	skeletal system morphogenesis	85	1.60E-20	2.50E-18
	GOTERM_BP_5	embryonic organ morphogenesis	101	1.10E-19	1.40E-17
	GOTERM_BP_5	embryonic morphogenesis	160	5.70E-19	6.90E-17

GOTERM_BP_5	embryonic skeletal system development	59	8.70E-19	1.00E-16
GOTERM_BP_5	embryonic skeletal system morphogenesis	49	1.40E-17	1.40E-15
GOTERM_BP_5	embryo development ending in birth or egg hatching	151	1.20E-10	3.70E-09
Annotation Cluster 4 heart development Enrichment Score: 16.85				
GOTERM_BP_5	muscle cell differentiation	130	3.40E-25	1.10E-22
GOTERM_BP_5	heart development	165	1.80E-24	4.70E-22
GOTERM_BP_5	striated muscle tissue development	128	3.00E-24	7.40E-22
GOTERM_BP_5	cardiac muscle tissue development	86	2.20E-22	4.60E-20
GOTERM_BP_5	striated muscle cell differentiation	87	3.70E-16	3.30E-14
GOTERM_BP_5	heart morphogenesis	79	1.30E-14	8.30E-13
GOTERM_BP_5	cardiac muscle cell development	38	1.90E-14	1.20E-12
GOTERM_BP_5	cardiocyte differentiation	57	2.30E-14	1.40E-12
GOTERM_BP_5	cardiac cell development	39	3.50E-14	2.00E-12
GOTERM_BP_5	muscle cell development	61	3.90E-14	2.20E-12
GOTERM_BP_5	striated muscle cell development	57	5.90E-14	3.20E-12
GOTERM_BP_5	cardiac muscle cell differentiation	47	9.40E-13	4.00E-11
Annotation Cluster 5 signaling Enrichment Score: 15.98				
GOTERM_BP_5	regulation of signal transduction	479	5.60E-29	2.10E-26
GOTERM_BP_5	negative regulation of cell communication	219	1.70E-11	6.20E-10
GOTERM_BP_5	negative regulation of signal transduction	191	1.20E-09	3.20E-08
Annotation Cluster 6 muscle organ and tissue development Enrichment Score: 15.71				
GOTERM_BP_5	striated muscle tissue development	128	3.00E-24	7.40E-22
GOTERM_BP_5	muscle organ development	112	1.10E-18	1.20E-16
GOTERM_BP_5	skeletal muscle organ development	49	2.30E-06	3.20E-05

Annotation Cluster 7		nervous system and cell development		Enrichment Score: 15.21	
		Count	P_Value	FDR	
GOTERM_BP_5	cell development	468	2.40E-34	1.20E-31	
GOTERM_BP_5	nervous system development	447	1.10E-28	4.00E-26	
GOTERM_BP_5	Neurogenesis	338	1.50E-24	4.20E-22	
GOTERM_BP_5	regulation of nervous system development	211	1.40E-20	2.30E-18	
GOTERM_BP_5	neuron differentiation	283	4.10E-20	6.00E-18	
GOTERM_BP_5	cell morphogenesis involved in differentiation	187	3.90E-19	4.90E-17	
GOTERM_BP_5	regulation of neurogenesis	181	1.20E-15	9.70E-14	
GOTERM_BP_5	axon development	117	3.20E-15	2.30E-13	
GOTERM_BP_5	neuron projection development	195	4.40E-15	3.10E-13	
GOTERM_BP_5	neuron development	221	8.80E-15	5.80E-13	
GOTERM_BP_5	neuron projection morphogenesis	133	1.10E-13	5.60E-12	
GOTERM_BP_5	cell morphogenesis involved in neuron differentiation	125	2.60E-13	1.20E-11	
GOTERM_BP_5	axon guidance	66	6.90E-13	3.00E-11	
GOTERM_BP_5	regulation of neuron differentiation	149	7.90E-13	3.40E-11	
GOTERM_BP_5	neuron projection guidance	66	8.80E-13	3.80E-11	
GOTERM_BP_5	cell morphogenesis	236	3.40E-11	1.20E-09	
GOTERM_BP_5	regulation of neuron projection development	104	1.80E-07	3.30E-06	
GOTERM_BP_5	cell projection morphogenesis	144	1.00E-05	1.20E-04	
GOTERM_BP_5	cell part morphogenesis	144	7.40E-05	7.30E-04	
Annotation Cluster 8		heart and muscle contraction		Enrichment Score: 13.12	
		Count	P_Value	FDR	
GOTERM_BP_5	regulation of muscle contraction	56	1.40E-15	1.10E-13	
GOTERM_BP_5	regulation of heart contraction	58	2.70E-14	1.60E-12	
GOTERM_BP_5	heart contraction	62	5.60E-14	3.10E-12	
GOTERM_BP_5	striated muscle contraction	50	1.70E-11	6.20E-10	

Annotation Cluster 9	immune system development	Enrichment Score: 11.55	Count	P_Value	FDR
	GOTERM_BP_5	hematopoietic or lymphoid organ development	197	9.00E-15	5.80E-13
	GOTERM_BP_5	immune system development	201	6.80E-14	3.70E-12
	GOTERM_BP_5	Hemopoiesis	186	9.30E-14	4.80E-12
	GOTERM_BP_5	myeloid cell differentiation	100	2.40E-13	1.10E-11
	GOTERM_BP_5	leukocyte differentiation	117	8.50E-10	2.30E-08
	GOTERM_BP_5	regulation of hemopoiesis	84	4.50E-08	9.10E-07
Annotation Cluster 10	signal transduction	Enrichment Score: 11.37	Count	P_Value	FDR
	GOTERM_BP_5	regulation of signal transduction	479	5.60E-29	2.10E-26
	GOTERM_BP_5	positive regulation of cell communication	315	1.30E-24	3.90E-22
	GOTERM_BP_5	positive regulation of signal transduction	285	3.20E-23	7.50E-21
	GOTERM_BP_5	positive regulation of phosphate metabolic process	230	1.00E-19	1.40E-17
	GOTERM_BP_5	positive regulation of phosphorus metabolic process	230	1.00E-19	1.40E-17
	GOTERM_BP_5	regulation of phosphate metabolic process	316	1.70E-18	1.90E-16
	GOTERM_BP_5	intracellular signal transduction	419	1.70E-16	1.70E-14
	GOTERM_BP_5	positive regulation of protein modification process	216	8.10E-14	4.30E-12
	GOTERM_BP_5	positive regulation of intracellular signal transduction	188	9.70E-14	4.90E-12
	GOTERM_BP_5	positive regulation of MAPK cascade	115	1.40E-13	6.70E-12
	GOTERM_BP_5	regulation of intracellular signal transduction	286	1.40E-13	6.70E-12
	GOTERM_BP_5	regulation of MAPK cascade	147	1.70E-12	6.70E-11
	GOTERM_BP_5	regulation of protein modification process	286	2.10E-11	7.50E-10
	GOTERM_BP_5	signal transduction by protein phosphorylation	145	6.50E-11	2.10E-09
	GOTERM_BP_5	MAPK cascade	144	8.40E-11	2.60E-09
	GOTERM_BP_5	positive regulation of protein metabolic process	251	8.00E-10	2.20E-08

GOTERM_BP_5	positive regulation of cellular protein metabolic process	237	9.60E-10	2.60E-08
GOTERM_BP_5	Phosphorylation	330	5.90E-08	1.20E-06
GOTERM_BP_5	regulation of protein metabolic process	382	3.20E-07	5.40E-06
GOTERM_BP_5	regulation of cellular protein metabolic process	357	3.20E-07	5.40E-06
GOTERM_BP_5	ERK1 and ERK2 cascade	62	5.30E-07	8.50E-06
GOTERM_BP_5	regulation of kinase activity	119	2.90E-05	3.20E-04
GOTERM_BP_5	positive regulation of transferase activity	86	6.50E-04	5.00E-03
GOTERM_BP_5	protein modification process	454	5.40E-02	1.90E-01
GOTERM_BP_5	cellular protein modification process	454	5.40E-02	1.90E-01
GOTERM_BP_5	cellular protein metabolic process	541	8.90E-01	8.90E-01
Annotation Cluster 11 leukocyte activation Enrichment Score: 11.25				
GOTERM_BP_5	myeloid leukocyte activation	68	1.10E-20	1.90E-18
GOTERM_BP_5	myeloid cell activation involved in immune response	30	4.90E-09	1.20E-07
GOTERM_BP_5	leukocyte activation involved in immune response	56	3.20E-06	4.30E-05
Annotation Cluster 12 wound healing Enrichment Score: 10.94				
GOTERM_BP_5	blood coagulation	68	3.90E-18	4.10E-16
GOTERM_BP_5	regulation of wound healing	52	8.20E-15	5.50E-13
GOTERM_BP_5	regulation of blood coagulation	40	1.50E-14	9.40E-13
GOTERM_BP_5	negative regulation of blood coagulation	25	3.10E-11	1.10E-09
GOTERM_BP_5	negative regulation of hemostasis	25	3.10E-11	1.10E-09
GOTERM_BP_5	negative regulation of coagulation	25	1.00E-10	3.20E-09
GOTERM_BP_5	negative regulation of wound healing	28	1.10E-10	3.40E-09
GOTERM_BP_5	negative regulation of response to wounding	29	2.50E-09	6.10E-08
GOTERM_BP_5	Fibrinolysis	10	2.80E-04	2.40E-03

Annotation Cluster 13 ion transport	Enrichment Score: 10.53	Count	P_Value	FDR
GOTERM_BP_5	regulation of ion transport	157	1.20E-22	2.70E-20
GOTERM_BP_5	regulation of metal ion transport	109	1.00E-19	1.40E-17
GOTERM_BP_5	regulation of ion transmembrane transport	111	2.10E-18	2.20E-16
GOTERM_BP_5	regulation of transmembrane transport	112	2.20E-17	2.20E-15
GOTERM_BP_5	regulation of cation transmembrane transport	76	4.60E-16	4.00E-14
GOTERM_BP_5	ion transport	265	9.60E-16	7.80E-14
GOTERM_BP_5	ion transmembrane transport	155	2.00E-14	1.20E-12
GOTERM_BP_5	cation transport	191	2.10E-14	1.30E-12
GOTERM_BP_5	cation transmembrane transport	128	2.80E-14	1.60E-12
GOTERM_BP_5	positive regulation of ion transport	75	1.30E-13	6.40E-12
GOTERM_BP_5	inorganic ion transmembrane transport	126	1.60E-12	6.40E-11
GOTERM_BP_5	regulation of ion transmembrane transporter activity	55	1.40E-09	3.60E-08
GOTERM_BP_5	transmembrane transport	187	1.50E-09	3.90E-08
GOTERM_BP_5	regulation of transmembrane transporter activity	55	5.60E-09	1.30E-07
GOTERM_BP_5	regulation of transporter activity	57	8.60E-09	2.00E-07
GOTERM_BP_5	positive regulation of calcium ion transport	37	1.00E-07	2.00E-06
GOTERM_BP_5	positive regulation of ion transmembrane transport	38	4.90E-07	8.00E-06
GOTERM_BP_5	positive regulation of cation transmembrane transport	34	8.50E-07	1.30E-05
GOTERM_BP_5	positive regulation of transmembrane transport	39	8.60E-07	1.30E-05
GOTERM_BP_5	positive regulation of ion transmembrane transporter activity	24	4.60E-05	4.80E-04
GOTERM_BP_5	positive regulation of transporter activity	24	2.80E-04	2.40E-03
GOTERM_BP_5	positive regulation of cation channel activity	14	1.70E-03	1.20E-02
GOTERM_BP_5	positive regulation of calcium ion transmembrane transporter activity	8	1.00E-01	3.00E-01

Annotation Cluster 14 ameoboidal-type cell migration					
	Count	P_Value	FDR		
GOTERM_BP_5	98	8.80E-16	7.30E-14	ameoboidal-type cell migration	
GOTERM_BP_5	71	4.30E-13	1.90E-11	epithelial cell migration	
GOTERM_BP_5	57	6.60E-12	2.50E-10	regulation of epithelial cell migration	
GOTERM_BP_5	35	4.60E-08	9.40E-07	positive regulation of epithelial cell migration	
GOTERM_BP_5	25	2.00E-07	3.60E-06	positive regulation of endothelial cell migration	
Annotation Cluster 15 heart development					
	Count	P_Value	FDR		
GOTERM_BP_5	86	2.20E-22	4.60E-20	cardiac muscle tissue development	
GOTERM_BP_5	79	1.30E-14	8.30E-13	heart morphogenesis	
GOTERM_BP_5	39	3.50E-14	2.00E-12	muscle tissue morphogenesis	
GOTERM_BP_5	52	9.20E-14	4.70E-12	cardiac chamber morphogenesis	
GOTERM_BP_5	40	2.30E-13	1.10E-11	muscle organ morphogenesis	
GOTERM_BP_5	60	1.20E-12	5.20E-11	cardiac chamber development	
GOTERM_BP_5	33	3.90E-12	1.50E-10	cardiac muscle tissue morphogenesis	
GOTERM_BP_5	35	1.00E-11	3.90E-10	cardiac ventricle morphogenesis	
GOTERM_BP_5	27	1.70E-09	4.30E-08	ventricular cardiac muscle tissue development	
GOTERM_BP_5	45	3.10E-09	7.60E-08	cardiac ventricle development	
GOTERM_BP_5	24	1.40E-08	3.10E-07	ventricular cardiac muscle tissue morphogenesis	
GOTERM_BP_5	16	3.70E-06	4.90E-05	cardiac atrium morphogenesis	
GOTERM_BP_5	16	1.90E-05	2.10E-04	cardiac atrium development	
GOTERM_BP_5	6	4.80E-02	1.70E-01	ventricular trabecula myocardium morphogenesis	
Annotation Cluster 16 chemical homeostasis					
	Count	P_Value	FDR		
GOTERM_BP_5	159	7.70E-14	4.10E-12	ion homeostasis	
GOTERM_BP_5	129	1.40E-10	4.10E-09	cellular ion homeostasis	
GOTERM_BP_5	146	2.30E-08	4.90E-07	cellular chemical homeostasis	

Annotation Cluster 17 sensory organ development		Enrichment Score: 9.99	Count	P_Value	FDR
GOTERM_BP_5	sensory organ development		147	2.30E-16	2.10E-14
GOTERM_BP_5	camera-type eye development		87	2.50E-10	7.40E-09
GOTERM_BP_5	eye development		95	3.20E-10	9.40E-09
GOTERM_BP_5	sensory organ morphogenesis		76	3.60E-10	1.00E-08
GOTERM_BP_5	eye morphogenesis		45	1.60E-06	2.30E-05
Annotation Cluster 18 digestive system development		Enrichment Score: 9.66	Count	P_Value	FDR
GOTERM_BP_5	digestive system development		55	8.90E-13	3.80E-11
GOTERM_BP_5	digestive tract development		51	2.50E-12	9.70E-11
GOTERM_BP_5	digestive tract morphogenesis		21	5.00E-06	6.50E-05
Annotation Cluster 19 appendage development		Enrichment Score: 9.65	Count	P_Value	FDR
GOTERM_BP_5	limb development		60	2.30E-11	8.10E-10
GOTERM_BP_5	appendage morphogenesis		55	3.60E-11	1.20E-09
GOTERM_BP_5	limb morphogenesis		55	3.60E-11	1.20E-09
GOTERM_BP_5	embryonic limb morphogenesis		46	1.20E-09	3.20E-08
GOTERM_BP_5	embryonic appendage morphogenesis		46	1.20E-09	3.20E-08
GOTERM_BP_5	forelimb morphogenesis		23	3.10E-09	7.60E-08
Annotation Cluster 20 negative regulation of cell motility		Enrichment Score: 9.5	Count	P_Value	FDR
GOTERM_BP_5	negative regulation of cellular component movement		73	5.50E-11	1.80E-09
GOTERM_BP_5	negative regulation of cell motility		65	5.20E-10	1.50E-08
GOTERM_BP_5	negative regulation of cell migration		62	1.10E-09	3.00E-08

Annotation Cluster 21	central nervous system development	Enrichment Score: 9.45	Count	P_Value	FDR
	GOTERM_BP_5	central nervous system development	209	2.50E-17	2.40E-15
	GOTERM_BP_5	forebrain development	102	3.10E-12	1.20E-10
	GOTERM_BP_5	brain development	150	4.20E-10	1.20E-08
	GOTERM_BP_5	telencephalon development	62	7.90E-07	1.20E-05
	GOTERM_BP_5	pallium development	40	2.10E-04	1.90E-03
Annotation Cluster 22	cellular response to growth factor stimulus	Enrichment Score: 9.42	Count	P_Value	FDR
	GOTERM_BP_5	cellular response to growth factor stimulus	158	1.00E-21	1.90E-19
	GOTERM_BP_5	response to transforming growth factor beta	66	1.20E-13	6.00E-12
	GOTERM_BP_5	regulation of transmembrane receptor protein serine/threonine kinase signaling pathway	65	1.40E-12	5.80E-11
	GOTERM_BP_5	transforming growth factor beta receptor signaling pathway	44	6.30E-09	1.50E-07
	GOTERM_BP_5	regulation of transforming growth factor beta receptor signaling pathway	31	2.40E-07	4.20E-06
	GOTERM_BP_5	negative regulation of transforming growth factor beta receptor signaling pathway	21	5.00E-06	6.50E-05
	GOTERM_BP_5	negative regulation of cellular response to transforming growth factor beta stimulus	21	6.80E-06	8.50E-05
	GOTERM_BP_5	negative regulation of transmembrane receptor protein serine/threonine kinase signaling pathway	28	4.60E-05	4.80E-04
Annotation Cluster 23	regulation of vasculature development	Enrichment Score: 9.38	Count	P_Value	FDR
	GOTERM_BP_5	regulation of vasculature development	81	7.50E-16	6.30E-14
	GOTERM_BP_5	regulation of angiogenesis	73	3.30E-14	1.90E-12

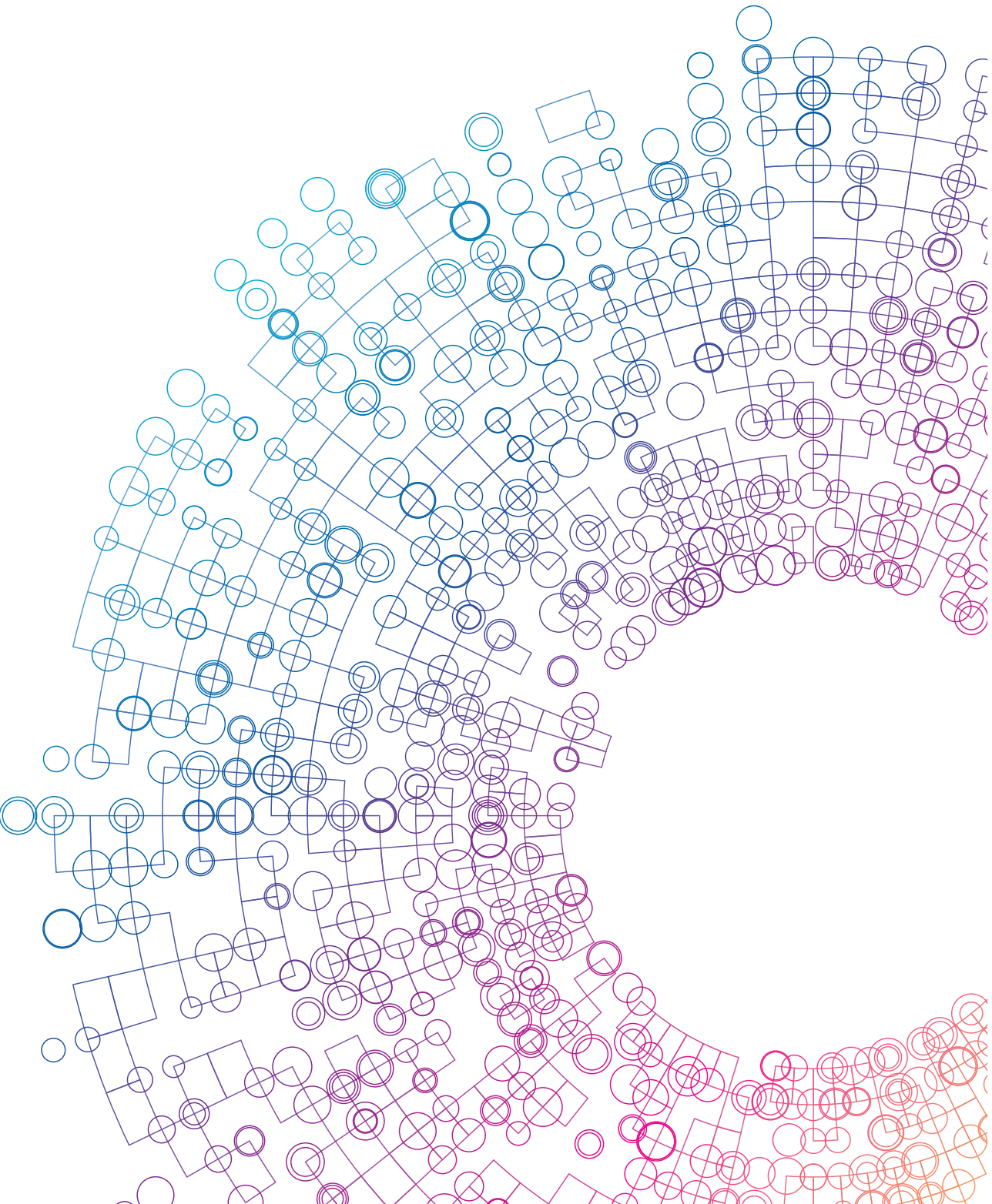
GOTERM_BP_5	negative regulation of vasculature development	31	3.10E-07	5.30E-06
GOTERM_BP_5	negative regulation of blood vessel morphogenesis	29	1.00E-06	1.50E-05
GOTERM_BP_5	negative regulation of angiogenesis	28	1.70E-06	2.40E-05
Annotation Cluster 24 regulation of nervous system development				
Enrichment Score: 9.29				
GOTERM_BP_5	regulation of nervous system development	211	1.40E-20	2.30E-18
GOTERM_BP_5	regulation of neurogenesis	181	1.20E-15	9.70E-14
GOTERM_BP_5	regulation of neuron differentiation	149	7.90E-13	3.40E-11
GOTERM_BP_5	positive regulation of nervous system development	128	1.40E-12	5.80E-11
GOTERM_BP_5	positive regulation of cell development	126	5.00E-10	1.40E-08
GOTERM_BP_5	positive regulation of neurogenesis	101	1.20E-07	2.30E-06
GOTERM_BP_5	regulation of neuron projection development	104	1.80E-07	3.30E-06
GOTERM_BP_5	positive regulation of neuron differentiation	81	2.20E-06	3.10E-05
GOTERM_BP_5	positive regulation of neuron projection development	56	1.50E-03	1.10E-02
GOTERM_BP_5	positive regulation of cell projection organization	69	1.60E-03	1.10E-02
Annotation Cluster 25 tube development				
Enrichment Score: 9.06				
GOTERM_BP_5	respiratory system development	72	4.90E-11	1.60E-09
GOTERM_BP_5	lung development	62	2.80E-09	7.00E-08
GOTERM_BP_5	respiratory tube development	62	4.90E-09	1.20E-07
Annotation Cluster 26 regulation of nervous system development				
Enrichment Score: 8.81				
GOTERM_BP_5	regulation of nervous system development	211	1.40E-20	2.30E-18
GOTERM_BP_5	regulation of neurogenesis	181	1.20E-15	9.70E-14
GOTERM_BP_5	regulation of neuron differentiation	149	7.90E-13	3.40E-11

GOTERM_BP_5	negative regulation of cell development	87	5.30E-10	1.50E-08
GOTERM_BP_5	negative regulation of neurogenesis	71	3.90E-08	8.00E-07
GOTERM_BP_5	negative regulation of nervous system development	74	7.20E-08	1.40E-06
GOTERM_BP_5	regulation of neuron projection development	104	1.80E-07	3.30E-06
GOTERM_BP_5	negative regulation of neuron differentiation	56	6.00E-07	9.50E-06
GOTERM_BP_5	negative regulation of neuron projection development	31	5.20E-03	3.00E-02
GOTERM_BP_5	negative regulation of cell projection organization	35	6.80E-03	3.70E-02
Annotation Cluster 27 chemotaxis				
Enrichment Score: 8.6				
GOTERM_BP_5	leukocyte migration	90	7.10E-16	6.10E-14
GOTERM_BP_5	cell chemotaxis	73	1.20E-11	4.40E-10
GOTERM_BP_5	regulation of leukocyte migration	55	2.20E-11	7.80E-10
GOTERM_BP_5	myeloid leukocyte migration	53	2.60E-11	9.20E-10
GOTERM_BP_5	leukocyte chemotaxis	59	5.80E-11	1.90E-09
GOTERM_BP_5	positive regulation of leukocyte migration	43	1.40E-09	3.60E-08
GOTERM_BP_5	positive regulation of chemotaxis	42	7.80E-09	1.80E-07
GOTERM_BP_5	regulation of leukocyte chemotaxis	35	1.30E-07	2.40E-06
GOTERM_BP_5	granulocyte chemotaxis	33	6.80E-07	1.10E-05
GOTERM_BP_5	positive regulation of leukocyte chemotaxis	28	3.50E-06	4.70E-05
GOTERM_BP_5	neutrophil migration	30	6.80E-06	8.50E-05
GOTERM_BP_5	neutrophil chemotaxis	27	9.00E-06	1.10E-04
Annotation Cluster 28 regulation of defense response				
Enrichment Score: 8.53				
GOTERM_BP_5	regulation of inflammatory response	79	3.10E-12	1.20E-10
GOTERM_BP_5	positive regulation of defense response	68	3.10E-08	6.40E-07
GOTERM_BP_5	positive regulation of inflammatory response	35	2.70E-07	4.60E-06

Annotation Cluster 29 muscle cell development		Enrichment Score: 8.47	Count	P_Value	FDR
GOTERM_BP_5	muscle cell development		61	3.90E-14	2.20E-12
GOTERM_BP_5	striated muscle cell development		57	5.90E-14	3.20E-12
GOTERM_BP_5	myofibril assembly		28	6.70E-11	2.10E-09
GOTERM_BP_5	actomyosin structure organization		46	2.40E-08	5.00E-07
GOTERM_BP_5	sarcomere organization		17	9.60E-07	1.40E-05
GOTERM_BP_5	cellular component assembly involved in morphogenesis		41	4.60E-01	8.30E-01
Annotation Cluster 30 cartilage development		Enrichment Score: 8.39	Count	P_Value	FDR
GOTERM_BP_5	cartilage development		78	3.90E-22	7.80E-20
GOTERM_BP_5	chondrocyte differentiation		38	1.70E-10	5.00E-09
GOTERM_BP_5	regulation of cartilage development		29	7.30E-10	2.00E-08
GOTERM_BP_5	regulation of chondrocyte differentiation		24	2.20E-09	5.40E-08
GOTERM_BP_5	positive regulation of cartilage development		17	3.50E-07	5.80E-06
GOTERM_BP_5	positive regulation of chondrocyte differentiation		12	1.70E-05	1.90E-04
GOTERM_BP_5	negative regulation of chondrocyte differentiation		10	2.80E-04	2.40E-03
GOTERM_BP_5	negative regulation of cartilage development		11	4.20E-04	3.40E-03
Annotation Cluster 31 urogenital system development		Enrichment Score: 8.05	Count	P_Value	FDR
GOTERM_BP_5	renal system development		92	3.00E-15	2.20E-13
GOTERM_BP_5	urogenital system development		100	4.40E-15	3.10E-13
GOTERM_BP_5	kidney development		85	1.10E-13	5.70E-12
GOTERM_BP_5	kidney epithelium development		52	1.90E-11	6.90E-10
GOTERM_BP_5	morphogenesis of a branching epithelium		64	2.20E-11	7.70E-10
GOTERM_BP_5	tube morphogenesis		98	9.70E-11	3.00E-09
GOTERM_BP_5	morphogenesis of an epithelium		119	9.90E-11	3.00E-09

GOTERM_BP_5	nephron development	49	2.20E-10	6.60E-09
GOTERM_BP_5	mesonephros development	40	6.00E-10	1.70E-08
GOTERM_BP_5	ureteric bud development	38	1.60E-09	4.00E-08
GOTERM_BP_5	mesonephric epithelium development	38	2.10E-09	5.20E-08
GOTERM_BP_5	mesonephric tubule development	38	2.10E-09	5.20E-08
GOTERM_BP_5	branching morphogenesis of an epithelial tube	52	9.80E-09	2.20E-07
GOTERM_BP_5	nephron epithelium development	38	6.50E-08	1.30E-06
GOTERM_BP_5	nephron tubule development	34	7.40E-08	1.40E-06
GOTERM_BP_5	metanephros development	32	1.10E-07	2.10E-06
GOTERM_BP_5	renal tubule development	34	2.10E-07	3.70E-06
GOTERM_BP_5	epithelial tube morphogenesis	80	4.00E-07	6.60E-06
GOTERM_BP_5	nephron tubule morphogenesis	28	5.70E-07	9.10E-06
GOTERM_BP_5	nephron morphogenesis	29	6.10E-07	9.70E-06
GOTERM_BP_5	renal tubule morphogenesis	29	6.10E-07	9.70E-06
GOTERM_BP_5	nephron epithelium morphogenesis	28	1.30E-06	1.90E-05
GOTERM_BP_5	mesonephric tubule morphogenesis	25	2.40E-06	3.30E-05
GOTERM_BP_5	branching involved in ureteric bud morphogenesis	23	3.50E-06	4.70E-05
GOTERM_BP_5	kidney morphogenesis	30	8.40E-06	1.00E-04
GOTERM_BP_5	positive regulation of kidney development	15	6.60E-04	5.10E-03
GOTERM_BP_5	regulation of kidney development	17	1.80E-03	1.20E-02
Annotation Cluster 32 stem cell differentiation				
Enrichment Score: 7.78				
GOTERM_BP_5	mesenchyme development	77	4.90E-15	3.40E-13
GOTERM_BP_5	mesenchymal cell differentiation	54	1.70E-09	4.40E-08
GOTERM_BP_5	mesenchymal cell development	51	2.90E-09	7.20E-08
GOTERM_BP_5	neural crest cell development	28	2.40E-07	4.20E-06

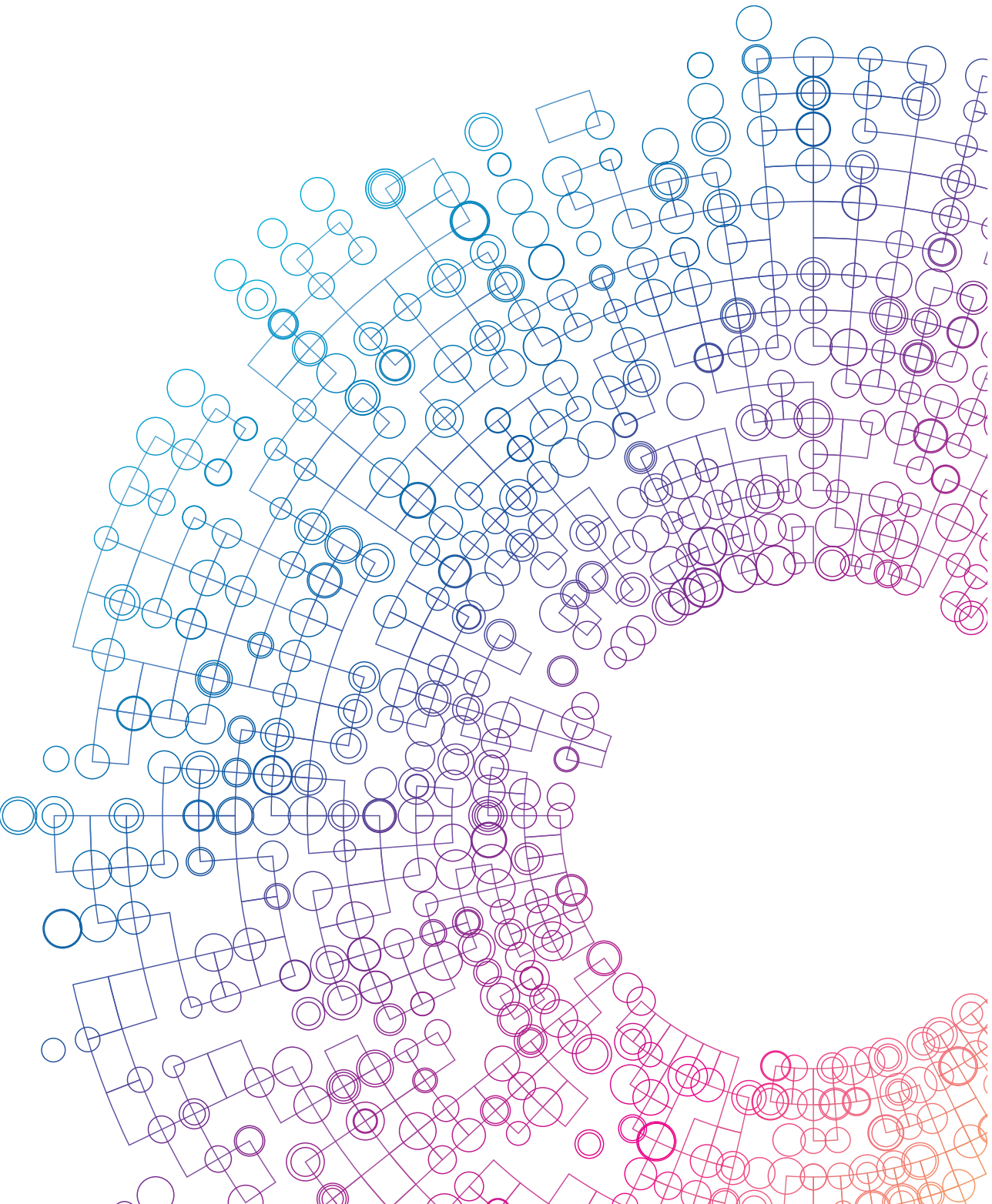
GOTERM_BP_5	neural crest cell migration	21	6.80E-06	8.50E-05
GOTERM_BP_5	epithelial to mesenchymal transition	26	5.30E-04	4.20E-03
Annotation Cluster 33 programmed cell death				
Enrichment Score: 7.72				
GOTERM_BP_5	regulation of programmed cell death	274	1.20E-12	5.20E-11
GOTERM_BP_5	regulation of apoptotic process	271	1.80E-12	6.90E-11
GOTERM_BP_5	apoptotic process	293	2.50E-08	5.20E-07
GOTERM_BP_5	negative regulation of cell death	185	9.30E-08	1.80E-06
GOTERM_BP_5	positive regulation of programmed cell death	114	2.90E-07	5.00E-06
GOTERM_BP_5	positive regulation of apoptotic process	113	3.30E-07	5.60E-06
GOTERM_BP_5	negative regulation of programmed cell death	168	5.40E-07	8.70E-06
GOTERM_BP_5	negative regulation of apoptotic process	165	7.90E-07	1.20E-05
GOTERM_BP_5	positive regulation of cell death	117	1.40E-06	2.10E-05
Annotation Cluster 34 regulation of defense response				
Enrichment Score: 7.41				
GOTERM_BP_5	regulation of inflammatory response	79	3.10E-12	1.20E-10
GOTERM_BP_5	negative regulation of defense response	43	1.10E-06	1.70E-05
GOTERM_BP_5	negative regulation of inflammatory response	32	1.60E-05	1.90E-04
Annotation Cluster 35 synapse assembly				
Enrichment Score: 7.35				
GOTERM_BP_5	synapse assembly	40	7.30E-09	1.70E-07
GOTERM_BP_5	regulation of synapse assembly	31	7.70E-08	1.50E-06
GOTERM_BP_5	positive regulation of synapse assembly	27	1.50E-07	2.80E-06



SECTION

Enhancing the sensitivity to
biomarkers





6

CHAPTER

Oxygen tension influences
embryonic stem cell
maintenance and has lineage
specific effects on neural and
cardiac differentiation

R.H. Mennen*, V.C. de Leeuw*, A.H. Piersma

Differentiation. Sep-Oct 2020;115:1-10.

DOI: 10.1016/j.diff.2020.07.001

* These authors contributed equally to the
manuscript.

Abstract

The importance of oxygen tension in *in vitro* cultures and its effect on embryonic stem cell (ESC) differentiation has been widely acknowledged. Research has mainly focussed on ESC maintenance or on one line of differentiation and only few studies have examined the potential relation between oxygen tension during ESC maintenance and differentiation. In this study we investigated the influence of atmospheric (20%) versus physiologic (5%) oxygen tension in ESC cultures and their differentiation within the cardiac and neural embryonic stem cell tests (ESTc, ESTn). Oxygen tension was set at 5% or 20% and cells were kept in these conditions from starting up cell culture until use for differentiation. Under these oxygen tensions, ESC culture showed no differences in proliferation and gene and protein expression levels. Differentiation was either performed in the same or in the alternative oxygen tension compared to ESC culture creating four different experimental conditions. Cardiac differentiation in 5% instead of 20% oxygen resulted in reduced development of spontaneously beating cardiomyocytes and lower expression of cardiac markers *Nkx2.5*, *Myh6* and MF20 (myosin), regardless whether ESC had been cultured in 5% or 20% oxygen tension. As compared to the control (20% oxygen during stem cell maintenance and differentiation), neural differentiation in 5% oxygen with ESC cultured in 20% oxygen led to more cardiac and neural crest cell differentiation. The opposite experimental condition of neural differentiation in 20% oxygen with ESC cultured in 5% oxygen resulted in more glial differentiation. ESC that were maintained and differentiated in 5% oxygen showed an increase in neural crest and oligodendrocytes as compared to 20% oxygen during stem cell maintenance and differentiation. This study showed major effects on ESC differentiation in ESTc and ESTn of oxygen tension, which is an important variable to consider when designing and developing a stem cell-based *in vitro* system.

Keywords: embryonic stem cells, oxygen tension, neural differentiation, cardiac differentiation, embryonic stem cell test

Introduction

The importance of oxygen tension on cell behaviour cannot be underestimated, as has been officially acknowledged in 2019 by awarding the Nobel Prize in Physiology or Medicine to William Kaelin Jr, Sir Peter Ratcliffe and Gregg Semenza for their important work in this field [1-3]. This also holds true for embryonic development in which oxygen levels range between around 2.4% between week 7 and 11 and 8% after week 11 [4, 5], which is considerably lower than atmospheric pressure. These oxygen levels vary since O_2 gradients play a crucial and dynamic role in directing differentiation into specific organs [6, 7]. The importance of oxygen tension is also widely acknowledged in therapeutic applications in which cells are cultured *in vitro* to be placed back *in vivo*. For example, oocytes that are grown for *in vitro* fertilisation survive better in 5% than 20% oxygen tension [8]. For regenerative medicine purposes, purer, healthier and better differentiated cells are obtained by culturing under low oxygen tension [9, 10].

Also in the field of cell culturing for basic research there is an increasing appreciation that oxygen tension, amongst other basic culture conditions, can have a substantial effect on the outcome of experiments [11]. In the case of stem cell differentiation, there is a link between the oxygen sensing system and the activation of specific differentiation pathways [12-14]. *In vitro* cell cultures are typically kept at 5% CO_2 and 18.5% oxygen [15], but a wealth of literature has shown that maintaining stem cells under lower oxygen tension is beneficial for keeping cells in an undifferentiated state [9, 14, 16, 17] and increases survival and expansion [14, 18]. The oxygen level can influence the differentiation track of stem cells, when stimulating them into one of the three germ lines and their derivatives. For example, differentiation to endoderm and subsequently lung cells may benefit from short 1% oxygen treatment [19] and hepatic cells from 5% oxygen [20]. Differentiation of mouse ESC to mesodermal cells and subsequently spontaneous beating cardiomyocytes, conversely, is inhibited by low oxygen tension [21-24]. Interestingly, short treatment with lower oxygen levels may actually increase cardiomyocyte differentiation [25, 26], in combination with other mechanistic agitation or addition of extracellular matrix proteins [27, 28]. Lower oxygen tension in ectodermal and subsequently neural differentiation increases the differentiation of neural precursors [29] and starting from these precursors, lower oxygen tension leads to enhanced multi-lineage competence [18, 30-32].

Most studies examined a single differentiation path for one cell type or tissue. Additionally, much research has focused on either the influence on stem cell maintenance or differentiation, while the state of the stem cells may affect the

differentiation potential and direction [33, 34]. In this study, the oxygen tension and its effects on the differentiation tracks of murine ESC used in the cardiac and neural embryonic stem cell test (ESTc and ESTn respectively) were investigated. ESTc and ESTn are typically used in developmental toxicology to study the effects of chemicals on early differentiation towards the cardiac or neural lineage [35]. Previous studies have shown the presence of cardiac and neural crest cells in ESTc [36] and neural, neural crest cells and glial cells in ESTn [37, 38], which may be modulated when differentiated under different oxygen tensions. Therefore, the aim of this study was to investigate the influence of physiological levels of oxygen (i.e. 5%) on ESC and their subsequent differentiation into the cardiac or neural lineage in terms of their differentiation potential and cell type expression.

Materials and Methods

Embryonic stem cell maintenance and differentiation

Maintenance

Murine ESC (ES-D3, ATCC, Manassas, VA, USA) were maintained on polystyrene 35 mm plates (Corning, New York, NY, USA) according to the protocol described by Spielmann *et al.* [39]. For the experiment, cells were kept under either physiological (5% O₂) or atmospheric (20% O₂) oxygen levels. Cells were passaged every two to three days. The culture medium (CM) consisted of Dulbecco's modified Eagle's medium (DMEM; Gibco, Waltham, MA, USA) supplemented with 20% fetal bovine serum (FBS; Greiner Bio-One, Kremsmünster, Austria), 200 mM L-glutamine (Gibco), 1% nonessential amino acids (Gibco), 1% 5000 IU/ml Penicillin/5000 µg/ml Streptomycin (Gibco), and 0.1mM β-mercaptoethanol (Sigma-Aldrich, Zwijndrecht, The Netherlands). CM was supplemented with 1000 units/ml murine leukemia inhibitory factor (mLIF; Millipore, Burlington, MA, USA) to maintain pluripotency of the cells. These cells were used for all subsequent experiments between passages 7 and 18.

Cardiac Differentiation

Cardiac differentiation of the ES-D3 cells was performed according to a protocol previously described [39, 40]. Embryoid Bodies (EBs) were formed in hanging drops from a cell suspension of $15 \cdot 10^4$ cells/ml in CM without mLIF that was put on ice and further diluted to a suspension of $3.75 \cdot 10^4$ cells/ml. Hanging drops were made by placing 56 20 µl droplets of the cell suspension to the inside of the lid of a 100/20

mm CELLSTAR® cell culture dish (Greiner Bio-One). The culture dish contained 5 ml of ice-cold phosphate buffered saline (PBS; Ca²⁺, Mg²⁺ free; Gibco). The hanging drops were incubated for 3 days at 37°C, 5% CO₂ at one of the four oxygen conditions. At differentiation day 3, EBs were transferred in 5 ml CM to a 60 mm bacterial petri dish (Greiner Bio-One). After two days of incubation at differentiation day 5, EBs were transferred to a 24-wells plate (TPP, Trasadingen, Switzerland) containing one EB per well in 1 ml CM. Each plate contained 24 replicates per condition and two plates per condition were tested. After five days of incubation, at differentiation day 10, the EBs were scored for presence or absence of beating cardiomyocytes. The fractions of beating EBs were calculated per 24-wells plate.

Neural Differentiation of embryonic stem cells

Neural differentiation was performed as described in Theunissen *et al.* [41]. Differentiation days 0 to 3 were the same as described for the cardiac differentiation of ESC, with the exception of adding 0.5 µM retinoic acid to CM on day 3 to induce neural differentiation. On differentiation day 5, EBs were transferred to 35 mm laminin-coated dishes (Sigma-Aldrich) in low serum medium (LS) supplemented with 2.5 µg/ml fibronectin. LS contained 10% FBS instead of 20% as in CM. On day 6, medium was exchanged for insulin-transferrin-selenite (ITS) medium supplemented with 2.5 µg/ml fibronectin. ITS was comprised of DMEM/Ham's nutrient mixture F12 medium (DMEM/F12; Gibco), 0.2 µg/ml bovine insulin (Sigma-Aldrich), 1% 5000 IU/ml Penicillin/5000 µg/ml Streptomycin (Gibco), 200 mM L-glutamine (Gibco), 30 nM sodium selenite (Sigma-Aldrich), and 50 µg/ml apo-transferrin (Sigma-Aldrich). On day 7, EBs were dissociated and placed on dishes coated with poly-L-ornithine (Sigma-Aldrich) and laminin containing N2 medium. This medium was comprised of DMEM/F12 medium (Gibco) supplemented with 0.2 µg/ml bovine insulin (Sigma-Aldrich), 1% 5000 IU/ml Penicillin/5000 µg/ml Streptomycin (Gibco), 30 nM sodium selenite (Sigma-Aldrich), 20 nM progesterone (Sigma-Aldrich), 100 µM putrescine (Sigma-Aldrich), and 50 µg/ml apo-transferrin (Sigma-Aldrich). Later on day 7, medium was replaced by N2 medium supplemented with 10 ng/ml basic fibroblast growth factor (Miltenyi Biotech, Bergisch Gladbach, Germany). EBs received one more medium refreshment on day 10 before the end of the test at day 13.

Oxygen tension conditions

Cells were all maintained in a humidified atmosphere at 37°C and 5% CO₂. Oxygen tension was set at 5% or 20% and cells were kept in these conditions from starting up the culture until use for differentiation. Differentiation was either performed in

the same or in the alternative oxygen tension as outlined in Table 1, creating four different experimental conditions.

Table 1: experimental set-up

Stem cell culture oxygen levels	Differentiation oxygen levels	Resulting experimental conditions
20%	20%	20-20%
20%	5%	20-5%
5%	20%	5-20%
5%	5%	5-5%

RNA isolation and quantitative real-time PCR

Following the cell differentiation protocol, sample collection was done for all four oxygen conditions for the ESC cultures, and for cardiac and neural differentiation protocols at the end-point of differentiation. Eight samples per condition were fixed in QIAzol (Qiagen, Hilden, Germany) and kept at -80°C until further use. The QIAshredder (Qiagen) was used to homogenise samples and the RNeasy mini kit (Qiagen) and protocol were used to perform the RNA isolation. Concentration of RNA was determined with the NanoDropTM 1000 spectrophotometer (Nanodrop Technologies, Wilmington, DE, USA) and purity was defined using the 2100 BioAnalyzer (Aligent Technologies, Amstelveen, the Netherlands). RNA samples were subsequently synthesised into cDNA using the cDNA archive kit, which contains random hexamer primers (Applied Biosystems, Foster City, CA, USA). Gene quantification was performed on a 7500 Fast Real-Time PCR system (Applied Biosystems) with the following thermal cycling conditions: 95°C for 20 s, followed by 40 cycles of 95°C for 3 s and 60°C for 30 s. Table 2 lists the primers (Applied Biosystems) used in all experiments.

Immunocytochemistry

Samples were rinsed with pre-warmed PBS and fixed for 30 minutes with 4% formaldehyde (Electron Microscopy Sciences, Hatfield, PA, USA). The fixed cells were stored at 4°C up to one week until starting the staining protocol. Samples were rinsed three times for 5 minutes with PBS before and after storage and in between each step of the process. The cells were permeabilised using 0.2% Triton X-100 in PBS (0.5% for

TWIST; T9284, Sigma-Aldrich) for 5 minutes. Then, samples were blocked with blocking buffer for 1 hour (1% bovine serum albumin (BSA, Sigma-Aldrich), 0.5% Tween-20 (Sigma-Aldrich) in PBS (TWIST staining: 5% BSA in PBS)). Rinsed cells were incubated with the primary antibodies in dilution buffer (0.5% BSA, 0.5% Tween-20 in PBS; TWIST staining: 5% normal goat serum (NGS, G9023, Sigma-Aldrich), 0.5% Tween-20 in PBS), which are listed in Table 3, overnight at 4°C. After incubation, samples were incubated with secondary antibodies (Table 2) for 1 hour in dilution buffer. Nuclei were stained with 1 µg/ml DAPI (Sigma-Aldrich), which was put on the samples for 10 minutes. Cells were rinsed once with PBS for 10 minutes and then covered with SlowFade® Diamond Antifade Mountant (Thermo Fisher) and a cover glass. Imaging of the samples was performed on a Leica DMI8 microscope system (Wetzlar, Germany) using a 10x objective and further processed in Fiji/ImageJ (version 1.51n; [42]).

Table 2: primers used for qPCR procedure

Gene name	Abbreviation	Marker for	Assay ID/primer sequence
POU domain, class 5, transcription factor 1	<i>Pou5f1</i>	Stem cell	Mm03053917_g1
Cadherin 1	<i>Cdh1</i>	Adhesion molecule present before neural tube closure	Mm01247357_m1
Bone morphogenetic protein 4	<i>Bmp4</i>	Mesoderm	Mm00432087_m1
Nestin	<i>Nes</i>	Ectoderm / Neural progenitor	Mm00450205_m1
	<i>Gata4</i>	Endoderm	Mm00484689_m1
Msh homeobox 2	<i>Msx2</i>	Early neural crest marker	Mm00442992_m1
Snail family zinc finger 2	<i>Snai2</i>	Epithelial-Mesenchymal Transition	Mm00441531_m1
NK2 transcription factor related, locus 5	<i>Nkx2.5</i>	Early cardiomyocyte	Mm01309813_s1
myosin, heavy polypeptide 6, cardiac muscle, alpha	<i>Myh6</i>	Cardiomyocyte	Mm00440359_m1
Tubulin, beta 3 class III	<i>Tubb3</i>	Neuron	Mm00727586_s1
Glial fibrillary acidic protein	<i>Gfap</i>	Early astrocyte	Mm01253033_m1
Myelin basic protein	<i>Mbp</i>	Oligodendrocyte	Mm01266402_m1
Glucuronidase beta	<i>Gusb</i>	Housekeeping gene	Mm01197698_m1
Hypoxanthine phosphoribosyltransferase 1	<i>Hprt1</i>	Housekeeping gene	Mm03024075_m1
RNA Polymerase II Subunit A	<i>Polr2a</i>	Housekeeping gene	Mm00839502_m1

Table 3: antibodies used for immunocytochemistry

Antibody	Abbreviation	Marker for	Product number	Company	Dilution
Mouse POU domain, class 5, transcription factor 1	OCT4	Stem cell	sc-5279	Santa Cruz	1:500
Mouse anti Stage Specific Embryonic Antigen-1	SSEA1	Stem cell	bs-1702R	Millipore	1:250
Rat anti E-cadherin	ECAD	Adhesion molecule present before neural tube closure	13-1900	Invitrogen	1:1000
Rabbit anti Paired homeobox 6	PAX6	Neural progenitor	901301	Biolegend	1:1000
Mouse anti Nestin	NES	Neural progenitor	N5413	Sigma-Aldrich	1:200
Mouse anti Activating Enhancer-Binding Protein 2-Alpha	AP2 α	Neural crest cell	sc-12726	Santa Cruz	1:400
Mouse anti Twist Family BHLH Transcription Factor 2	TWIST	Epithelial to mesenchymal transition	ab50887	Abcam	1:400
Mouse anti Myosin Heavy Chain	MF20	Cardiomyocyte	MAB4470	Sigma-Aldrich	1:100
Rabbit anti β -Tubulin III	TUBB3	Neuron	T2200	Sigma-Aldrich	1:1000
Rat anti Glial fibrillary acidic protein	GFAP	Early astrocyte	13-0300	Invitrogen	1:800
Goat anti rabbit Alexa 488			A11034	Invitrogen	1:1000
Goat anti rabbit Alexa 555			A21429	Invitrogen	1:1000
Goat anti mouse Alexa 555			A21424	Invitrogen	1:1000
Goat anti rat Alexa 555			A21434	Invitrogen	1:500
Goat anti mouse Alexa 647			A21236	Invitrogen	1:500

Data visualisation and statistics

Relative gene expression differences were calculated using the $2^{-\Delta\Delta Ct}$ method [43], which were all normalised against an average of the housekeeping genes *Hypoxanthine phosphoribosyltransferase 1 (Hprt1)*, *Glucuronidase beta (Gusb)*, and *RNA Polymerase II Subunit A (Polr2a)*. Statistical analysis was performed

using a one-way ANOVA test and post-hoc Sidak's multiple comparisons test using GraphPad Prism 8.1.2 (www.graphpad.com). The cell map was constructed in GraphPad Prism and the heatmap was made with R software [44]. For the heatmaps, each condition was plotted against the average of all conditions of a specific culture (stem cells, ESTc or ESTn).

Results

Oxygen tension had no effect on ESC viability, density and pluripotency

ESC cultures were tested for effects on cell growth under 20% and 5% oxygen tension and no differences in the levels of cell viability (fig. 1a) or cell density (fig. 1b) were found. The pluripotency markers SSEA-1, ECAD, and OCT4 showed clear protein expression in both groups without obvious differences (fig. 1c). The early neural differentiation markers NES and PAX6 were present in a small number of cells in both groups (fig. 1c). These results indicated that oxygen tension affected neither cell growth nor the level of pluripotency.

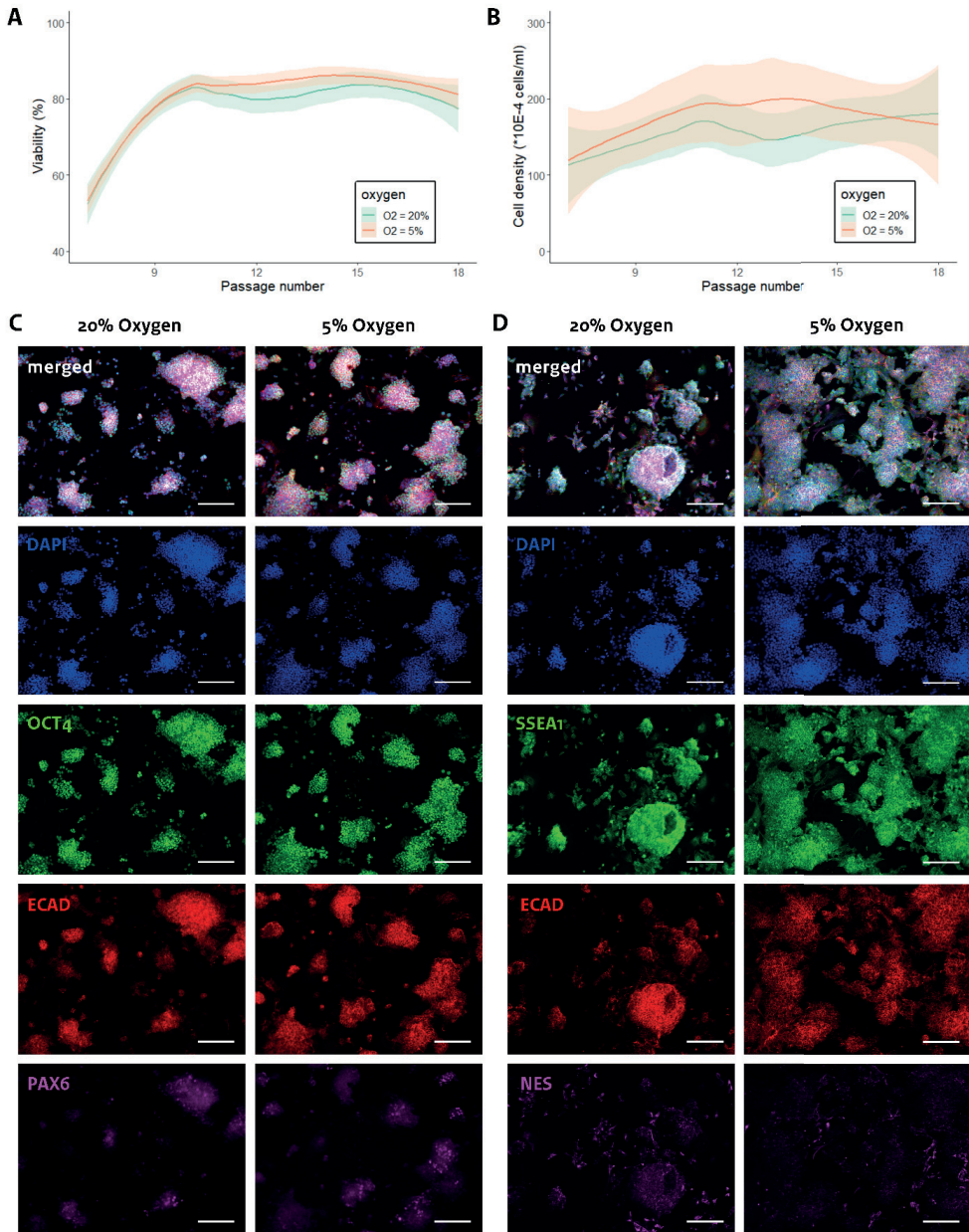


Figure 1: Characteristics of ESC grown under 5 or 20% oxygen tension. (A) Viability (as percentage of total number of cells) and (B) density ($\times 10^4$ cells/ml) of viable ESC from passage 7 to 18. (C) Expression of stem cell markers ECAD and OCT4, and differentiation marker PAX6. (D) Expression of stem cell markers SSEA1 and ECAD and differentiation marker NES. Scale bar: 200 μ m.

Oxygen tension had generally no effect on gene expression level during ESC culture

Various genes related to pluripotency or to one of the primordial germ layers were analysed for their expression levels (fig. 2a). Gene expression alterations were summarised in a heatmap (fig. 2b), which showed small differences with trends towards relatively higher expression of stem cell markers (*Pou5f1*, *Cdh1*) under 5% oxygen tension. Markers for early differentiation stages (*Nes*, *Gata4*, *Msx2*, *Snai2*, *Nkx2.5*) showed a tendency towards lower expression levels in the 5% oxygen group. Later markers for differentiation (*Myh6*, *Tubb3*, *Mbp*) tended to be upregulated in the 5% oxygen group. However, these limited tendencies were not significantly different between the two groups (fig. 2c), except for a statistically significant difference in *Nkx2.5* expression levels.

Oxygen tension affected morphology and cell differentiation in ESTc and ESTn

Next, the differentiation behaviour of stem cells into the cardiac and neural lineage was investigated. To this end, ESC grown under 5% and 20% oxygen tensions were differentiated in the same or in the other oxygen level, which resulted in four conditions as described in Table 1.

The development of beating cardiomyocytes was severely impaired when differentiated under 5% as compared to 20% oxygen (fig. 3). Also ESTc morphology was clearly affected when differentiated under 5% oxygen, resulting in necrosis in the 5-5% condition and evident balloon-like structures in 20-5% (fig. 4a), both accompanied by a change in colour of the medium to yellow (data not shown). Immunostainings showed neural crest cell marker AP2 α expression under all oxygen conditions (fig. 4b). The myosin marker MF20 was clearly expressed when ESTc was differentiated under 20% oxygen tension at day 7 (data not shown) and 10 (fig. 4c), but not when the oxygen tension was 5%.

ESTn also showed a particular morphological change per condition. Compared to the control (20-20%), ESC that were grown under 20% and differentiated under 5% oxygen showed an increase in cells migrating out of EB, while an opposite oxygen regimen (5-20%) resulted in less migration (fig. 4d). The 5-5% and 20-20% conditions showed comparable morphology. Staining of ESTn at day 7 revealed that the cells migrating out of the EB especially under 5% oxygen during differentiation were

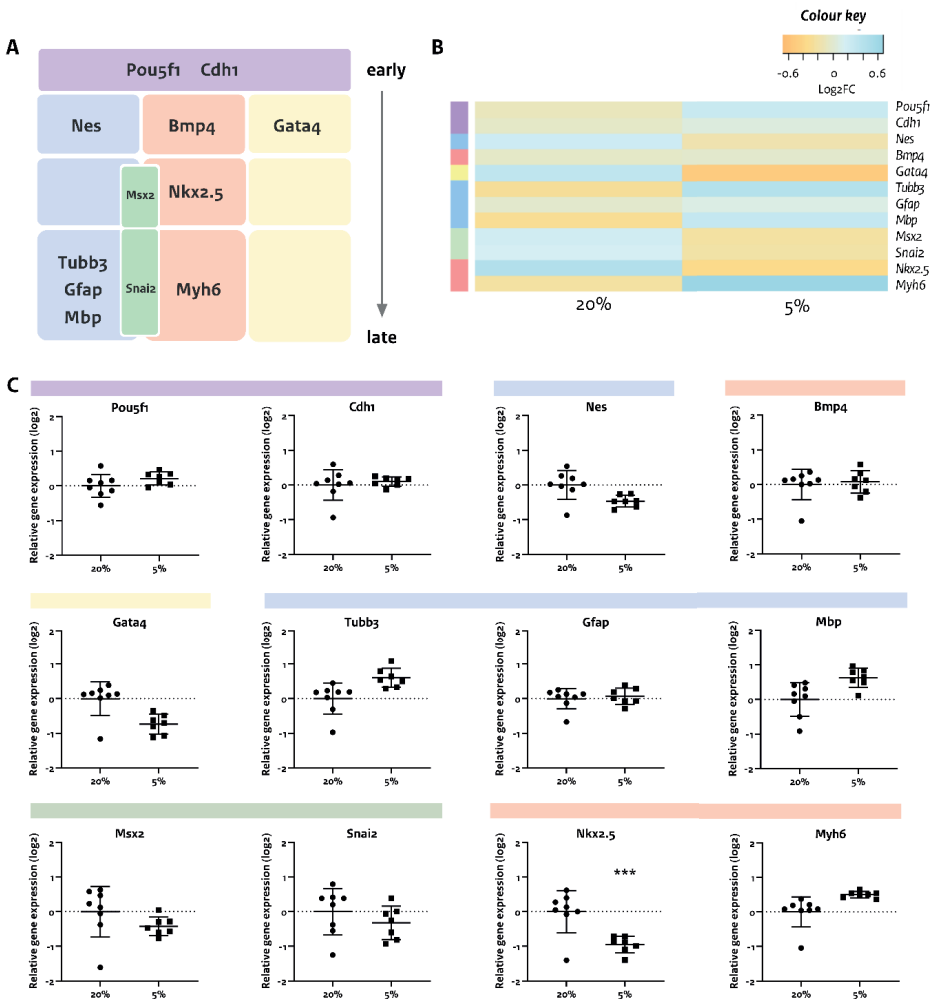


Figure 2: Gene expression alterations in ESC grown under 5 or 20% oxygen tension. (A) Overview of tested cell type markers in time related to pluripotency (purple), ectoderm (blue), mesoderm (red), endoderm (yellow) and neural crest (green). (B) Heatmap of relative gene expression (log₂) of cell type markers in ESC after culturing in 20% or 5% oxygen tension. (C) Relative gene expression (log₂) per cell type marker. Significance levels: *** p<0.001.

strongly positive for neural progenitor marker NES (fig. 4e). Neural marker TUBB3 was present in all conditions (fig. 4e), as well as AP2 α (data not shown). By day 13, cell type markers for neural progenitors (PAX6), late neural crest cells (TWIST) and astrocytes (GFAP, data not shown) were present in all conditions (fig. 4f).

In short, while oxygen tension did not seem to have effects of gene- or protein expression of cell type markers in ESC, differentiating these into cardiac or neural cells influenced morphology as well as the expression of certain cell types. For ESTc, regardless of the oxygen tension in the stem cell culture, 5% oxygen tension in the differentiation phase did not support the development of cardiac function and cardiac cells. ESTn morphology was mostly affected by a change from one oxygen level to the other, without obvious effects on cell type loss or gain, except for more NES⁺ staining in the 20-5% condition.

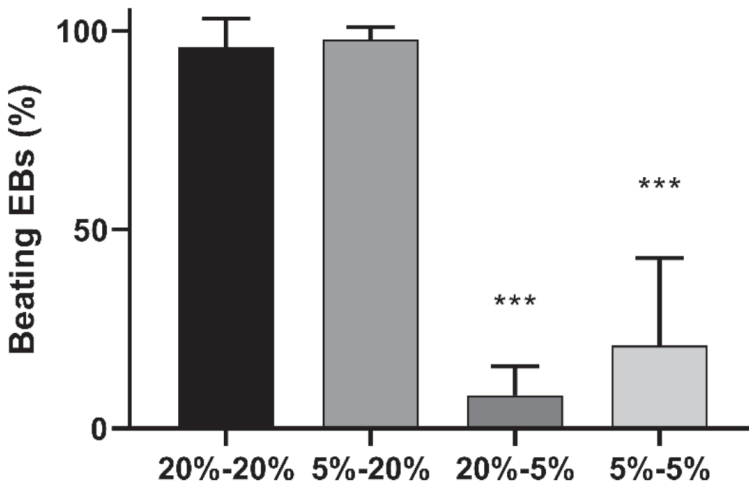


Figure 3: Differentiation of beating cardiomyocytes at different oxygen tensions. Groups were compared to the 20-20% control group using an one-way ANOVA with Sidak's multiple comparisons test *** p<0.001.

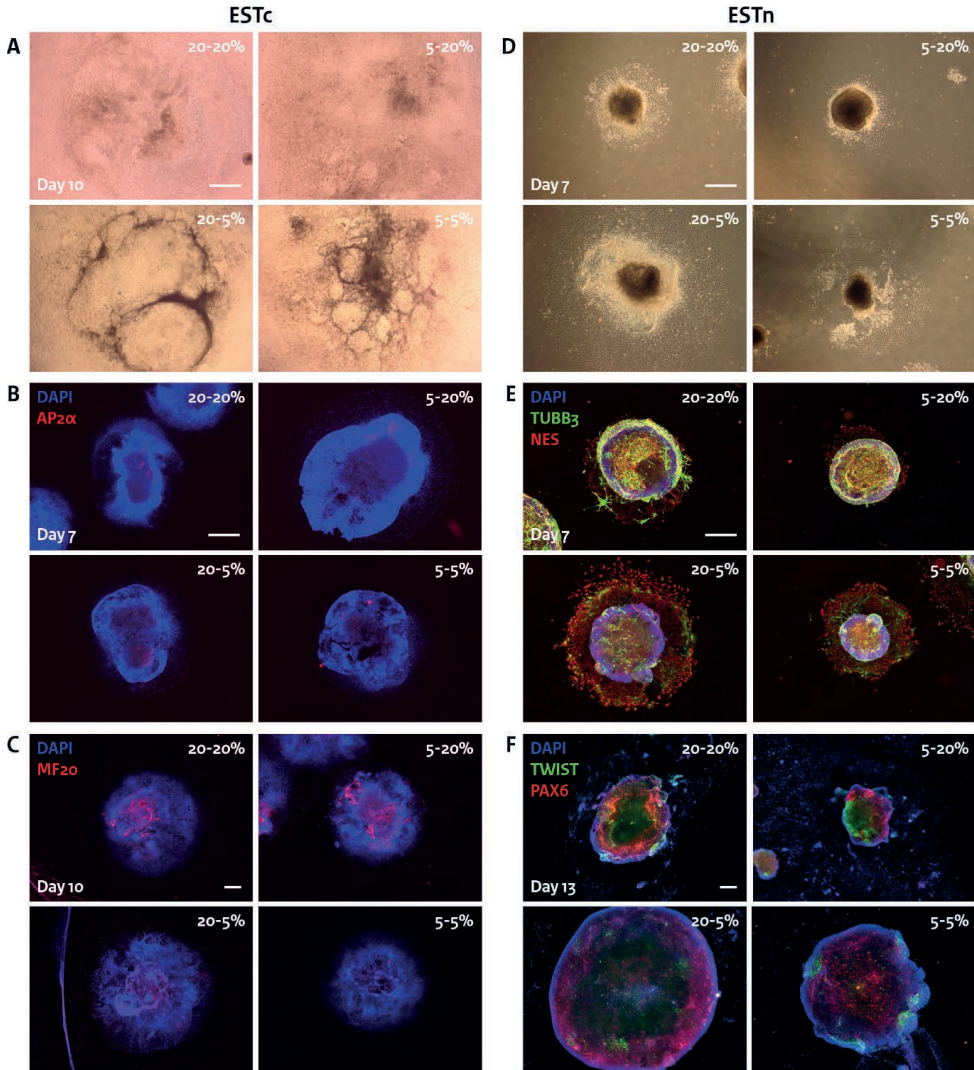


Figure 4: Morphology and cell type changes in ESTc and ESTn under different oxygen tension conditions. (A) Bright-field images of ESTc day 10. (B,C) Immunocytochemistry on ESTc showed expression of (B) early neural crest cell marker AP2 α at day 7 and (C) cardiac marker MF20 at day 10. (D) Bright-field images of ESTn day 7. (B,C) Immunocytochemistry on ESTn showed expression of (E) neural marker TUBB3 and neural progenitor marker NES at day 7, and (C) neural progenitor marker PAX6, astrocyte marker GFAP and late neural crest cell marker TWIST at day 13. Scale bar: 500 μ m.

Oxygen tension altered cell type gene expression in distinct ways in ESTc and ESTn

To quantitatively assess the changes in cell differentiation induced by differences in oxygen tension, qPCR was performed on ESTc and ESTn for each of the conditions with the same cell type markers as outlined in fig 2a.

Hierarchical clustering of the four oxygen conditions in ESTc based on their gene expression profiles revealed that, consistent with above results, oxygen tension in the differentiation phase was the dominant determinant for gene expression changes (fig. 5a). Most clear was the decreased appearance of the cardiac marker Myh6 upon differentiation under 5% as compared to 20% oxygen. Moreover, 5% rather than 20% oxygen tension in the differentiation phase caused higher expression of endoderm marker Gata4 and mesoderm marker Bmp4, and lower expression of stem cell marker Oct4, ectoderm marker Nes and cardiac differentiation marker Nkx2.5 expression (fig. 5c). Neural crest markers (Msx2, Snai2) and glial markers (Gfap, Mbp) were not affected. Interestingly, Tubb3 expression was less expressed in all conditions relative to 20-20% oxygen. The lower expression of cardiac markers in combination with the increased expression of endoderm marker Gata4 and mesoderm marker Bmp4 suggest that ESTc was pushed off its cardiac differentiation track under 5% versus 20% oxygen tension.

Hierarchical clustering of gene expression in ESTn showed that the 20-5% condition deviated most from the 20-20% condition, showing higher expression of non-neural markers and lower expression of neural differentiation related markers (fig. 5b). As with ESTc, oxygen tension during the differentiation phase determined most of the gene expression differences (fig. 5c). Expression of Cdh1, Bmp4, Gata4 and Snai2 were higher, and Tubb3 and Gfap expression were lower in 5% oxygen tension relative to ESTn differentiation under 20% oxygen tension. Switching stem cells from 20% to 5% oxygen additionally enhanced Msx2 and Myh6 expression, which together suggested higher expression of non-ectodermal (Cdh1, Bmp4, Gata4), cardiac (Myh6) and neural crest differentiation (Msx2, Snai2) and lower expression of neural (Tubb3) and astroglial differentiation (Gfap) compared to the 20-20% control group. Nes and Mbp expression were not affected. The 5-5% group did show higher expression of Nes and Mbp and lower expression of Nkx2.5, but no change in Msx2 and Myh6 expression relative to the 20-20% group, indicating a more complex phenotype compared to the 20-5% condition. Expression patterns indicated

higher expression of non-ectodermal differentiation (*Cdh1*, *Bmp4*, *Gata4*) in the 20-5% versus the 20-20% group, but additionally a lower expression of early cardiac differentiation and upregulation of early neural differentiation. Neural (*Tubb3*) and astroglial (*Gfap*) differentiation were less expressed in the presence of higher expression of oligodendrocyte (*Mbp*) and neural crest cell (*Snai2*) differentiation. ESC that were grown in 5% and differentiated in 20% oxygen resembled the 20-20% group most, although with some notable differences. Compared to the 20-20% condition, the 5-20% condition showed higher expression of glial (*Gfap* and *Mbp*) and early cardiac differentiation (*Nkx2.5*), together with less late cardiac (*Myh6*) and neural crest cell (*Msx2*, *Snai2*) expression.

In short, oxygen tension in the differentiation phases of ESTc as well as ESTn seemed to be most important for determining differences in cell differentiation. Cardiac and stem cell marker expression in ESTc was lower under 5% versus 20% oxygen tension and endoderm marker expression was higher, regardless of whether stem cells were grown under 5% or 20% oxygen. Other cell types were not influenced by the different oxygen tension regimens, except for neural differentiation (*Tubb3*). In ESTn a different distribution of cell types seemed to be generated, depending on both the ESC culture and differentiation oxygen tensions. A switch from 20 to 5% oxygen seemed to lead ESTn off the neural differentiation track to more cardiac and neural crest cell differentiation. Conversely, changing from 5 to 20% oxygen resulted in more glial differentiation and less neural crest cell differentiation. The 5-5% group presented a more mixed phenotype, but within the ectodermal lineage there was more neural crest and oligodendrocytes and less astroglial and neural differentiation.

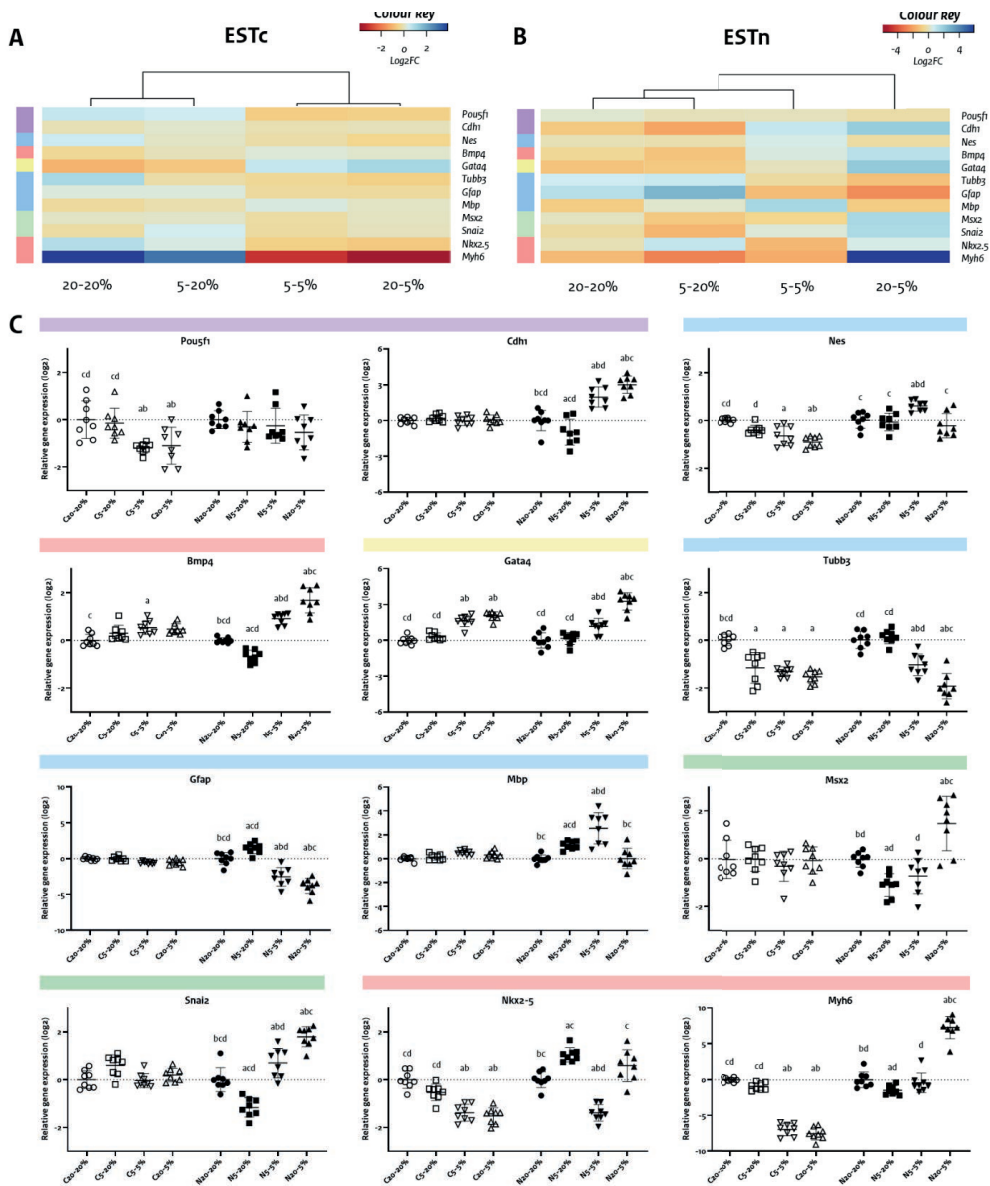


Figure 5: Gene expression of cell type markers in ESTc and ESTn under 5% and 20% oxygen tensions. (A,B) Heatmap summarising gene expression changes in (A) ESTc (day 10) and (B) ESTn (day 13), relative to the average expression per gene, per model. (C) Same data as shown in (A) and (B), plotted per gene, relative to the control condition (20-20%), per model. Significant difference from a condition is indicated as: a (different from 20-20%), b (5-20%), c (5-5%), d (20-5%). Significance levels are summarised in supplementary data 1.

Discussion

This study revealed the importance of oxygen tension within the ESTc and ESTn lineage differentiation. There were generally no significant differences between oxygen tensions when studying effects on ESC maintenance cultures alone. Differentiation into cardiomyocytes profited from 20% oxygen tension irrespective of the oxygen tension during ESC culture. An oxygen tension of 5% seemed to stimulate differentiation into endodermal differentiation rather than mesoderm-derived cardiomyocytes. Neural differentiation depended both on oxygen tension during stem cell maintenance and during differentiation, which resulted in different distributions of cell types. Relative to continuously culturing in 20% oxygen, the 20-5% oxygen condition seemed to push cells off the neural differentiation track, the 5-20% condition stimulated the cells more towards glial differentiation, and 5-5% showed a more mixed phenotype.

Although there were generally no statistically significant differences in cell density, viability and cell type markers between the oxygen tensions during ESC maintenance, cell density tended to be higher under 5% oxygen tension (fig. 1b). Increased cell density has been reported before under low oxygen tensions with ESC of different origin [16, 18]. However, studies that used murine ESC reported decreased cell density under 2% oxygen tension compared to 20% [33, 45]. This inconsistency may indicate that 2% oxygen tension is potentially too low for optimal ESC culture. This study showed trends of increased expression in stem cell markers, decreased expression in early differentiation markers, and increased expression in late differentiation markers (fig. 2b). Although these trends were not statistically significant, the tendencies were in line with results showing that low oxygen tension resulted in inhibition of differentiation [9, 14, 16, 17].

Differentiation into the cardiac lineage was lower under 5% versus 20% oxygen tension as shown by affected morphology including stimulation of necrosis (fig. 4a), reduced beating cardiomyocytes (fig. 3), and decreased gene expression of the early and late cardiomyocyte markers *Nkx2.5* and *Myh6* (fig. 5c). Also 5% oxygen tension resulted in a colour change of the medium to yellow indicating nutrient deprivation related to enhanced cell proliferation at the expense of differentiation into beating cardiomyocytes. However, cell death and reduced development of beating cardiomyocytes were previously reported in both mESCs and murine induced pluripotent stem cells (iPSCs), which were differentiated to cardiomyocytes at 2% oxygen or 5% oxygen tension,

respectively [22, 23]. Interestingly, iPSCs derived from mouse dermal fibroblasts could not be differentiated into beating cardiomyocytes at 2% oxygen levels, while showing an upregulation of cardiac markers like *Myh6* [26]. This contradiction was also seen in bone marrow derived mesenchymal stem cells from rats in which 0.5% oxygen tension did not result in functional cardiomyocyte differentiation, while cardiomyocyte gene and protein markers were upregulated [46]. Human ESCs showed more beating cardiomyocytes, a higher cardiac yield and a higher beating frequency when differentiated in 5% oxygen levels compared to 21% oxygen levels [27]. These contradictory results could be explained by e.g. methodological differences, species differences or nutrient depletion. For example, Wang *et al.* [26] performed only part of the differentiation in 2% oxygen and Choi *et al.* [46] measured gene expression already after 12 hours. This illustrates again the impact of the employed experimental procedure [9]. The decrease of the cardiomyocyte markers *Nkx2.5* and *Myh6* and concurring upregulation of endoderm marker *Gata4* suggests a stimulation of the endodermal lineage rather than the mesoderm-related cardiomyocyte route. One explanation may be that cardiomyocyte functioning needs sufficient oxygen for contraction and, in case of low oxygen, this severely impairs their development resulting in a differentiation in an alternative direction.

Differentiation into the neural lineage was, in contrast to cardiac differentiation, dependent of the oxygen tension during ESC culture and resulted in different morphologies for the different conditions. Compared to the control (20-20%), ESC that were grown in 20% and differentiated in 5% oxygen showed an increase in cells migrating out of EB, while an opposite oxygen regimen (5-20%) resulted in less migration (fig. 4d). This enlarged corona suggests an increase in proliferation, which is in line with previous findings showing increased proliferation of neural precursors in hypoxic conditions [47].

The changes in oxygen tension from ESC culture to differentiation not only affected morphology but also gene and protein expression levels, and indicated deviations from the differentiation tracks in all conditions compared to the 20-20% control condition. Rather than almost complete absence of a cell type as seen in ESTc it seemed that in ESTn the ratios between cell types were changed by different oxygen tensions. The oxygen tension level has an active role during the differentiation process [18]. Differentiation in 5% oxygen tension resulted in less neural (*Tubb3*) differentiation, which is consistent with previous research [16]. Another study has shown that 2% oxygen tension may enhance neural differentiation and that

changing oxygen tension between 0 and 10% can result in different proportions of cell types [29, 48]. The change of 20 to 5% oxygen tension in our study resulted in an upregulated expression of mesoderm and endoderm lineage markers instead of ectoderm lineage markers. Additionally, neural crest markers were upregulated during this condition, in line with previous research [18, 49]. Chen *et al.* [18] showed that a high oxygen tension of 20% led to a loss in cell density and a loss in astrocytes and oligodendrocytes compared to a low oxygen tension (2-5%) and Xie *et al.* [34] showed that 2% oxygen tension enhanced glial differentiation compared to 20% oxygen tension. This is partly consistent with results in our study only for oligodendrocyte (*Mbp*) but not astrocyte (*Gfap*) expression. Again, this may be due to methodological differences and more research is needed to further delineate the effects of oxygen tension with regard to conditions like timing, duration and cell source (e.g. ESCs versus neural progenitor cells)[9].

As mentioned before, oxygen tension and switching between high and low oxygen levels seems to have an active role in lineage commitment, which indicates a potential underlying mechanism. One of the potential mechanisms is through Hypoxia-Inducible Factor (HIF), which is activated upon a low oxygen tension and regulates differentiation [13, 34, 50-53]. A low oxygen tension can also regulate differentiation epigenetically in terms of myosin expression by inhibiting the oxygen sensitive KDM6A, which is a H3K27 histone demethylase [54]. These possible underlying mechanisms for oxygen dependent differentiation into specific lineages in the EST, should be investigated in future research.

In summary, this study exemplified the importance of oxygen tension for both maintenance and differentiation of murine ESCs into the neural and cardiac lineage. To our knowledge, this is the first study that assessed in parallel the effect of oxygen tension on two differentiation pathways from the same stem cell source. By separating the stem cell maintenance phase and the differentiation phase, we could distinguish specifically between the effects on either phase, and the relation between the two. ESTc and ESTn were affected in a different manner, which stresses that controlling oxygen tension during stem cell culture as well as during differentiation can greatly influence the differentiation path and can offer a valuable tool in optimising the desired *in vitro* system. Controlling oxygen tension can thus offer a valuable tool in optimizing ESC maintenance and differentiation, towards more realistic cell models for the purpose of for example personalised medicine, disease modelling, basic research and toxicology.

Acknowledgements

Victoria de Leeuw was funded by the Dutch NGO *Stichting Proefdiervrij* and the Dutch Ministry of Agriculture, Nature and Food Quality. Gina Mennen was supported by a CIFRE PhD grant, which was co-supervised by Nina Hallmark, Marc Pallardy, Remi Bars, and Helen Tinwell. Aldert Piersma was funded by the Dutch Ministry of Health, Welfare and Sports. We would like to thank Anne Kienhuis for a critical review of the manuscript.

References

1. Ivan, M., et al., *HIF1 α targeted for VHL-mediated destruction by proline hydroxylation: implications for O₂ sensing*. Science, 2001. **292**(5516): p. 464-8.
2. Maxwell, P.H., et al., *The tumour suppressor protein VHL targets hypoxia-inducible factors for oxygen-dependent proteolysis*. Nature, 1999. **399**(6733): p. 271-5.
3. Wang, G.L., et al., *Hypoxia-inducible factor 1 is a basic-helix-loop-helix-PAS heterodimer regulated by cellular O₂ tension*. Proc Natl Acad Sci U S A, 1995. **92**(12): p. 5510-4.
4. Jauniaux, E., et al., *In-vivo measurement of intrauterine gases and acid-base values early in human pregnancy*. Hum Reprod, 1999. **14**(11): p. 2901-4.
5. Rodesch, F., et al., *Oxygen measurements in endometrial and trophoblastic tissues during early pregnancy*. Obstet Gynecol, 1992. **80**(2): p. 283-5.
6. Panchision, D.M., *The role of oxygen in regulating neural stem cells in development and disease*. J Cell Physiol, 2009. **220**(3): p. 562-8.
7. Burr, S., et al., *Oxygen gradients can determine epigenetic asymmetry and cellular differentiation via differential regulation of Tet activity in embryonic stem cells*. Nucleic Acids Res, 2018. **46**(3): p. 1210-1226.
8. Kasterstein, E., et al., *The effect of two distinct levels of oxygen concentration on embryo development in a sibling oocyte study*. J Assist Reprod Genet, 2013. **30**(8): p. 1073-9.
9. Mas-Bargues, C., et al., *Relevance of Oxygen Concentration in Stem Cell Culture for Regenerative Medicine*. Int J Mol Sci, 2019. **20**(5).
10. Stacpoole, S.R., et al., *Derivation of neural precursor cells from human ES cells at 3% O₂ is efficient, enhances survival and presents no barrier to regional specification and functional differentiation*. Cell Death Differ, 2011. **18**(6): p. 1016-23.
11. Ast, T. and V.K. Mootha, *Oxygen and mammalian cell culture: are we repeating the experiment of Dr. Ox?* Nature Metabolism, 2019. **1**(9): p. 858-860.
12. Mohyeldin, A., T. Garzón-Muvdi, and A. Quiñones-Hinojosa, *Oxygen in Stem Cell Biology: A Critical Component of the Stem Cell Niche*. Cell Stem Cell, 2010. **7**(2): p. 150-161.
13. Zhao, Y., et al., *Dual functions of hypoxia-inducible factor 1 α for the commitment of mouse embryonic stem cells toward a neural lineage*. Stem Cells Dev, 2014. **23**(18): p. 2143-55.
14. Forristal, C.E., et al., *Hypoxia inducible factors regulate pluripotency and proliferation in human embryonic stem cells cultured at reduced oxygen tensions*. Reproduction, 2010. **139**(1): p. 85-97.
15. Keeley, T.P. and G.E. Mann, *Defining Physiological Normoxia for Improved Translation of Cell Physiology to Animal Models and Humans*. Physiol Rev, 2019. **99**(1): p. 161-234.
16. Gustafsson, M.V., et al., *Hypoxia requires notch signaling to maintain the undifferentiated cell state*. Dev Cell, 2005. **9**(5): p. 617-28.
17. Ezashi, T., P. Das, and R.M. Roberts, *Low O₂ tensions and the prevention of differentiation of hES cells*. Proc Natl Acad Sci U S A, 2005. **102**(13): p. 4783-8.
18. Chen, H.L., et al., *Oxygen tension regulates survival and fate of mouse central nervous system precursors at multiple levels*. Stem Cells, 2007. **25**(9): p. 2291-301.
19. Pimton, P., et al., *Hypoxia enhances differentiation of mouse embryonic stem cells into definitive endoderm and distal lung cells*. Stem Cells Dev, 2015. **24**(5): p. 663-76.

20. Katsuda, T., et al., *Hypoxia efficiently induces differentiation of mouse embryonic stem cells into endodermal and hepatic progenitor cells*. Biochemical Engineering Journal, 2013. **74**: p. 95-101.
21. Medley, T.L., et al., *Effect of oxygen on cardiac differentiation in mouse iPS cells: role of hypoxia inducible factor-1 and Wnt/beta-catenin signaling*. PLoS One, 2013. **8**(11): p. e80280.
22. Ramirez, M.A., et al., *Effect of long-term culture of mouse embryonic stem cells under low oxygen concentration as well as on glycosaminoglycan hyaluronan on cell proliferation and differentiation*. Cell Prolif, 2011. **44**(1): p. 75-85.
23. Brodarac, A., et al., *Susceptibility of murine induced pluripotent stem cell-derived cardiomyocytes to hypoxia and nutrient deprivation*. Stem Cell Res Ther, 2015. **6**(1): p. 83.
24. Huang, C.Y., et al., *Differentiation of embryonic stem cells into cardiomyocytes used to investigate the cardioprotective effect of salvianolic acid B through BNIP3 involved pathway*. Cell Transplant, 2015. **24**(3): p. 561-71.
25. Bianco, C., et al., *Cripto-1 is required for hypoxia to induce cardiac differentiation of mouse embryonic stem cells*. Am J Pathol, 2009. **175**(5): p. 2146-58.
26. Wang, Y., et al., *Hypoxia Enhances Direct Reprogramming of Mouse Fibroblasts to Cardiomyocyte-Like Cells*. Cell Reprogram, 2016. **18**(1): p. 1-7.
27. Horton, R.E. and D.T. Auguste, *Synergistic effects of hypoxia and extracellular matrix cues in cardiomyogenesis*. Biomaterials, 2012. **33**(27): p. 6313-9.
28. Correia, C., et al., *Combining hypoxia and bioreactor hydrodynamics boosts induced pluripotent stem cell differentiation towards cardiomyocytes*. Stem Cell Rev Rep, 2014. **10**(6): p. 786-801.
29. Mondragon-Teran, P., G.J. Lye, and F.S. Veraitch, *Lowering oxygen tension enhances the differentiation of mouse embryonic stem cells into neuronal cells*. Biotechnol Prog, 2009. **25**(5): p. 1480-8.
30. Pistollato, F., et al., *Oxygen tension controls the expansion of human CNS precursors and the generation of astrocytes and oligodendrocytes*. Mol Cell Neurosci, 2007. **35**(3): p. 424-35.
31. Storch, A., et al., *Long-term proliferation and dopaminergic differentiation of human mesencephalic neural precursor cells*. Exp Neurol, 2001. **170**(2): p. 317-25.
32. Lukmanto, D., et al., *Dynamic Changes of Mouse Embryonic Stem Cell-Derived Neural Stem Cells Under In Vitro Prolonged Culture and Hypoxic Conditions*. Stem Cells Dev, 2019. **28**(21): p. 1434-1450.
33. Fynes, K., et al., *The differential effects of 2% oxygen preconditioning on the subsequent differentiation of mouse and human pluripotent stem cells*. Stem Cells Dev, 2014. **23**(16): p. 1910-22.
34. Xie, Y., et al., *Defining the role of oxygen tension in human neural progenitor fate*. Stem Cell Reports, 2014. **3**(5): p. 743-57.
35. Theunissen, P.T., et al., *Complementary detection of embryotoxic properties of substances in the neural and cardiac embryonic stem cell tests*. Toxicol Sci, 2013. **132**(1): p. 118-30.
36. Mennen, R.H., J.L. Pennings, and A.H. Piersma, *Neural crest related gene transcript regulation by valproic acid analogues in the cardiac embryonic stem cell test*. Reprod Toxicol, 2019. **90**: p. 44-52.

37. de Leeuw, V.C., E.V.S. Hessel, and A.H. Piersma, *Look-alikes may not act alike: Gene expression regulation and cell-type-specific responses of three valproic acid analogues in the neural embryonic stem cell test (ESTn)*. *Toxicol Lett*, 2019. **303**: p. 28-37.
38. Theunissen, P.T., et al., *An abbreviated protocol for multilineage neural differentiation of murine embryonic stem cells and its perturbation by methyl mercury*. *Reprod Toxicol*, 2010. **29**(4): p. 383-92.
39. Spielmann, H., et al., *The embryonic stem cell test (EST), an in vitro embryotoxicity test using two permanent mouse cell lines : 3T3 fibroblasts and embryonic stem cells*. In *In Vitro and Molecular Toxicology: Journal of Basic and Applied Research*, 1997. **10**(1): p. 119-127.
40. Genschow, E., et al., *Validation of the Embryonic Stem Cell Test in the International ECVAM Validation Study on Three In Vitro Embryotoxicity Tests*. *Alternatives to Laboratory Animals*, 2004. **32**(3): p. 209-244.
41. Theunissen, P.T., et al., *Time-Response Evaluation by Transcriptomics of Methylmercury Effects on Neural Differentiation of Murine Embryonic Stem Cells*. *Toxicological Sciences*, 2011. **122**(2): p. 437-447.
42. Schindelin, J., et al., *Fiji: an open-source platform for biological-image analysis*. *Nature Methods*, 2012. **9**(7): p. 676-682.
43. Biosystems, A., *User Bulletin #2 ABI PRISM 7700 Sequence Detection System*. 2001, Thermo Fisher: Waltham (MA). p. 1-30.
44. Team, R.C., *R: A Language and Environment for Statistical Computing*. 2019: Vienna, Austria.
45. Fernandes, T.G., et al., *Different stages of pluripotency determine distinct patterns of proliferation, metabolism, and lineage commitment of embryonic stem cells under hypoxia*. *Stem Cell Res*, 2010. **5**(1): p. 76-89.
46. Choi, J.W., et al., *Alterations in Cardiomyocyte Differentiation-Related Proteins in Rat Mesenchymal Stem Cells Exposed to Hypoxia*. *Cell Physiol Biochem*, 2016. **39**(4): p. 1595-607.
47. Studer, L., et al., *Enhanced proliferation, survival, and dopaminergic differentiation of CNS precursors in lowered oxygen*. *J Neurosci*, 2000. **20**(19): p. 7377-83.
48. Mondragon-Teran, P., et al., *The full spectrum of physiological oxygen tensions and step-changes in oxygen tension affects the neural differentiation of mouse embryonic stem cells*. *Biotechnol Prog*, 2011. **27**(6): p. 1700-8.
49. Morrison, S.J., et al., *Culture in reduced levels of oxygen promotes clonogenic sympathoadrenal differentiation by isolated neural crest stem cells*. *J Neurosci*, 2000. **20**(19): p. 7370-6.
50. Mohyeldin, A., T. Garzon-Muvdi, and A. Quinones-Hinojosa, *Oxygen in stem cell biology: a critical component of the stem cell niche*. *Cell Stem Cell*, 2010. **7**(2): p. 150-61.
51. Ateghang, B., et al., *Regulation of cardiotrophin-1 expression in mouse embryonic stem cells by HIF-1alpha and intracellular reactive oxygen species*. *J Cell Sci*, 2006. **119**(Pt 6): p. 1043-52.
52. Kudova, J., et al., *HIF-1alpha Deficiency Attenuates the Cardiomyogenesis of Mouse Embryonic Stem Cells*. *PLoS One*, 2016. **11**(6): p. e0158358.
53. Simon, M.C. and B. Keith, *The role of oxygen availability in embryonic development and stem cell function*. *Nat Rev Mol Cell Biol*, 2008. **9**(4): p. 285-96.

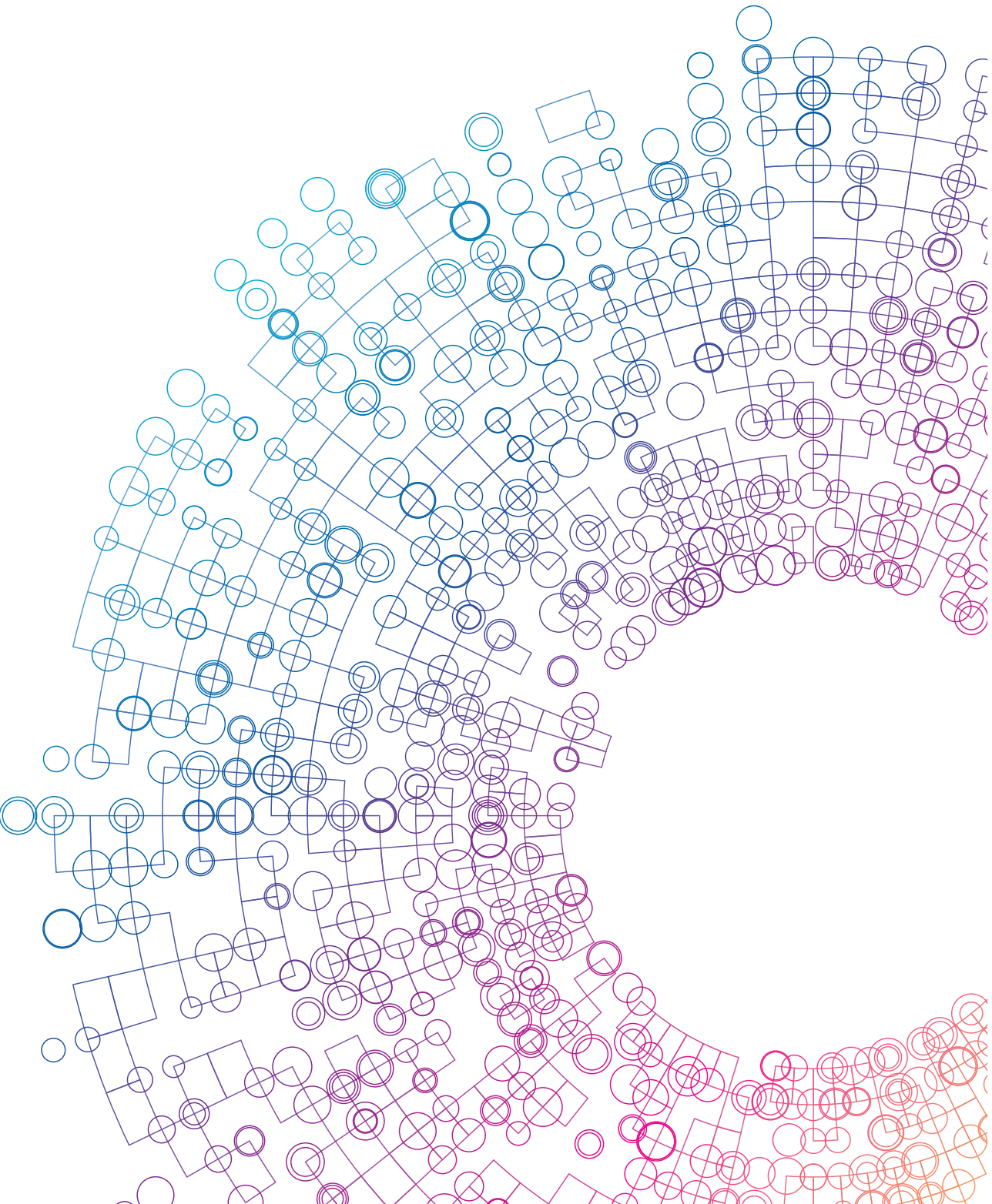
54. Chakraborty, A.A., et al., *Histone demethylase KDM6A directly senses oxygen to control chromatin and cell fate*. Science, 2019. **363**(6432): p. 1217-1222.

Supplementary

Gene	Sidak's multiple comparisons test	Mean Diff.	95.00% CI of diff.	Summary	Adjusted P Value
<i>Pou5f1</i>	C20-20% vs. C20-5%	1.103	0.2179 to 1.988	**	0.0052
	C20-20% vs. C5-5%	1.195	0.3105 to 2.080	**	0.0018
	C20-5% vs. C5-20%	-0.9523	-1.837 to -0.06746	*	0.0258
	C5-20% vs. C5-5%	1.045	0.1601 to 1.930	**	0.0098
<i>Cdh1</i>	N20-20% vs. N20-5%	-2.999	-3.929 to -2.069	****	<0.0001
	N20-20% vs. N5-20%	0.9775	0.04735 to 1.908	*	0.0323
	N20-20% vs. N5-5%	-1.969	-2.900 to -1.039	****	<0.0001
	N20-5% vs. N5-5%	1.03	0.09964 to 1.960	*	0.0196
	N20-5% vs. N5-20%	3.977	3.046 to 4.907	****	<0.0001
	N5-20% vs. N5-5%	-2.947	-3.877 to -2.017	****	<0.0001
<i>Nes</i>	C20-20% vs. C20-5%	0.9119	0.4321 to 1.392	****	<0.0001
	C20-20% vs. C5-5%	0.659	0.1792 to 1.139	**	0.0015
	C20-5% vs. C5-20%	-0.5017	-0.9815 to -0.02190	*	0.0338
	N20-20% vs. N5-5%	-0.5975	-1.077 to -0.1177	**	0.0053
	N20-5% vs. N5-5%	-0.8276	-1.307 to -0.3478	****	<0.0001
	N5-20% vs. N5-5%	-0.6726	-1.152 to -0.1928	**	0.0011
<i>Bmp4</i>	C20-20% vs. C5-5%	-0.5386	-1.014 to -0.06340	*	0.0154
	N20-20% vs. N20-5%	-1.679	-2.154 to -1.203	****	<0.0001
	N20-20% vs. N5-20%	0.6683	0.1931 to 1.143	**	0.001
	N20-20% vs. N5-5%	-0.9058	-1.381 to -0.4306	****	<0.0001
	N20-5% vs. N5-5%	0.7729	0.2977 to 1.248	****	<0.0001
	N20-5% vs. N5-20%	2.347	1.872 to 2.822	****	<0.0001
	N5-20% vs. N5-5%	-1.574	-2.049 to -1.099	****	<0.0001
<i>Gata4</i>	C20-20% vs. C20-5%	-2.051	-2.803 to -1.298	****	<0.0001
	C20-20% vs. C5-5%	-1.625	-2.378 to -0.8729	****	<0.0001
	C20-5% vs. C5-20%	1.735	0.9823 to 2.487	****	<0.0001
	C5-20% vs. C5-5%	-1.309	-2.062 to -0.5568	****	<0.0001
	N20-20% vs. N20-5%	-3.26	-4.013 to -2.508	****	<0.0001
	N20-20% vs. N5-5%	-1.165	-1.917 to -0.4123	***	0.0002
	N20-5% vs. N5-5%	2.095	1.343 to 2.848	****	<0.0001
	N20-5% vs. N5-20%	3.097	2.344 to 3.850	****	<0.0001
	N5-20% vs. N5-5%	-1.002	-1.754 to -0.2491	**	0.0023

Gene	Sidak's multiple comparisons test	Mean Diff.	95.00% CI of diff.	Summary	Adjusted P Value
<i>Tubb3</i>	C20-20% vs. C20-5%	1.55	0.9577 to 2.143	****	<0.0001
	C20-20% vs. C5-20%	1.174	0.5817 to 1.767	****	<0.0001
	C20-20% vs. C5-5%	1.341	0.7483 to 1.933	****	<0.0001
	N20-20% vs. N20-5%	1.941	1.349 to 2.534	****	<0.0001
	N20-20% vs. N5-5%	1.049	0.4560 to 1.641	****	<0.0001
	N20-5% vs. N5-5%	-0.8926	-1.485 to -0.3001	***	0.0004
	N20-5% vs. N5-20%	-2.065	-2.658 to -1.473	****	<0.0001
	N5-20% vs. N5-5%	1.173	0.5800 to 1.765	****	<0.0001
<i>Gfap</i>	N20-20% vs. N20-5%	3.819	2.802 to 4.836	****	<0.0001
	N20-20% vs. N5-20%	-1.434	-2.451 to -0.4167	***	0.001
	N20-20% vs. N5-5%	2.546	1.529 to 3.563	****	<0.0001
	N20-5% vs. N5-5%	-1.273	-2.291 to -0.2561	**	0.005
	N20-5% vs. N5-20%	-5.253	-6.270 to -4.236	****	<0.0001
	N5-20% vs. N5-5%	3.98	2.962 to 4.997	****	<0.0001
<i>Mbp</i>	N20-20% vs. N5-20%	-1.136	-1.988 to -0.2841	**	0.0022
	N20-20% vs. N5-5%	-2.543	-3.395 to -1.691	****	<0.0001
	N20-5% vs. N5-5%	-2.526	-3.378 to -1.674	****	<0.0001
	N20-5% vs. N5-20%	-1.12	-1.972 to -0.2677	**	0.0027
	N5-20% vs. N5-5%	-1.407	-2.259 to -0.5547	****	<0.0001
<i>Msx2</i>	N20-20% vs. N20-5%	-1.505	-2.503 to -0.5068	***	0.0004
	N20-20% vs. N5-20%	1.078	0.08000 to 2.077	*	0.0249
	N20-5% vs. N5-5%	2.2	1.202 to 3.199	****	<0.0001
	N20-5% vs. N5-20%	2.583	1.585 to 3.582	****	<0.0001
<i>Snai2</i>	N20-20% vs. N20-5%	-1.792	-2.480 to -1.103	****	<0.0001
	N20-20% vs. N5-20%	1.164	0.4755 to 1.853	****	<0.0001
	N20-20% vs. N5-5%	-0.6924	-1.381 to -0.003579	*	0.0479
	N20-5% vs. N5-5%	1.099	0.4104 to 1.788	***	0.0001
	N20-5% vs. N5-20%	2.956	2.267 to 3.645	****	<0.0001
	N5-20% vs. N5-5%	-1.857	-2.545 to -1.168	****	<0.0001
<i>Nkx2.5</i>	C20-20% vs. C20-5%	1.518	0.9033 to 2.132	****	<0.0001
	C20-20% vs. C5-5%	1.388	0.7739 to 2.002	****	<0.0001
	C20-5% vs. C5-20%	-0.9815	-1.596 to -0.3672	***	0.0001
	C5-20% vs. C5-5%	0.8521	0.2378 to 1.466	**	0.0013
	N20-20% vs. N5-20%	-1.039	-1.654 to -0.4252	****	<0.0001
	N20-20% vs. N5-5%	1.39	0.7753 to 2.004	****	<0.0001

Gene	Sidak's multiple comparisons test	Mean Diff.	95.00% CI of diff.	Summary	Adjusted P Value
	N20-5% vs. N5-5%	1.976	1.362 to 2.590	****	<0.0001
	N5-20% vs. N5-5%	2.429	1.815 to 3.043	****	<0.0001
<i>Myh6</i>	C20-20% vs. C20-5%	7.54	6.189 to 8.891	****	<0.0001
	C20-20% vs. C5-5%	6.954	5.603 to 8.305	****	<0.0001
	C20-5% vs. C5-20%	-6.615	-7.966 to -5.264	****	<0.0001
	C5-20% vs. C5-5%	6.029	4.678 to 7.379	****	<0.0001
	N20-20% vs. N20-5%	-7.295	-8.646 to -5.944	****	<0.0001
	N20-20% vs. N5-20%	1.461	0.1105 to 2.812	*	0.0246
	N20-5% vs. N5-5%	7.716	6.366 to 9.067	****	<0.0001
	N20-5% vs. N5-20%	8.757	7.406 to 10.11	****	<0.0001



CHAPTER

Cell differentiation in the cardiac embryonic stem cell test (ESTc) is influenced by the oxygen tension in its underlying embryonic stem cell culture

7

R.H. Mennen, V.C. de Leeuw, A.H. Piersma

Toxicology In Vitro. 2021 Dec; 77: 105247.

DOI: [10.1016/j.tiv.2021.105247](https://doi.org/10.1016/j.tiv.2021.105247)

Abstract

Oxygen (O_2) levels in the mammalian embryo range between 2.4% and 8%. The cardiac embryonic stem cell test (ESTc) is a model for developmental toxicity predictions, which is usually performed under atmospheric O_2 levels of 20%. We investigated the chemical sensitivity of the ESTc carried out under 20% O_2 , using embryonic stem cells (ESC) cultured under either 20% O_2 or 5% O_2 . ESC viability was more sensitive to valproic acid (VPA) but less sensitive to flusilazole (FLU) when cultured under 5% versus 20% O_2 . For beating cardiomyocyte differentiation, lower ID_{50} values were found for FLU and VPA when the ESCs had been cultured under 5% versus 20% O_2 . At differentiation day 4, gene expression values were primarily driven by the level of O_2 during ESC culture instead of exposure to FLU. In addition, using ESCs cultured under 5% O_2 tension, VPA enhanced *Nes* (ectoderm) expression. *Bmp4* (mesoderm) was enhanced by VPA when using ESCs cultured under 20% O_2 . At differentiation day 10, using ESCs cultured under 5% instead of 20% O_2 , *Nkx2.5* and *Myh6* (cardiomyocytes) were less affected after exposure to FLU or VPA. These results show that O_2 tension in ESC culture influences chemical sensitivity in the ESTc. This enhances awareness of the standard culture conditions, which may impact the application of the ESTc in quantitative hazard assessment of chemicals.

Introduction

The lungs inhale oxygen (O_2) which is spread throughout the body at concentrations lower than atmospheric pressure (~20%). During pregnancy, the embryo is receiving O_2 through the placenta resulting in varying O_2 levels in the embryo, between 2.4% (7-11 weeks) and 8% (>11 weeks) depending on the body part and developmental stage [1-3]. O_2 pressure homeostasis influences differentiation into specific cell lineages throughout the embryo [3, 4]. These physiological O_2 levels are taken into account for instance in *in vitro* fertilisation (IVF) for which a 5% O_2 tension is favourable for survival of the oocytes [5]. However, the effects of O_2 levels are less well studied for *in vitro* models in the field of developmental toxicology.

As an example, the field of cancer treatment research is taking advantage of the sensitivity of chemicals to O_2 pressure with multiple clinical trials ongoing. Tumours grow under hypoxic conditions and the formulation of hypoxia-activated prodrugs (HAPs) that become more potent under low O_2 levels benefits tumour treatment [6, 7]. The development of two of these HAPs is still ongoing, namely for evosfosfamide (TH-302) and tarloxotinib bromide (TH-4000), which are prodrugs for DNA damage and kinase inhibition, respectively [7, 8]. Other examples in which the level of O_2 influences the cell sensitivity to chemicals are for rotenone or copper oxide nanoparticles. Rotenone is suspected to interfere with O_2 homeostasis since exposure in neuronal SH-SY5Y cells under 5% O_2 resulted in a lower production of Reactive Oxygen Species (ROS) by the mitochondria [9]. The sensitivity to copper oxide nanoparticles in A549 pulmonary cells increased in lower O_2 conditions (13%) since the ROS production was increased relative to high O_2 (21%) [10]. O_2 is the primary electron (e^-) acceptor in biochemical reactions and is used by mitochondria to generate adenosine triphosphate (ATP) through e.g. glycolysis [11]. O_2 homeostasis is maintained by factors like hypoxia inducible factor (HIFs), mammalian target of rapamycin (mTOR), and endoplasmic reticulum (ER) response. Chemicals can interfere with these pathways and, in turn, O_2 can influence chemical behaviour within the body and foetus causing a change in the sensitivity to chemicals. Conversely, basic culture conditions can impact compound effects in individual *in vitro* assays, with consequences in the broader perspective of test batteries, integrated approaches to testing and assessment (IATA) and ultimately risk assessment.

Compound sensitivity to O_2 has only slightly been studied in embryonic stem cell (ESC) culture and in ESC differentiation in the cardiac embryonic stem cell test (ESTc), an animal-free alternative test method in developmental toxicology. In a

study using human embryonic stem cells (hESC), the sensitivity to sodium arsenite was tested under hypoxic and normoxic (21%) conditions where hypoxic conditions were protective to sodium arsenite because of a reduced oxidative stress response [12]. Moreover, hypoxia maintains the pluripotent state of these stem cells [12]. The effect of low O₂ levels on stem cell differentiation and chemical sensitivity is less well studied. A lowered O₂ tension keeps the ESCs in an undifferentiated state, but is also better for cell survival and expansion [13-15]. Once differentiating the ESCs into cardiomyocytes in the ESTc, low O₂ levels reduce this development and appear to be detrimental, which can even result in cell death [16-19]. These effects of O₂ levels on ESC pluripotency and cardiomyocyte differentiation have been studied before in our lab and showed no effect of a lowered O₂ level on ESC proliferation and gene and protein expression levels [20]. However, irrespective of the O₂ levels in which the ESCs were cultured, cardiac differentiation in lowered O₂ levels of 5% reduced gene and protein expression levels and related beating cardiomyocyte development [20].

Because of the lack of attention to compound sensitivity under physiological O₂ levels during ESC culture, we investigated the sensitivity of ESCs to developmental toxicants in atmospheric (20%) and low (5%) O₂ levels. Additionally, we studied the effects of these different O₂ tensions during ESC culture on subsequent differentiation and compound effects in the ESTc performed under 20% O₂.

Methods

Chemicals

Flusilazole (FLU, CAS# 85509-19-9), and valproic acid sodium salt (VPA, CAS# 99-66-1) were purchased from Sigma-Aldrich (Zwijndrecht, The Netherlands). The compounds were tested at concentrations up to 300 µM and 3 mM for FLU and VPA, respectively. RNA collections were performed at compound specific ID₅₀ concentrations identified in the ESTc. DMSO was used as a solvent for FLU. VPA was dissolved in complete medium. The medium contained 0.25% dimethyl sulfoxide (DMSO, Sigma-Aldrich) as the final solvent concentration for FLU, VPA and control conditions.

Stem cell culture

Murine ESCs (ES-D3, ATCC® (Manassas, VA, USA)) were continuously cultured under 5% O₂ or 20% O₂ tension (see fig. 1). Both conditions were maintained as described

previously [21, 22]. Every 2-3 days, the cells were cultured in 35 mm dishes (Corning, New York, NY, USA) in a humidified atmosphere of 37°C with 5% CO₂. The culture medium consisted of Dulbecco's Modified Eagle's Medium (DMEM; Gibco, Waltham, MA, USA), 20% Fetal Bovine Serum (FBS; Greiner Bio-One, Kremsmünster, Austria); 1% 5000 IU/ml Penicillin/5000 µg/ml Streptomycin (Gibco); 2 mM L-Glutamin (Gibco); 1% Non-Essential Amino Acids (NEAA; Gibco); 0.1 mM β-mercaptoethanol (Gibco); and 1000 units/ml leukemia inhibitory factor (LIF; ESGRO®, Millipore, Burlington, MA, USA) to keep the cells in a pluripotent state. After several passages these cultured cells were used for all subsequent experiments.

Cell viability assay

Cell viability testing of ESCs was performed under 5% O₂ or 20% O₂ tension and was performed as described previously [23]. 500 cells per well were plated in LIF containing culture medium in a 96-wells plate (Greiner Bio-One) and were incubated at 37°C and 5% CO₂ for two hours. After incubation, the test chemicals were added with highest concentrations and six subsequent lower concentrations including the in medium dissolved controls DMSO (0.25%; solvent control; Sigma-Aldrich), 5-fluoruracil (0.1 µg/ml; positive control; Sigma-Aldrich), and penicillin G (500 µg/ml; negative control; Sigma-Aldrich) in six replicates. The exposure medium was refreshed at identical end-concentrations after three days of incubation. Fluorescence measurements as an indication for cell viability were measured after incubation for another two days using CellTiter-Blue reagent (Promega, Leiden, The Netherlands) [24]. The extinction values were determined at 544_{Ex}/590_{Em} nm on the SpectraMax® M2 spectrofluorometer (Molecular Devices, Berkshire, United Kingdom) after two hours of incubation and were expressed relative to the solvent control. Three independent experiments were done for each test compound and the average and standard deviation of the six replicates of each experiment were analysed using PROAST v67.0 in R.

Cell differentiation assay

Cardiac differentiation was always performed under 20% O₂ tension starting with ESCs cultured under 5% O₂ or with ESCs cultured under 20% O₂ tension (fig. 1). The differentiation was performed according to a protocol previously described using culture medium without the addition of LIF to provide differentiation [22, 25]. Embryonic bodies (EBs) were formed by hanging drop formation from a cell

suspension in the lid of a 100/20 mm CELLSTAR® cell culture dish (Greiner Bio-One) at differentiation day 0 (fig. 1). The culture dish contained ice-cold phosphate buffered saline (PBS; Ca²⁺, Mg²⁺ free; Gibco). After 3 days of incubation at 37°C and 5% CO₂, the formed EBs were transferred to exposure medium in a 60 mm bacterial petri dish (Greiner Bio-One) (fig. 1). This exposure medium contained start concentrations of the test chemicals with six subsequent lower concentrations or controls. At differentiation day 5, the EBs were transferred to a 24-wells plate (Greiner Bio-One) containing one EB per well in the desired concentration of the test compounds or controls (fig. 1). Each plate contained 24 replicates per concentration and was performed in duplicate. At differentiation day 10, the EBs were scored for presence or absence of beating cardiomyocytes using a bright field microscope (Olympus BX51, Shinjuku, Japan) (fig. 1). The number of beating EBs was calculated relative to the total EBs per 24-wells plate. Two independent experiments were done for each test compound. The data were analysed as described in the statistics section.

Gene expression analysis

The differentiating EBs exposed to ID₅₀ concentrations or to the DMSO control (0.25%) were collected at differentiation day 4 and differentiation day 10 (fig. 1). Each condition consisted of two groups, with ESCs cultured under 5% O₂ tension or under 20% O₂ tension. 13 to 14 samples were collected in QIAzol (Qiagen, Hilden, Germany) from two independent experiments and were stored at -80°C prior to RNA isolation. RNA was isolated using the RNeasy Mini-kit (Qiagen, Cat. # 74104) according to manufacturer's protocol. Prior to isolation, the samples were homogenised using QIAshredder columns (Qiagen, Cat. # 79654). As an intermediate step, DNA contamination was prevented using a RNase-Free DNase set (Qiagen, Cat # 79254). RNA quantity and quality was examined with 260 nm/280 nm absorbance ratios between 1.8 and 2.2 and the RIN (RNA Integrity Number) scores >8.9 using the Nanodrop (Nanodrop Technologies Inc., Wilmington, Delaware) and the 2100 Bioanalyzer (Agilent Technologies, Amstelveen, The Netherlands). cDNA was formed according to manufacturer's prescriptions using a cDNA synthesis kit (Applied Biosystems, Foster City, CA, USA). Quantification of cDNA was performed using a 7500 Fast Real-Time PCR system (Applied Biosystems) with the thermal cycling conditions: 95°C for 20s, followed by 40 cycles of 95°C for 3s and 60°C for 30s. The used TaqMan® Assays (Thermo Fisher Scientific) used for gene expression

analysis are listed in table 1. The relative differences between gene expression levels were calculated using the $-\Delta\Delta C_t$ method [26]. These values were normalised against the average expression levels of the housekeeping genes *Hprt1*, *Gusb*, and *Polr2a* (Table 1).

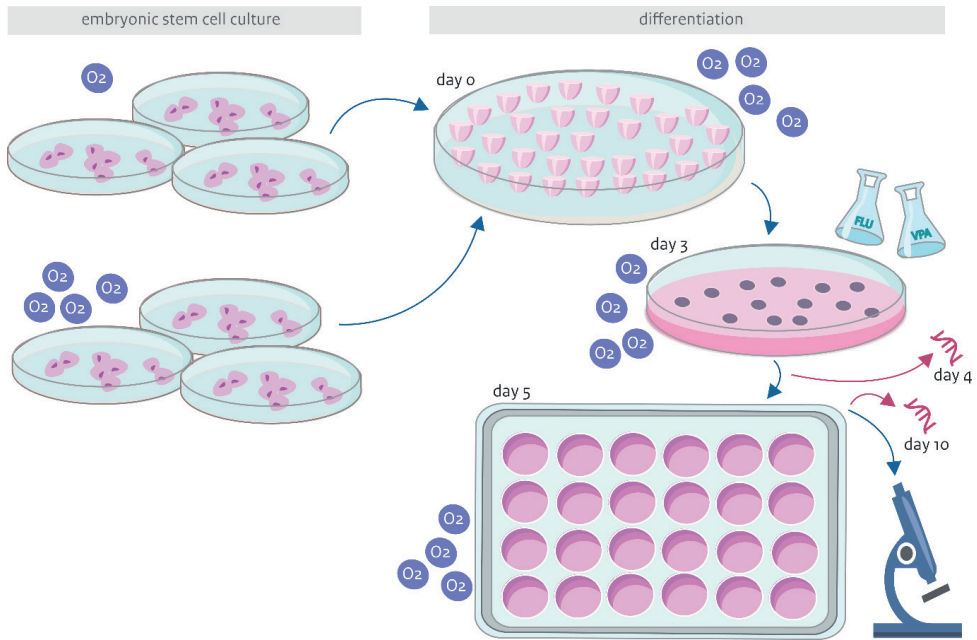


Figure 1: Procedure of ESC culture and the ESTc. One O_2 -circle equals 5% O_2 tension, four O_2 -circles equals 20% O_2 . ESCs were cultured under 5% or 20% O_2 tension. The ESCs from 5% or 20% O_2 cultures were used in the ESTc towards cardiomyocytes, which was completely performed under 20% O_2 . At differentiation day 0, hanging drops were formed facilitating the formation of cell aggregates. At differentiation day 3, the aggregates (EBs) were collected in exposure medium containing flusilazole (FLU), valproic acid (VPA), or vehicle control. At differentiation day 5, one EB was pipetted per well containing exposure medium. Beating muscle foci were scored by the microscope at differentiation day 10, and RNA was collected at differentiation day 4 and 10.

Table 1: Primers used for qPCR procedure

Gene name	Abbreviation	Marker for	Assay ID/primer sequence
POU domain, class 5, transcription factor 1	<i>Pou5f1</i> (or <i>Oct4</i>)	Stem cell	Mm03053917_g1
Bone morphogenetic protein 4	<i>Bmp4</i>	Mesoderm	Mm00432087_m1
Nestin	<i>Nes</i>	Ectoderm/Neural progenitor	Mm00450205_m1
GATA binding protein 4	<i>Gata4</i>	Endoderm	Mm00484689_m1
NK2 transcription factor related, locus 5	<i>Nkx2.5</i>	Early cardiomyocyte	Mm01309813_s1
myosin, heavy polypeptide 6, cardiac muscle, alpha	<i>Myh6</i>	Cardiomyocyte	Mm00440359_m1
Msh homeobox 2	<i>Msx2</i>	Early neural crest marker	Mm00442992_m1
Snail family zinc finger 2	<i>Snai2</i>	Epithelial-Mesenchymal Transition	Mm00441531_m1
Glucuronidase beta	<i>Gusb</i>	Housekeeping gene	Mm01197698_m1
Hypoxanthine phosphoribosyltransferase 1	<i>Hprt1</i>	Housekeeping gene	Mm03024075_m1
RNA Polymerase II Subunit A	<i>Polr2a</i>	Housekeeping gene	Mm00839502_m1
Hypoxia inducible factor 1 α	<i>Hif1α</i>	Homeostasis regulator in response to hypoxia	Mm00468869_m1

Statistics

The obtained data on cell viability and differentiation were fitted and statistically analysed using the exponential method within the PROAST software version 67.0 [27]. 50% inhibitory levels for viability and differentiation, IC₅₀ and ID₅₀ values respectively, were determined from the dose-response curves with 90% confidence lower and upper bench mark dose values (BMDL-BMDU). Control values were visualised using a dummy value. Gene expression data were compared to the control samples using an one-way ANOVA test with Sidak's multiple comparisons post-hoc test ($p < 0.05$) using GraphPad Prism 8.1.2 (www.graphpad.com). The data used for the heatmap were plotted against the average of all conditions and were visualised using R software [28].

Results

The sensitivity of ESC culture to compounds changes with changing O₂ tension

ESC viability under 5% or 20% O₂ tension was tested after exposure to flusilazole (FLU) and valproic acid (VPA) (fig. 2). The sensitivity of ESCs to VPA was higher under 5% O₂ tension, whilst the sensitivity of ESCs to FLU was higher in 20% O₂. This is confirmed by the derived IC₅₀ levels depicted in table 2, which show approximately two-fold differences between O₂ tension conditions.

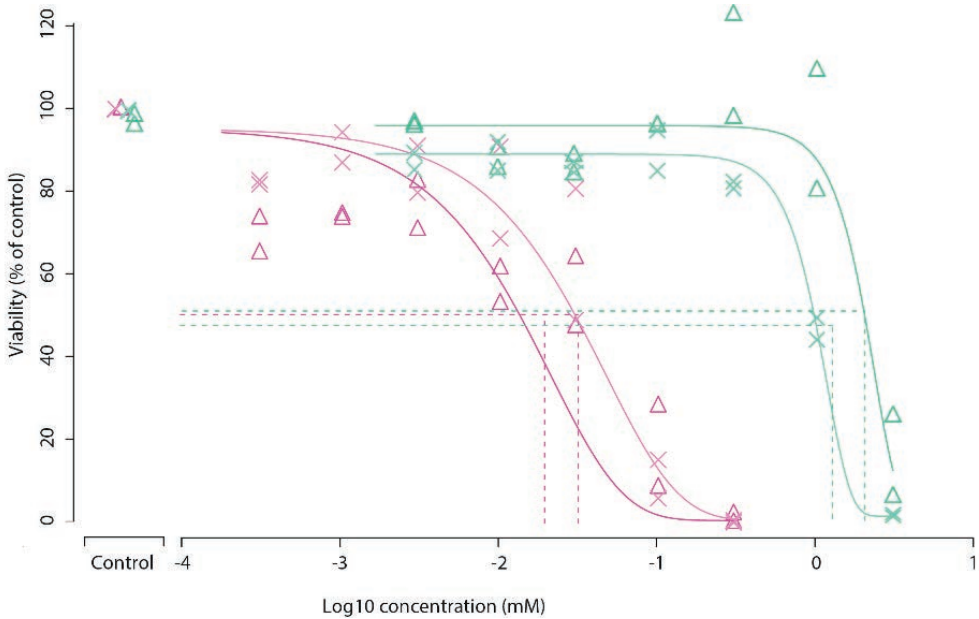


Figure 2: ESC viability in 5% O₂ (X) or 20% O₂ (Δ) after exposure to FLU or VPA. IC₅₀ levels are indicated by the dashed lines.

Table 2: IC₅₀ of FLU and VPA in ESC culture in 5% or 20% O₂ tension with lower and upper limit bench mark dose levels (BMDL-BMDU) with 90% confidence.

IC ₅₀ (BMDL-BMDU)	20% O ₂	5% O ₂
Flusilazole	14.3 μM (10.9-18.5)	32.1 μM (26.8-38.1)
Valproic acid	2.01 mM (1.69-2.23)	1.03 mM (0.991-1.08)

The influence of O₂ tension during ESC culture on sensitivity to compound exposure in the ESTc

Inhibition of beating cardiomyocyte differentiation

As to beating cardiomyocyte differentiation in the ESTc, applying 5% instead of 20% O₂ tension during ESC culture resulted in a small but statistically significantly higher sensitivity to FLU and VPA when these ESCs were subsequently used in the ESTc (fig. 3a, table 3). The benchmark dose lower and upper boundary intervals (BMDL-BMDU), indicating 90% confidence intervals, did not overlap. The ID₅₀ levels for FLU were 35.9 μM when ESCs had been cultured under 5% O₂ and 41.8 μM when cultured under 20% O₂ (table 3). For VPA these values were 1.30 mM when ESCs had been cultured under 5% O₂ and 1.74 mM when cultured under 20% O₂ (table 3).

Table 3: Differentiation inhibition of FLU and VPA in the ESTc after culturing ESCs in 5% or 20% O₂ tension with lower and upper bench mark dose levels (BMDL-BMDU) with 90% confidence.

ID ₅₀ (BMDL-BMDU)	20% O ₂	5% O ₂
Flusilazole	41.8 μM (41.8-42.4)	35.9 μM (34.4-37.1)
Valproic acid	1.74 mM (1.57-1.97)	1.30 mM (1.24-1.38)

Gene expression regulation

In the ESTc at differentiation day 4, unexposed differentiating cells showed higher expression of *Bmp4* (mesoderm marker) and of *Msx2* and *Snai2* (neural crest cell markers) when ESCs had been cultured under 5% O₂ compared to 20%, as shown by heatmap clustering (fig. 3b). At differentiation day 10, these unexposed cells showed lower expression of *Pou5f1* (pluripotency marker) and lower expression

of *Myh6* (cardiomyocyte marker) when ESCs had been cultured under 5% O₂ compared to 20% O₂ (fig. 3b).

The tested conditions clustered according to their gene expression profiles during differentiation in the ESTc as shown in figure 3b. The major clustering was driven by time, showing for example a relatively high expression of the pluripotency marker *Pou5f1* at differentiation day 4 as compared to differentiation day 10. The differentiation markers *Nkx2.5*, *Myh6* (cardiomyocyte differentiation), and *Snai2* (epithelial to mesenchymal transition marker for neural crest cells) showed the opposite direction of relative regulations with low gene expression values (in red) at differentiation day 4 and high values (in blue) at differentiation day 10.

In addition, clustering of expression levels in the ESTc occurred primarily per ESC O₂ condition with the exception of VPA at differentiation day 4 (fig. 3b). On the contrary, all exposure groups clustered per compound at differentiation day 10, indicating that with time the influence of the preceding ESC O₂ condition remained observable during the ESTc but declined in favour of the effect of compound exposure.

As to individual gene expression regulation during differentiation in the ESTc at differentiation day 4, pluripotency genes (*Pou5f1* c.q. *Oct4*) were significantly (up) regulated after FLU exposure when ESCs had been cultured under 5% O₂ tension, but not when ESCs had been cultured under 20% O₂ (fig. 3c). Also the germ layer markers *Nes* and *Bmp4* showed differences in significant exposure effects when ESCs had been cultured under different O₂ conditions. *Nes* expression (for ectoderm) was significantly regulated by FLU exposure when ESCs had been cultured under 20% O₂ tension only. VPA exposure significantly regulated *Nes* expression when ESCs had been cultured under 5% O₂ tension only. *Bmp4* expression (for mesoderm) was significantly regulated by VPA when ESCs had been cultured under 20% O₂ only. Also the early neural crest cell differentiation marker *Msx2* was significantly regulated by FLU when ESCs had been cultured under 20% O₂ tension only. The gene expression levels of the hypoxia inducible factor *Hif1a* were significantly regulated by VPA when ESCs had been cultured under 5% O₂ tension.

At differentiation day 10 in the ESTc, the pluripotency marker and differentiation markers showed statistically significant differences after developmental toxicant exposure depending on different O₂ tensions in the preceding ESC culture (fig.

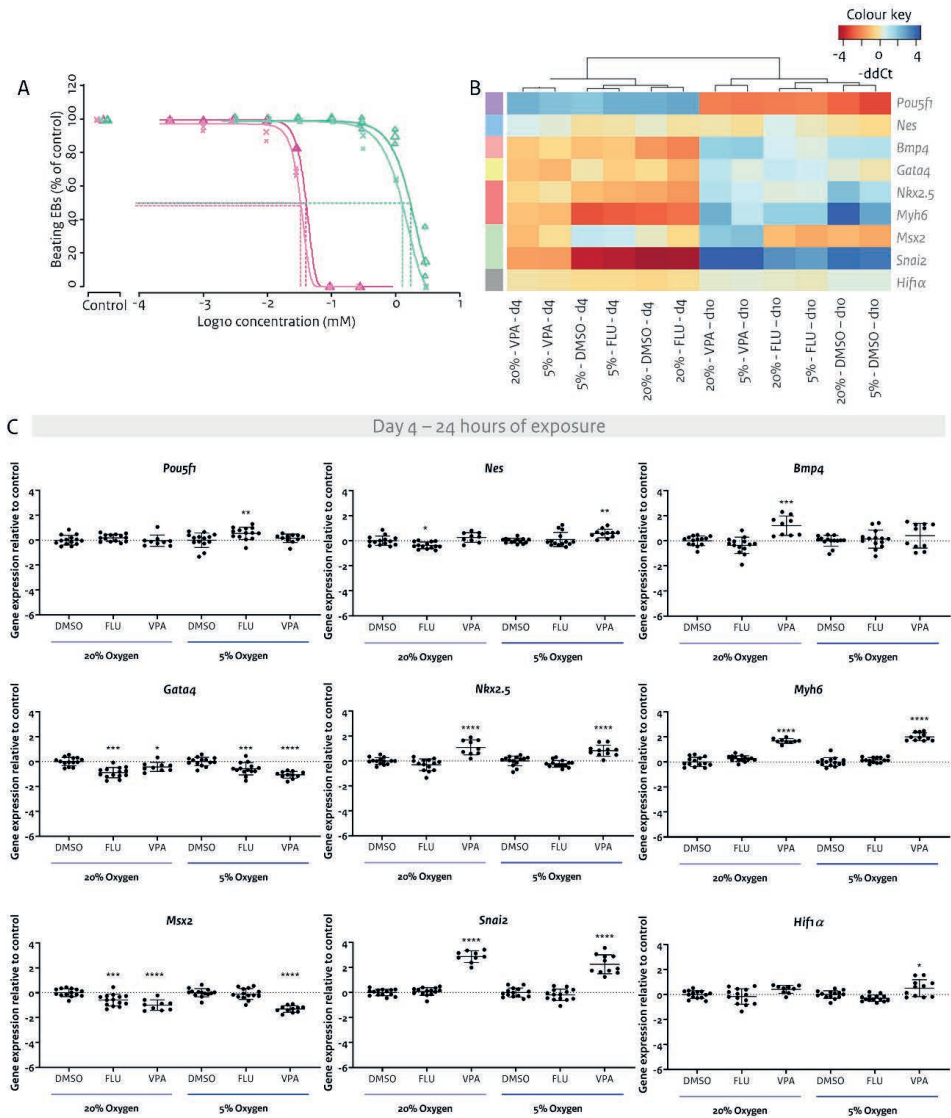
3d). The pluripotency marker *Pou5f1/Oct4* was statistically significantly regulated by FLU and VPA when ESCs had been cultured under 5% O₂ tension only. The cardiomyocyte differentiation markers (*Nkx2.5, Myh6*) were statistically significantly regulated by exposure to FLU when ESCs had been cultured under 20% O₂ but not when cultured under 5% O₂ tension. The epithelial-to-mesenchymal transition (EMT) marker for neural crest cell differentiation (*Snai2*) was statistically significantly regulated by VPA when ESCs had been cultured under 5% O₂ tension only. *Hif1a* was significantly regulated by FLU and VPA when ESCs had been cultured under 20% O₂ tension. When ESCs had been cultured under 5% O₂ tension, only FLU significantly regulated *Hif1a*.

Discussion

Culturing ESCs under 5% O₂ tension instead of 20%, affected the sensitivity to compound exposure. Furthermore, the use of undifferentiated ESCs cultured under 5% versus 20% O₂ prior to the ESTc differentiation assay, influenced the ESTc sensitivity to VPA and FLU as shown by statistically significant differences in both gene expression and in the ID₅₀ levels for cardiomyocyte differentiation. On differentiation day 4 in the ESTc, gene expression was affected by O₂ tension during ESC culture rather than by compound exposure in the ESTc as indicated by heatmap clustering. The opposite was found on differentiation day 10 as shown by gene expression levels clustered per compound rather than by previous ESC O₂ status. The O₂ tension during ESC culture caused differences in exposure effects and can be explained by the state of the pluripotent ESCs generated under 5% versus 20% O₂ tensions.

The lack of electron transfer to O₂ under low O₂ levels increases the production of reactive oxygen species (ROS) [11]. The production of ROS stimulates the activity of e.g. HIF, which interferes with differentiation [11, 29-34]. HIF1 α is regulated by histone deacetylase (HDAC) [11, 29-34], which epigenetically regulates various gene expression levels. In the heatmap results, different ESC O₂ culture conditions prior to the ESTc did not result in differences in *Hif1a* expression levels in the unexposed ESTc. This lack of differences is probably due to the fact that the ESTc was in each case performed under 20% O₂ tension. Therefore, effects of O₂ level during ESC culture were possibly already diminished at the time of gene expression assessment in the ESTc. Nonetheless, we did see differences in expression levels

of differentiation markers in the ESTc in controls dependent on O₂ preconditioning in ESCs. This shows that O₂ levels during ESC culture influence their subsequent differentiation in the ESTc.



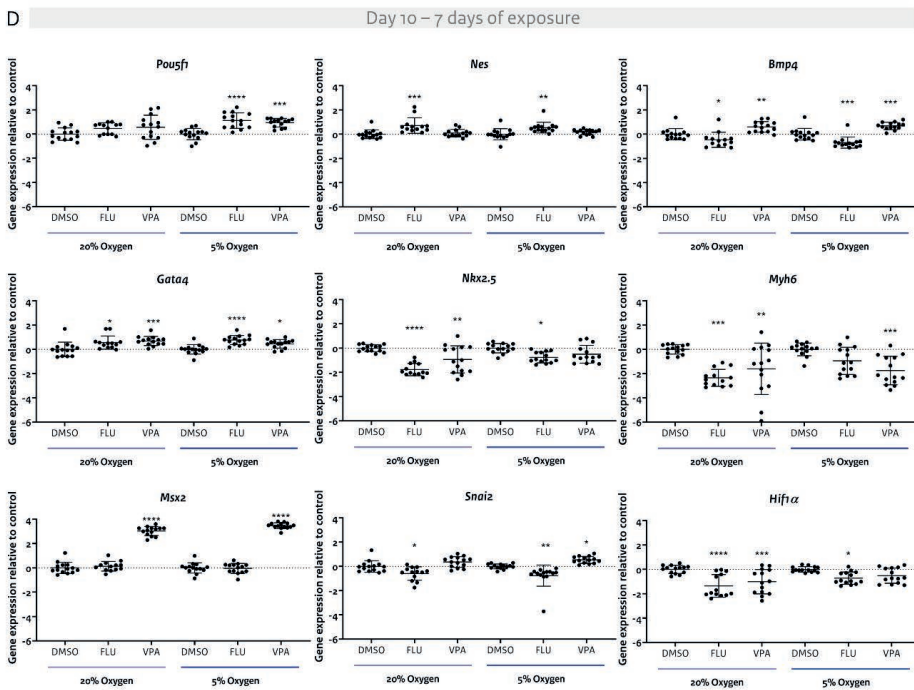


Figure 3: Chemical sensitivity in the ESTc in 20% O₂ tension after ESC were cultured under 20% versus 5% O₂ tension. A) Cardiomyocyte differentiation inhibition dose-response curves for FLU and VPA. Dotted lines indicate ID₅₀ concentrations in the ESTc, which were used for gene expression analysis. B) Heatmap representing gene expression levels relative to the average of all samples. Colour bar at the left indicates specificity of the tested genes for pluripotency (purple), ectoderm (blue), mesoderm (soft red), endoderm (yellow), cardiomyocyte differentiation (red), neural crest cell differentiation (green), and hypoxia inducible factor α (grey). Colour key indicates the level of gene expression per condition expressed as -ddCt. C) Gene expression levels relative to the DMSO control per O₂ condition at differentiation day 4. D) Gene expression levels relative to the DMSO control per O₂ condition at differentiation day 10. Error bars indicate standard deviation. N=2 with in total 13-14 samples. Asterisks indicate a statistically significant difference compared to the O₂ matched DMSO control (one-way ANOVA; Sidak's multiple comparisons post-hoc test). * p < 0.05, ** p < 0.01, *** p < 0.001, **** p < 0.0001.

Heatmap clustering showed an increase in *Bmp4* expression on differentiation day 4, an early differentiation marker indicative of a relative stimulation towards the mesodermal lineage, when ESCs had been cultured under 5% O₂ instead of 20% prior to the ESTc. Low O₂ tension stimulates HIF1 α overexpression and affects energy metabolism by stimulating pyruvate dehydrogenase kinase 1 (PDK1), which inhibits pyruvate dehydrogenase (PDH) from entering pyruvate in the citric acid

cycle resulting in lactate production and a lower mitochondrial O_2 consumption [34]. Pyruvate stimulates ESCs towards endodermal and mesodermal differentiation [35]. The stimulation towards the mesodermal lineage can therefore be explained by the O_2 dependent metabolic state causing a slowed citric acid cycle followed by pyruvate production. To explain this in more detail, pluripotent cells vary in gene expression patterns as described by Weinberger et al. as 'relative naivety' and consist of a gradient in cellular phenotypes [36]. These phenotypes differ in molecular and functional characteristics, but also in energy metabolism which likely plays an important part in differentiation [37]. Therefore, the ESC culture conditions in this study may steer the cells towards a certain metabolic preference because of O_2 availability that consequently influences cell characteristics and therefore the relative naivety and ESTc sensitivity [37]. Low O_2 levels alter mitochondrial activity by lowering ATP production which consequently causes a slowed citric acid cycle, meaning that glucose is transformed into pyruvic or lactic acid [11]. This elevated pyruvate explains the stimulation of mesodermal differentiation when ESCs had been cultured under 5% O_2 levels instead of 20% prior to the ESTc.

VPA stimulated cell commitment towards the ectodermal lineage in the ESTc when ESCs had been cultured under 5% O_2 tension prior to the ESTc. Also previous literature reported stimulation by VPA towards the ectodermal derived neuronal lineage, although when ESCs had been cultured under atmospheric O_2 levels [38]. The HDAC inhibitor VPA decreased HIF1 α protein levels under low O_2 conditions in murine ESCs and in human and mouse tumour cell lines after 24 hours of exposure [39, 40]. In those studies, VPA caused an upregulation of *Hif1a* in the ESTc after 24 hours of exposure. This difference could be explained by the fact that whereas we also performed the ESTc under 20% O_2 conditions, the preceding ESC culture was performed under 5% O_2 conditions. The *Hif1a* gene expression regulations by both VPA and FLU observed in our results, showed the same pattern as the regulations compared to the early cardiomyocyte marker *Nkx2-5*. HIF1 α deletion in ESCs resulted in an inhibition in cardiomyocyte differentiation [32, 33], which provides a mechanistic explanation of the common pattern of gene expression regulation of these two genes.

At differentiation day 4, gene expression levels were more affected by VPA exposure instead of O_2 tension during ESC culture prior to the ESTc as seen by the way how expression levels clustered (fig. 3b). *Bmp4* as an early differentiation marker for mesoderm was differently affected by VPA exposure when comparing the ESCs

O₂ conditions as opposed to the later differentiation markers *Nkx2-5* and *Myh6* which were to a lesser extent affected by the ESC O₂ tension preceding the ESTc on differentiation day 4. On differentiation day 10, *Nkx2-5* as an early cardiomyocyte differentiation marker was differently affected after VPA exposure when comparing the ESC O₂ conditions. These differences in compound exposure effects by the ESC O₂ conditions on early versus late differentiation markers seem to depend on the time-point of gene expression measurement. Overall, differentiation effects were more pronounced on differentiation day 4 because this time-point is closer to the preceding ESC culture compared to differentiation day 10.

FLU exposure in PC12 (rat dopaminergic pheochromocytoma cells) and MA-10 cells (murine Leydig tumour cell line) increased oxidative stress and ROS production under atmospheric O₂ tension [41, 42]. On differentiation day 10 in the ESTc, statistically significant gene expression effects of FLU were visible when ESCs had been cultured under 20% O₂ but not 5% O₂. When ESCs had been cultured under 5% O₂ tension instead of 20%, lower levels of cardiomyocyte markers were expressed in controls on differentiation day 10 (see heatmap, fig. 3b). When FLU causes an additional repression of these markers, the relative effect will be more clear in the conditions where control expression levels were highest, namely when ESCs had been cultured under 20% O₂ tension. Inhibition of cardiomyocyte differentiation by FLU has been observed in the ESTc under atmospheric O₂ conditions [43, 44]. A common explanation for effects caused by 5% O₂ ESCs culture before use in the ESTc and FLU exposure within the ESTc, could be because of ROS production, consequently influencing differentiation. Reliant on the state of development, ROS will stimulate or suppress cardiac maturation [45]. In a differentiation test using mouse ESCs, β-mercaptoethanol (an antioxidant) deprived culture medium resulted in elevated ROS levels and caused a reduction in cell growth and an improved cardiac differentiation [46]. In our study, we used β-mercaptoethanol in the culture medium, which possibly obstructs ROS production caused by both a low O₂ tension and FLU exposure. Therefore, it is unlikely that the observed differences are dependent on ROS. The differences in significant effects by FLU exposure most probably depend on the initial expression levels in controls, when comparing FLU exposure effects after ESCs had been cultured under 5% O₂ tension compared to 20% O₂ tension.

Whereas the effects on beating cardiomyocyte development showed lower ID₅₀ levels for both compounds when ESCs had been cultured under 5% O₂ instead

of 20%, the viability tests on ESCs resulted in IC_{50} levels that were lower (VPA) or higher (FLU) when performed under 5% O_2 tension instead of 20%. There is an important difference in O_2 conditions between the viability test using ESCs and the ESTc differentiation test. ESCs were exposed to the chemicals simultaneously with one of the two O_2 conditions during viability testing, whereas in the ESTc, cells were always exposed to the chemicals under atmospheric O_2 tension. Therefore, the differences in IC_{50} levels in the viability tests may be explained by the O_2 tension changing the (re)activity of the chemical (e.g. like in anti-cancer drug research) [9, 10, 12]. Although not explicitly found in literature for FLU, this may explain the relative difference in sensitivity between the viability test and the ESTc. Although the ID_{50} and IC_{50} levels were influenced by the O_2 level in our study, this does not necessarily change the predictivity of the standard EST as has been described by *Genschow et al.*, which divides potential hazardous compounds into categories [25]. In our study the basic O_2 levels in culture show effects on mechanistic details of differentiation and consequently on gene expression changes induced by VPA and FLU.

In summary, this study shows that O_2 concentration in ESC culture has a lasting effect upon the response of these cells to compound exposure in the subsequent ESTc. Also, undifferentiated ESC maintenance is optimal in 5% O_2 whereas functional cardiomyocyte differentiation in the ESTc benefits from 20% O_2 conditions [20], both similar to the *in vivo* situation in embryo development. Additional studies are needed to further finetune culture conditions towards mimicking *in vivo* cellular microenvironments in embryogenesis, and assessing their impact on effects of a wider array of compounds, to improve relevancy of *in vitro* test readouts. Realistic and relevant outcomes of individual *in vitro* assays are crucially important, as they affect the broader perspective of test batteries and integrated approaches to testing and assessment (IATA) and may ultimately impact quantitative risk assessment. Finetuning assay protocols to mimic physiological conditions is therefore advisable and should include consideration of the oxygenation schedule.

Acknowledgements

Gina Mennen was supported by the French National Association for Research and Technology (ANRT) through a CIFRE PhD grant no. 2018-0682, which was co-supervised by Aldert Piersma, Nina Hallmark, Marc Pallardy, Remi Bars, and Helen

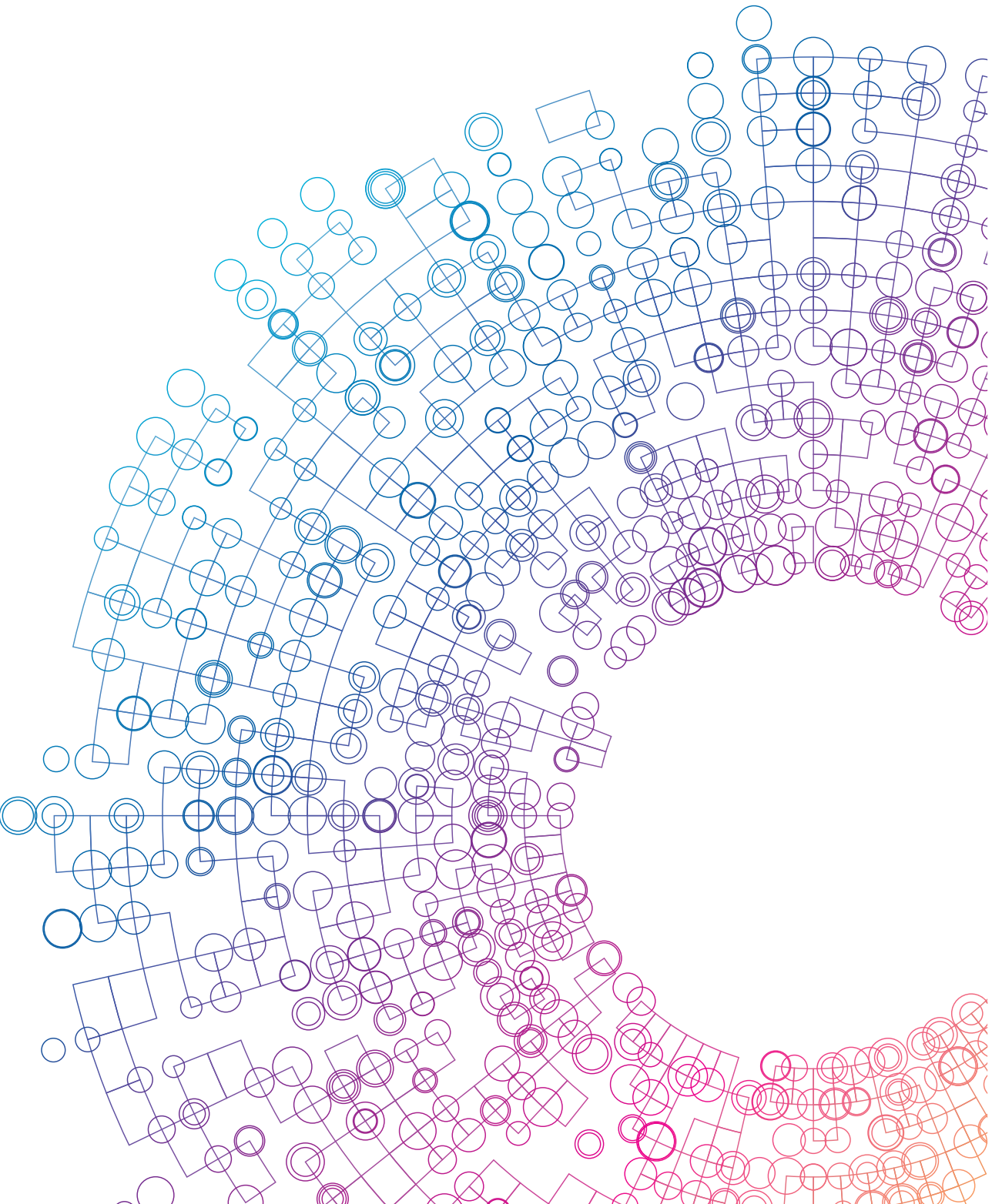
Tinwell. Victoria de Leeuw was funded by the Dutch NGO *Stichting Proefdiervrij* and the Dutch Ministry of Agriculture, Nature and Food Quality. Aldert Piersma was funded by the Dutch Ministry of Health, Welfare and Sports. We would like to thank Anne Kienhuis for a critical review of the manuscript.

References

1. Rodesch, F., et al., *Oxygen measurements in endometrial and trophoblastic tissues during early pregnancy*. *Obstet Gynecol*, 1992. **80**(2): p. 283-5.
2. Burton, G.J., A.L. Jauniaux E Fau - Watson, and A.L. Watson, *Maternal arterial connections to the placental intervillous space during the first trimester of human pregnancy: the Boyd collection revisited*. 2001(0002-9378 (Print)).
3. Burr, S., et al., *Oxygen gradients can determine epigenetic asymmetry and cellular differentiation via differential regulation of Tet activity in embryonic stem cells*. *Nucleic Acids Res*, 2018. **46**(3): p. 1210-1226.
4. Panchision, D.M., *The role of oxygen in regulating neural stem cells in development and disease*. *J Cell Physiol*, 2009. **220**(3): p. 562-8.
5. Kasterstein, E., et al., *The effect of two distinct levels of oxygen concentration on embryo development in a sibling oocyte study*. *Journal of Assisted Reproduction and Genetics*, 2013. **30**(8): p. 1073-1079.
6. Sharma, A., et al., *Hypoxia-targeted drug delivery*. *Chem Soc Rev*, 2019. **48**(3): p. 771-813.
7. Hunter, F.W., B.G. Wouters, and W.R. Wilson, *Hypoxia-activated prodrugs: paths forward in the era of personalised medicine*. *British Journal of Cancer*, 2016. **114**(10): p. 1071-1077.
8. Baran, N. and M. Konopleva, *Molecular Pathways: Hypoxia-Activated Prodrugs in Cancer Therapy*. *Clin Cancer Res*, 2017. **23**(10): p. 2382-2390.
9. Villeneuve, L., et al., *Quantitative proteomics reveals oxygen-dependent changes in neuronal mitochondria affecting function and sensitivity to rotenone*. *J Proteome Res*, 2013. **12**(10): p. 4599-606.
10. Kumar, A., et al., *Quantifying the magnitude of the oxygen artefact inherent in culturing airway cells under atmospheric oxygen versus physiological levels*. *FEBS Lett*, 2016. **590**(2): p. 258-69.
11. Simon, M.C. and B. Keith, *The role of oxygen availability in embryonic development and stem cell function*. *Nat Rev Mol Cell Biol*, 2008. **9**(4): p. 285-96.
12. Koutsouraki, E., S. Pells, and P.A. De Sousa, *Sufficiency of hypoxia-inducible 2-oxoglutarate dioxygenases to block chemical oxidative stress-induced differentiation of human embryonic stem cells*. *Stem Cell Res*, 2019. **34**: p. 101358.
13. Gustafsson, M.V., et al., *Hypoxia requires notch signaling to maintain the undifferentiated cell state*. *Dev Cell*, 2005. **9**(5): p. 617-28.
14. Forristal, C.E., et al., *Hypoxia inducible factors regulate pluripotency and proliferation in human embryonic stem cells cultured at reduced oxygen tensions*. *Reproduction*, 2010. **139**(1): p. 85-97.
15. Ezashi, T., P. Das, and R.M. Roberts, *Low O2 tensions and the prevention of differentiation of hES cells*. *Proc Natl Acad Sci U S A*, 2005. **102**(13): p. 4783-8.
16. Medley, T.L., et al., *Effect of oxygen on cardiac differentiation in mouse iPS cells: role of hypoxia inducible factor-1 and Wnt/beta-catenin signaling*. *PLoS One*, 2013. **8**(11): p. e80280.
17. Ramirez, M.A., et al., *Effect of long-term culture of mouse embryonic stem cells under low oxygen concentration as well as on glycosaminoglycan hyaluronan on cell proliferation and differentiation*. *Cell Prolif*, 2011. **44**(1): p. 75-85.

18. Brodarac, A., et al., *Susceptibility of murine induced pluripotent stem cell-derived cardiomyocytes to hypoxia and nutrient deprivation*. *Stem Cell Res Ther*, 2015. **6**(1): p. 83.
19. Huang, C.Y., et al., *Differentiation of embryonic stem cells into cardiomyocytes used to investigate the cardioprotective effect of salvianolic acid B through BNIP3 involved pathway*. *Cell Transplant*, 2015. **24**(3): p. 561-71.
20. Mennen, R.H., V.C. de Leeuw, and A.H. Piersma, *Oxygen tension influences embryonic stem cell maintenance and has lineage specific effects on neural and cardiac differentiation*. *Differentiation*, 2020. **115**: p. 1-10.
21. Mennen, R.H.G., J.L.A.J. Pennings, and A.H.A. Piersma, *Neural crest related gene transcript regulation by valproic acid analogues in the cardiac embryonic stem cell test*. *Reproductive toxicology* (Elmsford, N.Y.), 2019. **90**: p. 44-52.
22. Spielmann, H., et al., *The Embryonic Stem Cell Test, an In Vitro Embryotoxicity Test Using Two Permanent Mouse Cell Lines: 3T3 Fibroblasts and Embryonic Stem Cells*. *In Vitro Toxicology*, 1997. **10**: p. 119-127.
23. de Jong, E., et al., *Potency ranking of valproic acid analogues as to inhibition of cardiac differentiation of embryonic stem cells in comparison to their in vivo embryotoxicity*. *Reprod Toxicol*, 2011. **31**(4): p. 375-82.
24. *CellTiter-Blue Cell Viability Assay technical bulletin #TB317*. Promega Corporation.
25. Genschow, E., et al., *Validation of the embryonic stem cell test in the international ECVAM validation study on three in vitro embryotoxicity tests*. *Altern Lab Anim*, 2004. **32**(3): p. 209-44.
26. Pfaffl, M.W., *A new mathematical model for relative quantification in real-time RT-PCR*. *Nucleic Acids Res*, 2001. **29**(9): p. e45.
27. Slob, W., *Dose-response modeling of continuous endpoints*. *Toxicol Sci*, 2002. **66**(2): p. 298-312.
28. Team, R.C., *R: A Language and Environment for Statistical Computing (Version 3.5.2, R Foundation for Statistical Computing, Vienna, Austria, 2018)*. There is no corresponding record for this reference.[Google Scholar], 2019.
29. Zhao, Y., et al., *Dual functions of hypoxia-inducible factor 1 alpha for the commitment of mouse embryonic stem cells toward a neural lineage*. *Stem Cells Dev*, 2014. **23**(18): p. 2143-55.
30. Xie, Y., et al., *Defining the role of oxygen tension in human neural progenitor fate*. *Stem Cell Reports*, 2014. **3**(5): p. 743-57.
31. Mohyeldin, A., T. Garzon-Muvdi, and A. Quinones-Hinojosa, *Oxygen in stem cell biology: a critical component of the stem cell niche*. *Cell Stem Cell*, 2010. **7**(2): p. 150-61.
32. Ateghang, B., et al., *Regulation of cardiotrophin-1 expression in mouse embryonic stem cells by HIF-1alpha and intracellular reactive oxygen species*. *J Cell Sci*, 2006. **119**(Pt 6): p. 1043-52.
33. Kudova, J., et al., *HIF-1alpha Deficiency Attenuates the Cardiomyogenesis of Mouse Embryonic Stem Cells*. *PLoS One*, 2016. **11**(6): p. e0158358.
34. Heo, H.J., et al., *Mitochondrial pyruvate dehydrogenase phosphatase 1 regulates the early differentiation of cardiomyocytes from mouse embryonic stem cells*. *Exp Mol Med*, 2016. **48**(8): p. e254.

35. Song, C., et al., *Elevated Exogenous Pyruvate Potentiates Mesodermal Differentiation through Metabolic Modulation and AMPK/mTOR Pathway in Human Embryonic Stem Cells*. Stem Cell Reports, 2019. **13**(2): p. 338-351.
36. Weinberger, L., et al., *Dynamic stem cell states: naive to primed pluripotency in rodents and humans*. Nat Rev Mol Cell Biol, 2016. **17**(3): p. 155-69.
37. Tsogtbaatar, E., et al., *Energy Metabolism Regulates Stem Cell Pluripotency*. Front Cell Dev Biol, 2020. **8**: p. 87.
38. Theunissen, P.T., et al., *Complementary Detection of Embryotoxic Properties of Substances in the Neural and Cardiac Embryonic Stem Cell Tests*. Toxicological Sciences, 2012. **132**(1): p. 118-130.
39. Lee, H.J. and K.W. Kim, *Suppression of HIF-1 α by Valproic Acid Sustains Self-Renewal of Mouse Embryonic Stem Cells under Hypoxia In Vitro*. Biomol Ther (Seoul), 2012. **20**(3): p. 280-5.
40. Kim, S.H., et al., *Regulation of the HIF-1 α stability by histone deacetylases*. Oncol Rep, 2007. **17**(3): p. 647-51.
41. Heusinkveld, H.J., et al., *Azole fungicides disturb intracellular Ca²⁺ in an additive manner in dopaminergic PC12 cells*. Toxicol Sci, 2013. **134**(2): p. 374-81.
42. Roelofs, M.J.E., et al., *Conazole fungicides inhibit Leydig cell testosterone secretion and androgen receptor activation in vitro*. Toxicol Rep, 2014. **1**: p. 271-283.
43. Dimopoulou, M., et al., *A comparison of the embryonic stem cell test and whole embryo culture assay combined with the BeWo placental passage model for predicting the embryotoxicity of azoles*. Toxicol Lett, 2018. **286**: p. 10-21.
44. van Dartel, D.A., et al., *Concentration-dependent gene expression responses to flusilazole in embryonic stem cell differentiation cultures*. Toxicol Appl Pharmacol, 2011. **251**(2): p. 110-8.
45. Momtahan, N., C.O. Crosby, and J. Zoldan, *The Role of Reactive Oxygen Species in In Vitro Cardiac Maturation*. Trends in Molecular Medicine, 2019. **25**(6): p. 482-493.
46. Tu, C., et al., *Commonly used thiol-containing antioxidants reduce cardiac differentiation and alter gene expression ratios of sarcomeric isoforms*. Experimental Cell Research, 2018. **370**(1): p. 150-159.



CHAPTER

Endoderm and mesoderm
derivatives in embryonic stem
cell differentiation and their
use in developmental toxicity
testing

R.H. Mennen, M.M. Oldenburger, A.H. Piersma

Reproductive Toxicology. 2021 Nov 30; 107: 44-59.

DOI: 10.1016/j.reprotox.2021.11.009

Abstract

Embryonic stem cell differentiation models have increasingly been applied in non-animal test systems for developmental toxicity. After the initial focus on cardiac differentiation, attention has also included an array of neuro-ectodermal differentiation routes. Alternative differentiation routes in the mesodermal and endodermal germ lines have received less attention. This review provides an inventory of achievements in the latter areas of embryonic stem cell differentiation, with a view to possibilities for their use in non-animal test systems in developmental toxicology. This includes murine and human stem cell differentiation models, and also gains information from the field of stem cell use in regenerative medicine. Endodermal stem cell derivatives produced *in vitro* include hepatocytes, pancreatic cells, lung epithelium, and intestinal epithelium, and mesodermal derivatives include cardiac muscle, osteogenic, vascular and hemopoietic cells. This inventory provides an overview of studies on the different cell types together with biomarkers and culture conditions that stimulate these differentiation routes from embryonic stem cells. These models may be used to expand the spectrum of embryonic stem cell based new approach methodologies in non-animal developmental toxicity testing.

Introduction

New approach methodologies (NAMs) are increasingly being employed in chemical safety testing. They may reduce animal use and provide detailed mechanistic information that may benefit human hazard and risk assessment. The field of regulatory developmental toxicology, which uses large amounts of animals, can benefit from stem cell differentiation models. These cells have the potential to differentiate into every cell type in the body. As compared to intact animals, stem cell models are simplistic models, yet can help us in understanding mechanisms of early embryonic development. Monitoring differentiation to multiple cell types may expand mechanistic knowledge as well as enhance prediction of developmental toxicity potential of tested chemicals.

The aim of this paper is to review differentiation routes that have been studied in murine, human embryonic and/or human induced pluripotent stem cell cultures *in vitro* that could be of use in specifying heterogenous cell populations. Molecular markers and inducers for these differentiation routes may add to the detailed monitoring of compound effects on embryonic cell differentiation. Neuroectodermal cell differentiation is being studied in great detail already, given the importance of various neural-related cell types for proper central nervous system functioning [1-3]. Therefore for the present review we chose to focus on endodermal and mesodermal differentiation routes and a selection of their derivatives. For this we also included information obtained from regenerative medicine studies using differentiating stem cells. Search terms that were used in PubMed contained “murine” or “human”, “embryonic stem cells” or “induced pluripotent stem cells” in combination with variations of “developmental toxicity”, “endoderm differentiation”, “mesoderm differentiation” or a specific cell type of interest. No restriction as to year of publication was applied. All articles were individually assessed for quality and relevance by expert judgment. This literature search provides an overview of possible differentiation routes, which may not be complete, but gives examples that contribute to possibilities to monitor the development of additional cell types in heterogenic and therefore complex cell systems.

Toxicological stem cell models

After murine embryonic stem cell (mESC) models were firstly established also human stem cell models were developed. The idea arose that human instead of

murine test systems would be more applicable to the human biology, yet this is subject to discussion [4]. Therefore, we here discriminate and compare between murine and human differentiation models. This chapter briefly reviews those models already used in toxicology.

Murine stem cell differentiation models used in toxicology

The murine cardiac embryonic stem cell test (mESTc) provides an *in vitro* model to test for general embryotoxicity looking at cardiac differentiation and cytotoxicity. This is the only formally validated *in vitro* test using mESC for developmental toxicology [5]. Within this test, spontaneous differentiation of beating cardiomyocytes occurs [6]. Teratogens can cause an inhibition of cardiomyocyte differentiation in the mESTc. After its formal validation, additional assessments followed about the applicability domain of this test [7-9]. Although this is the only validated mESC test for developmental toxicology, other endpoints have also been investigated.

As an example, *Zur Nieden and Baumgartner* used an mEST in which effects of compounds on osteoblast differentiation can be assessed [10]. A different protocol for this differentiation route was established by *De Jong et al.*, called the osteogenic embryonic stem cell test (mESTo) [11]. *De Jong et al.* investigated the effects of compounds on gene expression as well as on calcium concentration within their cell population [11, 12]. The mESTo did replicate the known adverse effects of TCDD on osteogenesis, whilst the mESTc was negative, suggesting that the mESTo has added value when applied in parallel to the mESTc [12].

In addition, the applicability of mESC derived neural cells to predict neurodevelopmental toxicity of compounds has been studied extensively in the neural mEST (mESTn) [3, 13]. Their cell cultures mostly consisted of neuroectodermal cell lineages, whereas mesodermal and endodermal lineages were present to a lesser extent. Such neural differentiation protocols have further been characterised [14, 15], but also other approaches have been tested like reporter assays [16].

Human stem cell models and induced pluripotent stem cells used in toxicology

Test methods using human stem cells have not been formally validated yet. *Kugler et al.* and *Luz and Tokar* gave a summary of available *in vitro* developmental toxicity screens including human derived cells [4, 17]. These listed human methods mainly

described metabolomics as assay output with the advantage that different modes of action can be detected [4, 18-20]. However, in these models differentiation routes (of susceptible cell types) were not assessed. *Kameoka et al.* proposed a high-throughput screen by imaging cells with characteristics of the three germ layers: the endoderm, mesoderm, and ectoderm [21], which was a first start of assessing multiple differentiation routes for chemical perturbations towards specific cell type differentiation. Also neural differentiation routes, originating from the ectoderm, have been studied in great detail already [1-3]. In the following chapters, we will focus on the inducers and biomarkers of mesoderm and endoderm and a selection of their derivatives, which have so far received less attention in a developmental toxicity testing context.

Endoderm differentiation and derivatives

The late blastocyst contains three cell types: the trophectoderm, the epiblast and the primitive endoderm [22]. The primitive endoderm gives rise to the visceral and parietal endoderm. The visceral endoderm plays a role in the development of the visceral yolk sac, whereas the parietal endoderm forms the parietal yolk sac. The latter one provides protection to the embryo against mechanical damage and regulates the uptake of nutrients important for the development. These tissues also assist the progress of embryo-maternal interactions. From the epiblast, the definitive endoderm (DE) is derived [22]. The definitive endoderm gives rise to the gastrointestinal tract, the lungs, hepatocytes and pancreatic cells [23].

To differentiate ESC into cells of the gastrointestinal tract, lungs, urinary tract or pancreas, ESC must first differentiate into DE. The various ways of inducing DE and derivative differentiation as well as the biomarkers used to identify differentiated cell types, will be discussed and compared for ESC or iPSCs of mouse and human origin, as summarized in Table 1-4.

Endoderm

To specify the differentiation of DE, biomarkers like SOX17, FOXA2, and CXCR4 were most commonly used in both mouse and human endodermal differentiation (Table 1). Other endodermal markers that were both employed in mouse and human cells were GATA4, GATA6, alpha fetoprotein (AFP), and gooseoid (GSC). *Zhong et al.* also studied the expression of the transmembrane 4 superfamily 2 (*Tm4sf2*) gene

as an endoderm marker [24]. AFP is widely used as a general endodermal marker (Table 1), but also to specify hepatic endoderm and hepatocyte progenitors (Table 2).

A well-known inducer of the DE is Activin A, which plays a role in the nodal signalling pathway important in endoderm differentiation [24]. *Zhong et al.* investigated the signalling pathways of Wnt and Nodal in connection with DE differentiation and treated ESC with Activin A and WNT3A, which resulted in a more optimized DE differentiation than treatment with Activin A alone. This was similar to the synergistic effect of hypoxia in combination with Activin A on DE differentiation, described by *Pimton et al.* [25]. In mESC differentiation to DE, different inducers apart from Activin A induction have been tested. *Kim et al.* described a way to differentiate mESC into DE in a monolayer, using all-*trans*-retinoic acid (ATRA) and dibutyryl cyclic-AMP (DBcAMP) [26]. *Kaitsuka et al.* initiated the differentiation of mESC into DE using erythropoietin (EPO), which activated ERK signalling and thereby triggered the differentiation into DE [27]. ERK signalling induces the pluripotent cells from a self-renewal state into a state of differentiation.

DE differentiation by Activin A induction is also a standard method in hESC, and has been applied in combination with multiple other inducers to improve DE differentiation efficiency. The addition of WNT3A has been popular in multiple protocols up to the year 2015 (Table 1). Afterwards, WNT3A has no longer been used for human endodermal differentiation, and inducers as B27 or BMP4 were used more frequently. Interestingly, B27 is also sold as a supplement to stimulate neuronal cell culture (Thermo Fisher Scientific). Other constituents have been tested as well, like different inhibitors of e.g. GSK3 β (CHIR99021) or PI3K (Ly294002, PI-103). Also, DE differentiation from iPSC required Activin A as one of the basic inducers together with at least one of the inducers B27, BMP4, or WNT3A (from most used to least used). In addition, inhibitors for GSK3 β and PI3K have been used as DE inducers in some studies, as well as FGF2. Inducers of mESC that were not used in human embryonic stem cells (hESC) were DMSO, penicillin/streptomycin, and sodium pyruvate. Interestingly, DE stimulation by Activin A was tested in iPSC cells against the same medium composition excluding Activin A as a negative control [28]. The lack of Activin A resulted in no observed differences in SOX17 and FOXA2 expression levels, whereas the use of Activin A did enhance expression of these endodermal markers. This underlines the importance of Activin A in directed endodermal differentiation.

The comparison of DE differentiation between mESC and hESC revealed conserved mechanisms of action. *Daneshvar et al.* studied DE differentiation of both hESC and mESC using Activin A and identified the long non-coding RNA *DIGIT* as a key regulator of both human and mouse DE differentiation [29]. Also *Chen et al.* compared mESC and hESC studying hyperglycemic treatments, which downregulated DE differentiation in both mESC and hESC through histone methylation modifications [30]. Whereas DE differentiation per se seemed to be regulated in the same way in mESC and hESC, differentiation of DE to DE derivatives may not always share mechanisms between species. *Wang et al.* studied DE derivatives and showed that the primitive gut cell surface markers CD238, CD141, and CD49e were not induced in mESC derived endoderm after primitive gut differentiation stimulation, while they were detected in hESC [31].

Human DE differentiation efficiencies may be different between cell lines of hESC and hiPSC origin. *Jiang et al.* observed a low DE differentiation efficiency of about 15% for hiPSC (JT16) cells, whereas the hESC DE differentiation efficiency rates ranged from 10% (H7-E8), 20% (H9.2), 25% (HES3), and 45% (MEL-1) [32]. In a protocol using mesendogen in combination with the growth factors Activin A and WNT3A, *Geng and Feng* observed an efficiency of 89.41% (hiPSC) and 94.9% (hESC) through SOX17 and FOXA2 expression using FACS analysis [33]. *Jacobson et al.* also assessed SOX17 and FOXA2 using FACS for DE differentiation efficiency, which resulted in efficiencies of 87.5 \pm 8.8 % and 80.2 \pm 9.2 %, for hESC and hiPSC respectively [34]. *Eldridge et al.* only assessed the level of SOX17 positive cells and reported an efficiency of near 80% for both hiPSC and hESC [35]. These data showed that in general the DE differentiation efficiencies within each experiment are similar between hESC and hiPSC.

Table 1: from pluripotent stem cells to endoderm

literature	Cell model	Endpoint	Used markers	Inducers
[36]	mESC, miPSC	Endoderm	GATA6, AFP, SOX17, FOXA2, GATA4	Aggregation of cells in mESC medium without LIF
[26]	mESC	Definitive endoderm	<i>Sox17, Foxa2</i>	All-trans-retinoic acid, dibutyryl cyclic-AMP
[25]	mESC	Definitive endoderm	<i>Sox17, Foxa2, Cxcr4</i>	Hypoxia and Activin A
[24]	mESC	Definitive endoderm	<i>Sox17, Foxa2, Cxcr4, Gsc, Tm4sf2</i>	Activin A, WNT3A
[27]	mESC	Definitive endoderm	<i>Sox17, Foxa2</i>	Erythropoietin (EPO)
[37]	hESC (ReliCellhES1)	Germ layers	AFP, FOXA2, ALB	DMEM/F12, FBS, serum replacement NEAA, glutamine, b-mercaptoethanol, penstrep. Without β FGF
[38]	hESC (H9)	Germ layers	CXCR4+ KDR-	Activin A
[39]	hESC (H9)	Germ layers	SOX17	RPMI1640 with B27, Activin A
[40]	hESC (BG01V)	Germ layers	FOXA2, AFP, GLUC, GATA6, GATA4, SOX7, SOX17, APOA1, APOA4, COL4A2, FOXQ1, LAMB1.	α MEM spontaneous differentiation EBs
[41]	hESC (H7)	Germ layers	GATA4, GATA6, SOX17	Knockout Serum Replacement (KSR), β FGF
[42]	hESC (H1)	Germ layers	CER1, GATA6, CXCR4, SOX17	Differentiation: mTeSR, Retinoic acid Definitive endoderm differentiation: STEMdiff Definitive Endoderm Differentiation Kit
[43]	hESC (HUES8, HES3)	Germ layers	FOXA2, SOX17, GSC	RPMI1640, Activin A, CHIR miR-489-3p and miR-1263
[21]	hESC (H9)	Mesoendoderm	SOX17	RPMI1640, Activin A, WNT3A, FBS
[44]	hESC (H1)	Mesoendoderm	SOX17, FOXA2	mTeSR1, Thiazovivin, doxycycline, puromycin
[45]	hESC (Mel1, H9)	Mesoendoderm	GSC, SOX17, CXCR4	STEMDIFF trilineage differentiation kit with ROCKi
[46]	hESC (CA1, CA2)	Endoderm progenitors	SOX17, CXCR4, CER, GSC, DLX5, KRT8, BMP2	BMP4 or Activin A

literature	Cell model	Endpoint	Used markers	Inducers
[47]	hESC (surplus from IVF)	Definitive Endoderm	SOX17	Activin A
[31]	hESC (hS17), mESC (R1)	Definitive endoderm	SOX17	Mouse: Wnt, Activin A, FGF(1 and 4)/Noggin or FGF(1 and 4)/Noggin/Retinoic acid Human: WNT3A, Activin A FGF(1 and 4)/Noggin or FGF(1 and 4)/Noggin/RA
[32]	hESC (HUES8, H7, H9, MEL1, HES3, NKX2-5-GFP) hiPSC (JT-16)	Definitive endoderm	SOX17, GATA6, FOXA2, GSC, CXCR4	DMEM/F12, B27 without vitamin A, N2, Activin A Or WNT3A, XAV939
[48]	hESC (H9)	Definitive endoderm	CXCR4, SOX17	RPMI, Activin A, WNT3A, Ly294002
[49]	hESC (Hues8, Hues4)	Definitive endoderm	SOX17, FOXA2, GATA3, GATA4, GATA6	WNT3A, Activin A, KGF, CHIR99021
[33]	hESC (H9 and H1), hiPSC (MMW2)	Definitive endoderm	SOX17, FOXA2	Activin A, WNT3A Variations: mesendogen or B27 or Insulin-Transferrin-Selenium
[50]	hESC (H1, H9)	Definitive endoderm	SOX17, FOXA2	RPMI 1640, B27, Activin A, Variations: LY294002 or Torin-2 or wortmannin
[29]	hESC H1), mESC (W4)	Definitive endoderm	FOXA2, SOX17, CXCR4	hESC: RPMI, B27, Activin A mESC: Advanced DMEM, Activin A
[51]	hESC (H9, H1, H7) iPSCs (derived from fibroblasts or EPCs)	Definitive endoderm	SOX17, FOXA2, GATA6	BMP4, Activin A, LDN193189
[35]	hESC (H9), hiPSC (BOBSC)	Germ layers	SOX17	Activin A, FGF2, BMP4, Ly294002, CHIR99021
[52]	hESC (H1)	Endoderm	GATA6, CXCR4, FOXA2, SOX17	RPMI with B27, Activin A, CHIR99021, PI-103, LDN193189
[53]	hESC (H1)	Endoderm and neurectoderm	SOX17, FOXA2, GSC, GATA4, GATA6	RPMI/B27, Activin A
[34]	hESC (H9) hiPSC (IMR90)	Definitive endoderm	FOXA2, SOX17, CXCR4, GSC	Activin A, CHIR99021, insulin, selenium, transferrin

literature	Cell model	Endpoint	Used markers	Inducers
[54]	hiPSC (201B7, 253G1, 409B2, DYR0100, HYR0103, mc-iPS, R-1A, R-2A, R-12A, Tic)	Germ layers	FOXA2, AFP	Spontaneous differentiation without addition of growth factors
[55]	hiPSC (from female peripheral blood mononuclear cells)	Germ layers	GATA6	mTesR1 with infection of HIF1a and Act16a. Screening with Puromycin and Blasticidin S
[56]	hiPSC (Tic)	Early endoderm	GATA4, GATA6, SOX17	ReproStem medium containing β FGF
[57]	hiPSC (not indicated)	Definitive endoderm	FOXA2, SOX17	RPMI1640, B27 (with or without insulin), Activin A, LY294002
[58]	hiPSC (derived from eye conjunctiva stromal cells)	Definitive endoderm	SOX17, FOXA2, GSC	Activin A, WNT3A, Or, IDE1
[59]	hiPSC (Tic, YOW, FCL)	Definitive endoderm	GATA4, GSC, SOX17, FOXA2	RPMI1640, Activin A, B27 without vitamin A
[28]	hiPSC (201B7, 253G1)	Definitive endoderm	SOX17, FOXA2, CXCR4	DMEM, DMSO, B27 with vitamin A, with or without Activin A
[60]	hiPSC (TkDN4-M, 454E2)	Definitive endoderm	SOX17, FOXA2	RPMI1640, Activin A, FGF2, BMP4, CHIR99021, KSR, penicillin and streptomycin, sodium pyruvate
[61]	hiPSC (ChiPSC12, AICS-0074-026)	Definitive endoderm	SOX17	STEMdiff Definitive Endoderm Kit
[62]	hiPSC (ChiPSC12, Y00285)	Definitive endoderm	Not assessed	Cellartis Definitive Endoderm Differentiation Kit
[63]	hiPSC (derived from 125 donors)	Endoderm	GATA6	CDM-PVA, Activin A, FGF2, BMP4, Ly294002, CHIR99201
[64]	hiPSC (ABPSC-HDFAIPS)	Endoderm	FOXA2	RPMI/B27, Activin
[65]	hiPSC (>70 lines) hESC (HUES8)	Endoderm	FOXA2, HNF1 β , CXCR4, SOX17	Activin A, KSR, CHIR99021, PI-103, BMP4, FGF2, Doxycycline hyclate_

Hepatocyte-like cells

The liver has a large regenerative capacity containing typical oval hepatocyte stem cells that have the ability to differentiate into multiple hepatic cell lineages when there is severe damage due to toxins [66, 67]. In some cases, for instance when liver failure occurs, the liver loses the capacity to regenerate. Therefore, much research has been done in the field of regenerative medicine by investigating stem cell differentiation into hepatocytes.

To mark successful hepatocyte differentiation, the biomarkers α -fetoprotein (AFP), albumin (ALB) and HNF4 α are most often used in both mouse and human differentiation protocols (Table 2). Other markers that are both used in mouse and human hepatocyte differentiation are glucose 6-phosphatase (G6PC), cytokeratin 18 (CK18) and transthyretin (TTR).

To induce the formation of hepatocytes in mESC, hepatocyte growth factor (HGF) was used in all mentioned protocols, as was BMP4. Various forms of fibroblast growth factor (FGF) were added to stimulate mESC towards hepatocyte-like cells. Additional stimulators that specified these cells were dexamethasone, oncostatin M, vascular endothelial growth factor (VEGF), and TGF α .

When comparing human hepatocyte inducers to these mouse inducers, BMP4 is rarely used to induce hepatocyte-like cell differentiation and the same holds true for HGF. More often DMSO is used, almost always in combination with a serum replacement and hydrocortisone-21-hemisuccinate. Among other additional factors and similar to mESC protocols, hESC protocols sporadically contained dexamethasone, various forms of FGF, or oncostatin M. For all studied hiPSC protocols for hepatocyte-like differentiation, HGF in combination with oncostatin M was used with additional stimulators varying from amongst others hydrocortisone-21-hemisuccinate, DMSO, dexamethasone, FGF10, BMP4.

Comparison experiments were done for hESC and hiPSC hepatocyte differentiation. Although no differentiation efficiencies were assessed, there were some similarities and differences in the differentiation process and functionality [68-71]. *Siller et al.* showed that all assessed human cell lines (ESC and iPSC), except for the hiPSC line CRL S23, differentiated into functional hepatocyte-like cells based on CYP3A4 activity, albumin production and secretion, and glycogen synthesis and storage [69]. Albumin was also examined by *Du et al.* and seemed to be slightly more

present in hESC as compared to hiPSC, however this was not quantified [71]. *Wruck and Adjaye* assessed hepatocyte differentiation on the transcriptomic level and concluded hepatocyte-like cells are very similar between hESC and hiPSC based on k-means-clusters. A difference was observed in the hepatic endoderm that showed a peak in hiPSC derived cells that was less clear in hESC cells [70].

Table 2: from endoderm to hepatocyte-like cells

literature	Cell model	Endpoint	Used markers	Inducers
[72]	mESC	Hepatocyte-like cells	<i>Alb, Cyp7a1, Aat, Ttr, G6p</i>	Sodium butyrate, β FGF, BMP4 Dexamethasone, oncostatin M, HGF
[73]	miPSC (iPS-MEF-Ng-20D-17), mESC (Balb/c \times 129sv)	Hepatocyte-like cells	Early-committed hepatocytes: AFP matured hepatocytes: ALB	Activin A, β FGF
[74]	mESC	Hepatocyte-like cells	Hepatic endoderm: <i>Afp, Ttr, Hnf4a, Foxa2, Sox17</i>	Hepatic endoderm: BMP4, FGF2 Hepatoblasts: FGF1, FGF4, FGF8B Hepatocytes: HGF
[75]	miPSC (ST5, ST8, Oct4-GFP, 2D4), mESC (129/Ola, C57BL/6)	Hepatocyte-like cells	AFP, ALB	SFD medium, MTG, Activin A, BMP4, β FGF, VEGF, FGF2, HGF, TGF α , dexamethasone
[76]	mESC	Hepatocyte-like cells	ALB, AFP, AAT, CK18, CYP7A1	Plasmid containing <i>Foxa2</i> as lentivector
[67]	mESC	Oval cells	SCA-1, CD34, A6	EGF, HGF
[77]	hESC (NTU1, NTU2, and NTU3), primate ESC (ORMES-5 and ORMES-6)	Hepatocyte-like cells	CYP1A1, MT1E, TNMD, MET, AGT, GSTA5, G6PC, AGT, F5, FN1, AMBP, A2M, CK18, CYP3A64, MT2A, AKRIC3, CFB, CES1, C/EBP α , FN1, TMPRSS1, HMGCS2, a1-AT, OSMR, GSTA1, RBP1, IGFII, TIMP-1	DMEM/F12 with KSR and β FGF human ESC-derived fibroblast-like cells cocultured with the ESC secreted FGF2 and Activin A
[68]	hESC (H9), hiPSC (hFLF4)	Foregut endoderm and hepatocyte-like cells	AFP	Foregut endoderm and hepatocytes: FGF4, BMP2, SB431542, +/- sFRP-5

literature	Cell model	Endpoint	Used markers	Inducers
[69]	hESC (H1), hiPSC (207, Det RA, CRL S23),	Hepatocyte-like cells	CYP3A4 activity, Albumin production and secretion, glycogen synthesis and storage	Hepatocytes: P1: SR/DMSO medium P2: L15 medium with dihexa (without Hydrocortisone 21-hemisuccinate or dexamethasone) supplemented with Rifampicin (Sigma)
[70]	hESC (H1, H9), hiPSC (from foreskin fibroblasts)	Hepatocyte-like cells	ALB Hepatic endoderm: HNF4 α	B27, sodium butyrate, Activin A, FBS, tryptose phosphate broth, hydrocortisone-21-hemisuccinate, insulin, HGF, oncostatin M
[71]	hESC (H1, H7), hiPSC (not indicated)	Hepatocyte-like cells	AFP, ALB, HNF4 α , AIAT, APOA2, TTR, ASGR1, CYP1A1, CYP1A2, CYP2C9, CYP3A4	Hepatic progenitor cells: F12 basal medium, A83-01, sodium butyrate, DMSO Hepatocyte-like cells: Advanced F12 basal medium, FH1, FPH1, A83-01, dexamethasone, hydrocortisone
[78]	hESC (H9)	Hepatocyte-like cells	Hepatoblast and hepatocyte-like cells: AFP, ALB, HNF4 α Liver markers: AFP, ALB, HNF4A	Hepatoblast formation: knockout DMEM/KSR, DMSO Hepatocyte-like: L15 medium, insulin-tranferrin-selenium, ascorbic acid, hydrocortisone-21-hemisuccinate, N-heanoic-tyrile aminohexanoic amide, dexamethasone
[79]	hESC (H1)	Hepatocyte-like cells	Unclear how they defined the cells as hepatic	RPMI1640/B27 without insulin, Activin A, CHIR99021
[80]	hESC (H1)	Hepatocyte-like cells	Hepatocytes: HNF4 α Immature hepatocytes: AFP mature hepatocytes: ALBUMIN	Hepatic endoderm: RPMI1640/B27, BMP4, FGF Immature hepatocytes: RPMI1640/B27, HGF Mature hepatocytes: HCM medium with kit-supplied HCM Single Quots, oncostatin-M

literature	Cell model	Endpoint	Used markers	Inducers
[81]	hESC (H1)	Hepatocyte-like cells	HNF4A, AFP, ALB, FGA, FGB, FGG	Hepatoblasts: KO-DMEM/KSR, DMSO Hepatocyte-like cells: L15 medium, insulin-transferrin-selenium, ascorbic acid, hydrocortisone-21-hemisuccinate, dihexa, dexamethasone
[82]	hiPSC (JDM-IPSI, PGP9-IPSI)	Hepatocyte-like cells	Hepatic endoderm: albumin, E-cadherin. AFP, HNF4 α , CYP7A1 Hepatocytes produced/secreted: fibrinogen, fibronectin, transthyretin (TTR), alpha-fetoprotein.	RPMI/B27, Activin A, WNT3A, DMSO Maturation: L15, tryptose phosphate broth, hydrocortisone-21-hemisuccinate, insulin, glutamine, hepatocyte growth factor (HGF), oncostatin-M
[83]	hiPSC (Windy, Dotcom, Fetch)	Hepatocyte-like cells	ALB, AFP, TAT, PXR	Hepatic progenitors: DMSO Maturation: HGF, oncostatin-M, dexamethasone
[84]	hiPSC (not indicated)	Hepatocyte-like cells	Not assessed	DMEM/F12, Activin A, WNT3A
[85]	hiPSC (obtained from Stem Cells Technology Research Center, Tehran, Iran)	Hepatocyte-like cells	albumin, cytokeratin-18, tyrosine aminotransferase, hepatocyte nuclear factor-4 α , cytochrome-P450 7A1	5 hepatocyte differentiation culture media, protocols (P) P1: hepatocyte growth factor and fibroblast growth factor-4 (FGF-4), oncostatin-M and dexamethasone; P2: similar to P1 but FGF4; P3: similar to P1 but FGF-4 was not used; P4: similar to P1 but FGF-4 and dexamethasone were not used; P5: similar to P1 but FGF-4 and oncostatin-M were not used. P3 gave the best results

literature	Cell model	Endpoint	Used markers	Inducers
[86]	hiPSC (generated from dermal fibroblasts)	Hepatocyte-like cells	AFP, CYP3A7, ALBUMIN, CYP3A4	Hepatic differentiation: RPMI/B27, BMP4, FGF10, oncostatin-M, HGF
[87]	hiPSC (ChiPS18)	Hepatocyte-like cells	AFP, PROX1, HHEX, NR1H4, SERPINA, ASGR1, ALB, SLCO1B1, SLC22A1, SLC10A1, UGT1A1, ABCC3, KRT18, TBX3, TF, NR1I3, OTC, ASL, ARG1, TDO2, SLCO2B1, ABCB4, ABCG2	Hepatocytes: DMEM/F12/B27, FGF10, BMP4 HCM SingleQuot, HGF, Oncostatin M

Pancreatic like cells

The pancreas consists of exocrine and endocrine tissues [88]. Observed overlap in markers in both human and mouse derivatives comprised markers of both of the exocrine and endocrine cells (Table 3). The most frequently used markers are pancreatic and duodenal homeobox 1 (PDX1) and the pancreatic endoderm marker SRY-box 9 (SOX9). Also mediators secreted by pancreatic cells, such as c-peptide, glucagon, somatostatin, amylase and insulin, were indicative of successful pancreatic-like cell differentiation. Other markers used to specify these cells in both human and mouse cells were NGN3, NKX6.1, and NEUROD1.

To induce pancreatic-like cell differentiation in mouse protocols, pluripotent cells were generally first differentiated into DE as an intermediate step [30, 89, 90]. To further specify pancreatic-like cells, *Liu and Lee* used insulin, laminin and nicotinamide [90]. *Kaitsuka et al.* also used laminin next to fibronectin, which were both derived from the extracellular matrix from a carcinoma cell line (804G) and stimulated differentiation even more by transduction of pancreas specific genes [91]. *Salguero-Aranda et al.*, found that diethylenetriamine nitric oxide adduct (DETA-NO) in high concentrations activated *Pdx1* expression and promoted differentiation. Normally, *Pdx1* expression results in the release of P300 which plays a role in guiding differentiation to liver cells instead of pancreatic cells. To stimulate pancreatic differentiation, mESC were sequentially exposed to P300 inhibitor C646 [92].

A different approach was used for hESC differentiation into pancreatic-like cells for which retinoic acid is almost always used to stimulate the differentiation

(Table 3). Another inducer that was used frequently is (KAAD)-cyclopamide. Also nicotinamide was used in some studies. Inducers like noggin, ascorbic acid, FGF10, FGF7, and EGF were used in more than one protocol. For hiPSC differentiation comparable inducers were used as for hESC differentiation, such as retinoic acid, ascorbic acid (vitamin C), SANT, and LDN193189 (BMP inhibitor).

When comparing mouse and human pluripotent cell differentiation to pancreatic-like cells, *Bernardo et al.* showed a proof of principle with a pTP6pdx1VP16 (mESC) or Pdx1VP16 (hESC) induction resulting in a multi-endocrine pancreas phenotype [89]. *Kaitsuka et al.* on the other hand, needed to use two different protocols since the 804G extracellular matrix treatment was not successful in generating insulin producing cells from human pluripotent cells whereas it was successful for cells originating from mice [91]. Also *Chen et al.* used different inducers between human and mouse stem cell differentiation [30].

Comparing hESC and hiPSC in their pancreatic-like cell differentiation capacities showed comparable but also different results. *Santamaria et al.* examined pancreatic endoderm development and observed similar changes in several related differentiation markers in cells derived from hESC and hiPSC [93]. *Rostovskaya et al.* also determined the differentiation into PDX1 positive cells which accounted for >90% for both H9 and FiPS derivatives for the most efficient protocols that were tested [94]. *Pezzolla et al.* and *Trott et al.* on the other hand observed differences between the pancreatic differentiation capacity between hESC and hiPSC. *Pezzolla et al.* concluded that the differentiation efficiency of hiPSC was clearly lower compared to that of hESC based on the pancreas specific markers INS, PDX1 and PAX4 [95]. *Trott et al.* measured a pancreatic differentiation efficiency of 90% for H9 cells, but only 54% and 24% for the hiPSC F14 and F18, respectively [96]. This was based on flow cytometry of the pancreatic progenitor markers PDX1 and NKX6.1. However the F14 and F18 were missing a single copy of winged helix transcription factor regulatory factor X6 (RFX6), which is a gene that is mutated in patients with the Mitchell-Riley syndrome (MRS). *Trott et al.* say the differentiation protocol usually generates >80% pancreatic progenitors in cells of hiPSC origin [96].

Table 3: from endoderm to pancreatic lineage

literature	Cell model	Endpoint	Used markers	Inducers
[89]	mESC (CGR8C10), hESC (H9C7)	Beta-cells	<i>Ptfla</i> , <i>Sox9</i> , <i>Ngn3</i> , <i>MafB</i> , <i>Ins</i> , <i>IAPP</i> , <i>Nkx6.1</i> , <i>MafA</i> , Glucagon, pancreatic polypeptide, Somatostatin, Amylase	Mouse: transfected with pTP6pdx1VP16ER Human: Transfected with Pdx1VP16ER
[90]	mESC	Pancreatic cells	<i>Pax4</i> , <i>Pax6</i> , <i>amylase</i> , <i>insulin I and II</i> , <i>somatostatin</i> , <i>glucagon</i> , <i>C-peptide</i>	Pancreatic cells: insulin, laminin, nicotinamide
[91]	mESC, hiPSC	Pancreatic cells	<i>Glut2</i> , <i>Kir6.2</i> , <i>MafA</i> , <i>NeuroD</i> , <i>Pdx1</i>	Extracellular matrix from a carcinoma cell line (804C) containing fibronectin, laminin 5 Transduction of <i>NeuroD</i> , <i>MafA</i> , <i>Pdx1</i>
[92]	mESC	Pancreatic cells	<i>Glut2</i> , <i>Gck</i> , <i>Ins1</i> , <i>Kir6.2</i> , <i>Pdx1</i>	Diethylenetriamine nitric oxide, C646
[30]	mESC (L4), hESC (VAL3)	Pancreas	PDX1, NKX6-1	STEMdiff definitive endoderm kit (hESC) Inducer of definitive endoderm 1 (IDE1; mESC) STEMdiff pancreatic progenitor kit (hESC)
[97]	hESC (H1, H9)	Beta-cells	Pancreatic endocrine markers: PDX1, HLXB9, C-peptide, glucagon, somatostatin Exocrine marker: amylase	Pancreatic differentiation: All-trans retinoic acid Maturation: DMEM/F12, β FGF, nicotinamide
[98]	hESC (ENVY)	Pancreatic progenitor cells	Pancreatic gut epithelium: SOX9 Gut-tube endoderm marker: HNF1B posterior foregut and pancreatic epithelium markers: HNF6, CDX2, PDX1	Activin A, FBS, FGF10, cyclopamine, B27 supplement, retinoic acid, DAPT gamma-secretase inhibitor, exendin 4, nicotinamide, IGF1, HGF
[99]	hESC (H9, HUES1, HUES9)	Pancreatic endoderm	Pancreatic foregut: HNF6 Pancreatic endoderm: PDX1	Primitive gut tube: KGF Posterior foregut: retinoic acid, cyclopamine, noggin, B27 Pancreatic endoderm: B27, NOGGIN, KGF, EGF

literature	Cell model	Endpoint	Used markers	Inducers
[93]	hESC (ES4), hiPSC (KiPS4F1, KiPS3F1)	Pancreatic endoderm	pancreatic precursor: HNF4 α , HNF1 β , NKX2.2, NKX6.1, HEX Committed pancreatic epithelium: ISL1, PDX1, SLC2A	RPMI1640/B27, WNT3A, ActivinA, sodium butyrate, FBS, FGF7, KAADcyclopamine, retinoic acid, noggin, DMEM/B27
[100]	hESC (H9)	Pancreas	Not assessed	RPMI1640, Activin A and low serum
[94]	hESC (H9, Shef6), hiPSC (FiPS, AdiPS),	Pancreatic endoderm	Pancreatic endoderm: PDX1, SOX9, NKX6.1, NGN3, NEUROD1	P1: FCS, FGF7, ATRA, SANTI, DM3189 P2: WNT3A, FGF10, DM3189, ATRA, SANTI P3: DM3189, IWP2, PDO325901, ATRA, SANTI P4: Ascorbic acid P5: FGF7, SANTI, ATRA, DM3189, TPB, Ascorbic acid P6: Ascorbic acid, FGF7, SANTI, ATRA
[101]	hESC (S17d5, H1), hiPSC (from newborn fibroblasts)	Pancreatic progenitors	INS, PDX1, CHGA	Insulin-producing cells: P1: B27, CHIR99021, Activin A P2: B27 without vitamin A P3: B27 without antioxidants P4: BSA P5: N2
[95]	hESC (HS-181), hiPSC (MSUH-001)	Beta-cell like cells	pancreatic progenitor markers: ISL1, NGN3, PDX1 Endocrine markers: PDX1, SST, GCG, INS	Pancreatic differentiation: retinoic acid, noggin, cyclopamine
[102]	hESC (RH5, RH6)	Pancreatic progenitor cells	PDX1, NKX6.1, INSULIN	Pancreatic progenitor differentiation: DMEM/F12/B27 without vitamin A, FGF10, KAAD-cyclopamine, PDBu, retinoic acid, LDN193189, ascorbic acid, EGF, nicotinamide
[96]	hESC (H9), hiPSC (F14, F18)	Pancreatic endoderm and progenitors	pancreatic endoderm: PDX1, SOX9 pancreatic progenitors: PDX1, NKX6-1	STEMdiff pancreatic progenitor kit

literature	Cell model	Endpoint	Used markers	Inducers
[103]	hiPSC (derived from pancreatic beta-cells)	Pancreas	PDX1, NKX2-2, HNF1A	GDF8, MCX-928, FGF7, vitamin C, retinoic acid, SANT, TPB, LDN193189, ALK5 inhibitor II, T3, LDN, GS inhibitor XX, N-Cys, AXL inhibitor
[104]	hiPSC (derived from fibroblasts and pancreatic cells)	Pancreas	PDX1, INS	DMEM/B27 (spontaneous)

Lung-like cells

The regenerative capacity of the lungs is very limited, therefore multiple researchers investigated the generation of lung lineages from ESC, with the purpose to use it for regenerative medicine [105-107]. To specify lung specific cells, the following markers were both used in mouse and human derivatives: NKX2.1 for lung progenitor cells; FOXJ1 for ciliated cells; SP-C for type II alveolar cells; and CC10 for Club cells (Table 4).

To induce the differentiation of lung-like cells from mESC, researchers have used different protocols. In general, the differentiation to DE is initiated first by using Activin A or IDE2 (Table 4). Stimulators that have been used towards lung-like cell development were nodal, noggin, retinoic acid, SHH and BMP4 [106], decellularized lung matrixes (L-Mat) [108], or A549 conditioned medium, FGF2 and hydrocortisone [105].

Human ESC differentiation to lung-like cells, like *Ninomiya et al.*, used ATRA and BMP4 (Table 4). Different from the mouse protocols, the human ones mainly used inhibitors to get to lung cell differentiation. Mainly SB431542 (inhibitor of the TGF- β /Activin/NODAL pathway) and dorsomorphin (AMPK inhibitor) were used. Other inhibitors were CHIR99021 (GSK3 β inhibitor), 1-thioglycerol (glycerol kinase inhibitor), and Y-27632 (ROCK inhibitor). Also when stimulating hiPSC to lung-like cells ATRA, noggin and BMP4 were used, similar as for the mouse protocols. Comparable to hESC stimulation, hiPSC were induced by using inhibitors Y27632 (ROCK inhibitor) for DE differentiation, SB431542 (inhibitor of the TGF- β /Activin/NODAL pathway) for anteriorization, and CHIR99021 (GSK3 β inhibitor) and PD032519 (inhibitor of MEK1/MEK2 part of the MAPK/ERK pathway) for proximal lung progenitor differentiation.

Sahabian et al. compared the differentiation of hESC and hiPSC to lung progenitor cells by quantifying NKX2.1, which resulted in 29% of positive cells derived from hESC and 47% when derived from hiPSC [109]. For this differentiation only stimulators for DE were used and not specific lung cell inducers [109]. *Li et al.* showed that the use of a JNK inhibitor increased the frequency of NKX2.1 positive cells from 20% to 70% by flow cytometry [110]. This was tested in only one hESC cell line, so no comparison can be made.

Table 4: endoderm to lung-like cells

Literature	Cell model	Endpoint	Used markers	Inducers
[106]	mESC	Lung progenitor cells and lung cells	Lung progenitor: <i>Nkx2.1</i> Ciliated cells: <i>Foxj1</i> , Type II alveolar cells: <i>SP-C</i> , Type I alveolar cells <i>T1a</i> , Goblet cells: <i>Muc5aC</i> , Club cells: <i>CC10</i>	Lung progenitor cells: Activin A, nodal, noggin Ciliated cells: Activin A, retinoic acid, SHH Type II alveolar cells: Noggin, retinoic acid Type I alveolar cells: Nodal, retinoic acid Goblet cells: low BMP4, Activin A Club cells: high BMP4, Nodal
[25]	mESC	Definitive endoderm and distal lung	<i>Aqp5</i> , <i>Sftpc</i> , <i>Scgb1a1</i>	Hypoxia, Activin A
[108]	mESC	Lung cells	Club cells: CC10 ATI cells: AQP5 ATII cells: TTF-1, SP-C	Decellularized lung matrixes (L-Mat)
[105]	mESC	ATII cells	ATII cells: SP-C, SP-A, NKX2.1	A549 conditioned medium, FGF2, hydrocortisone
[110]	hESC (H1, HUES6, HUES8), hiPSC (BJ, CV)	lung progenitor cells	NKX2.1	Base medium: IMDM, Ham's Modified F12, N2, B27, BSA, L-glutamine, ascorbic acid, MTC Lung base medium: SB431542, Dorsomorphin, BMP4, ATRA, CHIR99021
[109]	hESC (HES3), hiPSC (MHHi001-A)	Lung progenitor cells	NKX2.1, p63	Lung basal medium: KSR, 1-thioglycerol, dorsomorphin, SB435142, Y-27632 Anterior foregut medium: LBM, IWP-2, SB435142 B4CF10 medium, LBM, BMP4, CHIR99021, FGF10

Literature	Cell model	Endpoint	Used markers	Inducers
[111]	hiPSC (XCL-ER2.2, 3D1, BC1, RC 202)	Proximal and distal lung precursor cells	NKX2.1, PITX2, FOXJ1, CC10, SPC	Ant. Endoderm: SB431542, Noggin, FGF2, EGF Proximal lung: CHIR99021, PD032519, FGF7, BMP7, RA, Noggin Distal lung: BMP2, BMP4, FGF2, FGF10, WNT3A

Intestinal cells

It was suggested that patients that have intestinal failure, could perhaps be treated with ESC [112]. Therefore, *Konuma et al.* investigated the capacity of mESC to differentiate into gut-like cells or structures as well as refining culture conditions for an efficient differentiation into these cells [112]. Multiple markers were used to specify intestinal-like cell differentiation, including the markers leucine-rich-repeat-containing G protein-coupled receptor 5 (LGR5) for intestinal stem cells and *Cdx2* for intestinal epithelium [112]. These two markers were also used to specify intestinal differentiation of human pluripotent cells (Table 5).

For differentiation into intestinal cells, completely different inducers were used among mouse and hESC and hiPSC (Table 5). The inducers for hiPSC intestinal differentiation had more in common with hepatocyte differentiation protocols (Table 5), including the use of Activin A, B27, DMSO and KSR. The addition of BIO and glucose stimulated the cells towards intestinal epithelium. *Sahabian et al.* used a different protocol with inducers as FGF4 and CHIR99021 for both hiPSC and hESC stimulation to intestinal epithelium [109]. By immunofluorescence staining of CDX2, 92-96% of the cells were positive in both hiPSC and hESC [109].

Table 5: endoderm to intestinal lineage

Literature	Cell model	Endpoint	Used markers	Inducers
[112]	mESC	Gut-like cells	Intestinal stem cells: LGR5, MSI-1 Intestinal epithelium: <i>Shh, Cdx1, Cdx2</i> Absorptive markers: <i>Fabp2, Fabp6</i>	15% serum-replacement
[113]	mESC	Intestinal cells	Definitive endoderm: <i>Cxcr4, Gsc, Foxa2, Sox17</i> gut: <i>Id2</i> Intestinal cells: <i>Cdx2, Fabp2, Muc2</i>	Intestinal differentiation: Fibroblast-conditioned medium, WNT3A
[114]	mESC (mutation in DF508)	Intestinal cells	<i>Lgr5</i>	DF508 mutation for cystic fibrosis transmembrane conductance regulator
[115]	mESC	Stomach cells	<i>Barx1, Sox2, Pepsinogen A</i>	SHH, DKK1
[109]	hESC (HES3), hiPSC (MHHi001-A)	Intestinal progenitors	CDX2, HOXC5, HOXB6, HOXD13	DMEM/F12, FBS, FGF4, CHIR99021, Penstrep
[116]	hiPSC (201B7)	Intestinal epithelium	Gut epithelium: VILLIN, CDX2, LGR5 Enterocytes: PEPT1, VILLIN, ALP (alkali phosphatase activity), CYP3A4, CDX2, MDR1, MRP3, OATP2B1, EAAC1, TAUT, CYP2E1, CES2	DMEM, Activin A, B27, DMSO, BIO, DAPT, KSR, glucose

Mesoderm differentiation and derivatives

Within the early mouse embryo, pluripotent epiblast cells arise from the primitive streak (PS) [117]. On day 6 of embryogenesis, mesodermal cells emerge from the epiblast. Epithelial cells detach during breakdown of the basement membrane and are able to migrate into the embryo and generate the endoderm and mesoderm [118]. Cells that do not migrate will later become ectodermal cells. The newly formed mesodermal cells lose their pluripotency. Depending on the location where mesodermal cells arise from the PS, the mesoderm contributes to different cell types and tissues. At the posterior side of the PS, extra-embryonic mesoderm is formed. Extra-embryonic mesoderm contributes to the visceral yolk sac and it also gives rise to red blood cells and early vasculature. On the anterior side of the

PS, mesoderm is committed to become cells of the cranial and cardiac lineages. In between the anterior and posterior side, axial, paraxial, intermediate and lateral plate mesoderm is formed [117]. The axial mesoderm at the anterior side of the PS gives rise to the notochord [119]. Paraxial mesoderm is clustered in segments called somites [117]. Somites consist of dermomyotome and sclerotome, which give rise to muscles and the axial skeleton. Intermediate mesoderm gives rise to the gonads, tissues of the urogenital tract and the adrenal cortex [117]. Cells from the lateral plate mesoderm participate in the formation of the heart [120]. In short, mesodermal cells give rise to the cardiovascular system, musculoskeletal system (cartilage, bones, muscles), urogenital system, connective tissues and notochord [117].

Mesoderm

To specify mesodermal cells, both human and mouse pluripotent cell differentiation to mesoderm used the markers T (Brachyury), PDGFR α , FLK1, MSGN1, and MEOX1 from which MSGN1 (Mesogenin 1) is specific to the paraxial mesoderm [121]. mESC can be stimulated towards mesoderm without the use of chemical inducers. However, chemical inducers have been used like for instance a combination of JAK inhibitors, LY294002 (PI3K inhibitor), and CCG1423 (Rho/Ras inhibitor), but also ATRA was used to stimulate mesoderm differentiation (Table 6). Human mesoderm differentiation has also been achieved without the use of chemical inducers, but multiple inducers have been tested. Mainly the addition of Activin A, BMP4, VEGF and β FGF have been used, but after 2017 ROCK inhibitors were used instead. In hiPSC differentiation mainly the GSK3 β inhibitor CHIR99021 has been tested next to mesoderm differentiation without the use of chemical inducers.

Song et al. investigated the effect of pyruvate on BMP4 induced mesoderm differentiation and showed presence of the mesoderm specific markers TBXT and MIXL1 for both hESC (H1, H9) and hiPSC (ND1, ND2) cell lines [122]. However, a comparison was difficult to make due to the normalized control which doesn't contain pyruvate. Relatively, pyruvate stimulated the highest expression levels of TBXT in ND2 cells and of MIXL1 in ND2 cells [122]. *Geng and Feng* actually quantified the differentiation efficiency by FACS analysis of EOMES and T (brachyury) after inducing pluripotent cells with mesendogen followed by a combination of Activin A, BMP4, VEGF, and β FGF and resulted in 85.2% of mesodermal cells in H9 cells and 89.63% in MMW2 cells [33].

Table 6: from pluripotent stem cells to mesoderm

literature	Cell model	Endpoint	Used markers	Inducers
[123]	mESC	Intermediate mesoderm	Brachyury, <i>Pdgfra</i> , OSR1, PAX2	JAKi, LY294002, CCG1423, RA
[124]	mESC	Intermediate mesoderm	WT1, OSR1	Activin A, RA
[37]	hESC (ReliCellhES1)	Germ layers	ACTC1, MSX1, CD34	Spontaneous differentiation EBs (advanced DMEM/F12 without β FGF)
[125]	hESC (H9)	Germ layers	HAND2, PITX2, GATA5, MYL4, TNNT2, COL1A1 and COL1A2	Spontaneous differentiation EBs (advanced DMEM/F12 without β FGF)
[38]	hESC (H9)	Germ layers	KDR+, SSEA3-	Mesoderm: BMP4 Lateral mesoderm: VEGF
[39]	hESC (H9)	Germ layers	PDGFRA and FOXF1	RPMI1640 with B27, Activin A, BMP4, β FGF
[40]	hESC (BG01V)	Germ layers	FLK1, HAND1, LHX1, VEGFR2, ACTA2, TNNT2, BRACHYURY	<u>aMEM</u> (spontaneous differentiation EBs)
[41]	hESC (H7)	Germ layers	MYF5, MYOD1, BRACHYURY	Knockout Serum Replacement (KSR), β FGF
[42]	hESC (H1)	Germ layers	BRACHYURY, EOMES, GSC, MIXL1	mTeSR, retinoic acid
[43]	hESC (HUES8, HES3)	Germ layers	PDGFRA, KDR, CD34	BMP4, CHIR, BMP4 miR-483-3p, miR-199a-3p, and miR214-3p
[126]	hESC (H9)	Germ layers	CD56, CD34 and PDGFR- α	Activin A, BMP4, VEGF, β FGF
[122]	hESC (H1, H9), hiPSC (ND1, ND2)	Germ layers	Brachyury	BMP4 in E8 medium
[127]	hESC (H9)	Germ layers	Not assessed	DMEM/F12 with VEGF
[21]	hESC (H9)	Mesoendoderm	EOMES, Brachyury	RPMI1640, Activin A, WNT3A, FBS
[33]	hESC (H9 and H1), hiPSC (MMW2)	mesoderm	Brachyury, EOMES, MIXL1, EVX1, TBX6, HAND1, MESP1, MEOX1	RPMI1640 with B27, Activin A, BMP4, VEGF, β FGF Variations: mesendogen addition or BMP4, VEGF, and β FGF or BMP4 and β FGF

literature	Cell model	Endpoint	Used markers	Inducers
[128]	hESC (H7 and H9)	Mesoderm	NCAM, BRACHYURY, GSC, MIXL1, HLX, KDR	Activin, β FGF, VEGF, BMP4
[129]	hESC (H9)	Mesoderm	Brachyury	Plasmids with shRNA targeting CHAC2 and CHAC1
[130]	hESC (ESI017)	Mesoderm	Brachyury	mTeSR1 medium with ROCK inhibitor
[44]	hESC (H1)	Mesoendoderm	CALPONIN, T, RUNX1	mTeSR1, Thiazovivin, doxycycline, puromycin
[45]	hESC (Mel1, H9)	Mesoendoderm	Brachyury, HAND1	STEMDIFF trilineage differentiation kit with ROCKi
[54]	hiPSC (201B7, 253G1, 409B2, DYR0100, HYR0103, mc-iPS, R-1A, R-2A, R-12A, Tic)	Germ layers	GATA4, T, KDR	Spontaneous differentiation without addition of growth factors
[131]	hiPSC (A18945)	Germ layers	ABCA4, ALOX15, BMP10, CDH5, CDX2, ESM1, FCN3, FOXF1, HAND1, HAND2, HEY1, RGS4, ODAM, NKX2-5, PDGFRA, PLVAP, SNAI2, TBX3, TM4SF1, COLEC10, HOPX, IL6ST	Spontaneous EB formation
[132]	hiPSC (201B7-0063)	Mesoderm	TRA-1-60, BRACHYURY	CHIR99021
[133]	hiPSC (from sondylocostal dysostosis patients)	Somatic mesoderm	T, TBX6, MSGN1, MEOX1	Primitive streak: Activin A, CHIR99021, β FGF, PIK90. Presomitic mesoderm: A8301, CHIR99021, LDN193189 Early somites: A8301, XAV939, LDN193189, PD0325901
[134]	hiPSC (201B7)	Mesoderm	CD34, HAND1, RUNX1, HNF4A	hESF6 medium with activin, CHIR99021, and y-27632

Cardiomyocytes

In the field of regenerative medicine, treatment of heart failure is investigated by replacing injured heart tissue with cardiomyocytes grown from ESC or iPS cells [135]. To specify cardiomyocytes markers as α MHC, TNNT2 (=CTNT), TBX5, and α ACTININ were used in both mouse and human derivatives and mainly code for the typical cardiomyocyte structures myosin, troponin and actinin (Table 7).

Kokkinopoulos et al. stimulated cardiomyocytes from mESC into mesoderm using BMP4, Activin A and human VEGF as a first step to induce cardiomyocytes. To specify further cardiomyocyte differentiation, cells were exposed to fibroblast growth factor 10 (FGF10), β FGF, VEGF, ascorbic acid and L-glutamine [135]. *Lu et al.* also used ascorbic acid as inducer, but in combination with rapamycin [136].

In hESC differentiation, B27 (without insulin) supplement was often added to serum free media to promote growth and proliferation of cells without differentiation. Later in the differentiation process, this component was often replaced by B27 containing insulin. Also Wnt inhibition plays an important role in hESC cardiomyocyte differentiation. The inhibitor IWR-1 was most often used, but also DKK1, XAV939 and IWP4 were used to inhibit Wnt and stimulate cardiomyocyte differentiation. Other inhibitors that some protocols used were CHIR99021 (GSK3 β inhibitor), SB203580 (TGF β /Nodal pathway inhibitor), and SB431542 (NODAL inhibitor). hESC differentiation to cardiomyocytes also sometimes made use of inducers, like β FGF, Activin A, BMP4, VEGF. These inducers were also used in mesoderm stimulation. The protocols for hESC and hiPSC cells to induce cardiomyocyte differentiation were very similar.

Wei et al. compared the percentage of contracting EBs from total EB aggregates in H9 cells and hiPSC cell lines, indicating a significantly lower cardiomyocyte differentiation for the hiPSC lines (28.7 \pm 3% and 23.5 \pm 3%) compared to H9 differentiation (50 \pm 5%) [137]. *Liu et al.*, on the other hand, yielded comparable cardiomyocyte populations of 85-95% [138]. The differentiation depended on confluence of the cells that were cultured in monolayers. Confluencies ranged from 50-65% for C15 cells, 60-70% for H1, 70-80% for H9, and 80-85% for C20 cells [138].

Table 7: from mesoderm to cardiomyocytes

literature	Cell model	Endpoint	Used markers	Inducers
[5]	mESC	cardiomyocytes	beating cardiomyocytes	Spontaneous differentiation
[135]	mESC	Mesoderm and cardiomyocytes	<i>cTnT</i> , <i>Mlc2v</i> , <i>Tbx5</i> , <i>Mesp1</i>	FGF10, β FGF, VEGF, ascorbic acid, L-glutamine
[136]	mESC	Cardiomyocytes	Alpha-actinin <i>Tnnt2</i> , <i>Tbx5</i> , α - <i>Mhc</i> , β - <i>Mhc</i>	Ascorbic acid and rapamycin
[139]	hESC	Cardiac mesoderm and cardiac progenitors	Mesoderm: LHX1, FGF4, FLK1, BRACHYURY Cardiac mesodermal cells: NKX2.5, ISLET1 Cardiac progenitors: NKX2.5, α MHC	GSI (NOTCH inhibitor) in reduced-volume culture medium (RVCM) Cardiac differentiation: knock-out DMEM with B27
[140]	hESC (PKU1.1)	Cardiomyocytes	Precursors: NKX2.5, GATA4, TNNT2	Ascorbic acid
[137]	hESC (H9), hiPSC (from dermal fibroblasts)	Mesenchymal stem cells and Cardiomyocytes	MSC markers: CD29, CD44, CD73, CD90, CD105, CD146, α -actinin, titin cardiomyocytes: MLC, β -MHC	SB203580
[141]	hESC (KIND1, KIND2)	Mesoderm and cardiomyocytes	NKX2.5, α MHC	B27, Activin A, β FGF, BMP4, DKK1
[142]	hESC (HES3, H7)	Cardiomyocytes	Cardiac mesoderm: MESP117 or KDR+, PDGFR α - cardiomyocytes: GATA4, TBX5, NKX2-5, MEF2C6	SB203580 in DMEM or CHIR99021 and IWR-1 in RPMI/B27-insulin
[143]	hESC (H9)	Cardiomyocytes	cardiac progenitor markers: HAND1, NKX2.5 cardiomyocytes: cTNT and MYH7	StemPro-34, BMP4, DKK1, VEGF, SB, β FGF
[144]	hESC (H1, H9), hiPSC (C15, C20)	Cardiomyocytes	Cardiac mesoderm: MESP1, NKX2-5 Cardiomyocytes: TNNT2	PSC cardiomyocyte differentiation kit followed by glucose starvation with RPMI/B27
[145]	hESC (not indicated)	Cardiomyocytes	ACTN2	DMEM/F12 with B27 without insulin, CHIR99021, IWR-1, DMEM/F12 with B27 with insulin

literature	Cell model	Endpoint	Used markers	Inducers
[146]	hESC (H1), hiPSC (C15)	Cardiomyocytes	NKX2-5, TNNT2	PSC cardiomyocyte differentiation kit
[147]	hESC (H1, H9)	Cardiomyocytes	Cardiac markers: ISL-1, TBX5, NKX2.5 Cardiomyocytes: ACTN2, TNNT2, TNNI3, MYH6, MYL7, MYL2, IRX4	RPMI1640 with B27 minus insulin, CHIR99021, IWR-1, RPMI1640 with B27
[148]	hESC (not indicated)	Cardiomyocytes	TNNT2, NKX2.5	Mesoderm: CHIR99021 Cardiomyocytes: Neutral condition Or IWR-1, Insulin
[149]	hiPSC (DYR0100)	Cardiomyocytes	GATA4, NKX2-5, cTnT, α MHC, β MHC	BMP4, resveratrol, β FGF, Activin A, and DKK1 or WNT3A
[150]	hiPSC (3 cell lines generated from cardiac or dermal fibroblasts)	Cardiomyocytes	Early cardiac progenitor: GATA4, ISL1 Late cardiac progenitor: HAND1, NKX2.5 Cardiomyocytes: cTnT, MYL2, α -actinin, CX43	RPMI1640/B27 without insulin, CHIR99021, IWR1, RPMI1640/B27 with insulin
[151]	hiPSC (iPS- DF19-9-7T and iPS-DF6- 9-9T)	Cardiomyocytes	TNNC, TNT	RPMI/B27 without insulin, CHIR99021, IWR1, SB431542
[152]	hiPSC (836B3, 253G1, 1201C1)	Cardiomyocytes	cTNT, α -actinin ventricular cardiomyocytes: MLC2a	RPMI1640/B27 without insulin, Activin A, BMP 4, β FGF After purification PDGFR α positive cells: RPMI1640/B27 with XAV939 and/or IWP4, Y-27632
[153]	hiPSC	Cardiomyocytes	cardiac progenitors: GATA4, ISL1 cardiomyocytes: α -actinin, cTNT	RPMI1640/B27 without insulin, IWR1, RPMI1640/ B27

Osteogenic cells

The self-renewing and pluripotent characteristics of embryonic stem cells make it a useful model to investigate normal osteogenesis and bone tissue related diseases [154]. Osteocalcin is the marker that was most used when comparing species (Table 8). In differentiation of mESC often inducers as ascorbic acid, dexamethasone and different forms of glycerol (β -glycerol, β -glycerophosphate, mono-thioglycerol, β -glycerophosphate) were mostly used in osteogenesis stimulation. In hESC differentiation similar components were used, with the addition of vitamin D3. This is also true in hiPSC osteogenesis stimulation, in which also dexamethasone, ascorbic acid-2-phosphate, and TGF β were used.

Table 8: mesoderm to osteogenic lineage

Literature	Cell model	Endpoint	Used markers	Inducers
[155]	mESC	Osteogenic cells	Osteocalcin	Ascorbic acid, dexamethasone, β -glycerol
[156]	ESC (marmoset, rhesus and mouse)	Osteogenic cells	Mineralization	β -glycerophosphate, ascorbic acid, vitamin D3
[157]	mESC	Osteogenic cells	<i>Alp, Bsp, Ocn, Osx, Runx2</i>	Retinoic acid, dexamethasone
[158]	miPSC (APS0003), mESC (E14tg2A)	Chondrogenic cells	Flk-1, SOX9, Collagen II, aggrecan, Collagen I, Collagen X	IMDM/DMEM:F12, L-ascorbic acid, BSA, N2, B27, mono-thioglycerol chondrogenic differentiation: β FGF, Gdf5
[159]	mESC (ES-E14TG2a)	Osteogenic cells	RUNX2, OSX, <i>Hoxa1, Ctgf, Fgfr1, Col5a2</i>	Ascorbic acid, β -glycerophosphate, dexamethasone and low oxygen tension
[160]	hESC (H9)	Osteogenic cells	Osteocalcin (OCN)	Vitamin D3, β -glycerophosphate, ascorbic acid
[161]	hiPSC (from dermal skin fibroblasts)	Osteogenic cells	RUNX1	Osteoblasts: MSC, α MEM, FCS, dexamethasone, ascorbic acid-2-phosphate, β -glycerophosphate Chondrogenic differentiation: complete chondrogenic medium (Lonza), TGF- β 3
[162]	hiPSC (from healthy donors)	Osteoclasts	TRAP, NFATc1, CATHEPSIN K, CALCITONIN R	DMEM, IL-3, MCSF Osteoclasts: DMEM, Vitamin D, TGF- β , MCSF, RANKL

Vascular and hematopoietic cells

From the mesoderm, hemangioblasts are derived [163]. These cells can either give rise to endothelial lineages or hematopoietic lineages. Hematopoietic stem cells (HSCs) are normally located in the bone marrow [164]. These HSCs can be derived from ESC and can be transplanted in patients that have a hematopoietic disease [164]. Another method for collecting HSCs is by collecting these cells from the bone marrow of donors. However, the yield of this method is low and to harvest these cells, an invasive procedure is required. Hematopoietic stem cells could also be further differentiated into its derivatives. Most approaches that aim to differentiate stem cells towards hematopoietic lineages make use of hESC or hiPSC cells, for use in clinical therapies.

For the differentiation towards hematopoietic cells, CD34 was often used to specify the cells (Table 9). Endothelial cells were often specified by the markers VE-CAD, vWF, and CD31. To induce mESC cells to hematopoietic differentiation inducers as IGFII, VEGF, EPO, dexamethasone, SCF, and IL3 were used. Like for the mouse, human hematopoietic differentiation was stimulated by VEGF, SCF, EPO, and IL3. These inducers were mainly used for erythroid induction. To differentiate into myeloid progenitors, SFM, Fit3, granulocyte-macrophage colony stimulating factor, and thrombopoietin were additionally employed.

Inducers for endothelial cell differentiation included mainly VEGF for both hiPSC and hESC (Table 9). Also SB431542 (TGF β /NODAL pathway inhibitor) and β FGF were frequently used for differentiation of both derivatives. The inducers BMP4 and Activin A, also used for stimulation towards mesoderm, added to a successful endothelial cell specification. A wide range of inducers were used in hiPSC and hESC endothelial cell differentiation: endothelial growth factor, fibronectin, ascorbic acid, 2-phosphate magnesium, sodium selenite, holo-transferrin, insulin, FGF2, CHIR99021. Only *White et al.* compared the efficiency of endothelial cell differentiation between hiPSC and hESC derivatives specific for CD31 and CD144 by FACS and resulted in almost completely homogenic cell cultures of 95+/-3.7 % for hESC and 93+/-4.8 % for hiPSCs.

Table 9: mesoderm to vascular and hematopoietic cells

Literature	Cell model	Endpoint	Used markers	Inducers
[165]	mESC	Erythroid cells	<i>Epor, Eklf, Gata1</i>	IGFII, VEGF, EPO, dexamethasone, stem cell factor, IL3
[164]	mESC	Hematopoietic cells	CD117, CD34, SCA-1	Exosomes from hematopoietic stem cells containing microRNAs (e.g. miR126)
[166]	hESC (H1, H7, H9)	Hematopoietic cells	SCL, CD34, ϵ -GLOBIN, γ -GLOBIN	BMP4, Noggin, FGF
[167]	hESC (H1, H7, H9), hiPSC (iPS1, iPS2, iPS3)	Endothelial cells	KDR, PECAM1, VE-CAD, vWF, eNOS	Arterial endothelial cells: VEGF, β FGF, Fibronectin
[168]	hESC (H1, H9), hiPSC (hFib2-iPSS)	Blood cells	CD34, CD45, CD56, KDR, VEGFR2	Hematopoietic mesoderm: β FGF, BMP4, VEGF, SCF myeloid progenitors: SFM, Flt3, granulocyte-macrophage colony stimulating factor, IL-3, SCF, EPO, thrombopoietin Erythroid induction: SFM, SCF, IL-3, EPO
[169]	hESC	Hematovascular precursors	KDR, SCL, VE-CAD	BMP4
[170]	hESC (H1)	Perineural vascular plexus	Endothelial cells: CD31, VE-CAD	DMEM/F12, L-ascorbic acid, 2-phosphate magnesium, sodium selenite, holo-transferrin, insulin, FGF2, VEGF Endothelial cells: E8 with Activin A, BMP4, CHIR99021, SB431542
[171]	hiPSC (BC1)	Endothelial cells	VE-CAD, CD31, vWF, and eNOS	Early vascular differentiation: EGM, SB431542, VEGF, FBS,
[172]	hiPSC	Endothelial cells	CD31, VE-CAD, vWF	DMEM/F12, CHIR99021 Endothelial cell basal medium (Promocell), β FGF, VEGF, Activin A, BMP4, EMV2 medium, VEGFA

Discussion and future perspectives

A vast amount of research has been invested in the differentiation of pluripotent stem cells into other cell types in *in vitro* cell culture systems. Whereas differentiation into the human neuroectodermal germ line has been studied in relatively great detail from the perspective of developmental toxicity testing, embryonic stem cell differentiation into cell types of the endodermal and mesodermal germ line have received less attention thus far. For mouse stem cell differentiation, developmental toxicity testing has been investigated using the cardiomyocyte, osteogenic, and neural cell types. For most of the other endoderm and mesoderm derivatives, multiple differentiation approaches have been developed, but these lines have hardly if at all been employed yet in chemical safety testing. This information can be useful in selecting additional cell differentiation routes for study in developmental toxicity testing, as well as for detecting additional differentiation routes present in existing EST assays, which could be of added value in hazard predictions of developmental toxicity.

In this review we showed resemblances and differences in biomarkers and inducers between mouse and human derivatives, indicative of differences in mechanisms. To summarise, the differentiation into endoderm and mesoderm showed partly similar inducers between species. Differentiation of human and mouse stem cells into endoderm needs induction with Activin A and differentiation into mesoderm can occur without the addition of chemical inducers (Table 1 and 6). The interspecies differences in mesoderm induction mainly pertain to the need for additional inducers when using human derivatives (Table 6). Also osteogenic and hematopoietic differentiation seem to show similar inducers between species, although the information collected was less extensive as compared to the other differentiation routes (Table 8 and 9). Also the collected information for lung-like differentiation was less extensive and additionally showed more variation and therefore less similarities in inducers (Table 4). This variation was also seen in cardiomyocyte differentiation when comparing mouse and human derivatives, but nevertheless both lung-like and cardiomyocyte differentiation still showed resemblances a well (Table 4 and 7). When comparing species, the opposite was true for the differentiation routes to intestine, hepatocyte and pancreatic cells which need different inducers for mouse and human stem cell differentiation (Table 2, 3, and 5). The observed similarities are indicative of comparable mechanisms *in vitro* needed for differentiation.

To be able to make predictions about the human *in vivo* situation, we need to know whether these *in vitro* mechanisms actually mimic the mechanisms in a whole organism. Although a comparison to the *in vivo* situation was not within the scope of this review, human *in vivo* comparisons are difficult to make, since such detailed information on human embryo development is obviously lacking. Although the early human embryo has been visualized on the organ and cellular levels (Belle et al., 2017), an overview of mechanisms in the human embryo is largely limited to the first 14 days of development, restricting research to mechanisms of e.g. gastrulation and later stages of organogenesis (Pera, 2017; Shahbazi, 2020). *In vivo* animal data on the other hand are more abundant. Data on the mouse embryo have been mapped on the single-cell level at the stages of mouse fertilization through gastrulation [173], gastrulation and early organogenesis [174], and mouse organogenesis from E9.5-E13.5 [175]. Such animal studies provide useful information to improve our understanding of embryo development. To predict the development in the human situation, initiatives for human embryo computational model systems are under development using *in vitro* and *in silico* human data for prediction of e.g. developmental vascular and palate fusion disturbances (Hutson et al., 2017; Saito et al., 2019).

Interpreting *in vitro* data also comes with challenges given that the differentiation efficiencies not only differ between species but also between cell lines. The possibility to use human pluripotent cells is promising to make predictions for human safety, although the use of these cells obviously also comes with ethical and legal issues for performing toxicity testing with hESC [17]. An alternative is the use of human induced pluripotent stem cells (hiPSC), but questions about comparable differentiation potentials still exist as reviewed by Kugler et al. [4]. In addition, hiPSC based assays may need the time-consuming process of validation every time new cell batches are induced to pluripotency. Although originating from another species, mESCs more closely resemble stem cells of the early embryo [17]. Additionally, species-specific differences are often due to *in vivo* differences in metabolism or toxicokinetics, which may not apply to *in vitro* assays [4, 17]. Moreover, the metabolic capacity of these stem cell differentiation cultures needs further study also in view of possible *in vitro* metabolism of test compounds. Nevertheless, the differentiation routes as readout for toxicological screens originating from mESC, hESC and hiPSC can be of added value in case these routes are applicable to the mechanisms present within the human early embryo.

Although *in vitro* assays have usually focussed on individual cell types for effect assessment, stem cell differentiation *in vitro* is always heterogeneous. Therefore, these tests may be missing out on additional informative data of chemical effects by focussing on one cell type instead of the complete heterogeneous cell population. Additionally, in heterogeneous cell populations cell fate decisions can be studied which, like in a whole embryo, are made by the cell responding to stimuli of surrounding cells. During gastrulation for example, when the three germ layers are formed, the ectoderm is migrating and transforms into mesoderm cells after stimulation by its surroundings [176]. This cellular communication regulates differentiation. Studying these processes and perturbations thereof without the use of animals, asks for the use of more complex engineered living systems (ELS) (Glen et al., 2018). Monitoring the heterogeneous properties within pluripotent stem cell test systems such as the EST would add to the understanding of differentiation processes and potential chemical perturbations.

ESC differentiation models provide an intermediate complexity level among developmental toxicity assays. High throughput molecular and cellular assays are often focused on single readout parameters, whereas 3D models and organ-on-a-chip models are more complex, but have a lower throughput level. A smart combination of complementary assays as to endpoints and complexity might allow an integral *in vitro* assessment of mechanisms of embryotoxicity. The use of adverse outcome pathways (AOPs) could help to design relevant combinations of *in vitro* assays including stem cell differentiation assays with related biomarkers, depending on the adverse outcome of interest. The integration of this information to the level of the intact organism, preferably the human, provides the real challenge for a future of toxicity testing without animal experimentation. Efforts such as the virtual physiological human program could be used as a feeder for providing the biological backbone of an ontology describing the adverse outcome pathway networks that drive toxicity [177-179]. Based on those networks, *in vitro* test batteries could be defined that mimic its critical key events. Computational data integration could then lead to predictions on compound toxicity and safety [180]. Additional EST differentiation routes may help filling gaps in the spectrum of assays available to cover the developmental toxicity adverse outcome pathway network.

In conclusion, this review summarizes cell type specific inducers and biomarkers used in pluripotent stem cell differentiation of the endoderm, the mesoderm,

and a selection of its derivatives. In the future, the described differentiation approaches in combination with the corresponding biomarkers might be useful to investigate effects of compounds on the differentiation of specific cell types during development. Further research should be conducted to see whether these approaches are fit to use in developmental and reproductive toxicology.

Acknowledgements

Gina Mennen was supported by the French National Association for Research and Technology (ANRT) through a CIFRE PhD grant no. 2018-0682, which was co-supervised by Aldert Piersma, Nina Hallmark, Marc Pallardy, Remi Bars, and Helen Tinwell. Aldert Piersma was funded by the Dutch Ministry of Health, Welfare and Sports. We would like to thank Victoria de Leeuw for a critical review of the manuscript.

References

1. Engel, M., et al., *Common pitfalls of stem cell differentiation: a guide to improving protocols for neurodegenerative disease models and research*. Cellular and Molecular Life Sciences, 2016. **73**(19): p. 3693-3709.
2. Kuegler, P.B., et al., *Markers of murine embryonic and neural stem cells, neurons and astrocytes: reference points for developmental neurotoxicity testing*. ALTEX -HEIDELBERG-, 2010. **27**(1): p. 15-42.
3. Fritsche, E., et al., *Current Availability of Stem Cell-Based In Vitro Methods for Developmental Neurotoxicity (DNT) Testing*. Toxicological Sciences, 2018. **165**(1): p. 21-30.
4. Kugler, J., et al., *Embryonic stem cells and the next generation of developmental toxicity testing*. Expert Opin Drug Metab Toxicol, 2017. **13**(8): p. 833-841.
5. Genschow, E., et al., *Validation of the embryonic stem cell test in the international ECVAM validation study on three in vitro embryotoxicity tests*. Altern Lab Anim, 2004. **32**(3): p. 209-44.
6. Seiler, A.E. and H. Spielmann, *The validated embryonic stem cell test to predict embryotoxicity in vitro*. Nat Protoc, 2011. **6**(7): p. 961-78.
7. Liu, S., N. Yin, and F. Faiola, *Prospects and Frontiers of Stem Cell Toxicology*. Stem Cells Dev, 2017. **26**(21): p. 1528-1539.
8. Chapin, R., et al., *Struggles for equivalence: in vitro developmental toxicity model evolution in pharmaceuticals in 2006*. Toxicol In Vitro, 2007. **21**(8): p. 1545-51.
9. Marx-Stoelting, P., et al., *A review of the implementation of the embryonic stem cell test (EST). The report and recommendations of an ECVAM/ReProTect Workshop*. Altern Lab Anim, 2009. **37**(3): p. 313-28.
10. zur Nieden, N.I. and L. Baumgartner, *Assessing developmental osteotoxicity of chlorides in the embryonic stem cell test*. Reprod Toxicol, 2010. **30**(2): p. 277-83.
11. de Jong, E., L. van Beek, and A.H. Piersma, *Osteoblast differentiation of murine embryonic stem cells as a model to study the embryotoxic effect of compounds*. Toxicol In Vitro, 2012. **26**(6): p. 970-8.
12. de Jong, E., L. van Beek, and A.H. Piersma, *Comparison of osteoblast and cardiomyocyte differentiation in the embryonic stem cell test for predicting embryotoxicity in vivo*. Reprod Toxicol, 2014. **48**: p. 62-71.
13. Barenys, M. and E. Fritsche, *A Historical Perspective on the Use of Stem/Progenitor Cell-Based In Vitro Methods for Neurodevelopmental Toxicity Testing*. Toxicological Sciences, 2018. **165**(1): p. 10-13.
14. de Leeuw, V.C., et al., *Differential effects of fluoxetine and venlafaxine in the neural embryonic stem cell test (ESTn) revealed by a cell lineage map*. Neurotoxicology, 2020. **76**: p. 1-9.
15. de Leeuw, V.C., E.V.S. Hessel, and A.H. Piersma, *Look-alikes may not act alike: Gene expression regulation and cell-type-specific responses of three valproic acid analogues in the neural embryonic stem cell test (ESTn)*. Toxicol Lett, 2019. **303**: p. 28-37.
16. Kobayashi, K., et al., *Editor's Highlight: Development of Novel Neural Embryonic Stem Cell Tests for High-Throughput Screening of Embryotoxic Chemicals*. Toxicol Sci, 2017. **159**(1): p. 238-250.

17. Luz, A.L. and E.J. Tokar, *Pluripotent Stem Cells in Developmental Toxicity Testing: A Review of Methodological Advances*. Toxicological sciences : an official journal of the Society of Toxicology, 2018. **165**(1): p. 31-39.
18. West, P.R., et al., *Predicting human developmental toxicity of pharmaceuticals using human embryonic stem cells and metabolomics*. Toxicol Appl Pharmacol, 2010. **247**(1): p. 18-27.
19. Kleinstreuer, N.C., et al., *Identifying developmental toxicity pathways for a subset of ToxCast chemicals using human embryonic stem cells and metabolomics*. Toxicol Appl Pharmacol, 2011. **257**(1): p. 111-21.
20. Palmer, J.A., et al., *Establishment and assessment of a new human embryonic stem cell-based biomarker assay for developmental toxicity screening*. Birth Defects Res B Dev Reprod Toxicol, 2013. **98**(4): p. 343-63.
21. Kameoka, S., et al., *A high-throughput screen for teratogens using human pluripotent stem cells*. Toxicol Sci, 2014. **137**(1): p. 76-90.
22. Kim, P.T. and C.J. Ong, *Differentiation of definitive endoderm from mouse embryonic stem cells*. Results Probl Cell Differ, 2012. **55**: p. 303-19.
23. Marikawa, Y. and V.B. Alarcón, *Establishment of trophectoderm and inner cell mass lineages in the mouse embryo*. Mol Reprod Dev, 2009. **76**(11): p. 1019-32.
24. Zhong, W., et al., *Wnt and Nodal signaling simultaneously induces definitive endoderm differentiation of mouse embryonic stem cells*. Rom J Morphol Embryol, 2017. **58**(2): p. 527-535.
25. Pimton, P., et al., *Hypoxia enhances differentiation of mouse embryonic stem cells into definitive endoderm and distal lung cells*. Stem Cells Dev, 2015. **24**(5): p. 663-76.
26. Kim, P.T., et al., *Differentiation of mouse embryonic stem cells into endoderm without embryoid body formation*. PLoS One, 2010. **5**(11): p. e14146.
27. Kaitsuka, T., et al., *Erythropoietin facilitates definitive endodermal differentiation of mouse embryonic stem cells via activation of ERK signaling*. Am J Physiol Cell Physiol, 2017. **312**(5): p. C573-c582.
28. Shoji, M., et al., *Different murine-derived feeder cells alter the definitive endoderm differentiation of human induced pluripotent stem cells*. PLoS One, 2018. **13**(7): p. e0201239.
29. Daneshvar, K., et al., *DIGIT Is a Conserved Long Noncoding RNA that Regulates GSC Expression to Control Definitive Endoderm Differentiation of Embryonic Stem Cells*. Cell Rep, 2016. **17**(2): p. 353-365.
30. Chen, A.C.H., et al., *Hyperglycemia impedes definitive endoderm differentiation of human embryonic stem cells by modulating histone methylation patterns*. Cell Tissue Res, 2017. **368**(3): p. 563-578.
31. Wang, P., et al., *A molecular signature for purified definitive endoderm guides differentiation and isolation of endoderm from mouse and human embryonic stem cells*. Stem Cells Dev, 2012. **21**(12): p. 2273-87.
32. Jiang, W., et al., *WNT3 is a biomarker capable of predicting the definitive endoderm differentiation potential of hESCs*. Stem Cell Reports, 2013. **1**(1): p. 46-52.
33. Geng, Y. and B. Feng, *Mesendogen, a novel inhibitor of TRPM6, promotes mesoderm and definitive endoderm differentiation of human embryonic stem cells through alteration of magnesium homeostasis*. Heliyon, 2015. **1**(4): p. e00046.

34. Jacobson, E.F., et al., *Non-xenogeneic expansion and definitive endoderm differentiation of human pluripotent stem cells in an automated bioreactor*. *Biotechnol Bioeng*, 2021. **118**(2): p. 979-991.
35. Eldridge, C.B., et al., *A p53-Dependent Checkpoint Induced upon DNA Damage Alters Cell Fate during hiPSC Differentiation*. *Stem Cell Reports*, 2020. **15**(4): p. 827-835.
36. Smith, K.N., A.M. Singh, and S. Dalton, *Myc represses primitive endoderm differentiation in pluripotent stem cells*. *Cell Stem Cell*, 2010. **7**(3): p. 343-54.
37. Mehta, A., et al., *Assessment of drug induced developmental toxicity using human embryonic stem cells*. *Cell Biol Int*, 2008. **32**(11): p. 1412-24.
38. Outten, J.T., et al., *A high-throughput multiplexed screening assay for optimizing serum-free differentiation protocols of human embryonic stem cells*. *Stem Cell Res*, 2011. **6**(2): p. 129-42.
39. Wrighton, P.J., et al., *Signals from the surface modulate differentiation of human pluripotent stem cells through glycosaminoglycans and integrins*. *Proc Natl Acad Sci U S A*, 2014. **111**(51): p. 18126-31.
40. Dzobo, K., M. Vogelsang, and M.I. Parker, *Wnt/ β -Catenin and MEK-ERK Signaling are Required for Fibroblast-Derived Extracellular Matrix-Mediated Endoderm Differentiation of Embryonic Stem Cells*. *Stem Cell Rev Rep*, 2015. **11**(5): p. 761-73.
41. Gokhale, P.J., et al., *Culture adaptation alters transcriptional hierarchies among single human embryonic stem cells reflecting altered patterns of differentiation*. *PLoS One*, 2015. **10**(4): p. e0123467.
42. Wade, S.L., et al., *MiRNA-Mediated Regulation of the SWI/SNF Chromatin Remodeling Complex Controls Pluripotency and Endodermal Differentiation in Human ESCs*. *Stem Cells*, 2015. **33**(10): p. 2925-35.
43. Ishikawa, D., et al., *miRNome Profiling of Purified Endoderm and Mesoderm Differentiated from hESCs Reveals Functions of miR-483-3p and miR-1263 for Cell-Fate Decisions*. *Stem Cell Reports*, 2017. **9**(5): p. 1588-1603.
44. Xiao, L., et al., *Tuning FOXD3 expression dose-dependently balances human embryonic stem cells between pluripotency and meso-endoderm fates*. *Biochim Biophys Acta Mol Cell Res*, 2019. **1866**(12): p. 118531.
45. Fang, Y., et al., *Histone crotonylation promotes mesoendodermal commitment of human embryonic stem cells*. *Cell Stem Cell*, 2021. **28**(4): p. 748-763.e7.
46. Séguin, C.A., et al., *Establishment of endoderm progenitors by SOX transcription factor expression in human embryonic stem cells*. *Cell Stem Cell*, 2008. **3**(2): p. 182-95.
47. Zhou, J., et al., *Human feeder cells support establishment and definitive endoderm differentiation of human embryonic stem cells*. *Stem Cells Dev*, 2008. **17**(4): p. 737-49.
48. Guo, S., et al., *Activin A supplement in the hESCs culture enhances the endoderm differentiation efficiency*. *Cell Biol Int*, 2014. **38**(7): p. 849-56.
49. Naujok, O., U. Diekmann, and S. Lenzen, *The generation of definitive endoderm from human embryonic stem cells is initially independent from activin A but requires canonical Wnt-signaling*. *Stem Cell Rev Rep*, 2014. **10**(4): p. 480-93.
50. Yu, J.S., et al., *PI3K/mTORC2 regulates TGF- β /Activin signalling by modulating Smad2/3 activity via linker phosphorylation*. *Nat Commun*, 2015. **6**: p. 7212.

51. Carpenedo, R.L., et al., *Transcriptomically Guided Mesendoderm Induction of Human Pluripotent Stem Cells Using a Systematically Defined Culture Scheme*. Stem Cell Reports, 2019. **13**(6): p. 1111-1125.
52. Daneshvar, K., et al., *lncRNA DIGIT and BRD3 protein form phase-separated condensates to regulate endoderm differentiation*. Nat Cell Biol, 2020. **22**(10): p. 1211-1222.
53. He, Y., et al., *Involvement of LIMK2 in actin cytoskeleton remodeling during the definitive endoderm differentiation*. In Vitro Cell Dev Biol Anim, 2021.
54. Kuroda, T., et al., *SALL3 expression balance underlies lineage biases in human induced pluripotent stem cell differentiation*. Nat Commun, 2019. **10**(1): p. 2175.
55. Cui, P., et al., *HIF-1 α /Actl6a/H3K9ac axis is critical for pluripotency and lineage differentiation of human induced pluripotent stem cells*. Faseb j, 2020. **34**(4): p. 5740-5753.
56. Kim, M.H. and M. Kino-oka, *Switching between self-renewal and lineage commitment of human induced pluripotent stem cells via cell-substrate and cell-cell interactions on a dendrimer-immobilized surface*. Biomaterials, 2014. **35**(22): p. 5670-8.
57. Sekine, K., et al., *Highly efficient generation of definitive endoderm lineage from human induced pluripotent stem cells*. Transplant Proc, 2012. **44**(4): p. 1127-9.
58. Hoveizi, E., et al., *Definitive endoderm differentiation of human-induced pluripotent stem cells using signaling molecules and IDE1 in three-dimensional polymer scaffold*. J Biomed Mater Res A, 2014. **102**(11): p. 4027-36.
59. Hanawa, M., et al., *Hepatocyte Nuclear Factor 4 Alpha Promotes Definitive Endoderm Differentiation from Human Induced Pluripotent Stem Cells*. Stem Cell Rev Rep, 2017. **13**(4): p. 542-551.
60. Yabe, S.C., et al., *Definitive endoderm differentiation is promoted in suspension cultured human iPS-derived spheroids more than in adherent cells*. Int J Dev Biol, 2019. **63**(6-7): p. 271-280.
61. Arkenberg, M.R., et al., *Dynamic Click Hydrogels for Xeno-Free Culture of Induced Pluripotent Stem Cells*. Adv Biosyst, 2020. **4**(11): p. e2000129.
62. Oka, S., et al., *ROS control in human iPS cells reveals early events in spontaneous carcinogenesis*. Carcinogenesis, 2020. **41**(1): p. 36-43.
63. Cuomo, A.S.E., et al., *Single-cell RNA-sequencing of differentiating iPS cells reveals dynamic genetic effects on gene expression*. Nat Commun, 2020. **11**(1): p. 810.
64. Saili, K.S., et al., *Molecular characterization of a toxicological tipping point during human stem cell differentiation*. Reprod Toxicol, 2020. **91**: p. 1-13.
65. Peaslee, C., et al., *Doxycycline Significantly Enhances Induction of iPSCs to Endoderm by Enhancing survival via AKT Phosphorylation*. Hepatology, 2021.
66. Gilgenkrantz, H. and A. Collin de l'Hortet, *Understanding Liver Regeneration: From Mechanisms to Regenerative Medicine*. Am J Pathol, 2018. **188**(6): p. 1316-1327.
67. Yin, D.Z., et al., *Mouse A6-positive hepatic oval cells derived from embryonic stem cells*. J Huazhong Univ Sci Technolog Med Sci, 2014. **34**(1): p. 1-9.
68. Hoepfner, J., et al., *Biphasic modulation of Wnt signaling supports efficient foregut endoderm formation from human pluripotent stem cells*. Cell Biol Int, 2016. **40**(5): p. 534-48.

69. Siller, R., et al., *Development of a rapid screen for the endodermal differentiation potential of human pluripotent stem cell lines*. Sci Rep, 2016. **6**: p. 37178.
70. Wruck, W. and J. Adjaye, *Human pluripotent stem cell derived HLC transcriptome data enables molecular dissection of hepatogenesis*. Sci Data, 2018. **5**: p. 180035.
71. Du, C., et al., *Highly efficient and expedited hepatic differentiation from human pluripotent stem cells by pure small-molecule cocktails*. Stem Cell Res Ther, 2018. **9**(1): p. 58.
72. Cao, J., et al., *Differentiation of embryonic stem cells into hepatocytes that coexpress coagulation factors VIII and IX*. Acta Pharmacol Sin, 2010. **31**(11): p. 1478-86.
73. Iwamuro, M., et al., *Comparative analysis of endoderm formation efficiency between mouse ES cells and iPS cells*. Cell Transplant, 2010. **19**(6): p. 831-9.
74. Pauwelyn, K., et al., *Culture of mouse embryonic stem cells with serum but without exogenous growth factors is sufficient to generate functional hepatocyte-like cells*. PLoS One, 2011. **6**(8): p. e23096.
75. Christodoulou, C., et al., *Mouse ES and iPS cells can form similar definitive endoderm despite differences in imprinted genes*. J Clin Invest, 2011. **121**(6): p. 2313-25.
76. Liu, T., et al., *Induction of hepatocyte-like cells from mouse embryonic stem cells by lentivirus-mediated constitutive expression of Foxa2/Hnf4a*. J Cell Biochem, 2013. **114**(11): p. 2531-41.
77. Huang, H.P., et al., *Factors from human embryonic stem cell-derived fibroblast-like cells promote topology-dependent hepatic differentiation in primate embryonic and induced pluripotent stem cells*. J Biol Chem, 2010. **285**(43): p. 33510-33519.
78. Hu, B., et al., *Silver nanoparticles (AgNPs) and AgNO₃ perturb the specification of human hepatocyte-like cells and cardiomyocytes*. Sci Total Environ, 2020. **725**: p. 138433.
79. Li, S., et al., *TGF β -dependent mitochondrial biogenesis is activated during definitive endoderm differentiation*. In Vitro Cell Dev Biol Anim, 2020. **56**(5): p. 378-385.
80. Munroe, M., et al., *Telomere Dysfunction Activates p53 and Represses HNF4 α Expression Leading to Impaired Human Hepatocyte Development and Function*. Hepatology, 2020. **72**(4): p. 1412-1429.
81. Liang, X., et al., *Evaluation of the effects of low nanomolar bisphenol A-like compounds' levels on early human embryonic development and lipid metabolism with human embryonic stem cell in vitro differentiation models*. J Hazard Mater, 2021. **407**: p. 124387.
82. Sullivan, G.J., et al., *Generation of functional human hepatic endoderm from human induced pluripotent stem cells*. Hepatology, 2010. **51**(1): p. 329-35.
83. Kondo, Y., et al., *Histone deacetylase inhibitor valproic acid promotes the differentiation of human induced pluripotent stem cells into hepatocyte-like cells*. PLoS One, 2014. **9**(8): p. e104010.
84. Hoveizi, E., et al., *Differential effect of Activin A and WNT3a on definitive endoderm differentiation on electrospun nanofibrous PCL scaffold*. Cell Biol Int, 2015. **39**(5): p. 591-9.
85. Jafarpour, Z., et al., *Efficient Production of Hepatocyte-like Cells from Human-induced Pluripotent Stem Cells by Optimizing Growth Factors*. Int J Organ Transplant Med, 2018. **9**(2): p. 77-87.
86. Alsaeedi, F., et al., *Expression of serine/threonine protein kinase SGK1F promotes an hepatoblast state in stem cells directed to differentiate into hepatocytes*. PLoS One, 2019. **14**(6): p. e0218135.

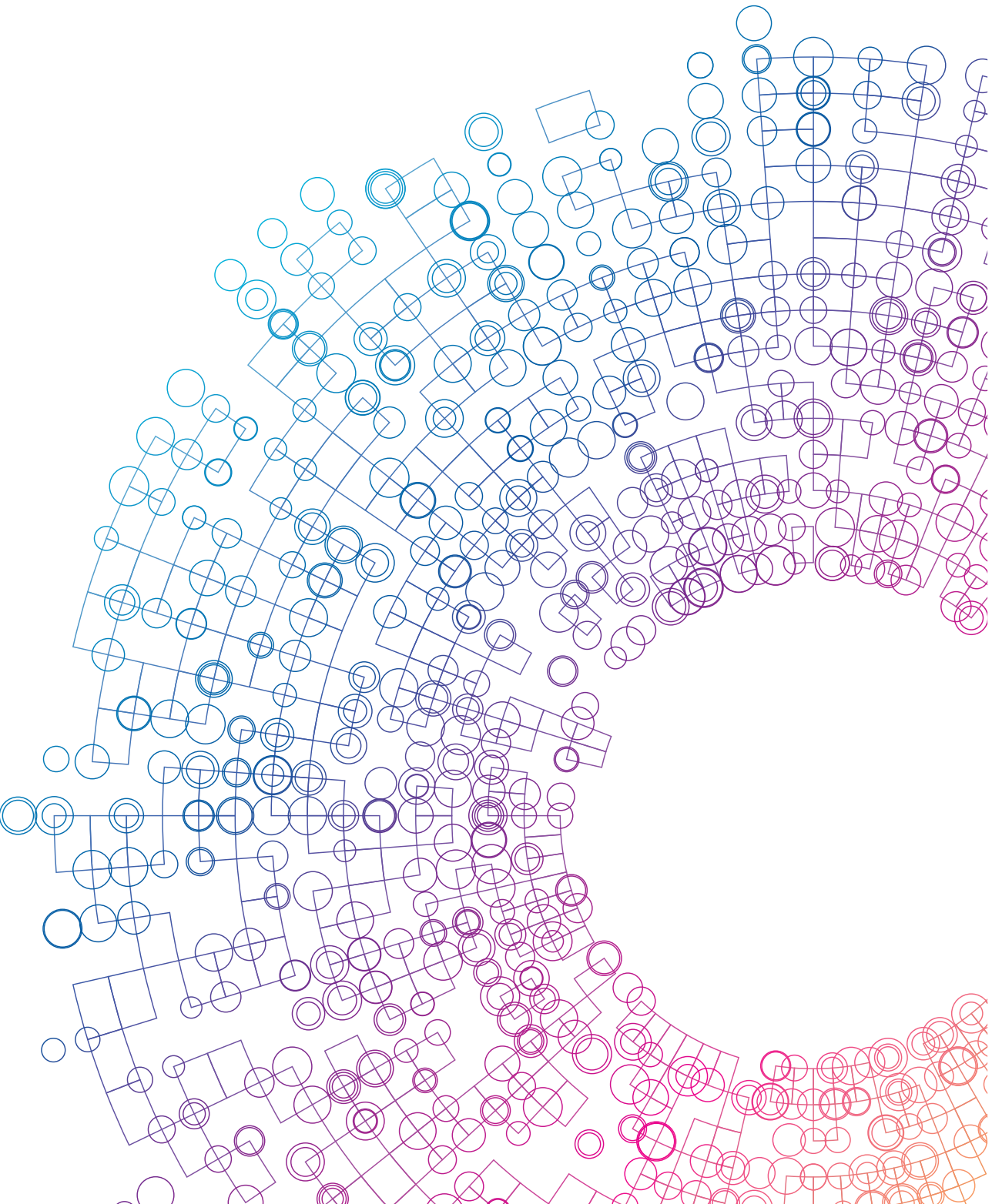
87. Nakai, S., et al., *Collagen vitrigel promotes hepatocytic differentiation of induced pluripotent stem cells into functional hepatocyte-like cells*. Biol Open, 2019. **8**(7).
88. Jennings, R.E., et al., *Human pancreas development*. Development, 2015. **142**(18): p. 3126-37.
89. Bernardo, A.S., et al., *Biphasic induction of Pdx1 in mouse and human embryonic stem cells can mimic development of pancreatic beta-cells*. Stem Cells, 2009. **27**(2): p. 341-51.
90. Liu, S.H. and L.T. Lee, *Efficient differentiation of mouse embryonic stem cells into insulin-producing cells*. Exp Diabetes Res, 2012. **2012**: p. 201295.
91. Kaitsuka, T., et al., *Generation of functional insulin-producing cells from mouse embryonic stem cells through 804G cell-derived extracellular matrix and protein transduction of transcription factors*. Stem Cells Transl Med, 2014. **3**(1): p. 114-27.
92. Salguero-Aranda, C., et al., *Differentiation of Mouse Embryonic Stem Cells toward Functional Pancreatic β -Cell Surrogates through Epigenetic Regulation of Pdx1 by Nitric Oxide*. Cell Transplant, 2016. **25**(10): p. 1879-1892.
93. Santamaria, P., et al., *Turning human epidermis into pancreatic endoderm*. Rev Diabet Stud, 2010. **7**(2): p. 158-67.
94. Rostovskaya, M., N. Bredenkamp, and A. Smith, *Towards consistent generation of pancreatic lineage progenitors from human pluripotent stem cells*. Philos Trans R Soc Lond B Biol Sci, 2015. **370**(1680): p. 20140365.
95. Pezzolla, D., et al., *Resveratrol ameliorates the maturation process of β -cell-like cells obtained from an optimized differentiation protocol of human embryonic stem cells*. PLoS One, 2015. **10**(3): p. e0119904.
96. Trott, J., et al., *Mitchell-Riley syndrome iPSCs exhibit reduced pancreatic endoderm differentiation due to a mutation in RFX6*. Development, 2020. **147**(21).
97. Jiang, W., et al., *In vitro derivation of functional insulin-producing cells from human embryonic stem cells*. Cell Res, 2007. **17**(4): p. 333-44.
98. Lie, K.H., B.E. Tuch, and K.S. Sidhu, *Suppression of NANOG induces efficient differentiation of human embryonic stem cells to pancreatic endoderm*. Pancreas, 2012. **41**(1): p. 54-64.
99. Brafman, D.A., et al., *Regulation of endodermal differentiation of human embryonic stem cells through integrin-ECM interactions*. Cell Death Differ, 2013. **20**(3): p. 369-81.
100. Lee, D.H., et al., *Proteomic identification of overexpressed adenomatous polyposis coli and cyclin B3 during endoderm differentiation from human embryonic stem cells*. Pancreas, 2011. **40**(2): p. 271-80.
101. Wang, H., et al., *Improvement of Cell Survival During Human Pluripotent Stem Cell Definitive Endoderm Differentiation*. Stem Cells Dev, 2015. **24**(21): p. 2536-46.
102. Tsei, A., et al., *Suppression of p38-MAPK endows endoderm propensity to human embryonic stem cells*. Biochem Biophys Res Commun, 2020. **527**(3): p. 811-817.
103. Thurner, M., et al., *Genes Associated with Pancreas Development and Function Maintain Open Chromatin in iPSCs Generated from Human Pancreatic Beta Cells*. Stem Cell Reports, 2017. **9**(5): p. 1395-1405.
104. Tsugata, T., et al., *Role of Egr1 on Pancreatic Endoderm Differentiation*. Cell Med, 2018. **10**: p. 2155179017733177.
105. Mokhber Dezfouli, M.R., et al., *Hydrocortisone Promotes Differentiation of Mouse Embryonic Stem Cell-Derived Definitive Endoderm toward Lung Alveolar Epithelial Cells*. Cell J, 2019. **20**(4): p. 469-476.

106. Ninomiya, N., et al., *BMP signaling regulates the differentiation of mouse embryonic stem cells into lung epithelial cell lineages*. *In Vitro Cell Dev Biol Anim*, 2013. **49**(3): p. 230-7.
107. Noguchi, T.K. and A. Kurisaki, *Formation of Stomach Tissue by Organoid Culture Using Mouse Embryonic Stem Cells*. *Methods Mol Biol*, 2017. **1597**: p. 217-228.
108. Kawai, N., et al., *Induction of lung-like cells from mouse embryonic stem cells by decellularized lung matrix*. *Biochem Biophys Res Commun*, 2018. **15**: p. 33-38.
109. Sahabian, A., et al., *Chemically-Defined, Xeno-Free, Scalable Production of hPSC-Derived Definitive Endoderm Aggregates with Multi-Lineage Differentiation Potential*. *Cells*, 2019. **8**(12).
110. Li, Q.V., et al., *Genome-scale screens identify JNK-JUN signaling as a barrier for pluripotency exit and endoderm differentiation*. *Nat Genet*, 2019. **51**(6): p. 999-1010.
111. Banerjee, P., et al., *Long Noncoding RNA RP11-380D23.2 Drives Distal-Proximal Patterning of the Lung by Regulating PITX2 Expression*. *Stem Cells*, 2018. **36**(2): p. 218-229.
112. Konuma, N., et al., *Mouse embryonic stem cells give rise to gut-like morphogenesis, including intestinal stem cells, in the embryoid body model*. *Stem Cells Dev*, 2009. **18**(1): p. 113-26.
113. Cao, L., et al., *Intestinal lineage commitment of embryonic stem cells*. *Differentiation*, 2011. **81**(1): p. 1-10.
114. Li, P., et al., *CFTR constrains the differentiation from mouse embryonic stem cells to intestine lineage cells*. *Biochem Biophys Res Commun*, 2019. **510**(2): p. 322-328.
115. Noguchi, T.K., et al., *Generation of stomach tissue from mouse embryonic stem cells*. *Nat Cell Biol*, 2015. **17**(8): p. 984-93.
116. Ogaki, S., et al., *A cost-effective system for differentiation of intestinal epithelium from human induced pluripotent stem cells*. *Sci Rep*, 2015. **5**: p. 17297.
117. Ferretti, E. and A.K. Hadjantonakis, *Mesoderm specification and diversification: from single cells to emergent tissues*. *Curr Opin Cell Biol*, 2019. **61**: p. 110-116.
118. Acloque, H., et al., *Epithelial-mesenchymal transitions: the importance of changing cell state in development and disease*. *J Clin Invest*, 2009. **119**(6): p. 1438-49.
119. Balmer, S., S. Nowotschin, and A.K. Hadjantonakis, *Notochord morphogenesis in mice: Current understanding & open questions*. *Dev Dyn*, 2016. **245**(5): p. 547-57.
120. Pu, Q., K. Patel, and R. Huang, *The lateral plate mesoderm: a novel source of skeletal muscle*. *Results Probl Cell Differ*, 2015. **56**: p. 143-63.
121. Shelton, M., et al., *Derivation and expansion of PAX7-positive muscle progenitors from human and mouse embryonic stem cells*. *Stem Cell Reports*, 2014. **3**(3): p. 516-29.
122. Song, C., et al., *Elevated Exogenous Pyruvate Potentiates Mesodermal Differentiation through Metabolic Modulation and AMPK/mTOR Pathway in Human Embryonic Stem Cells*. *Stem Cell Reports*, 2019. **13**(2): p. 338-351.
123. Mae, S., et al., *Combination of small molecules enhances differentiation of mouse embryonic stem cells into intermediate mesoderm through BMP7-positive cells*. *Biochem Biophys Res Commun*, 2010. **393**(4): p. 877-82.
124. Oeda, S., et al., *Induction of intermediate mesoderm by retinoic acid receptor signaling from differentiating mouse embryonic stem cells*. *Int J Dev Biol*, 2013. **57**(5): p. 383-9.

125. Jagtap, S., et al., *Cytosine arabinoside induces ectoderm and inhibits mesoderm expression in human embryonic stem cells during multilineage differentiation*. Br J Pharmacol, 2011. **162**(8): p. 1743-56.
126. Peng, Q., et al., *Connexin 43 is involved in early differentiation of human embryonic stem cells*. Differentiation, 2019. **105**: p. 33-44.
127. Venables, J.P., et al., *MBNL1 and RBFOX2 cooperate to establish a splicing programme involved in pluripotent stem cell differentiation*. Nat Commun, 2013. **4**: p. 2480.
128. Przybyla, L., J.N. Lakins, and V.M. Weaver, *Tissue Mechanics Orchestrate Wnt-Dependent Human Embryonic Stem Cell Differentiation*. Cell Stem Cell, 2016. **19**(4): p. 462-475.
129. Wang, C.K., et al., *CHAC2 is essential for self-renewal and glutathione maintenance in human embryonic stem cells*. Free Radic Biol Med, 2017. **113**: p. 439-451.
130. Chhabra, S., et al., *Dissecting the dynamics of signaling events in the BMP, WNT, and NODAL cascade during self-organized fate patterning in human gastruloids*. PLoS Biol, 2019. **17**(10): p. e3000498.
131. Jaklin, M., et al., *Focus on germ-layer markers: A human stem cell-based model for in vitro teratogenicity testing*. Reprod Toxicol, 2020. **98**: p. 286-298.
132. Tachikawa, S., et al., *Thalidomide induces apoptosis during early mesodermal differentiation of human induced pluripotent stem cells*. In Vitro Cell Dev Biol Anim, 2018. **54**(3): p. 231-240.
133. Otomo, N., et al., *Bi-allelic loss of function variants of TBX6 causes a spectrum of malformation of spine and rib including congenital scoliosis and spondylocostal dysostosis*. J Med Genet, 2019. **56**(9): p. 622-628.
134. Shimizu, M., et al., *Thalidomide affects limb formation and multiple myeloma related genes in human induced pluripotent stem cells and their mesoderm differentiation*. Biochem Biophys Rep, 2021. **26**: p. 100978.
135. Kokkinopoulos, I., et al., *Cardiomyocyte differentiation from mouse embryonic stem cells using a simple and defined protocol*. Dev Dyn, 2016. **245**(2): p. 157-65.
136. Lu, Q., et al., *Rapamycin efficiently promotes cardiac differentiation of mouse embryonic stem cells*. Biosci Rep, 2017. **37**(3).
137. Wei, H., et al., *One-step derivation of cardiomyocytes and mesenchymal stem cells from human pluripotent stem cells*. Stem Cell Res, 2012. **9**(2): p. 87-100.
138. Liu, Q., et al., *Genome-Wide Temporal Profiling of Transcriptome and Open Chromatin of Early Cardiomyocyte Differentiation Derived From hiPSCs and hESCs*. Circ Res, 2017. **121**(4): p. 376-391.
139. Jang, J., et al., *Notch inhibition promotes human embryonic stem cell-derived cardiac mesoderm differentiation*. Stem Cells, 2008. **26**(11): p. 2782-90.
140. Zhu, M.X., et al., *Early embryonic sensitivity to cyclophosphamide in cardiac differentiation from human embryonic stem cells*. Cell Biol Int, 2011. **35**(9): p. 927-38.
141. Pethe, P., V. Pursani, and D. Bhartiya, *Lineage specific expression of Polycomb Group Proteins in human embryonic stem cells in vitro*. Cell Biol Int, 2015. **39**(5): p. 600-10.
142. Yeo, H.C., et al., *Genome-Wide Transcriptome and Binding Sites Analyses Identify Early FOX Expressions for Enhancing Cardiomyogenesis Efficiency of hESC Cultures*. Sci Rep, 2016. **6**: p. 31068.

143. Jiang, Y., et al., *Disruption of cardiogenesis in human embryonic stem cells exposed to trichloroethylene*. *Environ Toxicol*, 2016. **31**(11): p. 1372-1380.
144. Liu, Q., et al., *Genome-Wide Temporal Profiling of Transcriptome and Open Chromatin of Early Cardiomyocyte Differentiation Derived From hiPSCs and hESCs*. *Circulation research*, 2017. **121**(4): p. 376-391.
145. Pan, L., et al., *Quantitative Proteomics Study Reveals Changes in the Molecular Landscape of Human Embryonic Stem Cells with Impaired Stem Cell Differentiation upon Exposure to Titanium Dioxide Nanoparticles*. *Small*, 2018. **14**(23): p. e1800190.
146. Liu, Q., et al., *Disruption of mesoderm formation during cardiac differentiation due to developmental exposure to 13-cis-retinoic acid*. *Sci Rep*, 2018. **8**(1): p. 12960.
147. Fu, H., et al., *Dioxin and AHR impairs mesoderm gene expression and cardiac differentiation in human embryonic stem cells*. *Sci Total Environ*, 2019. **651**(Pt 1): p. 1038-1046.
148. Yang, Y., et al., *Endogenous IGF Signaling Directs Heterogeneous Mesoderm Differentiation in Human Embryonic Stem Cells*. *Cell Rep*, 2019. **29**(11): p. 3374-3384.e5.
149. Liu, H., et al., *Resveratrol Enhances Cardiomyocyte Differentiation of Human Induced Pluripotent Stem Cells through Inhibiting Canonical WNT Signal Pathway and Enhancing Serum Response Factor-miR-1 Axis*. *Stem Cells Int*, 2016. **2016**: p. 2524092.
150. Zhao, M., et al., *Deciphering Role of Wnt Signalling in Cardiac Mesoderm and Cardiomyocyte Differentiation from Human iPSCs: Four-dimensional control of Wnt pathway for hiPSC-CMs differentiation*. *Sci Rep*, 2019. **9**(1): p. 19389.
151. Yechikov, S., et al., *NODAL inhibition promotes differentiation of pacemaker-like cardiomyocytes from human induced pluripotent stem cells*. *Stem Cell Res*, 2020. **49**: p. 102043.
152. Fukushima, H., et al., *Specific induction and long-term maintenance of high purity ventricular cardiomyocytes from human induced pluripotent stem cells*. *PLoS One*, 2020. **15**(11): p. e0241287.
153. Ye, D., et al., *Inhibition of cardiomyocyte differentiation of human induced pluripotent stem cells by Ribavirin: Implication for its cardiac developmental toxicity*. *Toxicology*, 2020. **435**: p. 152422.
154. Buttery, L., et al., *Osteogenic differentiation of embryonic stem cells in 2D and 3D culture*. *Methods Mol Biol*, 2011. **695**: p. 281-308.
155. Smith, L.A., et al., *Enhancing osteogenic differentiation of mouse embryonic stem cells by nanofibers*. *Tissue Eng Part A*, 2009. **15**(7): p. 1855-64.
156. Walker, L., et al., *Non-human primate and rodent embryonic stem cells are differentially sensitive to embryotoxic compounds*. *Toxicology reports*, 2014. **2**: p. 165-174.
157. Yu, Y., L. Al-Mansoori, and M. Opas, *Optimized osteogenic differentiation protocol from R1 mouse embryonic stem cells in vitro*. *Differentiation*, 2015. **89**(1-2): p. 1-10.
158. He, P., J. Fu, and D.A. Wang, *Murine pluripotent stem cells derived scaffold-free cartilage grafts from a micro-cavitory hydrogel platform*. *Acta Biomater*, 2016. **35**: p. 87-97.
159. An, S.Y. and J.S. Heo, *Low oxygen tension modulates the osteogenic differentiation of mouse embryonic stem cells*. *Tissue Cell*, 2018. **52**: p. 9-16.
160. Martinez, I.K.C., et al., *Video-based kinetic analysis of calcification in live osteogenic human embryonic stem cell cultures reveals the developmentally toxic effect of Snus tobacco extract*. *Toxicol Appl Pharmacol*, 2019. **363**: p. 111-121.

161. Jin, H., et al., *Increased activity of TNAP compensates for reduced adenosine production and promotes ectopic calcification in the genetic disease ACDC*. *Sci Signal*, 2016. **9**(458): p. ra121.
162. Chen, I.P., *Differentiation of Human Induced Pluripotent Stem Cells (hiPSCs) into Osteoclasts*. *Bio Protoc*, 2020. **10**(24): p. e3854.
163. Fehling, H.J., et al., *Tracking mesoderm induction and its specification to the hemangioblast during embryonic stem cell differentiation*. *Development*, 2003. **130**(17): p. 4217-27.
164. Liao, F.L., et al., *Hematopoietic stem cell-derived exosomes promote hematopoietic differentiation of mouse embryonic stem cells in vitro via inhibiting the miR126/Notch1 pathway*. *Acta Pharmacol Sin*, 2018. **39**(4): p. 552-560.
165. Hirayama, T., et al., *Establishment of mouse embryonic stem cell-derived erythroid progenitor cell lines able to produce functional red blood cells*. *PLoS One*, 2008. **3**(2): p. e1544.
166. Zhang, P., et al., *Short-term BMP-4 treatment initiates mesoderm induction in human embryonic stem cells*. *Blood*, 2008. **111**(4): p. 1933-41.
167. White, M.P., et al., *Limited gene expression variation in human embryonic stem cell and induced pluripotent stem cell-derived endothelial cells*. *Stem Cells*, 2013. **31**(1): p. 92-103.
168. Yuan, X., et al., *Generation of glycosylphosphatidylinositol anchor protein-deficient blood cells from human induced pluripotent stem cells*. *Stem Cells Transl Med*, 2013. **2**(11): p. 819-29.
169. Zhang, B., et al., *Prostaglandin E(2) Is Required for BMP4-Induced Mesoderm Differentiation of Human Embryonic Stem Cells*. *Stem Cell Reports*, 2018. **10**(3): p. 905-919.
170. Kaushik, G., et al., *Engineered Perineural Vascular Plexus for Modeling Developmental Toxicity*. *Adv Healthc Mater*, 2020. **9**(16): p. e2000825.
171. Smith, A.S., et al., *Human iPSC-derived cardiomyocytes and tissue engineering strategies for disease modeling and drug screening*. *Biotechnol Adv*, 2017. **35**(1): p. 77-94.
172. Liu, X., et al., *Differentiation of functional endothelial cells from human induced pluripotent stem cells: A novel, highly efficient and cost effective method*. *Differentiation*, 2016. **92**(4): p. 225-236.
173. Chan, M.M., et al., *Molecular recording of mammalian embryogenesis*. *Nature*, 2019. **570**(7759): p. 77-82.
174. Pijuan-Sala, B., et al., *A single-cell molecular map of mouse gastrulation and early organogenesis*. *Nature*, 2019. **566**(7745): p. 490-495.
175. Cao, J., et al., *The single-cell transcriptional landscape of mammalian organogenesis*. *Nature*, 2019. **566**(7745): p. 496-502.
176. Gadue, P., et al., *Germ layer induction from embryonic stem cells*. *Experimental Hematology*, 2005. **33**(9): p. 955-964.
177. Van Sint Jan, S. and L. Geris, *Modelling towards a more holistic medicine: The Virtual Physiological Human (VPH)*. *Morphologie*, 2019. **103**(343): p. 127-130.
178. Vinken, M., et al., *Safer chemicals using less animals: kick-off of the European ONTOX project*. *Toxicology*, 2021. **458**: p. 152846.
179. Piersma, A.H., et al., *The virtual human in chemical safety assessment*. *Current Opinion in Toxicology*, 2019. **15**: p. 26-32.
180. Baker, N., et al., *Building a developmental toxicity ontology*. *Birth Defects Res*, 2018. **110**(6): p. 502-518.



CHAPTER

Summary and general
discussion

9

Summary and general discussion

This dissertation describes investigations on the murine cardiac embryonic stem cell test (mESTc), expanding on the merits of stem cell research as a tool for predicting chemical hazards to early embryo development. Additionally, this work contributed to our mechanism-based knowledge for hazard assessment of chemicals which in general is of added value as compared to the lacking mechanistic information from the standard developmental toxicity studies conducted in laboratory animals. The achievements in this dissertation include the broad characterization of heterogenous cell differentiation in the mESTc, identifying additional non-cardiomyocyte cell types like neural crest cells (chapter 2 and 3) and neural cells (chapter 4). Further insight was gained on the impact of *in vitro* culture conditions and their impact on the discrimination between different chemical compounds within the mESTc (chapter 6 and 7). Finally, a review of endoderm- and mesoderm-derived cellular pathways employed in embryonic stem cell differentiation research was performed (chapter 8), exploring additional embryonic stem cell differentiation pathways that might be used in the future in novel EST systems.

The overall aim of the research described in this dissertation was to explore the biological domain of the ESTc and to use this knowledge to better discriminate between molecules of the same class of structurally related chemicals, by selecting gene-expression based biomarker profiles beyond cardiac differentiation. This aim was supported by the following objectives:

1. To expand our knowledge on the biological domain of the mESTc.
2. To make progress towards setting a biomarker profile related to mechanisms important in developmental toxicity.
3. To explore whether this biomarker profile can distinguish between similar chemical structures within the same chemical class.
4. To enhance the sensitivity of the assay for detecting biomarkers.

Two approaches were used for identifying gene transcripts as potential biomarkers. A hypothesis-driven targeted approach of biomarker selection based on existing mechanistic knowledge, by studying selected gene pathways based on existing literature. A hypothesis-generating data driven approach of biomarker selection was also taken based on genome wide expression screening.

Summary

Part I: Monitoring selected gene pathways for defining biomarkers in the mESTc

Chapter 2: VPA analogues and neural crest cells

In this study, the presence of NC cells in the ESTc was confirmed by the expression of known NC protein markers. The AP2 α staining indicated the specification of NC cells within ESTc (differentiation day 7), followed by epithelial to mesenchymal transition (EMT) shown by TWIST staining (differentiation day 10). Gene expression analysis confirmed the upregulation of NC marker transcripts with time. This study showed an increased expression of neural plate border specifiers/NC precursor genes (*Msx2*, *Pax3*), NC specifiers (*Sox9*, *Ap2 α*), of NC related genes responsible for its migration and differentiation (*p75*, *Sox9*), and of epithelial to mesenchymal transition (EMT) genes (*Snail*, *Snai2*, *Twist1*) in controls between differentiation days 4 and 10. Additionally, the sensitivity to exposure of the VPA analogues tested differed depending on exposure duration. In summary, we have confirmed the presence of NC cells in the ESTc and demonstrated that gene markers for these cells are more sensitive than those for cardiomyocytes to VPA exposure. The presence of NC in the ESTc and the relations between the different functional gene groups expand our understanding of the biological domain of the ESTc.

Chapter 3: Organophosphates and neural crest cells

Exposure to three OPs resulted in similar patterns between inhibition of beating cardiomyocyte differentiation and reduction of their myosin protein expression on day 10 of the mESTc. However, these three chemically related compounds induced distinctive effects on NC cell differentiation, indicated by changes in gene transcript expression levels of the NC precursor (*Msx2*), NC marker (*Ap2 α*), and epithelial to mesenchymal transition (EMT; *Snai2*). This study shows that investigating NC markers can provide added value for ESTc outcome profiling and may enhance the applicability of this assay for screening and discriminating structurally related test chemicals.

Chapter 4: Morpholines, piperidines and neurogenesis

Whereas in chapter 2 and 3 neural crest (NC) cells contributed in distinguishing within the two structurally related chemical families: the VPA analogues class and within the organophosphate class, this was not the case for a further two: within

the classes of morpholines and piperidines. In this chapter a clear difference was observed in the early gene expression levels in the retinoic acid and cholesterol biosynthesis pathways and in the late gene expression levels related to cell type specific markers for cardiomyocyte differentiation and neurogenesis.

Taken together the results of part I in this dissertation, the selected gene pathways in the mESTc contributed to our mechanistic knowledge of the biological domain. Different structurally related chemical families can perturb a different part within that biological domain. Within structurally similar chemical families, the use of additional pathways can enhance the sensitivity of the mESTc.

Part II: Genome-wide monitoring of gene expression for defining biomarkers in the mESTc

Chapter 5: morpholines, piperidines and differentiation routes

A genome-wide gene expression screening was performed to map the range of differentiation routes in the ESTc and to search for a biomarker profile predictive of embryotoxicity. The detected differentiation routes included circulatory system development, skeletal system development, heart development, muscle and organ tissue development, and nervous system and cell development. The morpholines and piperidines were assessed for perturbation of these differentiation routes. In addition to the cardiomyocyte readout, alternative differentiation routes were also regulated, in a concentration-response fashion. Despite the structural differences between the test compounds, their gene expression effect patterns were largely comparable. However, uniquely regulated genes were found for each test compound that could help predict specific adverse effects of individual test compounds, without testing *in vivo*. These similar and unique regulations of gene expression by the tested compounds add to our knowledge of the chemical applicability domain of the ESTc.

Part III: The influence of culture conditions on embryonic stem cell differentiation

Chapter 6: The influence of oxygen on pluripotency and differentiation to cardiomyocytes (ESTc) and neurons (ESTn)

The influence of oxygen tension (O₂) in the incubation chamber was studied on ESC pluripotency and differentiation to cardiomyocytes (ESTc) and neurons (ESTn).

Usually, atmospheric levels of 20% oxygen are available during ESC culture and the ESTc and ESTn, however 5% oxygen is considered to be more physiologically relevant. Cardiac differentiation in 5% instead of 20% oxygen in the ESTc resulted in reduced development of spontaneously beating cardiomyocytes and lower expression of cardiac markers *Nkx2.5*, *Myh6* and MF20 (myosin). This observation was independent of whether the ESC had been cultured in 5% or 20% oxygen tension prior to their use in the ESTc. ESCs cultured in 20% oxygen and directed to neural differentiation in 5% oxygen using the ESTn led to relatively more cardiac and neural crest cell differentiation as compared to 20%. The opposite experimental condition with ESCs cultured in 5% oxygen and neural differentiation in 20% oxygen in the ESTn resulted in more glial differentiation. ESC maintained and differentiated in 5% oxygen in the ESTn showed an increase in neural crest and oligodendrocytes as compared to 20% oxygen during stem cell maintenance and differentiation. This study showed major effects of oxygen tension on ESC differentiation in the ESTc and ESTn, making this an important variable to consider when designing and developing a stem cell and biomarker based *in vitro* system.

Chapter 7: The influence of oxygen on compound sensitivity in the ESTc

The influence of O₂ on FLU and VPA sensitivity in the ESTc were studied including effects on gene transcript biomarkers. At differentiation day 4, gene expression values were primarily driven by the level of O₂ during ESC culture instead of exposure to FLU. In addition, using ESCs cultured under 5% O₂ tension, VPA exposure enhanced *Nes* (ectoderm) expression. *Bmp4* (mesoderm) was enhanced in the ESTc by VPA exposure when using ESCs cultured under 20% O₂. At differentiation day 10, using ESCs cultured under 5% instead of 20% O₂, *Nkx2.5* and *Myh6* (cardiomyocytes) were less affected after exposure to FLU or VPA. These results show that O₂ tension in ESC culture influences chemical sensitivity in the ESTc. This enhances awareness of the importance of standardization of culture conditions, which may influence the readout of the ESTc and consequently may impact the interpretation of the test outcome.

Chapter 8: The influence of inducers on differentiation routes between species

This review summarizes the current approaches to differentiate murine and human pluripotent stem cells towards the endoderm and mesoderm and a selection of its derivatives. Also, a list of biomarkers corresponding to these differentiated cell types is provided. In the future, these differentiation approaches in combination with the

linked biomarkers could be used to investigate teratogenic effects of compounds on multiple differentiation routes present in heterogenic stem cell differentiation. This would contribute to an enlarged EST spectrum and incorporation of multiple (EST) test systems into a test battery could lead to an improvement of *in vitro* hazard assessments.

Summarizing part III of this dissertation, culture conditions as oxygen level and specific inducers influence the status of the ESC or the direction of pluripotent stem cell differentiation. Consequently, the sensitivity to gene transcript biomarkers was affected when exposure chemicals were tested for developmental perturbation within the mESTc. This should be taken into account when applying the mESTc in a test battery for quantitative hazard assessment of chemicals.

General discussion

1. The biological domain

Biology related to developmental pathways

In general, identifying the biological domain of an assay contributes to understanding which part of the human biology is represented. The available biology within an assay can be compared to known human biological processes [1]. Understanding this biology gives mechanistic insight and can add to substantiated predictions of chemical interference with human biology [2-4]. The intended effects and the adverse effects are usually predicted by animal studies, which may differ from the human biology but consist of a complete biological system. *In vitro* assays only represent a part of the biology that needs to be protected. To overcome false negatives, it is of use to know to what part of the biology chemicals may respond. This comparison is more established for medicinal drugs as they are generally developed to have a therapeutic effect on human biology. For plant protection products (PPPs), the identification of the affected biological domain is more complex as the effects on human biology are often unclear because the intended mode of action (MOA) is directed to non-mammalian organisms including fungi, insects or plants. These pesticide target MOAs are summarised in the MOA posters by the Fungicide Resistance Action Committee (FRAC), the Insecticide Resistance Action Committee (IRAC), and the Herbicide Resistance Action Committee (HRAC) [5-7]. Since the intended PPP's MOA can differ from the adverse effects on

mammalian biology and because these PPP's are not developed to treat human disease, these potential unintended effects require to be investigated.

The mESTc assay consists of a heterogeneous cell population. The targeted cardiomyocytes are formed from the mesodermal germ layer, which forms when the ectoderm and endoderm interact. Clearly, other cell types are needed to enable cardiomyocyte differentiation as exemplified by homogenous mesenchymal stem cells that on their own can't form beating EBs [8, 9]. Each cell type in this heterogeneous population may respond uniquely to the same chemical perturbations resulting in distinct signals and changing transcription factors [10]. Although differentiation to beating cardiomyocytes comprises the targeted differentiation outcome of the mESTc, the identity of concurrent additional cell types has still been largely unknown. Chapters 2-4 describe additional cell types within the mESTc, namely neural crest cells and neural cells. To compare the mESTc situation with *in vivo* development, differentiation day 4, 5, and 6 of the mESTc have been shown to be comparable to embryonic days E5.5, E6.5, and E7.5 in mice, respectively [11]. In the case of neural crest cells, development and migration commences from embryonic day E9.0 onwards in mice [12]. Therefore, embryonic day E9.0 in mice should compare to differentiation day 7 or 8 in the mESTc, which is in concordance with our immunocytochemistry results of AP2 α and TWIST. Monitoring these additional cell types for chemical interference showed added value because of unique effects on their differentiation by the test compounds.

The sub-population of neural crest cells are of relevance to mammalian biology and were regulated by the VPA analogues and organophosphorus compounds (chapter 2 and 3). Also, other studies showed perturbations of *in vitro* cultures of NC cell function and migration by VPA [13-16]. The effects of the OPs CPF, MLT or TPP specifically on NC cell differentiation have been previously studied to a limited extent in other vertebrate species test systems. Tussellino et al. (2016) showed developmental defects caused by CPF on anatomical NC derived cranial structures and NC gene expression levels in *Xenopus laevis* [17]. In the chick (*Gallus domesticus*), exposure to a mixture of CPF and cypermethrin (50%; 5%) during embryo development affected the cranial NC cells and resulted in craniofacial dysmorphism [18]. In zebrafish, impairments in cardiac looping and function defects were observed after exposure to TPP [19-24]. The morpholines, piperidines, and FLU did not affect NC expression levels in the ESTc and were also not known to affect NC cell development (chapter 4). In addition to the NC cell readout, the readout

of neural cell differentiation after regulation by morpholines and piperidines also added to the understanding of the scope of the sensitivity of the biological domain of the ESTc. In studies with the neural embryonic stem cell test (ESTn), neural cell differentiation was also regulated by FLU [25].

In addition to specific cell type differentiation routes, the all-trans retinoic acid (ATRA) homeostasis pathway in the mESTc was affected by VPA analogues, the morpholines and piperidines (chapter 2 and 4). ATRA homeostasis is important in normal embryo development as perturbed ATRA signalling disrupts for example cardiac development and NC cell migration from the neural tube into the pharynx and eventually the heart [26-28]. Effects of VPA on enzyme expression levels of the ATRA homeostasis pathway described in chapter 2 are in concordance with previous findings in literature [29, 30]. The tested morpholines and piperidines had not been well studied in relation to the ATRA pathway before and were shown here to also regulate ATRA related gene expression and therefore showed novel results. The differences in gene expression regulation in the ESTc between these compounds and FLU, indicate differences in the detailed mechanisms of action. Based on the various *in vitro* studies published in ToxCast, modulation of the Cyp26 was identified as the molecular initiating event (MIE) linked to perturbed ATRA homeostasis, resulting in cleft palate formation following exposure to some triazoles such as FLU [31]. In the whole embryo culture (WEC) assay, FLU was predicted as an embryotoxicant because of time-dependent significant upregulation of Cyp26a1 gene expression [32]. Organophosphates were not tested in this dissertation in relation to the ATRA homeostasis pathway. However, literature search reveals that the OPs seem to affect this pathway as well since this was reported following TPP exposure effects in zebrafish [20, 22].

Biology related to the intended MOAs of test compounds

The presence of the NC and neural cell types and the ATRA homeostasis pathway add to our knowledge on the biological domain of the ESTc and this domain can be challenged by the test chemicals with known developmental toxicological properties. This biological domain and therefore the biological processes present within the ESTc determine which chemicals may or may not be suitable in this particular assay and therefore which chemicals may trigger a response in the ESTc. The spectrum of compounds (chemical structures) for which an *in vitro* test is suitable in terms of coverage of their mechanisms of action is described as the

chemical applicability domain. To test this, compounds from different chemical classes have been tested in the ESTc. These chemicals have a range of known MOAs which could be measured within the ESTc in terms of gene expression levels. This is indicative of opportunities for testing chemical classes with the same MOAs. The MOAs examined in this dissertation were the sterol biosynthesis pathway, acetylcholine esterase (AChE) inhibition, and histone deacetylase (HDAC) inhibition.

The sterol biosynthesis pathway is target for the MOA of several fungicides and was investigated for regulation by chemical exposure in order to confirm comparable effects of chemicals with shared MOAs. Triazoles were designed to interfere with this pathway and are known to be predicted correctly as *in vivo* embryotoxicants in the ESTc. Testing the morpholines and piperidines confirmed the robustness of the assay to be able to predict interference with the sterol biosynthesis pathway for ESTc embryotoxicity predictions. Triazoles, morpholines and piperidines all inhibit sterol synthesis in fungi, although interfering at different levels in the sterol biosynthesis pathway. Morpholines and piperidines primarily inhibit sterol $\Delta 14$ -reductase and sterol $\Delta 8, \Delta 7$ -isomerase in the formation of 4,4-dimethylzymosterol or ergosterol, respectively [33]. Azoles inhibit the sterol 14 α -demethylase cytochrome P450 (CYP51), important in demethylation of lanosterol [34, 35].

The tested organophosphates challenge a different part of the biological domain, since they are intended to interfere with AChE for which we showed measurable regulation of gene expression within the ESTc. The effects of OPs on AChE have been extensively studied and they usually inhibit the activity of this enzyme [36-38]. In chapter 3, *Ache* gene expression regulations seemed to be augmented by CPF and TPP (Fig. 3c). Although an inhibition of *Ache* would be expected in default situations, the opposing upregulation of its gene expression after exposure to CPF has been measured before in embryonic stem cells in conditions where the enzymatic activity was inhibited [39]. This exemplifies that an inhibition of an enzyme on protein level does not necessarily show an effect in the same direction on gene expression level.

The previously proposed primary molecular effect of VPA is HDAC inhibition [40]. In the EBs, the *Hdac* gene expression regulations gradually decreased with time (Fig. 3a). This corresponded to HDAC being necessary for pluripotency and therefore decreases as the cells differentiate [41-44]. Cardiac differentiation and

development are also regulated epigenetically, but this mechanism needs more research to identify specific target genes and histone modification mechanisms as reviewed by Kim *et al.* [45].

Overall, selected member genes of these three pathways which are target for MOAs were all detected within the ESTc. This describes additional knowledge of parts of the biological domain that can consequently contribute to the chemical applicability domain of the ESTc. The selected pathways act on different levels. Whereas the cholesterol biosynthesis pathway and AChE captured regulations on an enzymatic level, HDAC influences differentiation on an epigenetic level.

2. A predictive biomarker profile

With the aim to derive sensitive gene expression biomarkers for predicting developmental toxicity, this dissertation used two approaches, a hypothesis-driven targeted approach based on existing literature and a hypothesis-generating data driven approach using genome-wide expression screening. Both approaches were useful in view of the research question.

The hypothesis-driven targeted approach confirmed the presence of a sub-population of NC cells in the ESTc and demonstrated that gene expression markers for these cells can be more sensitive than those for cardiomyocytes demonstrated with VPA exposure (chapter 2). The three chemically related OPs showed distinctive on NC cell markers, indicated by changes in expression levels of the NC precursor (Msx2), NC marker (Ap2 α), and epithelial to mesenchymal transition (EMT; Snai2) gene transcripts (chapter 3). However, this profile is not always sufficient for discriminating compounds as the NC cell related markers contributed to making a distinction within the chemical classes of VPA analogues and organophosphates but were of no added value in the case of testing morpholines and piperidines (chapter 4).

Although this approach is especially successful for addressing and monitoring specific additional cell types within the ESTc, it is not always possible and therefore this method has limitations. A literature driven approach may result in focussing on the 'usual suspects' (known knowns), with the risk of missing out on other relevant but yet less known biomarkers. This literature driven approach also depends on having certain *a priori* knowledge such as the chemical or biological mode of action, whereas making a prediction is especially challenging when starting to

test chemicals with unknown (adverse) effects. Another limitation is that during development key marker genes can be repurposed as they can apply to multiple cell types which can lead to cell type misinterpretation when used alone [46]. Combining markers for the cell type of interest is therefore required [47]. Lastly, evaluating key marker genes risks bias towards a limited set of characterized cell types. For monitoring the full biological domain of an *in vitro* model, single-cell RNA-sequencing is proving to be an extremely powerful tool and would allow for the identification of rare and potentially sensitive cell populations [46, 48-51].

The hypothesis-generating approach can give a more holistic view on effects of chemical classes as in this case which analysed the transcriptomic data of all the genes expressed, not a pre-selected sub-set. As shown in chapter 5, gene expression regulations within GO-terms were concentration dependent and showed differences of the chemical classes of the morpholines and piperidines as compared to the triazole FLU, which seems to be more directed to nervous system development. In previous studies the usefulness of transcriptomics in developmental toxicity predictions has been demonstrated as well. Previous and current findings confirm the utility of assessing gene expression profiling at an early time-point as part of the toxicity screening with the ESTc [52-54]. Also, transcriptomics is useful in describing the mechanistic understanding of adverse events in stem cell differentiation. Liu et al and Merrick even see potential use of transcriptomics in future risk assessment [55-57]. Also, machine learning methods using these transcriptomics data have been employed to evaluate drug toxicity. These methods can help to screen and understand mechanisms of toxicity especially in the early stages of chemical development where early toxicity assessment can greatly reduce expenses and labor time [58].

3. Distinguishing compounds within the same chemical class

In previous studies different structural classes of developmental toxicants were discriminated using gene expression profiling in the ESTc [53]. In this dissertation, the aim was to discriminate structurally related chemicals within classes using the same method but with and additional differentiation-related biomarkers, combined with to cardiomyocyte differentiation. Using the first approach, the chapters 2-4 showed differences in effect levels of additional biomarkers to ESTc which refined the ability to make distinctions on the mechanistic level between

structurally related compounds within the chemical classes. The discriminating capacity of the additional readout depended on the chemical class that was tested.

When studying the VPA analogues, VPA appeared to be the most potent molecule in the ESTc as compared to EHA and EHOL based on our NC related gene expression results, as the most significant changes were induced by VPA (chapter 2). This correlated with *in vivo* rat data indicating VPA as most potent, followed by EHA and EHOL as roughly equipotent compounds as to effective dose [59]. A potency ranking of VPA analogues with respect to inhibition of cardiomyocyte differentiation in the ESTc, compared to *in vivo* embryotoxicity has been conducted before, but used a different set of analogues that showed greater differences related to the cardiomyocyte endpoint as compared to our set of analogues [60]. The assessment of organophosphates also benefitted from the additional readout of NC related gene expression and allowed discrimination between the test compounds that was not observable with the classical readout parameters of beating cardiomyocyte perturbations. The upregulation of the NC cell differentiation marker *Ap2a* by FLU discriminated this compound from the other compounds tested. Both other NC markers showed no difference between compounds. FLU has been shown to alter NC cells in an *ex vivo* model, *in line with the in vitro Ap2a* effect in the ESTc, as Menegola *et al.* exposed rat embryos in culture to teratogenic concentrations of triazoles including FLU, which resulted in a delay in neuropore development, branchial arch alterations, cleft palate formation, but also in alterations in NC cell migration [61, 62]. The additional readout of neural cell differentiation in the current experiments increased the possibility to discriminate between morpholine and piperidine compounds. This was illustrated e.g. by both protein (*TUBB3*), gene expression (*Tubb3*) and axon-like structures, that were affected by all tested compounds but not TDM. In studies with the neural embryonic stem cell test (ESTn), neural cell differentiation was also regulated by FLU [25].

The hypothesis-generating approach to distinguish compounds within the same chemical class indicated which differentiation routes as expressed in GO-terms were affected, indicating a range of possible perturbations *in vivo*, linked to the multiple differentiation routes affected (chapter 5). Other studies have also attempted to prioritise between compounds of the same chemical class using transcriptomics, e.g. phthalates or polycyclic aromatic compounds [54, 63, 64]. Discriminating between compounds of the same chemical class was challenging, as the transcriptomic perturbations were in similar directions for the

morpholines and piperidines (chapter 5). This readout would be particularly useful to differentiate between responders versus non-responders among structurally related compounds.

4. Experimental considerations

Test model and species

To set up a reliable *in vitro* model, every step of the assay should be as well understood as possible including the entire complex of culture conditions. As discussed in chapter 6 and 7, the importance of oxygen tension within the ESTc and ESTn models was identified. There were generally no significant differences between oxygen tensions when studying effects on ESC maintenance cultures alone. Differentiation into cardiomyocytes profited from 20% oxygen tension irrespective of the oxygen tension during ESC culture. An oxygen tension of 5% seemed to stimulate differentiation into endodermal differentiation rather than mesoderm derived cardiomyocytes. Neural differentiation in the ESTn was affected both by different oxygen tensions during stem cell maintenance and during differentiation, which resulted in different distributions of cell types. Relative to continuously culturing in 20% oxygen, the 20-5% oxygen condition seemed to push cells off the neural differentiation track, the 5-20% condition stimulated the cells more towards glial differentiation, and 5-5% showed a more mixed phenotype. Culturing ESCs under 5% O₂ tension instead of 20%, affected the sensitivity to compound exposure of VPA and FLU in the subsequent ESTc.

Other culture conditions can also influence the test outcome, as observed in the ESTn when the culture media concentrations of the nutrients folic acid and methionine influenced sensitivity to methotrexate exposure [65]. Further, the use of serum-free culture media instead of serum containing media would also enhance standardisation and the reproducibility of the ESTc due to the variable composition of natural serum compared to synthetic serum [66]. Additional studies are needed to further finetune culture conditions towards mimicking *in vivo* cellular microenvironments in embryogenesis as well as assessing their impact on effects of a wider array of compounds, to improve relevancy of *in vitro* test readouts. Realistic and relevant outcomes of individual *in vitro* assays are crucially important, as they affect the broader perspective of test batteries and integrated approaches to testing and assessment (IATA) and may ultimately impact quantitative risk assessment.

When aiming to predict the human safety of chemicals, the biological relevance of a test model is important. The ESTc is a murine model and the question is to what extent it applies to human biology. The idea arose that human test systems would be more applicable to the human biology, yet this is still unknown [67]. When comparing species for similarities, such likenesses between species are more comparable on cellular level than at the organism level. The molecular level makes it easier to extrapolate between species, which makes it an advantage to assess the molecular level within the ESTc. The possibility to use human pluripotent cells is promising to make predictions for human safety since interspecies extrapolation is not needed, although the access to and the use of these cells obviously also comes with ethical and legal issues for performing toxicity testing with hESC [68]. *Luz and Tokar* also questioned the level of hESC naivety by means of pluripotency, as the mESC more closely resemble stem cells of the early embryo [68]. Both *Kugler et al.* and *Luz and Tokar* state that species-specific differences are often due to *in vivo* differences in metabolism or toxicokinetics, which may not apply to *in vitro* assays [67, 68]. This means for mESC, hESC and hiPSC, the differentiation routes as a readout for toxicological screens can be of added value if applicable to the human early embryo development. Additionally, differences may exist between cell lines from one species also when derived from one human, linked to inter-individual variability [69, 70]. Such differences were also exemplified in the review in chapter 8. An alternative is the use of human induced pluripotent stem cells (hiPSC), but questions about comparable differentiation potentials still exist as reviewed by *Kugler et al.* [67].

Test protocol

Not only the test model and conditions may influence the possibility to detect developmental toxic chemicals within the assay, but the test set-up related to exposure duration and also influence the study outcome. After all, in developmental toxicology not only the dose makes the poison as Paracelsus described, but also timing. As the ESTc ordinarily takes ten days before differentiation perturbation is examined by beating cardiomyocyte differentiation, the test would benefit from a shorter timeframe when aiming for an HTS method that at the same time would provide more mechanistic information. Previously day four of the differentiation test was proven to show robust gene expression changes already for some known developmental toxicants (azoles, phthalates, etc.) [53, 71-73], and this also seemed to be applicable as a relevant timepoint to detect gene expression perturbations for

the VPA analogues (chapter 2). Also, for the organophosphates the same exposure duration and readout on day four benefitted detection of NC cell gene expression regulations over cardiomyocyte regulations (chapter 3). However, morpholine and piperidine results showed only general cell process regulation effects at day four and cell differentiation-specific effects at day ten (chapter 4 and 5). Since these compounds showed no effect on NC cell expression levels, the early timepoint was less useful. The possibility to use an early timepoint therefore also depends on the differentiation route that is affected and the concurring differentiation timeline of interest. For example, the myosin structures start to form on differentiation day 7 [74]. Also on the gene expression level, *Myh6* for myosin is expressed later during development and was most evidently expressed on differentiation day 14 of the embryonic stem cell line HM1 [75]. The test readout timepoint thus represents a certain window of differentiation that may be differentially perturbed between compound classes.

The chemical concentration influences the assay readout as increasing concentration induced a change in the magnitude of gene expression, making different patterns of gene regulations visible in addition to the classical read-out of beating cardiomyocyte differentiation inhibition. This was exemplified by the differences in statistically significant gene expression regulation at concentrations when 50% of the EBs were inhibited in beating cardiomyocyte differentiation compared to 10%. This phenomenon compares to other literature since Venn diagram analysis revealed that carbamazepine and VPA showed concentration-dependent changes in gene expression in the ESTn, including common genes as well as unique genes regulated by either compound [76, 77]. The PCA plot confirmed these findings, with additional concentration-dependent effects at the level of regulation of the entire genome [77].

Limitations of embryonic stem cell models

Embryonic stem cell models in general are challenged in the determination of the effective concentration *in vitro* and its extrapolation to the effective dose *in vivo*. The biologically effective dose (BED) is the dose that causes a toxicological effect at a target site (receptors, DNA or cytoplasm) and represents the fraction of the dose that interacts inside the cell [78]. These concentrations should not induce overt cell death as this is an indicator but also a confusing factor. However, it is challenging to extrapolate the concentration that is toxic to the cells *in vitro* and

predict the dose that is toxic *in vivo*, since several processes may reduce the cellular uptake of compounds in the mESTc. For example, compounds may interact with laboratory equipment, constituents of the medium, test system or evaporate [78, 79]. Moreover, there is the issue of chemicals that are not water soluble and therefore precipitate in the medium at biological relevant concentrations.

Extrapolating developmental toxicity concentrations to effective human doses is challenged by the limited knowledge on human biology. Investigating human biology is complicated with ethical concerns and our existing knowledge on embryo development is generally based on laboratory animal studies. This means that in practice *in vivo* animal data will probably be needed in order to validate and compare the *in vitro* perturbed mechanisms. The emerging process that may improve this translation is called Quantitative *In Vitro* to *In Vivo* Extrapolation (QIVIVE). The metabolizing capacity of *in vitro* systems is limited if the tissue is not metabolically competent such as in embryonic tissue. Additional test methods that are able to metabolise xenobiotics can overcome this limitation. Additionally, pharmacokinetic parameters differ between *in vitro* and *in vivo* systems [80]. In order to know which transcriptomic regulations are adverse and to what extent, additional *in vitro* or *in silico* tests are necessary including QIVIVE. *In vitro* tests would benefit from prediction models that describe the kinetic behaviour within the organism by e.g. predicting the interaction with organ system and barriers like the placenta [81-83]. Such models could be additional *in silico* test methods, like quantitative structure-activity relationship (QSAR) models [84]. Such models would also improve the prediction of developmental toxicity using the ESTc, where the morpholines and piperidines showed a different potency compared to the *in vivo* findings in rat and rabbit studies and this could be due to kinetic differences (chapter 4 and 5). Also for the organophosphates such additional information would be useful to improve the prediction capacity of the ESTc, since the reactive metabolites that affect embryo development *in vivo* may be different from the *in vivo* dosed 'parent' compound which would be used in the *in vitro* test (chapter 3).

Future perspectives

This dissertation demonstrated a hypothesis-driven literature-based approach and a hypothesis-generating genome-wide sequencing approach for transcriptome based biomarker profile selection. Whereas a hypothesis-driven approach can

apply well for compounds with known MOA, a hypothesis-generating approach will be more useful within chemical classes or structures with unknown MOA. Both approaches gave additional insight into the mechanistic perturbations induced by structurally similar compounds and that could in the future result in a more mechanism-based predictions for toxicity [85]. Alternative methods are already proving useful in terms of screening for indications of compound effects, prioritisation and mechanistic understanding [86]. Knowledge about the biological response scope (applicability domain) of the ESTc should be elaborated e.g. by single cell RNA sequencing or protein-based methods like proteomics or flow cytometry. Since the ESTc consists of a heterogenic cell population, certain genes can apply to multiple cell types and single cell analysis would correct for that. However, no single test can comprehensively predict the safety of a chemical for the complete embryo development.

Adverse outcome pathways (AOPs) describe molecular initiating events (MIE) and key events (KE) from the molecular, to cellular, to tissue, to organ, and to adverse outcomes (AO) on an organism level. The AOP can function as an anchor for the selection of multiple animal alternative test methods in order to generate Integrated Approaches to Testing and Assessment (IATA). Such a strategy has already been implemented for regulatory assessment of skin sensitisation using a combination of *in vitro* and *in silico* methods (OECD, 2021). Testing strategies can be formed based on quantitative adverse outcome pathways (qAOPs) which can describe perturbation of a metabolism pathway such as with ATRA and the formation of craniofacial defects [87, 88].

In order to be able to generate robust AOPs, a systematic representation of knowledge about developmental toxicity (i.e., an ontology) is needed [89]. The generated information in this dissertation could add to ontology formation for developmental toxicity. This could serve as a tool for an integrated assessment of developmental toxicity by combining all existing knowledge into a single developmental ontology for each organism to be protected.

In order to improve the robustness of the ESTc, next steps are needed based on obtained results in this dissertation. The culture conditions should be as optimal as possible in terms of sensitivity and should be improved to meet culture conditions which are as realistic as possible to the human situation. Additionally, in terms of moving forward to a complete animal-free method there is the need to step away

from animal materials as foetal bovine serum (FBS) and in case of histochemistry if possible the use of antibodies. Replacing FBS has already been proven to be successful and can additionally improve standardisation of the test since FBS contains variable components [66].

When knowing the optimal culture conditions and the complete biology of the ESTc, the test should be combined with other test methods by integrating it in test strategies for hazard assessment and prioritisation including modelling of kinetics. To gain awareness and trust in animal alternative test methods it is key to make a change to eventually be able to apply alternatives to animals to the actual practice for risk assessment in the future.

References

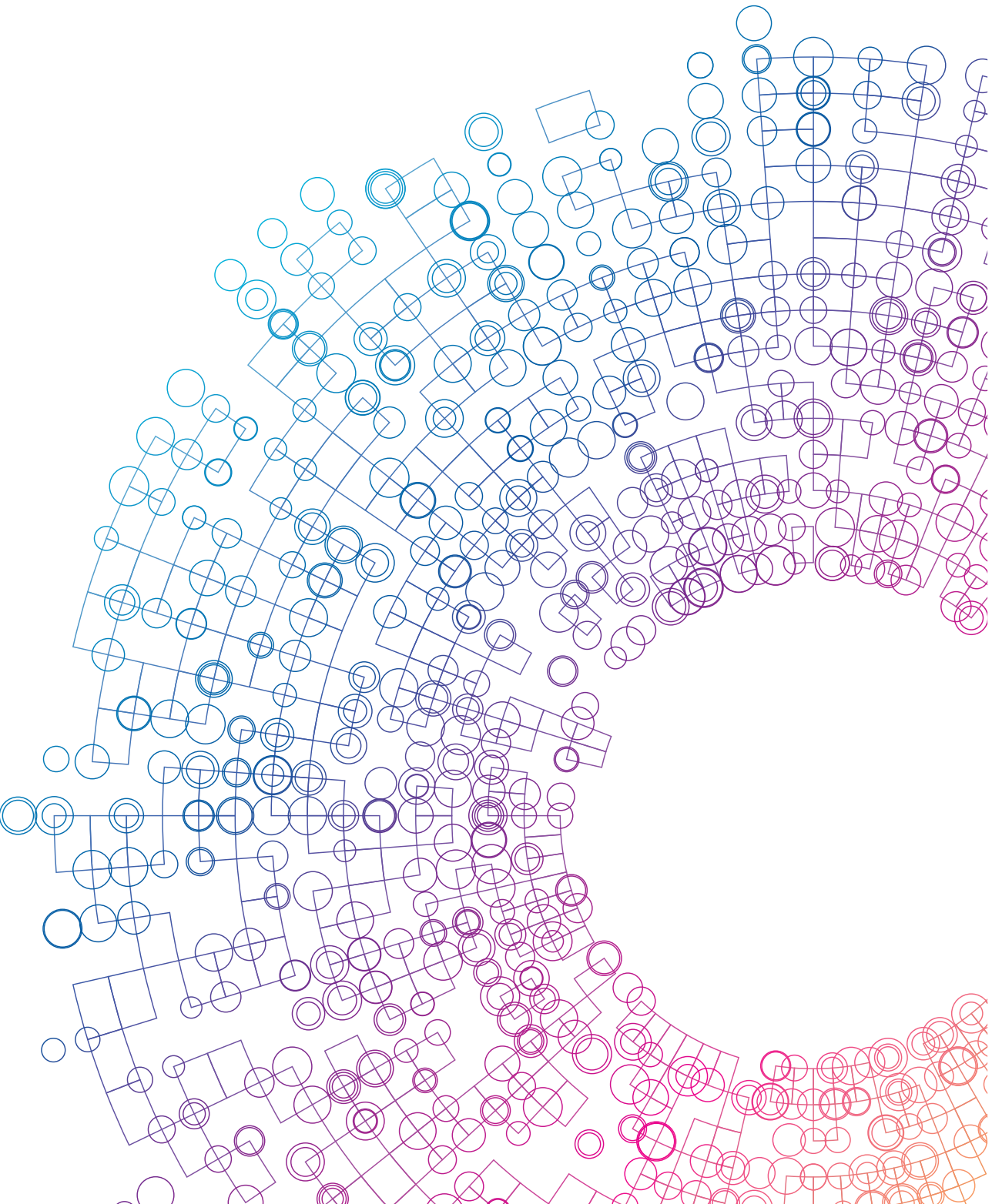
1. ROCHE. *Biochemical pathways*. 2021 [cited 2021 (accessed September 18, 2021)]; Available from: <http://biochemical-pathways.com/#/map/1>.
2. OECD, *Guidance document on the validation and international acceptance of new or updated test methods for hazard assessment*. 2005.
3. Hartung, T., et al., *A modular approach to the ECVAM principles on test validity*. *Altern Lab Anim*, 2004. **32**(5): p. 467-72.
4. Hartung, T., et al., *Systems toxicology*. *Altex*, 2012. **29**(2): p. 119-28.
5. FRAC, *FRAC Classification of Fungicides*. 2021: Fungicide Resistance Action Committee.
6. HRAC, *HRAC Mode of Action Classification 2021*. 2021: Herbicide Resistance Action Committee.
7. IRAC, *IRAC Mode of Action Classification*. 2019: Insecticide Resistance Action Committee.
8. Miskon, A., et al., *A suspension induction for myocardial differentiation of rat mesenchymal stem cells on various extracellular matrix proteins*. *Tissue Eng Part C Methods*, 2010. **16**(5): p. 979-87.
9. Tong, S., et al., *Development of functional If channels in mMSCs after transfection with mHCN4: effects on cell morphology and mechanical activity in vitro*. *Cardiology*, 2009. **112**(2): p. 114-21.
10. Jang, S., et al., *Dynamics of embryonic stem cell differentiation inferred from single-cell transcriptomics show a series of transitions through discrete cell states*. *Elife*, 2017. **6**.
11. Yu, R., et al., *A Modified Murine Embryonic Stem Cell Test for Evaluating the Teratogenic Effects of Drugs on Early Embryogenesis*. *PLoS One*, 2015. **10**(12): p. e0145286.
12. Baggiolini, A., et al., *Premigratory and migratory neural crest cells are multipotent in vivo*. *Cell Stem Cell*, 2015. **16**(3): p. 314-22.
13. Zimmer, B., et al., *Evaluation of developmental toxicants and signaling pathways in a functional test based on the migration of human neural crest cells*. *Environ Health Perspect*, 2012. **120**(8): p. 1116-22.
14. Dreser, N., et al., *Grouping of histone deacetylase inhibitors and other toxicants disturbing neural crest migration by transcriptional profiling*. *Neurotoxicology*, 2015. **50**: p. 56-70.
15. Colleoni, S., et al., *A comparative transcriptomic study on the effects of valproic acid on two different hESCs lines in a neural teratogenicity test system*. *Toxicol Lett*, 2014. **231**(1): p. 38-44.
16. Fuller, L.C., et al., *Neural crest cell motility in valproic acid*. *Reprod Toxicol*, 2002. **16**(6): p. 825-39.
17. Tussellino, M., et al., *Chlorpyrifos exposure affects fgf8, sox9, and bmp4 expression required for cranial neural crest morphogenesis and chondrogenesis in Xenopus laevis embryos*. *Environmental and molecular mutagenesis*, 2016. **57**(8): p. 630-640.
18. Sharma, S., et al., *A combination insecticide at sub-lethal dose debilitated the expression pattern of crucial signalling molecules that facilitate craniofacial patterning in domestic chick Gallus domesticus*. *Neurotoxicology and teratology*, 2019. **76**: p. 106836-106836.
19. Reddam, A., et al., *mRNA-Sequencing Identifies Liver as a Potential Target Organ for Triphenyl Phosphate in Embryonic Zebrafish*. *Toxicological sciences : an official journal of the Society of Toxicology*, 2019. **172**(1): p. 51-62.

20. Mitchell, C.A., et al., *Disruption of Nuclear Receptor Signaling Alters Triphenyl Phosphate-Induced Cardiotoxicity in Zebrafish Embryos*. Toxicological sciences : an official journal of the Society of Toxicology, 2018. **163**(1): p. 307-318.
21. Shi, Q., et al., *Developmental neurotoxicity of triphenyl phosphate in zebrafish larvae*. Aquatic toxicology (Amsterdam, Netherlands), 2018. **203**: p. 80-87.
22. Isales, G.M., et al., *Triphenyl phosphate-induced developmental toxicity in zebrafish: potential role of the retinoic acid receptor*. Aquat Toxicol, 2015. **161**: p. 221-30.
23. Du, Z., et al., *Aryl organophosphate flame retardants induced cardiotoxicity during zebrafish embryogenesis: by disturbing expression of the transcriptional regulators*. Aquatic toxicology (Amsterdam, Netherlands), 2015. **161**: p. 25-32.
24. McGee, S.P., et al., *Aryl phosphate esters within a major PentaBDE replacement product induce cardiotoxicity in developing zebrafish embryos: potential role of the aryl hydrocarbon receptor*. Toxicol Sci, 2013. **133**(1): p. 144-56.
25. Theunissen, P.T., et al., *Compound-specific effects of diverse neurodevelopmental toxicants on global gene expression in the neural embryonic stem cell test (ESTn)*. Toxicol Appl Pharmacol, 2012. **262**(3): p. 330-40.
26. Piersma, A.H., E.V. Hessel, and Y.C. Staal, *Retinoic acid in developmental toxicology: Teratogen, morphogen and biomarker*. Reprod Toxicol, 2017. **72**: p. 53-61.
27. Keyte, A. and M.R. Hutson, *The neural crest in cardiac congenital anomalies*. Differentiation, 2012. **84**(1): p. 25-40.
28. Stefanovic, S. and S. Zaffran, *Mechanisms of retinoic acid signaling during cardiogenesis*. Mech Dev, 2017. **143**: p. 9-19.
29. Kultima, K., et al., *Early transcriptional responses in mouse embryos as a basis for selection of molecular markers predictive of valproic acid teratogenicity*. Reprod Toxicol, 2010. **30**(3): p. 457-68.
30. Jergil, M., et al., *Short-time gene expression response to valproic acid and valproic acid analogs in mouse embryonic stem cells*. Toxicol Sci, 2011. **121**(2): p. 328-42.
31. Baker, N.C., et al., *Characterizing cleft palate toxicants using ToxCast data, chemical structure, and the biomedical literature*. Birth Defects Res, 2020. **112**(1): p. 19-39.
32. Dimopoulou, M., et al., *Flusilazole induces spatio-temporal expression patterns of retinoic acid-, differentiation- and sterol biosynthesis-related genes in the rat Whole Embryo Culture*. Reprod Toxicol, 2016. **64**: p. 77-85.
33. Pan, J., C. Hu, and J.-H. Yu, *Lipid Biosynthesis as an Antifungal Target*. Journal of Fungi, 2018. **4**(2): p. 50.
34. Pan, J., C. Hu, and J.H. Yu, *Lipid Biosynthesis as an Antifungal Target*. J Fungi (Basel), 2018. **4**(2).
35. He, M., et al., *Mutations in the human SC4MOL gene encoding a methyl sterol oxidase cause psoriasisform dermatitis, microcephaly, and developmental delay*. J Clin Invest, 2011. **121**(3): p. 976-84.
36. Costa, L.G., *Current issues in organophosphate toxicology*. Clinica chimica acta; international journal of clinical chemistry, 2006. **366**(1-2): p. 1-13.
37. Commission, E., *Draft Renwal Assessment Report prepared according to the Commission Regulation (EU) No 1107/2009, in Chlorpyrifos*. 2017.
38. Farag, A.T., A.M. El Okazy, and A.F. El-Aswed, *Developmental toxicity study of chlorpyrifos in rats*. Reprod Toxicol, 2003. **17**(2): p. 203-8.

39. Estevan, C., E. Vilanova, and M.A. Sogorb, *Chlorpyrifos and its metabolites alter gene expression at non-cytotoxic concentrations in D3 mouse embryonic stem cells under in vitro differentiation: considerations for embryotoxic risk assessment*. *Toxicol Lett*, 2013. **217**(1): p. 14-22.
40. Eikel, D., A. Lampen, and H. Nau, *Teratogenic effects mediated by inhibition of histone deacetylases: evidence from quantitative structure activity relationships of 20 valproic acid derivatives*. *Chem Res Toxicol*, 2006. **19**(2): p. 272-8.
41. Lv, W., et al., *Histone deacetylase 1 and 3 regulate the mesodermal lineage commitment of mouse embryonic stem cells*. *PLoS One*, 2014. **9**(11): p. e113262.
42. Kidder, B.L. and S. Palmer, *HDAC1 regulates pluripotency and lineage specific transcriptional networks in embryonic and trophoblast stem cells*. *Nucleic Acids Res*, 2012. **40**(7): p. 2925-39.
43. Dovey, O.M., C.T. Foster, and S.M. Cowley, *Histone deacetylase 1 (HDAC1), but not HDAC2, controls embryonic stem cell differentiation*. *Proc Natl Acad Sci U S A*, 2010. **107**(18): p. 8242-7.
44. Jamaladdin, S., et al., *Histone deacetylase (HDAC) 1 and 2 are essential for accurate cell division and the pluripotency of embryonic stem cells*. *Proc Natl Acad Sci U S A*, 2014. **111**(27): p. 9840-5.
45. Kim, Y.J., et al., *Epigenetic Regulation of Cardiomyocyte Differentiation from Embryonic and Induced Pluripotent Stem Cells*. *Int J Mol Sci*, 2021. **22**(16).
46. Posfai, E., et al., *All models are wrong, but some are useful: Establishing standards for stem cell-based embryo models*. *Stem Cell Reports*, 2021. **16**(5): p. 1117-1141.
47. Roost, M.S., et al., *KeyGenes, a Tool to Probe Tissue Differentiation Using a Human Fetal Transcriptional Atlas*. *Stem Cell Reports*, 2015. **4**(6): p. 1112-24.
48. Minn, K.T., et al., *High-resolution transcriptional and morphogenetic profiling of cells from micropatterned human ESC gastruloid cultures*. *Elife*, 2020. **9**.
49. Posfai, E., et al., *Evaluating totipotency using criteria of increasing stringency*. *Nature Cell Biology*, 2021. **23**(1): p. 49-60.
50. Tyser, R.C.V., et al., *A spatially resolved single cell atlas of human gastrulation*. *bioRxiv*, 2020: p. 2020.07.21.213512.
51. van den Brink, S.C., et al., *Single-cell and spatial transcriptomics reveal somitogenesis in gastruloids*. *Nature*, 2020.
52. van Dartel, D.A., et al., *Evaluation of developmental toxicant identification using gene expression profiling in embryonic stem cell differentiation cultures*. *Toxicol Sci*, 2011. **119**(1): p. 126-34.
53. van Dartel, D.A., et al., *Discriminating classes of developmental toxicants using gene expression profiling in the embryonic stem cell test*. *Toxicol Lett*, 2011. **201**(2): p. 143-51.
54. Schulpen, S.H., et al., *Dose response analysis of monophthalates in the murine embryonic stem cell test assessed by cardiomyocyte differentiation and gene expression*. *Reprod Toxicol*, 2013. **35**: p. 81-8.
55. Liu, Z., et al., *Toxicogenomics: A 2020 Vision*. *Trends Pharmacol Sci*, 2019. **40**(2): p. 92-103.
56. Merrick, B.A., *Next generation sequencing data for use in risk assessment*. *Curr Opin Toxicol*, 2019. **18**: p. 18-26.
57. Merrick, B.A., R.S. Paules, and R.R. Tice, *Intersection of toxicogenomics and high throughput screening in the Tox21 program: an NIEHS perspective*. *Int J Biotechnol*, 2015. **14**(1): p. 7-27.

58. Vo, A.H., et al., *An Overview of Machine Learning and Big Data for Drug Toxicity Evaluation*. Chem Res Toxicol, 2020. **33**(1): p. 20-37.
59. Ritter, E.J., et al., *Teratogenicity of di(2-ethylhexyl) phthalate, 2-ethylhexanol, 2-ethylhexanoic acid, and valproic acid, and potentiation by caffeine*. Teratology, 1987. **35**(1): p. 41-6.
60. de Jong, E., et al., *Potency ranking of valproic acid analogues as to inhibition of cardiac differentiation of embryonic stem cells in comparison to their in vivo embryotoxicity*. Reprod Toxicol, 2011. **31**(4): p. 375-82.
61. Menegola, E., et al., *Study on the common teratogenic pathway elicited by the fungicides triazole-derivatives*. Toxicol In Vitro, 2005. **19**(6): p. 737-48.
62. Menegola, E., et al., *Antifungal triazoles induce malformations in vitro*. Reprod Toxicol, 2001. **15**(4): p. 421-7.
63. Yuan, X., et al., *Finding maximal transcriptome differences between reprotoxic and non-reprotoxic phthalate responses in rat testis*. J Appl Toxicol, 2011. **31**(5): p. 421-30.
64. Hsieh, J.-H., et al., *Harnessing In Silico, In Vitro, and In Vivo Data to Understand the Toxicity Landscape of Polycyclic Aromatic Compounds (PACs)*. Chemical Research in Toxicology, 2021. **34**(2): p. 268-285.
65. de Leeuw, V.C., et al., *Culture Conditions Affect Chemical-Induced Developmental Toxicity In Vitro: The Case of Folic Acid, Methionine and Methotrexate in the Neural Embryonic Stem Cell Test*. Altern Lab Anim, 2020. **48**(4): p. 173-183.
66. Riebeling, C., et al., *Defined culture medium for stem cell differentiation: applicability of serum-free conditions in the mouse embryonic stem cell test*. Toxicol In Vitro, 2011. **25**(4): p. 914-21.
67. Kugler, J., et al., *Embryonic stem cells and the next generation of developmental toxicity testing*. Expert Opin Drug Metab Toxicol, 2017. **13**(8): p. 833-841.
68. Luz, A.L. and E.J. Tokar, *Pluripotent Stem Cells in Developmental Toxicity Testing: A Review of Methodological Advances*. Toxicological sciences : an official journal of the Society of Toxicology, 2018. **165**(1): p. 31-39.
69. Allegrucci, C. and L.E. Young, *Differences between human embryonic stem cell lines*. Hum Reprod Update, 2007. **13**(2): p. 103-20.
70. Osafune, K., et al., *Marked differences in differentiation propensity among human embryonic stem cell lines*. Nat Biotechnol, 2008. **26**(3): p. 313-5.
71. van Dartel, D.A., et al., *Early gene expression changes during embryonic stem cell differentiation into cardiomyocytes and their modulation by monobutyl phthalate*. Reprod Toxicol, 2009. **27**(2): p. 93-102.
72. van Dartel, D.A., et al., *Transcriptomics-based identification of developmental toxicants through their interference with cardiomyocyte differentiation of embryonic stem cells*. Toxicol Appl Pharmacol, 2010. **243**(3): p. 420-8.
73. Dimopoulou, M., et al., *A comparison of the embryonic stem cell test and whole embryo culture assay combined with the BeWo placental passage model for predicting the embryotoxicity of azoles*. Toxicol Lett, 2018. **286**: p. 10-21.
74. Mennen, R.H.G., J.L.A.J. Pennings, and A.H.A. Piersma, *Neural crest related gene transcript regulation by valproic acid analogues in the cardiac embryonic stem cell test*. Reproductive toxicology (Elmsford, N.Y.), 2019. **90**: p. 44-52.

75. Rungarunlert, S., et al., *Enhanced cardiac differentiation of mouse embryonic stem cells by use of the slow-turning, lateral vessel (STLV) bioreactor*. *Biotechnol Lett*, 2011. **33**(8): p. 1565-73.
76. Schulpen, S.H., et al., *Comparison of gene expression regulation in mouse- and human embryonic stem cell assays during neural differentiation and in response to valproic acid exposure*. *Reprod Toxicol*, 2015. **56**: p. 77-86.
77. Schulpen, S.H., J.L. Pennings, and A.H. Piersma, *Gene Expression Regulation and Pathway Analysis After Valproic Acid and Carbamazepine Exposure in a Human Embryonic Stem Cell-Based Neurodevelopmental Toxicity Assay*. *Toxicol Sci*, 2015. **146**(2): p. 311-20.
78. Groothuis, F.A., et al., *Dose metric considerations in in vitro assays to improve quantitative in vitro-in vivo dose extrapolations*. *Toxicology*, 2015. **332**: p. 30-40.
79. Kramer, N.I., et al., *Development of a partition-controlled dosing system for cell assays*. *Chemical research in toxicology*, 2010. **23**(11): p. 1806-1814.
80. Daston, G.P., *The theoretical and empirical case for in vitro developmental toxicity screens, and potential applications*. *Teratology*, 1996. **53**(6): p. 339-44.
81. Bremer, S., et al., *Detection of the embryotoxic potential of cyclophosphamide by using a combined system of metabolic competent cells and embryonic stem cells*. *Altern Lab Anim*, 2002. **30**(1): p. 77-85.
82. Sogorb, M.A., et al., *An integrated approach for detecting embryotoxicity and developmental toxicity of environmental contaminants using in vitro alternative methods*. *Toxicol Lett*, 2014. **230**(2): p. 356-67.
83. Fragki, S., et al., *In vitro to in vivo extrapolation of effective dosimetry in developmental toxicity testing: Application of a generic PBK modelling approach*. *Toxicol Appl Pharmacol*, 2017. **332**: p. 109-120.
84. Hareng, L., et al., *The Integrated Project ReProTect: A novel approach in reproductive toxicity hazard assessment*. *Reproductive Toxicology*, 2005. **20**(3): p. 441-452.
85. Krewski, D., et al., *Toxicity testing in the 21st century: progress in the past decade and future perspectives*. *Arch Toxicol*, 2020. **94**(1): p. 1-58.
86. Clements, J.M., et al., *Predicting the safety of medicines in pregnancy: A workshop report*. *Reprod Toxicol*, 2020. **93**: p. 199-210.
87. Menegola, E., et al., *An adverse outcome pathway on the disruption of retinoic acid metabolism leading to developmental craniofacial defects*. *Toxicology*, 2021. **458**: p. 152843.
88. Tonk, E.C., J.L. Pennings, and A.H. Piersma, *An adverse outcome pathway framework for neural tube and axial defects mediated by modulation of retinoic acid homeostasis*. *Reprod Toxicol*, 2015. **55**: p. 104-13.
89. Baker, N., et al., *Building a developmental toxicity ontology*. *Birth Defects Res*, 2018. **110**(6): p. 502-518.



APPENDIX

Nederlandse samenvatting

List of publications

Curriculum Vitae

Dankwoord

Nederlandse samenvatting

Deel I: Monitoring van geselecteerde genroutes voor het definiëren van biomarkers in de embryonale stam cel test (mESTc)

Hoofdstuk 2: valproaat-analogen en neurale lijstcellen

In deze studie werd door expressie van neurale lijst-eiwitmarkers aangetoond dat neurale lijstcellen gevormd worden in de mESTc. De AP2 α -kleuring gaf de specificatie van neurale lijstcellen binnen de mESTc aan (differentiatie dag zeven), gevolgd door epitheliale naar mesenchymale overgang (EMT) aangetoond door middel van een TWIST-kleuring (differentiatie dag tien). Genexpressie analyse bevestigde de opregulatie van transcriptmarkers van neurale lijstcellen in de loop der tijd. Deze studie toonde een verhoogde expressie aan tussen differentiatie dag vier en tien van neurale plaatgrens/neurale lijst-precursorgen (Msx2, Pax3), neurale lijst-specifieke genen (Sox9, Ap2 α), neurale lijst-gerelateerde genen die verantwoordelijk zijn voor de migratie en differentiatie (p75, Sox9), en epitheliaal naar mesenchymaal transitie (EMT) genen (Snai1, Snai2, Twist1). Samenvattend hebben we de aanwezigheid van neurale lijstcellen in de mESTc bevestigd en hebben we aangetoond dat genmarkers voor deze cellen gevoeliger zijn dan die voor cardiomyocyten wanneer blootgesteld aan valproaat (VPA). Bovendien verschilde de gevoeligheid voor blootstelling van de geteste VPA-analogen en was daarnaast de gevoeligheid afhankelijk van de blootstellingsduur. De aanwezigheid van neurale lijstcellen in de mESTc en de relaties tussen de verschillende functionele gengroepen dragen bij aan een beter beeld van het biologische domein van de mESTc.

Hoofdstuk 3: Organofosfaten en neurale lijstcellen

Blootstelling aan organofosfaten (OP's) in de mESTc resulteerde in vergelijkbare patronen van remming van differentiatie naar kloppende cardiomyocyten en van de cardiomyocyt specifieke myosine-eiwitexpressie op dag tien. De drie chemisch verwante OP's induceerden echter onderscheidende effecten op neurale lijstcel differentiatie, aangetoond door veranderingen in expressieniveaus van de neurale lijst precursor (Msx2), neurale lijst-marker (Ap2 α) en epitheliale naar mesenchymale transitie (EMT; Snai2) gen transcripten. Deze studie toont aan dat het onderzoeken van neurale lijst-markers een toegevoegde waarde kan bieden voor de mESTc en daarmee ook de toepasbaarheid van deze test kan verbeteren voor het screenen en onderscheiden van structureel gerelateerde teststoffen.

Hoofdstuk 4: Morfolines, piperidines en neurogenese

Terwijl in hoofdstuk 2 en 3 neurale lijstcellen hebben bijgedragen aan het onderscheid tussen VPA-analogen en organofosfaten, was dit niet het geval voor morfolines en piperidines. In dit hoofdstuk was juist een duidelijk verschil zichtbaar tussen enerzijds vroege genexpressieregulatie in de retinolzuur- en cholesterol biosynthese routes en anderzijds late genexpressieregulatie gerelateerd aan celtype-specifieke markers voor cardiomyocyt differentiatie en neurogenese.

Deel II: Genoombrede monitoring van genexpressie voor het definiëren van biomarkers in de mESTc

Hoofdstuk 5: morfolinen, piperidines en differentiatieroutes

Een expressiescreening van het gehele genoom werd uitgevoerd om aanwezige differentiatieroutes in de ESTc in kaart te brengen en om een voorspellend biomarkerprofiel voor embryotoxiciteit te selecteren. De differentiatieroutes die werden gedetecteerd, waren: de ontwikkeling van het bloedsomloopstelsel, de ontwikkeling van het skelet, de ontwikkeling van het hart, de ontwikkeling van spier- en orgaanweefsel en de ontwikkeling van het zenuwstelsel en zenuwcellen. De morfolinen en piperidines werden getest op verstoring van deze differentiatieroutes. Naast differentiatie naar cardiomyocyten, werden ook alternatieve differentiatieroutes gereguleerd volgens een concentratie-respons relatie. Ondanks de chemisch structurele verschillen tussen de stoffen, waren hun genexpressie-effectpatronen grotendeels vergelijkbaar. Er werden echter ook uniek gereguleerde genen gevonden voor elke testverbinding die kunnen helpen bij het identificeren van specifieke effecten van individuele stoffen. Deze vergelijkbare en unieke regulaties van genexpressie dragen bij aan onze kennis van het chemische toepasbaarheidsdomein van de ESTc.

Deel III: De invloed van kweekomstandigheden op de gevoeligheid van biomarkers in de embryonale stamceldifferentiatie

Hoofdstuk 6: De invloed van zuurstof op pluripotentie en differentiatie naar cardiomyocyten (in de mESTc) en neuronen (in de mESTn)

De invloed van zuurstof werd bestudeerd op pluripotentie van embryonale stamcellen (ESC) en op differentiatie tot cardiomyocyten (mESTc) en neuronen (mESTn). Cardiale differentiatie in 5% in plaats van 20% zuurstof in de mESTc resulteerde

in verminderde ontwikkeling van spontaan kloppende hartspiercellen en lagere expressie van cardiale markers Nkx2.5, Myh6 en MF20 (myosine), ongeacht of ESC was gekweekt in 5% of 20% zuurstofspanning voorafgaand aan hun gebruik in de mESTc. ESCs gekweekt in 20% zuurstof en gericht op neurale differentiatie in 5% zuurstof met behulp van de mESTn leidden tot relatief meer cardiale en neurale cel differentiatie in vergelijking met de controle situatie (20% zuurstof tijdens ESC-kweek en differentiatie). De tegenovergestelde experimentele conditie met ESCs gekweekt in 5% zuurstof en neurale differentiatie in 20% zuurstof in de mESTn resulteerde in meer differentiatie van gliale cellen. ESCs die werden gekweekt en gedifferentieerd in 5% zuurstof in de mESTn vertoonden een toename van neurale lijst en oligodendrocyten in vergelijking met 20% zuurstof tijdens stamcelkweek en differentiatie. Deze studie toonde grote effecten van zuurstofspanning aan op ESC-differentiatie in de mESTc en mESTn. Een geschikte zuurstofspanning is van belang bij het ontwerpen en ontwikkelen van een stamcel- en biomarker gebaseerde *in vitro* systemen.

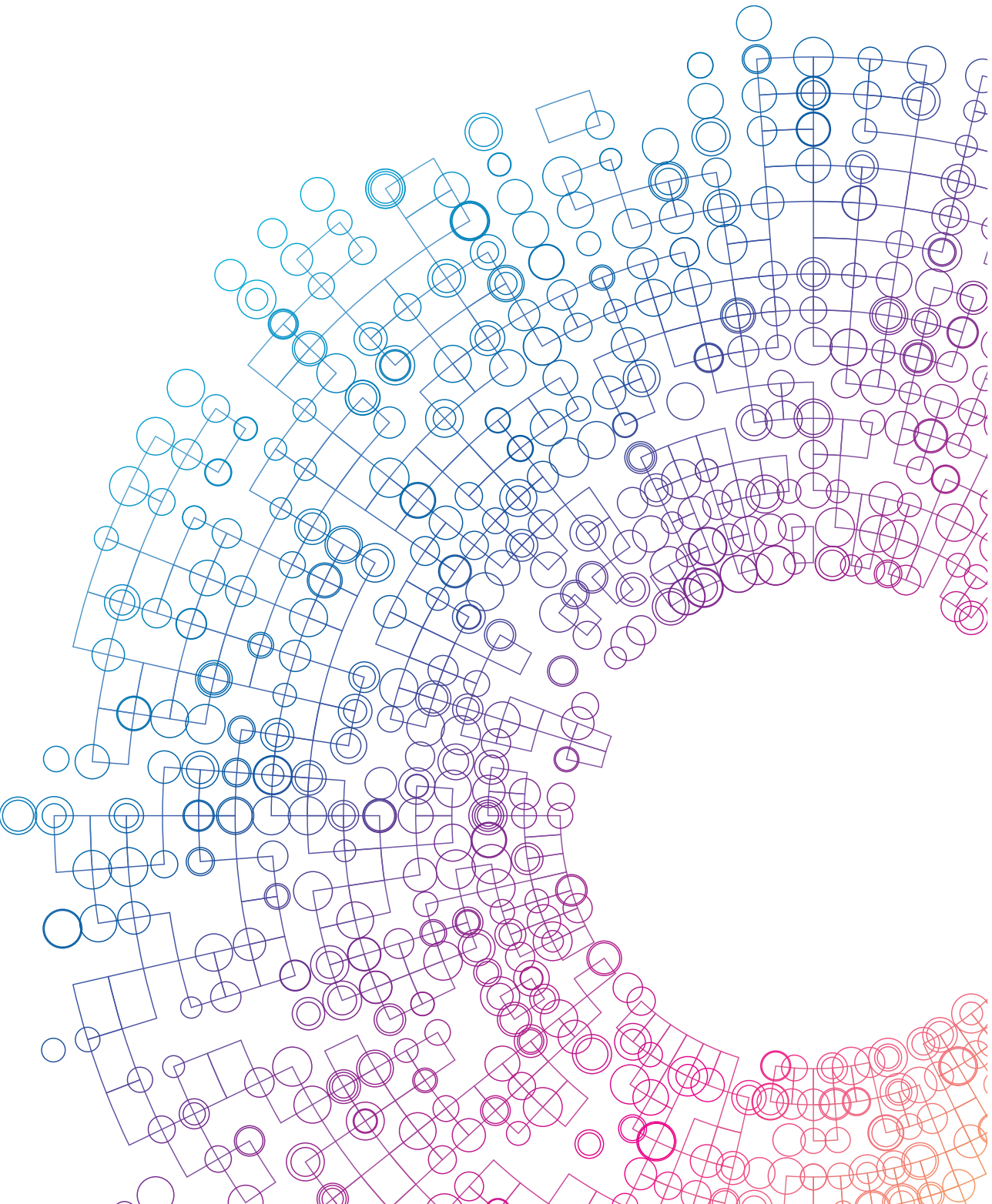
Hoofdstuk 7: De invloed van zuurstof op de gevoeligheid van stoffen in de ESTc

De invloed van O₂ op de gevoeligheid voor flusilazole (FLU) en valproaat (VPA) in de mESTc werd bestudeerd, inclusief effecten op gen transcript biomarkers. Op differentiatie dag vier werden genexpressiewaarden voornamelijk bepaald door het niveau van O₂ tijdens ESC-kweek in plaats van blootstelling aan FLU. Bovendien resulteerde ESC-kweek onder 5% O₂-spanning in een verhoogde Nes (ectoderm) expressie na blootstelling aan VPA. Bmp4 (mesoderm) gen expressie werd verhoogd door blootstelling aan VPA bij gebruik van ESCs gekweekt onder 20% O₂. Op differentiatie dag tien waren Nkx2.5 en Myh6 (cardiomyocyten) minder aangetast na blootstelling aan FLU of VPA wanneer de ESC waren gekweekt onder 5% in plaats van 20% O₂. Deze resultaten laten zien dat de O₂-spanning in de ESC-kweek de stofgevoeligheid in de mESTc beïnvloedt. Deze resultaten benadrukken het belang van standaardisatie van kweekomstandigheden die de gevoeligheid van de mESTc kunnen beïnvloeden en daarmee van invloed kunnen zijn op de toepassing van de mESTc bij kwantitatieve gevarenbeoordeling van stoffen.

Hoofdstuk 8: De invloed van inductoren op differentiatieroutes tussen soorten

Deze review vat de huidige benaderingen samen om pluripotente stamcellen te differentiëren naar endodermale en mesodermale cellen en een selectie van afgeleiden daarvan. Er wordt ook een lijst gegeven van biomarkers die

overeenkomen met deze celtypen. In de toekomst kunnen deze differentiatie routes in combinatie met de gekoppelde biomarkers worden gebruikt om teratogene effecten van stoffen op meerdere differentiatieroutes die aanwezig zijn in heterogene stamceldifferentiatie te onderzoeken. Dit zou bijdragen aan een groter EST-spectrum en de integratie van meerdere (EST)-testsystemen in een testbatterij zou kunnen leiden tot een verbetering van *de in vitro* gevarenbeoordelingen.



APPENDIX

Nederlandse samenvatting

List of publications

Curriculum Vitae

Dankwoord

List of publications

Mennen R.H., Hallmark N., Pallardy M., Bars R., Tinwell H., Piersma A.H. (2022). Genome-wide expression screening in the cardiac embryonic stem cell test shows additional differentiation routes that are regulated by morpholines and piperidines. *Submitted to Current Research in Toxicology*

Mennen, R. H., Oldenburger, M. M., & Piersma, A. H. (2021). Endoderm and mesoderm derivatives in embryonic stem cell differentiation and their use in developmental toxicity testing. *Reproductive toxicology (Elmsford, N.Y.)*, 107, 44–59. Advance online publication. <https://doi.org/10.1016/j.reprotox.2021.11.009>

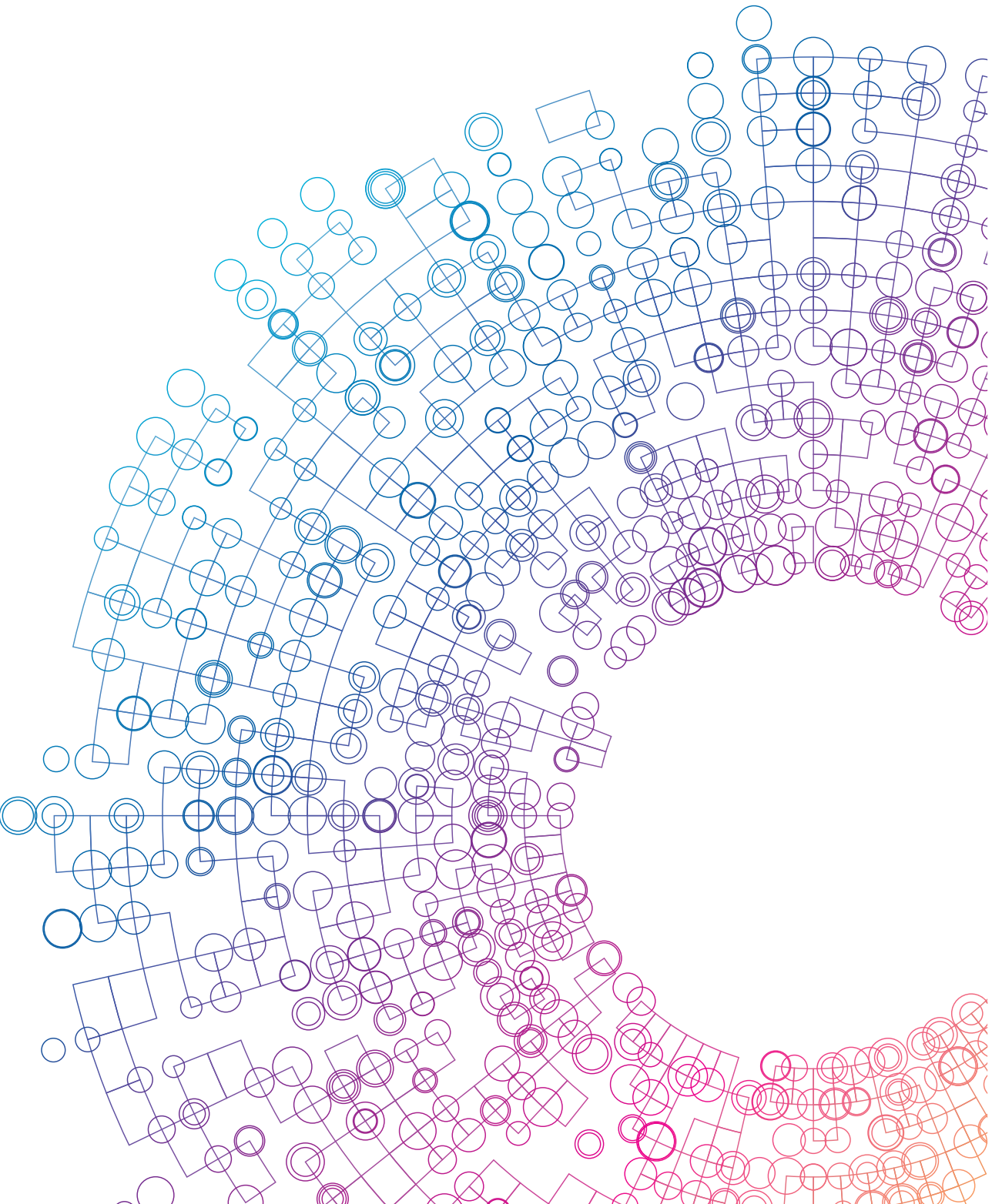
Mennen R.H., Hallmark N., Pallardy M., Bars R., Tinwell H., Piersma A.H. (2021). Gene regulation by morpholines and piperidines in the cardiac embryonic stem cell test. *Toxicol Appl Pharmacol.* 15;433:115781. doi: 10.1016/j.taap.2021.115781

Mennen, R. H., de Leeuw, V. C., & Piersma, A. H. (2021). Cell differentiation in the cardiac embryonic stem cell test (ESTc) is influenced by the oxygen tension in its underlying embryonic stem cell culture. *Toxicol In Vitro*, 105247. doi:10.1016/j.tiv.2021.105247

Mennen, R. H., Hallmark, N., Pallardy, M., Bars, R., Tinwell, H., & Piersma, A. H. (2021). Molecular neural crest cell markers enable discrimination of organophosphates in the murine cardiac embryonic stem cell test. *Toxicology reports*, 8, 1513-1520. doi:<https://doi.org/10.1016/j.toxrep.2021.07.017>

Mennen, R. H., de Leeuw, V. C., & Piersma, A. H. (2020). Oxygen tension influences embryonic stem cell maintenance and has lineage specific effects on neural and cardiac differentiation. *Differentiation*, 115, 1-10. doi:10.1016/j.diff.2020.07.001

Mennen, R. H., Pennings, J. L. A., & Piersma, A. H. (2019). Neural crest related gene transcript regulation by valproic acid analogues in the cardiac embryonic stem cell test. *Reprod Toxicol*, 90, 44-52. doi:10.1016/j.reprotox.2019.08.013



APPENDIX

Nederlandse samenvatting

List of publications

Curriculum Vitae

Dankwoord

Curriculum Vitae

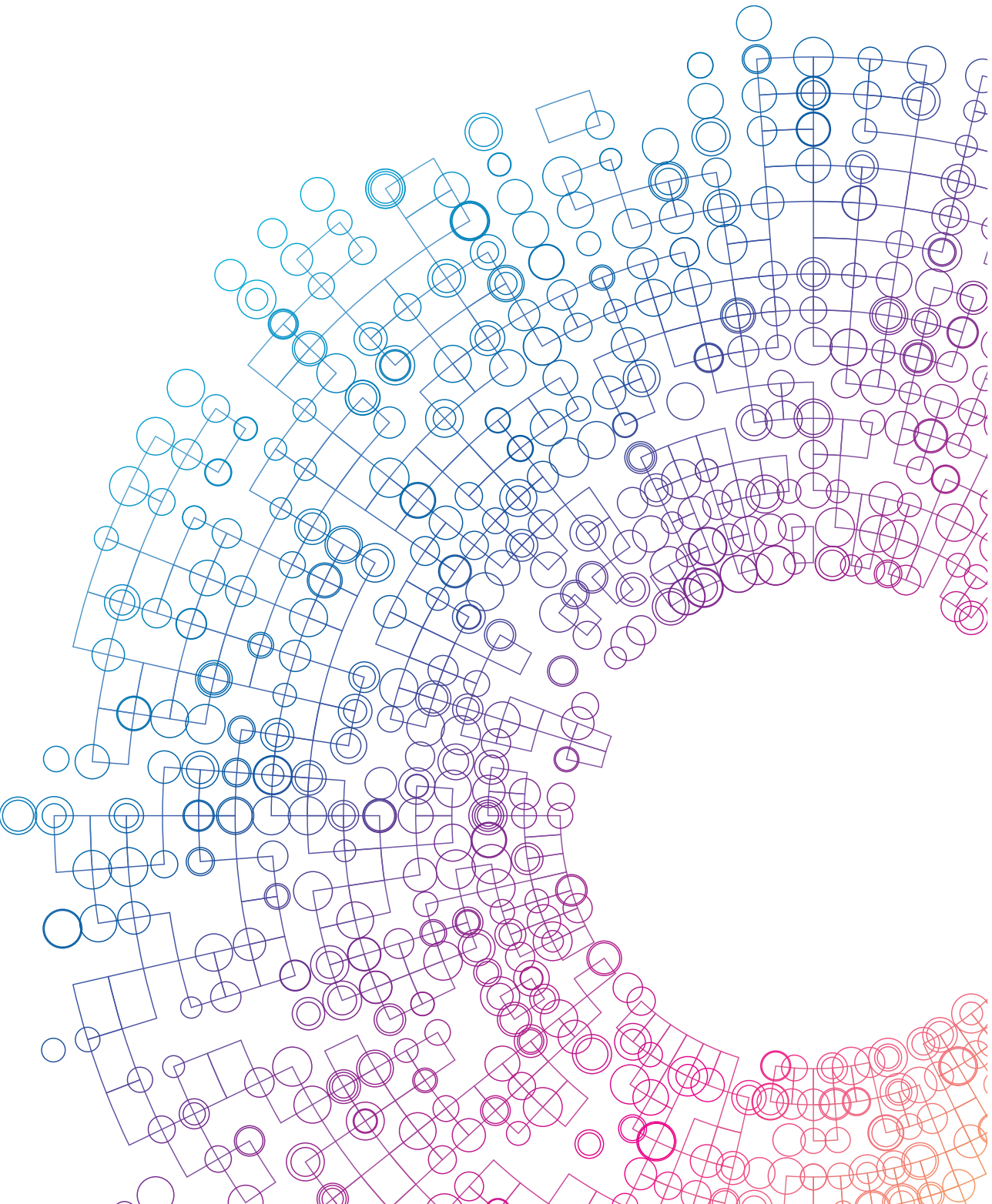


Gina Mennen was born on the 15th of August 1992 in Helmond, the Netherlands. After graduating the gymnasium from *Peellandcollege* in Deurne in 2010, she studied medical biology for her bachelor degree at the *Radboud University* in Nijmegen. As she gained special interest in disease prevention by a healthy lifestyle, she moved to Wageningen and studied the master Nutrition and Health from the *Wageningen University and Research centre*. She specialized herself in the direction of molecular nutrition and toxicology and did her master thesis in the human nutrition lab of the *WUR* under supervision of dr. Lily Boutens and assistant professor dr. Rinke Stienstra. For her thesis she studied inflammation of fat tissue under a high fat diet. Gina Mennen did her internship at the Gastroenterology department of the *Radboudumc* where she studied the effects of the antimicrobial taurolidine, used to prevent infections in catheters, on peripheral blood mononuclear cells. This was under the supervision of dr. Yannick Wouters and dr. Geert Wanten. Gina Mennen graduated in 2016 for her MSc degree.

In 2017, she started her PhD project at the Centre for Health Protection of the *National Institute for Public Health and the Environment (RIVM)*. To finance the remaining three years of her PhD, she moved to Sophia-Antipolis, France in 2018. While she was applying for a CIFRE grant of the *Association Nationale Recherche Technologie (ANRT)*, she worked at *Bayer Crop Sciences* and introduced the embryonic stem cell test. At the end of 2018, she started her 3-year CIFRE PhD contract for which she was situated at the *RIVM* under the supervision of prof. dr. Aldert Piersma, prof. dr. Marc Pallardy, dr. Nina Hallmark, dr. Rémi Bars and dr. Helen Tinwell.

During her research, she completed the Postdoctoral Education in Toxicology to become a European Registered Toxicologist. During her PhD she was also actively engaged in organizing the annual two-day meetings for the *Dutch Toxicology Society (NVT)* for which she was chair of the PhD-committee in 2020 and 2021.

After her PhD contract, she started as a project intern at the *Health and Environmental Sciences Institute (HESI)* in the HESI DARTable genome group. For almost four months she worked on the development of an AOP related to retinoic acid and heart development. As of March 2022, Gina will start her new job as scientific staff member of the Dutch Expert Committee on Occupational Safety (DECOS) of the *Health Council of the Netherlands*.



APPENDIX

Nederlandse samenvatting

List of publications

Curriculum Vitae

Dankwoord

Dankwoord

Dit is dan toch echt het einde van mijn promotietijd. Het was een erg mooie tijd waarin ik ontelbaar veel heb geleerd op wetenschappelijk vlak maar ook op persoonlijk vlak. Dit was me allemaal niet gelukt zonder de steun en hulp van een hele hoop mensen, die ik allemaal graag wil bedanken.

Als allereerste wil ik **Aldert Piersma** bedanken. Wat was het een bijzonder promotie traject. Met name het niet-inhoudelijk vlak maakte dit traject bijzonder door onder andere de verschillende contracten waarbij het vaak toch net een beetje anders ging dan bij een regulier promotietraject. Het begon allemaal in december 2016 toen we in twee dagen op en neer naar de Côte d'Azur vlogen voor de sollicitatie rondes. Ik zat in het vliegtuig naast jou, de professor waarmee ik later nog een sollicitatiegesprek had. Mega spannend! Op de terugweg ging je al druk bladerend nog eens alle CV's door en ik zag dat het een moeilijke beslissing voor je was. In april 2017 mocht ik dan eindelijk beginnen en deze anekdote geeft denk ik al een beetje aan hoe ingewikkeld het soms was. Ik ben dankbaar dat je me de kans hebt gegeven, voor je vertrouwen al die tijd, dat je de hoop niet hebt opgegeven, voor je creativiteit, maar ook bedankt dat je deur altijd open stond. Onze wetenschappelijk discussies voerde ik met heel veel plezier en het was erg fijn om met je samen te werken.

I would also like to thank my other supervisors, who we sometimes called the 'French Connection'. Thank you, **Remi Bars**, for initiating the idea for this collaboration, for always being as friendly, and for asking the right questions at the right time. **Marc Pallardy** for your support from Université Paris-Saclay, for your scientific contributions and for your flexibility. **Helen Tinwell**, for the fruitful discussions and for your very much appreciated critical points of view. I especially would like to thank **Nina Hallmark**. No matter how busy you were, you always took the time to help me with my questions or hurdles. You tried to make me feel at home during my stay in France by showing me around occasionally. I thank you for your inexhaustible support on personal and scientific basis.

I would also like to thank the members of the assessment committee who took the time to read my dissertation, **prof. dr. André Guillouzo**, **prof. dr. Chris Evelo**, **prof. dr. Christine Mummery**, **dr. Anne Kienhuis**, **prof. dr. Juliette Legler**, and **prof. dr. Ellen Moors**.

Het merendeel van mijn promotietijd bracht ik door op het RIVM en ik wil graag mijn collega's bedanken van het centrum gezondheidsbescherming (GZB) en de afdeling vernieuwing Teststrategieën (VTS). Ik ben me ervan bewust dat dit hele project niet had kunnen beginnen zonder **Jan van Benthem**. Dankjewel voor je geduld, je ruimdenkendheid en vertrouwen. Dankjewel **Janine Ezendam** voor de stimulerende gesprekken en ondersteuning. Dankjewel aan alle **VTS-collega's** voor de inhoudelijke discussies en in het bijzonder **Jeroen Pennings**, voor je ondersteuning in de analyses en **Anne Kienhuis, Harm Heusinkveld** en **Ellen Hessel** voor het zo nu en dan meelesen van de manuscripten. Ook dank aan alle analisten voor de fijne sfeer op het lab en voor het delen van jullie ervaringen, maar in het bijzonder dank aan **Conny van Oostrom** vanwege je ondersteuning in het lab en je expertise in de stamcellen.

Tijdens mijn promotie heb ik ook twee stagiaires mogen begeleiden. **Joey** en **Marcia** heel erg bedankt voor jullie harde werk. Joey, heel veel succes als research analist bij het Amsterdam UMC. Marcia, jij hebt je plek gevonden als PhD'er bij VTS en ik wens je een hele mooie promotietijd. Ook de andere collega PhD'ers wil ik graag bedanken. Mijn promotietijd was een erg mooie tijd mede door jullie gezelligheid binnen en buiten het werk, de kletspraatjes en de support. Hiervoor heel erg bedankt **Myrto, Christina, Coen, Stella, Laura, Erna, Christy, Alessandro, Nienke, Els, Kirsten, Job** en **Ina**. In het bijzonder wil ik **Charlotte, Kim, Astrid** en **Victoria** bedanken met wie een bijzondere vriendschap is ontstaan en we hebben er samen al een paar mooie reisjes op zitten. Op naar de volgende! **Victoria**, mijn 'partner-in-crime', ook bedankt voor je wetenschappelijk inhoudelijke steun. Het was fantastisch om samen met jou aan de stamcellen te werken. Naarmate we elkaar beter leerden kennen, bleek dat die stamcellen niet de enige gelijkenis was tussen ons. Heel erg bedankt dat je mijn paranimf wilde zijn.

The year 2018 was an unforgettable year for me in the south of France. I would like to thank my colleagues in Sophia-Antipolis for your hospitality and warm welcome. I want to thank the colleagues from the Early Toxicology team for the interesting discussions. Thank you, **Angela Becker**, for having me as part of your team. Thank you to my colleagues with whom I shared the office for our scientific conversations and for the good atmosphere: **Isabelle, Ainhua, Davy, Benedicte, Caroline, Laurent, Ingrid, Benoît, Benjamin, Oscar** and **Amandine**. Thank you to all the analysts in the lab and especially **Agnes** for supporting me. A special thank you to **Marie-Frantz Figaro-Bessac, Marie Taminau** and the GIE AIFOR administrator

Chrystel Francisoud for supporting me with all the administration (in French!), for your help to apply for the CIFRE grant and to make it a success. Marie-Frantz, it was by far from easy and I know it has been a pain in the ass and I am thankful for your perseverance. I also want to thank **Benjamin, Camille, Oscar, Aracelia, Amandine** and **Guillaume** for your friendship during my stay and I am grateful that we discovered the south of France together. It was 'Nice'!!

Tijdens mijn verblijf aan de Côte d'Azur, wat ik absoluut niet had willen missen, ben ik me ook gaan realiseren hoe dankbaar ik mag zijn voor de warme kring om me heen van vrienden en familie. Dankjewel aan mijn lieve vriendinnen voor de juiste ontspanning op zijn tijd met al die leuke etentjes, stapavondjes, en vriendinnenweekenden. Een speciaal dankjewel aan **Virginie, Caroline, Tiffany**, en **Marjolein** voor jullie luisterend oor, dat ik mijn enthousiasme met jullie kon delen en voor dat extra steuntje in de rug. Ik weet dat jullie er alles aan hebben gedaan om proberen te begrijpen wat ik allemaal uitspookte in dat lab. Ook dankjewel aan mijn schoonfamilie, **Ton, Franka, Ruud, Nicole, Lea, Walter** en de kinderen voor jullie betrokkenheid en voor dat warme nest waar ik al een hele tijd deel van mag uitmaken.

Lieve **Arie en Rini Mennen**, mijn vader en moeder, oftewel 'ons pap en mam', bedankt voor alles! Dankjewel voor jullie steun en voor de rustige en fijne thuishaven. Jullie hebben altijd ontzettend hard gewerkt om ons te kunnen laten doen wat we wilden doen binnen onze opleiding maar ook daarbuiten. Jullie zijn voorbeelden voor mij op meerdere vlakken: Pap vanwege jouw maatschappelijk betrokkenheid, nauwkeurigheid en gedrevenheid. Mam vanwege jouw doorzettingsvermogen, leergierigheid en zorgzaamheid. Mijn lieve zusje en broertje **Lenny** en **Corné**, bedankt en ik ben trots op jullie! Lenny, wat ben jij een ontzettend harde werker en jouw doelmatige opstelling in werk en sport is van topniveau. Heel erg bedankt dat je mijn paranimf wilde zijn. Corné, jouw brede nieuwsgierigheid naar alles gerelateerd aan energie, milieu, natuur en financiën is aanstekelijk en het is mooi om te zien hoe jij je volledig in iets kan onderdompelen. Dankjewel **Teun** en **Anne** dat jullie al zo lang bij ons zijn en ieder op je eigen manier een toevoeging zijn aan het gezin. Lieve **Annie** en **Bert**, jullie maken al heel lang deel uit van onze familie en kennen me al van peuter af aan. Bedankt voor jullie oprechte interesse en voor alles wat jullie al die tijd voor ons hebben gedaan.

Lieve **Gijs**. Dankjewel voor je onuitputtelijke steun om te doen wat ik graag wilde doen. Jij bent voor mij goud waard. Dit hele avontuur is niet altijd makkelijk voor jou en voor ons geweest. Vooral niet tijdens dat jaar in Frankrijk, maar ook die lange reistijden waardoor ik vaak laat thuis was en de onzekerheden die het soms met zich meebracht. Jij ving mij op en we vulden elkaar aan en we zijn daardoor een mooi team en dat maakt me trots. Ik bewonder jouw gedrevenheid en hoe jij je kunt vastbijten in het opzetten van jouw eigen bedrijf, wat je fantastisch doet. Er is voor ons veel veranderd in de tijd van mijn promotie. Dat alles maakte het ook een erg mooi avontuur. Ons volgende hoofdstuk wordt alleen nog maar mooier.

Zonder jullie allemaal was het me niet gelukt en dankzij jullie heb ik me heel erg gesteund gevoeld. Heel erg bedankt!!

Merci , Thank you, Dankjewel. Gina

